New mechanisms underlying the variable phenotypes caused by N- and C-terminal mutations in the cardiac sodium channel.

Azza Isleem Ziyadeh

THESE DE DOCTORAT DE L'UNIVERSITE PIERRE ET MARIE CURIE

Ecole doctorale : Complexité du Vivant ED515

Spécialité

Physiologie et Physiopathologie

Présentée par

Madame Azza ISLEEM ZIYADEH

Pour obtenir le grade de

DOCTEUR DE l'UNIVERSITE PIERRE ET MARIE CURIE

Nouveaux mécanismes contribuant à la variabilité phénotypiques de mutations N- et C-terminales du canal sodique cardiaque

Soutenue le 04 Avril 2014

Devant le jury composé de :

Pr. Rose KATZ	Présidente du jury
Pr. Eric RADDATZ	Rapporteur
Pr. Vincent PROBST	Rapporteur
Dr. Pascale GUICHENEY	Directrice de thèse

Membre invité :

Dr. Nathalie NEYROUD	Co-encadrante

Résumé des travaux de thèse

Titre : Nouveaux mécanismes contribuant à la variabilité phénotypiques de mutations N- et C-terminales du canal sodique cardiaque

L'activité électrique cardiaque est étroitement contrôlée par l'activité coordonnée de multiples canaux ioniques voltage-dépendants. L'un des plus importants est le canal sodique cardiaque formé d'une sous-unité α, $Na_v1.5$, constituant le canal lui-même et de nombreuses protéines partenaires régulatrices. Ce canal permet la génération du courant sodique entrant I_{Na}, qui est un déterminant essentiel de la vitesse de conduction de l'influx électrique cardiaque, qui se transmet du nœud sinusal aux oreillettes, puis aux ventricules le long du tissu conducteur, puis à travers le myocarde ventriculaire. Des mutations dans le gène *SCN5A*, codant $Na_v1.5$, ont été impliquées dans de nombreuses arythmies cardiaques héréditaires, telles que le syndrome du QT long (SQTL), le syndrome de Brugada (SBr), les dysfonctions du nœud sinusal (DNS), et la fibrillation auriculaire (FA). Les arythmies liées à des mutations de *SCN5A* ont d'abord été considérées comme des entités cliniques distinctes. Plus récemment, un large spectre de phénotypes mixtes a été rapporté dans les arythmies liées aux mutations de *SCN5A* regroupés sous le terme d'«overlap syndromes». En plus de leur expression variable, les arythmies liées à *SCN5A* sont caractérisées par une pénétrance incomplète. L'origine des phénotypes mixtes causés par une même mutation de *SCN5A*, et la pénétrance incomplète de ces canalopathies, restent encore mal comprises. Cela a conduit à souligner la complexité des maladies liées aux mutations de *SCN5A*, et à suggérer que d'autres facteurs génétiques ou environnementaux pouvaient moduler le phénotype clinique. Dans notre travail, nous avons étudié trois facteurs qui pourraient expliquer les phénotypes variables induits par des mutations de *SCN5A* : l'interaction entre les sous-unités α de $Na_v1.5$, les propriétés électriques différentes entre les cardiomyocytes auriculaires et ventriculaires, et le terrain génétique des patients.

Dans la première partie de ce travail de thèse, nous avons caractérisé la mutation R104W située dans la partie N-terminale du canal sodique cardiaque $Na_v1.5$, identifiée chez un patient de 33 ans atteint de SBr. Ce syndrome est une canalopathie cardiaque héréditaire à transmission autosomique dominante et à pénétrance incomplète, où des mutations perte-de-fonction de $Na_v1.5$ sont trouvées chez environ 25% des cas. Par des études biochimiques et électrophysiologiques, nous avons montré que le mutant R104W exprimé seul dans les cellules HEK293 n'était associé à aucun courant sodique I_{Na}, et est dégradé par le système

ubiquitine-protéasome. Lorsqu'il est co-exprimé avec le canal sauvage, imitant l'état hétérozygote du patient, le mutant exerce un effet dominant négatif sur les canaux sauvages, et conduit à un décalage de la courbe d'activation vers des potentiels positifs. L'immunocytochimie de cardiomyocytes de rats nouveaux-nés transfectés avec R104W et/ou $Na_v1.5$ sauvage a montré que le mutant seul est principalement retenu dans le réticulum endoplasmique. De plus, sa co-expression avec le sauvage conduit à la rétention de ce dernier. Par ailleurs, la co-transfection de R104W avec R878C, un canal mutant capable d'atteindre la membrane mais non fonctionnel, restaure une très petite activité de R104W. Ces résultats nous ont amené à penser qu'une coopération entre les sous-unités α $Na_v1.5$ pouvait exister. Par des études de co-immunoprécipitation, nous avons démontré pour la première fois que les sous-unités α sauvages interagissaient entre elles, ainsi qu'avec les sous-unités α mutées R104W. L''interaction entre les sous-unités α $Na_v1.5$ est un nouveau mécanisme qui pourrait moduler l'effet fonctionnel de mutations de *SCN5A* ainsi que le phénotype clinique ; ceci démontre l'importance de l'expression hétérozygote lorsque l'on étudie les effets fonctionnels de mutations dans *SCN5A*.

Dans la deuxième partie de ce travail de thèse, nous avons caractérisé la mutation R1860Gfs*12, mutation tronquante dans la région C-terminale de $Na_v1.5$, identifiée dans une famille présentant un tableau clinique mixte de DNS, FA, flutter atrial, et de troubles de la conduction sans SBr. La mutation a été identifiée chez le cas index, son père et son oncle.

Les analyses biochimiques et les études de patch-clamp ont objectivé que dans les cellules HEK293 les canaux mutants R1860Gfs*12 sont partiellement dégradés par le système ubiquitine-protéasome, et associés à une réduction de I_{Na}, un décalage positif de la courbe d'activation, un décalage négatif de la courbe d'inactivation et une augmentation du courant persistant I_{NaL} par rapport au canal sauvage. À l'état hétérozygote, le mutant n'exerce pas d'effet dominant négatif sur le sauvage, mais induit un décalage négatif de la courbe d'inactivation, ainsi qu'un courant sodique persistant. Le décalage négatif de la courbe d'inactivation conduit à une réduction marquée de la disponibilité de $Na_v1.5$, ce qui indique une perte-de-fonction du mutant R1860Gfs*12. Par ailleurs, en mesurant I_{Na} dans des cellules HEK293 exprimant le mutant, maintenues à des potentiels imitant le potentiel de repos des myocytes auriculaires ou celui des myocytes ventriculaires, nous avons montré que le mutant induit une perte-de-fonction nettement plus prononcée dans les cellules auriculaires que dans les cellules ventriculaires. Ces résultats ont été confirmés par modélisation informatique (des potentiels d'action membranaires de cellules uniques auriculaires ou ventriculaires) et pourraient expliquer la survenue d'arythmies auriculaires dans cette famille sans SBr, ni

arythmies ventriculaires. En outre, en recherchant la présence de polymorphismes associés au risque de FA dans cette famille, nous avons mis en évidence que le cas index, qui a développé la maladie à un jeune âge avec des symptômes plus sévères que son père et son oncle, est porteur d'allèles à risque en amont de *PITX2*, un gène largement associé au développement de la FA. De plus, dans cette étude, nous avons mis en évidence que les sous-unités α tronquées R1860Gfs*12 étaient encore capables d'interagir entre elles ainsi qu'avec des sous-unités α sauvages, indiquant que les derniers 156 acides aminés de $Na_v1.5$ ne sont pas essentiels pour l'interaction entre les sous-unités α. Ces résultats suggèrent que les différences électrophysiologiques entre les oreillettes et les ventricules, combinées au terrain génétique des patients, sont des facteurs modulant l'expression phénotypique des mutations *SCN5A*.

$Na_v1.5$ interagit avec de nombreuses protéines partenaires, y compris le facteur homologue au facteur de croissance des fibroblastes (FHF1B), qui se lie à la partie C-terminale de $Na_v1.5$ et module l'inactivation du canal. Cependant, le site exact de l'interaction de FHF1B sur le C-terminus de $Na_v1.5$ fait l'objet d'un débat et serait situé dans sa région proximale ou ses régions proximale et distale. Dans la troisième partie de ce travail de thèse, nous avons confirmé par des études de co-immunoprécipitation de FHF1B et de deux mutants tronqués R1860Gfs*12*10 et L1821fs*10, que les deux régions proximale et distale de $Na_v1.5$ sont essentielles à l'interaction entre FHF1B et $Na_v1.5$. En outre, nous avons démontré par PCR quantitative que FHF1B est l'isoforme FHF la plus exprimée dans les ventricules humains.

Puisque 75% des cas de SBr ne sont pas liés aux gènes connus à l'origine de SBr, nous avons criblé le gène candidat *FGF12B* codant une protéine partenaire, FHF1B, chez 182 patients atteints de SBr avec un génotype négatif pour la plupart des gènes connus et nous avons identifié le variant V127M chez un patient. La valine en position 127 est conservée dans plusieurs espèces, ainsi que dans les autres FHFs humains (FHF2, FHF3, FHF4), ce qui est en faveur d'un possible rôle dans la fonction de cette protéine. Néanmoins, l'analyse électrophysiologique de cellules HEK293 transfectées avec $Na_v1.5$ et FHF1B sauvage ou muté n'a pas montré de différence fonctionnelle.

Conclusion: l'interaction entre les sous-unités α $Na_v1.5$ est un nouveau mécanisme qui pourrait moduler les effets fonctionnels de certaines mutations du *SCN5A* ainsi que les phénotypes cliniques. Cela met en évidence l'importance de l'expression hétérozygote lorsque l'on étudie les effets fonctionnels des mutations *SCN5A*. En outre, les propriétés électriques différentes entre les cardiomyocytes auriculaires et ventriculaires, et la présence de

polymorphismes chez les patients porteurs des mutations pourraient modifier le phénotype clinique et aider à expliquer la grande variabilité phénotypique des canalopathies sodiques.

Mots Clés : Arythmie, Syndrome de Brugada, Fibrillation auriculaire, $Na_v1.5$, *SCN5A*, *PITX2*, Polymorphisme

Inserm-UPMC UMR_S 1166
Institut de recherche sur les maladies cardiovasculaires, du métabolisme et de la nutrition
Faculté de médecine Pierre et Marie Curie
75634 Paris Cedex 13
Tél : 33 1 40 77 98 05
Fax : 33 1 40 77 96 45

Thesis summary

Title: New mechanisms underlying the variable phenotypes caused by N- and C-terminal mutations in the cardiac sodium channel

Mutations in the *SCN5A* gene, which encodes the α-subunit of the cardiac sodium channel $Na_v1.5$, are implicated in different inherited cardiac arrhythmias. The incomplete penetrance observed in these diseases suggests the existence of other factors modulating the phenotype of these mutations. In this thesis work, we characterized two mutations identified in *SCN5A*.

The R104W mutant identified in a patient with Brugada syndrome is retained in the endoplasmic reticulum (ER), degraded by the proteasome and abolishes the sodium current. Co-expressed with wild type (WT) channels, R104W leads to WT channels ER retention, causing a dominant-negative effect. We demonstrated that interaction between $Na_v1.5$ α-subunits is responsible for the retention and the dominant-negative effect.

The R1860Gfs*12 mutation was identified in a family with atrial arrhythmias. In a heterologous system, this mutant induces both loss- and gain-of-function effects on $Na_v1.5$. Computer-model simulation showed that the loss-of-function was more pronounced in atrial than in ventricular cells. In addition, we showed that the presence of polymorphisms upstream of the *PITX2* gene could explain the observed phenotypic variability in this family.

In conclusion, the interaction between the α-subunits of $Na_v1.5$, the different electrical properties between atria and ventricles and the presence of polymorphisms in patients with *SCN5A* mutations, are important factors in the interpretation of the functional effects of these mutations, which could explain the phenotypic variability of sodium channelopathies.

Keywords: Arrhythmia, Brugada syndrome, Atrial fibrillation, $Na_v1.5$, *SCN5A*, *PITX2*, Polymorphism

Acknowledgement

I would like to thank all the people who have contributed, in one way or another, to the work described in this thesis. My first and sincere gratitude goes to Dr. Pascal Guicheney, my thesis supervisor, whose expertise, understanding, direction and invaluable ideas and suggestions added considerably to make this work a success. I appreciate her vast knowledge in her domain, and her assistance in writing the non-stop reports concerning my scholarship and stay in France. Besides, I am deeply grateful to my co-supervisor, Dr. Nathalie Neyroud, for her continuous support during the last four years, her patience, presence and kindness. I owe her most, if not all, the techniques I learnt in the laboratory since my arrival. The guidance and support of both of my supervisors have facilitated remarkably my research experience and the writing of the articles and this thesis, it would have been so difficult to accomplish this whole work without your insights.

My special thanks go to Dr. Alain Coulombe and my colleague Dr. Jérôme Clatot, for their valuable inputs in the work of this thesis and its articles. I am also grateful to every member in our team; Myriam Berthet, Dr. Martin Grauso, Dr. Eric Villard, Agathe Korniat, Dr. Alexia Vite, Dr. Darouna Kattygnarath, Gilles Dilanian and Dr. Sabine Duchatelet. I must also acknowledge Valérie Cornillault for her kindness and help with the administrative paper work, Pr. Stéphane Hatem, director of the whole unit. I would also like to thank Dr. Rachel Peat, for the time she spent to help correct my written English. You are adorable as usual.

Furthermore, I have been privileged to know and collaborate with many other great people. Dr. Estelle Gandjbakhch, cardiologist at the Pitié-Salpêtrière University Hospital, and her team, for providing patients' medical data as well as ECG interpretations. Dr. Isabelle Denjoy, cardiologist at the Bichat University Hospital, for her nice help in revising and correcting the section of cardiac arrhythmias in the introduction. Dr. Isabelle Deschenes, from Cleveland Heart and Vascular Research Centre in USA, thank you for your suggestions and help.

In addition, I would like to express my gratitude to Pr. Eric Raddatz from Lausanne University, and Pr. Vincent Probst from Nantes University Hospital, for their acceptance to be members in my thesis jury, their valuable time spent to critically read and comment on my thesis work. My special thanks are owed to Pr. Rose Katz, president of the jury and representative of Paris VI University in the cooperation program with the Palestinian Medical School for more than ten years. Thank you for your patience and availability to solve our problems in difficult moments. You are unforgettable!

I am greatly indebted to Pr. Anwar Dudin, ex-Dean of Annajah Medical School, who encouraged and helped me come here to do my first research experience. To Annajah University in Nablus, Palestine, for the grant I have been awarded to do this PhD degree.

Finally, I would like to thank from the depth of my heart my husband, Jawad, for his unconditional support, encouragement, love and assistance. I am deeply and forever indebted to my father, the soul of my mother, and my brothers and sister who have accompanied me from far away during my stay in France. My parents-in-law for their continuous payers for our success. Love you all, and forever!

I dedicate this thesis to my husband Jawad and my family Love you all

Table of contents

List of figures

List of tables

Abbreviations

ABS: Ankyrin-B syndrome
AF: Atrial fibrillation
AFL: Atrial flutter
AP: Action potential
ARVC: Arrhythmogenic right ventricular cardiomyopathy
ATS: Andersen-Tawil syndrome
AV: Atrio-ventricular
AVN: Atrio-ventricular node
AVNRT: Atrio-ventricular nodal re-entrant tachycardia
AVRT: Atrio-ventricular reciprocating tachycardia
bpm: Beats per minute
BrS: Brugada syndrome
BSA: Bovine serum albumin
Ca^{2+}: Calcium ion
CaM: Calmodulin
CaMKII: $Ca2^{+}$/calmodulin-dependent protein kinase II
cAMP: Cyclic adenosine monophosphate
CASQ2: Calsequestrin 2
CCD: Cardiac conduction diseases
CCW: Counterclockwise
CFTR: Cystic fibrosis transmembrane conductance regulator
CHO: Chinese hamster ovary
CPVT: Catecholaminergic polymorphic ventricular tachycardia
DAD: Delayed after-depolarization
DCC: Direct current cardioversion
DHAP: Dihydroxyacetone phosphate
DMSO: Dimethyl sulfoxide
dNTPs: Deoxynucleosidetriphosphates
DTT: Dithiothreitol
EAD: Early after-depolarization
ECG: Electrocardiogram
ER: Endoplasmic reticulum
ERAD: ER-associated degradation
ESC: European society of cardiology
FCS: Fetal calf serum
FGF: Fibroblast growth factor
FHFs: Fibroblast growth factor homologous factors
G3P: Glycerol-3-phosphate
GAPDH: Glyceraldehyde 3-phosphate dehydrogenase
GPD1L: Glycerol phosphate dehydrogenase 1-like protein
GWAS: Genome-wide association study
$G\alpha_s$: Stimulatory heterotrimeric G-protein
HCN: Hyperpolarization-activated cyclic nucleotide–gated channels
HEK: Human embryonic kidney

HPRT: Hypoxanthine guanine phosphoribosyl transferase
HV: His-ventricular
IB2: Islet-brain-2
$I_{Ca,L}$, $I_{Ca,T}$: Calcium currents
ICC: Interstitial cells of Cajal
ICD: Implantable cardioverter defibrillator
I_f : Funny current
IFM: Isoleucine, Phenylalanine, Methionine
I_{Na}: Inward sodium current
I_{NaL}: Late sodium current
I_{to}: Transient outward potassium current
IV: Intravenous
IVF: Idiopathic ventricular fibrillation
JLNS: Jervell and Lange-Nielsen syndrome
K^+: Potassium ion
KChIP2: K^+ channel-interacting protein
LB: Lysogeny broth medium
LGMD2G: Limb girdle muscular dystrophy
LQTS: Long QT syndrome
MAGUK: Membrane associated guanylate kinase
MAP: Mitogen activated protein
MDP: Maximum diastolic potential
MOG1: Multicopy of suppressor gsp1
Na^+: Sodium ion
$Na_v1.5$: Sodium channel 1.5
NCX: Na^+/Ca^{2+} exchanger
Nedd4-2: Ubiquitin-protein ligases
NHS: N-hydroxysuccinimide
NPPA: Atrial natriuretic peptide
PAC: Premature atrial contraction
PBS: Phosphate buffered saline
PCCD: Progressive cardiac conduction disease
PKA: Protein kinase A
PKC: Protein kinase C
PMCA: Plasma membrane Ca^{2+} ATPase
PTPH1: Protein tyrosine phosphatase 1
PVC: Premature ventricular contraction
PY: Proline, Tyrosine
qPCR: Quantitative reverse-transcriptase polymerase chain reaction
RBBB: Right bundle branch block
RFP: Red fluorescent protein
RPL32: Ribosomal protein L32
RVOT: Right ventricular outflow tract
RyR2: Ryanodine receptors
SAN: Sinoatrial node
SAP97: Synapse associated protein 97
SCA27: Spinocerebellar ataxia 27
SCD: Sudden cardiac death
SERCA: Sarco/endoplasmic reticulum Ca^{2+} ATPase
SIDS: Sudden infant death syndrome

SND: Sinus node dysfunction
SNP: Single nucleotide polymorphism
SOC: Super optimal broth medium
SOCC: Store-operated Ca^{2+} channels
SQTS: Short QT syndrome
SR: Sarcoplasmic reticulum
SSS: Sick sinus syndrome
SUNDS: Sudden unexplained nocturnal death syndrome
SVT: Supraventricular tachycardia
T tubules: Transverse tubules
TdP: Torsade de pointes
TfnR: Transferrin receptor
TS: Timothy syndrome
VF: Ventricular fibrillation
VGSCs: Voltage-gated sodium channels
VT: Ventricular tachycardia
WPW: Wolff-Parkinson-White syndrome
WT: Wild type
ZO-1: Zonula occludens-1

Preface

Sudden cardiac death (SCD) is defined as an unexpected death due to a cardiac cause, which occurs within one hour following the onset of symptoms. Ventricular tachycardia (VT) degenerating into ventricular fibrillation (VF) and to asystole is the most common mechanism underlying SCD. The disorganized and ineffective ventricular contraction during VF will deprive the vital organs from the oxygenated blood and result in a loss of consciousness. If not treated quickly by an electric shock using an automated external defibrillator, death occurs within few minutes. It is a major health problem accounting for 20% of total mortality, and 50% of cardiovascular mortality[1]. Consequently, identifying the patients at high risk of SCD and treating them, became one of the medical challenges of the beginning of the 21st century.

Eighty percent of SCDs occur in individuals older than 40 years with coronary heart disease[2]. However, SCDs also occur in young people where cardiomyopathies and primary electrical diseases (channelopathies) are the major causes of VF[2]. Brugada syndrome (BrS), long QT syndrome (LQTS), and catecholaminergic polymorphic ventricular tachycardia (CPVT) constitute the main channelopathies leading to SCD[3]. Our knowledge of the cellular and molecular mechanisms underlying these channelopathies is still insufficient, leading to inadequate risk stratification of patients and families, and treatment options restricted mainly to cardioverter defibrillator implantation. Nevertheless, basic research, using heterologous expressing systems or animal models, has proved its efficacy in improving our understanding of the pathophysiology of these channelopathies.

In this thesis work, we studied the cardiac sodium channelopathies associated with *SCN5A* mutations, which are involved in a wide spectrum of disease phenotypes: LQTS, BrS, progressive cardiac conduction disease (PCCD), atrial fibrillation (AF), sick sinus syndrome (SSS), and dilated cardiomyopathies. Despite important progresses in understanding the mechanisms underlying the sodium channel dysfunction, risk stratification and management of patients with this channelopathy are still limited, mainly because of its reduced penetrance and variable expressivity. Moreover, some *SCN5A* mutations were linked to a mixed clinical picture known as cardiac sodium channel "overlap syndromes". The variable expressivity of the *SCN5A* mutations suggests an involvement of additional unknown mechanistic, genetic, and environmental factors in the determination of the phenotypic expression of a given *SCN5A* mutation. Better understanding of these modifiers is essential to ameliorate the diagnosis, risk stratification, and treatment options in patients with sodium channelopathy.

In this thesis we aimed to address the mechanisms underlying the variable phenotypes

of *SCN5A* mutations, by the characterization of two *SCN5A* mutations, R104W and R1860Gfs*12 identified in patients with hereditary cardiac arrhythmias. Moreover, by candidate gene approach in genotype-negative BrS patients, which accounts approximately for 75% of BrS cases, we aimed to identify a new gene involved in this hereditary arrhythmia.

INTRODUCTION

I. The anatomical structure and electrical activity of the heart

I.1 General anatomical structure and function

The heart is a hollow striated muscular pump, which supplies the whole body with the requirements of nutrients and oxygen through the blood circulation. It is divided into right and left halves by a muscular wall that is called septum. Another muscular wall separates the upper parts of the heart from the lower parts, resulting in four chambers: right and left upper atria, right and left lower ventricles (Figure 1A). Each one of these chambers has a specific role in the circulatory system. The right atrium receives the non-oxygenated, waste-rich blood from the whole body through two large veins; the superior and inferior vena cava. Then, by the contraction of the right atrium, the blood passes through the one-way tricuspid valve into the right ventricle. The right ventricle contracts in turn and the non-oxygenated blood passes through the pulmonary valve into the pulmonary artery up to the lung. Once oxygenated, blood returns to the left atrium through the pulmonary veins. During the contraction of the left atrium, blood passes through the one-way mitral valve into the left ventricle. Then, it is ejected into the systemic circulation through the largest artery, the aorta (Figure 1B).

Each cardiac cycle consists of two basic phases: diastole and systole**.** During the diastolic phase, the ventricles are relaxed, and blood passes passively from right and left atria into the right and left ventricles. At the end of diastole, the atria contract to eject an additional amount of blood into the ventricles. In the systolic phase, the left and right ventricles contract and blood moves into the aorta and the pulmonary artery, respectively. This succession of diastolic and systolic phases is produced through the spontaneous activity of pacemaker cells. The trigger activity of these cells is not under the control of the nervous system. However, cardiac frequency can be modulated by the autonomic nervous system.

A B

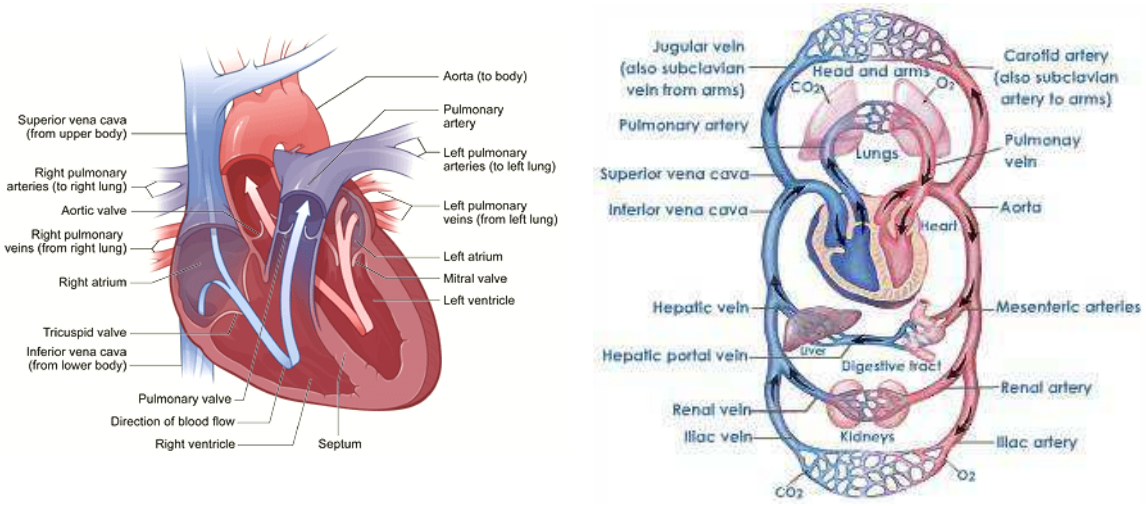

Figure 1: Anatomical structure of the heart and blood circulation
http://babyheart.in/tag/normal-structure-of-heart/
http://www.tutorvista.com/content/biology/biology-iv/circulation-animals/blood-circulation-mammalian-heart.php

I.2 Cardiac cells

The heart is composed of different cell types: the cardiomyocytes, which account for approximately 75% of the total volume of normal myocardial tissue but represent 30-40% of total cell numbers, and the non-myocyte cells which make up 70% of cardiac cells[4]. The non-myocyte cells include (1) the fibroblasts which represent 90% of non-myocyte cells, having many critical functions such as extracellular matrix synthesis and deposition, and cardiac remodeling[5], (2) endothelial cells that line the entire circulatory system from the heart to the smallest capillaries, (3) smooth muscle cells, (4) neurons and (5) inflammatory cells, mainly macrophages[6].

The cardiomyocytes are divided into two main cell types: working (contracting) myocytes and conduction cells.

I.2.1 Working or contracting cardiomyocytes

Adult cardiomyocytes have a cylindrical shape, are approximately 100 µm long by 10-25 µm in diameter, and are organized as a network of branched fibers. They have a specialized structure called a sarcolemma, which is a fusion of plasma and basement membrane surrounding the cells. The sarcolemma forms two specialized structures: the intercalated discs at the junction between adjacent cells, and the transverse tubules at the lateral membrane.

The intercalated discs play an important role in the function of cardiac muscle, and consist of three types of membrane junctions: adherens junctions, desmosomes and gap junctions. Adherens junctions (containing N-cadherin, catenins, and vinculin), and desmosomes (containing desmoplakin, desmocollin, desmoglein, plakophilin, and plakoglobin), mediate cell-cell adhesion and anchor underlying cytoskeletal structures to the cell membrane. Gap junctions allow the conduction of electrical signals between cardiomyocytes and exchanges of metabolites.

The transverse tubules (T tubules) are deep invaginations of the sarcolemma communicating with the sarcoplasmic reticulum (SR), an intracellular calcium (Ca^{2+}) reserve whose release is controlled by the ryanodine receptors (RyR2). The transmission of electrical signals through the T-tubules causes massive release of Ca^{2+} from the SR, leading to contraction of the myofibrils (excitation-contraction coupling). This contractile activity of cardiomyocytes is generated by the fundamental contractile unit, the sarcomere, which consists of thin (actin) and thick (myosin) filaments (Figure 2).

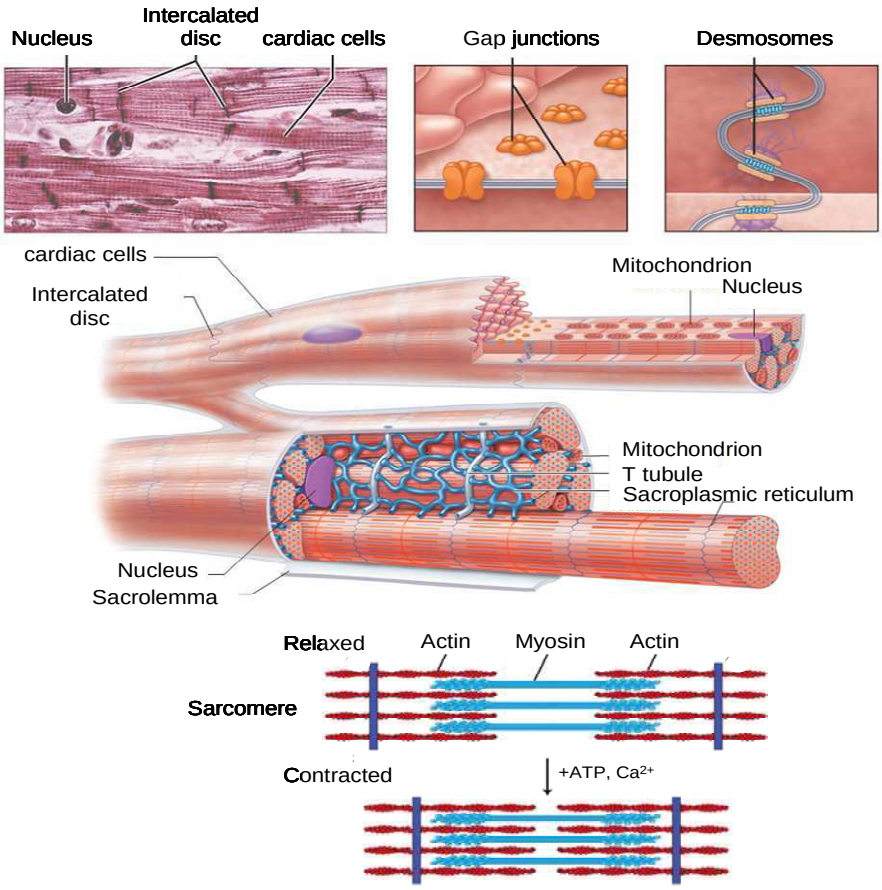

Figure 2: Anatomical structure of cardiomyocytes
Modified from http://antranik.org/myocardium/

I.2.2 Cardiac conduction cells

Specialized cardiomyocytes are responsible for the initiation, conduction and propagation of electrical signals, due to their ability to autonomously fire. These cells are present in the sinoatrial node (SAN), the atrio-ventricular node (AVN), the bundle of His and Purkinje fibers (Figure 3). In the normal heart, the electrical signal begins by the spontaneous excitation in the SAN, which is an area of specialized cells located at the junction between the superior vena cava and the right atrium. It is the natural and primary pacemaker of the heart since it is responsible for the initiation of electrical signals at faster rate than other areas of the heart with pacemaker potential. This rate of electrical discharge, called sinus rhythm, will determine the number of heartbeats per minute (bpm), which is normally between 60-100 bpm. From the SAN, the signal is rapidly conducted through the atria to the AVN, which also contains specialized nodal cells, located between the atria and the ventricles, in the interatrial septum near the opening of the coronary sinus. The AVN delays the propagation of impulse to the ventricles, this delay is extremely important to ensure that the atria have contracted and

ejected blood into the ventricles before ventricular contraction. It is also important to protect the ventricles from excessive heart rate such as in cases of atrial arrhythmia. From the AVN down to the apex, the electrical signal propagates through specialized bundle of conduction fibers called the bundle of His. The bundle of His enters the inter-ventricular septum and divides rapidly into right and left branches that end in the cardiac apex as Purkinje fibers. This network of fibers ensures synchronized ventricular contraction.

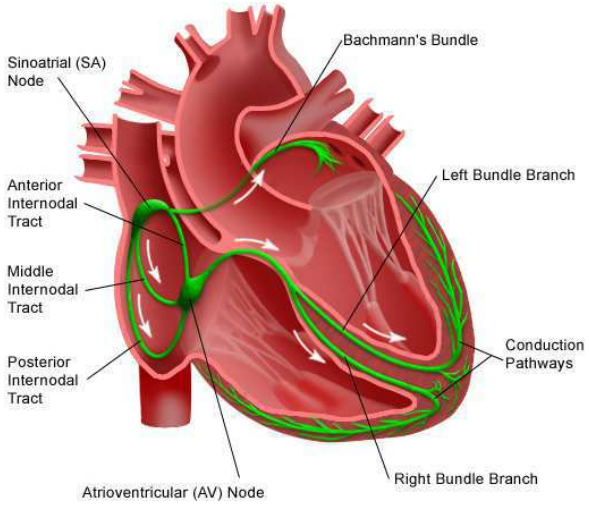

Figure 3: The cardiac conduction system
http://mdmedicine.wordpress.com/2011/04/24/heart-conduction-system/

I.3 The electrical activity of the heart

I.3.1 Membrane potential

The sarcolemma of the cardiomyocyte defines two different aqueous ionic compositions of intracellular and extracellular, by maintaining large gradients of ions across these two compartments. This uneven distribution of ionic species, mainly potassium (K^+) and sodium (Na^+), across the membrane, leads to an electro-diffusion membrane potential, which is equal to the differential electrical potential across the sarcolemma. Cations diffuse passively (following their concentration gradients) across the sarcolemma through embedded selective ion channels. The opening and closing of these channels depend on the change in membrane potential. Thus these ion channels are called voltage-dependent. The intracellular medium is rich in K^+ (150 mM) and the extracellular medium is rich in both Na^+ (135-145 mM) and Ca^{2+} (1-2 mM). These ion concentration gradients are maintained by the presence of ion pumps such as the Na^+/K^+ ATPase, PMCA (Plasma Membrane Ca^{2+} ATPase) and the Na^+/Ca^{2+} exchanger (NCX), which move ions against their electrochemical gradients.

I.3.2 Resting membrane potential

Like most excitable cells, atrial and ventricular cardiomyocytes have a resting state in which the electrical potential is stable across the sarcolemma. This state is called the resting membrane potential. It results from the selective permeability of the sarcolemma to K^+ ions. At resting membrane potential, most ion channels are closed except the potassium channel Kir2.1 (responsible for I_{K1}). The efflux of K^+ ions through this channel leads to a potential difference across the membrane of about -80 and -85 mV for atrial and ventricular cardiomyocytes, respectively, a value that is closest to the Nernst equilibrium potential of the K^+ ion. The resting membrane potential is less polarised in the atrial cells (Figure 5B) since they have lower expression of Kir2.1 transcripts compared to ventricular cells (Figure 4)[7]. In addition, atrial I_{K1} has 5- to 10- fold smaller current density, smaller elementary conductance, and shorter channel open times compared to ventricular I_{K1}[8,9]. As a consequence, less depolarizing current is required to reach the firing action potential threshold in atrial cells compared to ventricular cells, explaining the higher excitability of atrial cells.

In contrast to atrial and ventricular myocytes, SAN myocytes do not polarize enough to reach the level of the resting membrane potential and show slow spontaneous depolarization during diastole (Figure 5B). These diastolic depolarizations contribute to the ability of SAN to generate spontaneous and repetitive action potentials in the absence of external electrical stimulation. This depolarization results from low intensity of $I_{K1,}$ and the high expression of hyperpolarization-activated channel that conducts the inward-rectifying mixed Na^+ - K^+ 'funny' current (I_f) when the membrane potentials descend below –40 to –45 mV during the repolarization phase[10].

I.3.3 Cardiac action potential and ionic currents

The cardiac action potential (AP) represents a transient depolarization wave that starts when the membrane depolarizes. It is the consequence of a cascade of ion movements, depending mostly on changes in ion channel permeability. Each cell type exhibits a different shape and duration of cardiac AP (Figure 4). This diversity is due to the variable expression of ion channels[7,11].

The cardiac AP consists of five phases (Figure 5):

- Phase 0: The rapid depolarization phase (initial upstroke)

Excitation by electrical signals from adjacent cells activates the voltage-dependent sodium channels. Opening of these channels gives rise to the inward sodium current I_{Na},

which has a short duration but high intensity, and which triggers the very fast change in the membrane potential (upstroke of the AP) toward the equilibrium (Nernst) potential of Na^+. Indeed, entrance of sodium ions further depolarizes the membrane, opening more sodium channels and leading to phase 0 depolarization (initial upstroke). Closing of these channels is rapid, but they need time to be reactivated. This time is called the refractory period, it is essential for cardiac cells as it prevents the genesis of any new AP until these channels are able to open a second time.

In nodal cells, the slow depolarization during the resting membrane potential leads to the inactivation of most sodium channels, inhibiting them from participating in the depolarization phase. As a consequence, the depolarization phase in these cells is mainly due to the $I_{Ca,L}$ and the $I_{Ca,T}$ calcium currents (Figure 5B).

- Phase 1: The early repolarization phase

Inactivation of sodium channels, and opening of certain potassium channels ($K_v4.2$, $K_v4.3$, $K_v1.4$) responsible for the transient potassium current $I_{to,}$ lead to a rapid outflow of K^+ and early membrane repolarization. In human ventricles, differences in density and rate-dependent properties of I_{to} in endocardial and epicardial layers lead to transmural electrical gradients and variation in the AP duration[12].

- Phase 2: The plateau phase

The plateau phase of the cardiac AP represents the balance between the inward depolarizing and the outward repolarizing currents. The inward L-type Ca^{2+} current, generated by $Ca_v1.2$ calcium channels, is the main current maintaining the plateau phase. The $Ca_v1.2$ channels activate slowly at membrane potentials higher than -40mV, and their inactivation depends on membrane potential and intracellular Ca^{2+} concentration. They also have an important role in triggering the entry of Ca^+ into the cell, which, in turn, leads to SR Ca^{2+} release that is responsible for excitation-contraction coupling. At the end of the plateau phase, the rectifier potassium channels start to be activated accounting for the replarization phase.

- Phase 3: The repolarization phase

The rectifying potassium channels are in charge of the predominant outward repolarizing currents. They consist of two channels with different kinetics and conductance:

the rapid activating ($K_v11.1$, I_{Kr} current) and the slow activating ($K_v7.1$, I_{Ks} current) channels. In the atrium, the ultra rapid activating potassium channel ($K_v1.5$, I_{Kur} current) also exists.

Calcium channel closure and the increase in the outward potassium currents I_{Ks}, I_{Kr}, I_{Kur} and I_{K1} lead to membrane repolarization and phase 3 of the cardiac AP. In the ventricles, the beginning of Phase 3 is mainly due to the I_{Ks} and I_{Kr} currents, then I_{K1} current participates at the end of the membrane repolarization and in the maintenance of the resting membrane potential. The atrial AP (Figure 5B) has a less pronounced plateau phase compared to the ventricular AP. This is due to differences in the repolarizing channels. The $K_v1.5$ channel is highly expressed in the atrium compared to the ventricles (Figure 4) as it is specific to atrial cardiomyocytes[7,9], and I_{kur} activates more rapidely than $I_{Kr.}$

- Phase 4: The resting membrane potential

When the repolarization is complete, the cell membranes return back to their resting membrane potential, which is maintained by the Kir2.1 potassium channel (I_{K1} current).

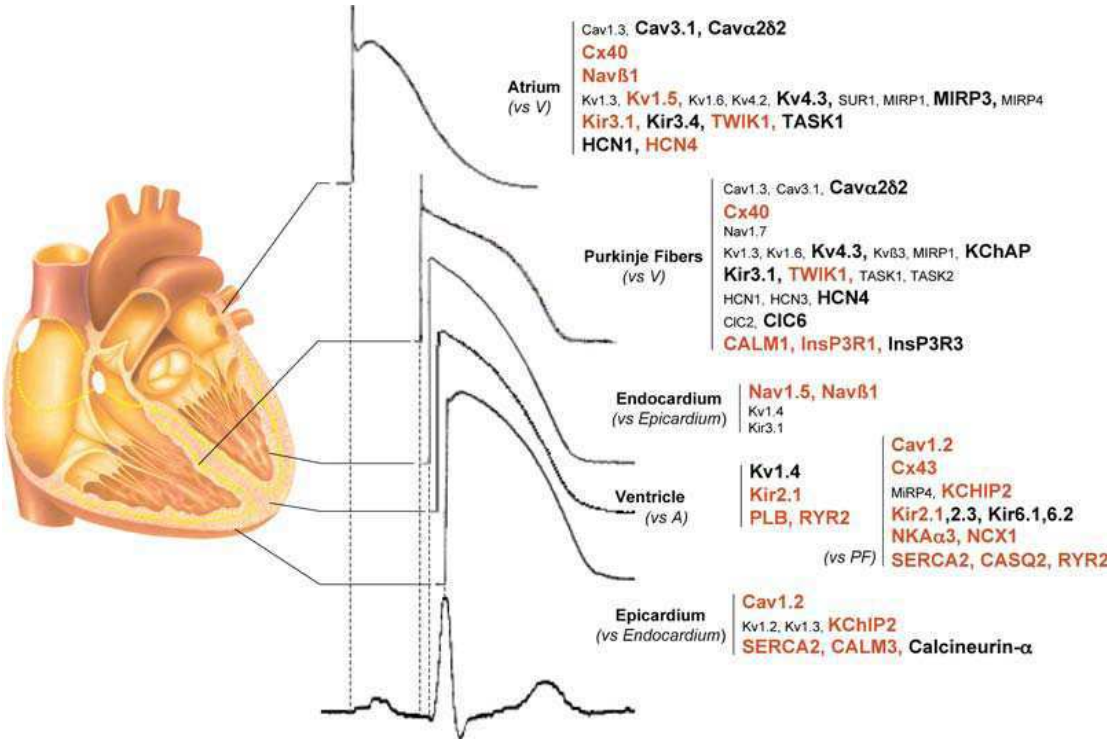

Figure 4: Ion-channel genes expression in various cardiac regions
The absolute expression levels of genes that are significantly more strongly expressed in a region of interest relative to the reference region indicated are provided by colour coding: genes expressed > 20-fold compared to the reference gene (*HPRT:* hypoxanthine guanine phosphoribosyl transferase) in the tissue/region of interest are indicated in bold and genes expressed at > 185 times the reference gene level are shown in bold red. Values shown are differences that were statistically significant for both right and left-sided comparisons for atrium *versus* ventricle and epicardium *versus* endocardium. Modified from Gaborit N. *et al*. J Physiol 2007[7]

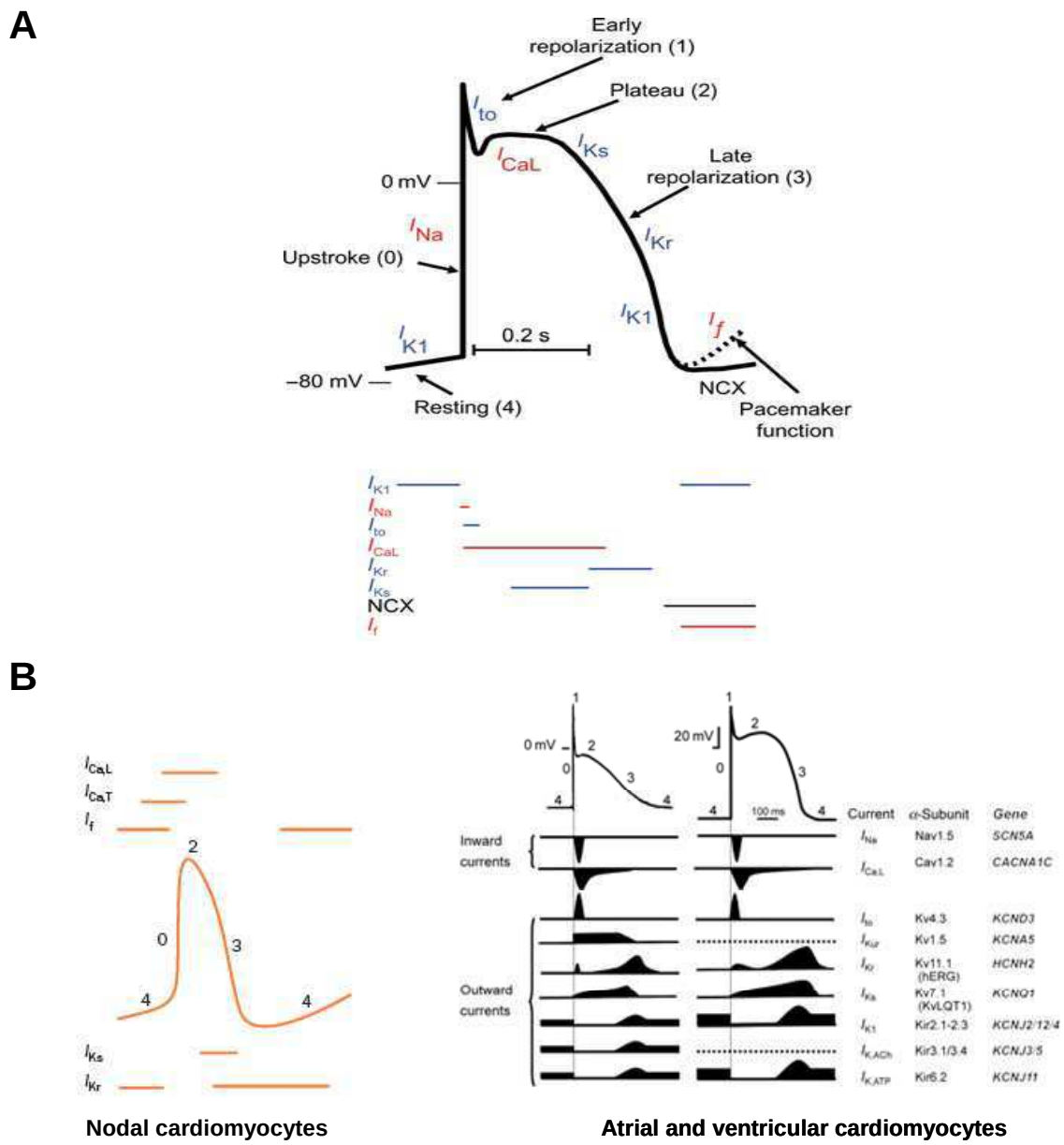

Figure 5: Cardiac action potential (AP)
(A) Phases and principal corresponding ion currents involved in cardiac AP. Inward (depolarizing) currents are in red, outward (repolarizing) currents are in blue. Modified from Michael G. *et al.* Cardiovasc Res 2009[13]. (B) Differences between nodal, atrial and ventricular cardiac APs. Modified from Giudicessi J. R. *et al.* Nat Rev Cardiol 2012[10] and Ravens U. *et al.* Europace 2008 [14]

I.3.4 Electrical communication between cardiac cells

The propagation of electrical activity in the heart needs special intercellular junctions, called gap junctions. These structures directly connect the cytoplasm of two adjacent cardiomyocytes and form low resistance pathways allowing the electrical impulse to pass rapidly between cells, ensuring synchronous contraction of the myocardium. Gap junctions

consist of connexins, which are four transmembrane domain proteins with N- and C-terminal cytoplasmic domains. They are arranged in groups of six to form hemichannels, or connexons, containing an aqueous pore in the center. Two connexons of two adjacent cells are aligned together to form a junctional channel (Figure 6). In working myocytes, gap junctions are present at the intercalated discs with desmosomes and fasciae adherens junctions. In nodal cells, only small and dispersed gap junctions are present. Various connexins have been identified in the heart[7,15]. Connexin 43 is highly expressed in the ventricles and atria, while connexin 40 is more expressed in the atria. Nodal cells contain connexin 45.

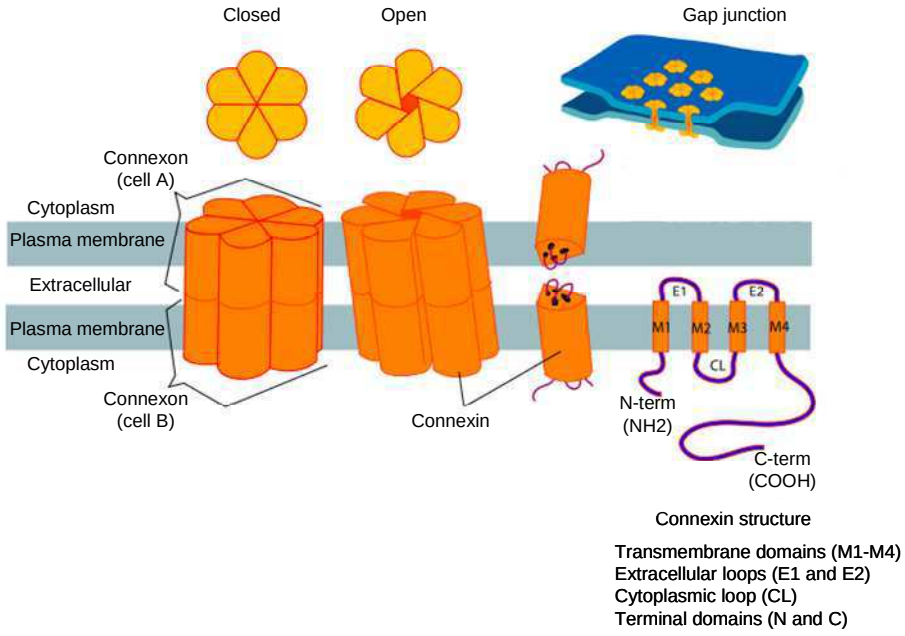

Figure 6: Gap junctions
http://en.wikipedia.org/wiki/Connexin

I.3.5 Excitation-contraction coupling

The contractile unit of the working myocytes is the sarcomere. It consists of thin (actin) and thick (myosin) filaments (Figure 2). At rest, actin and myosin do not interact with each other through the effect of two other proteins; tropomyosin and the Ca^{2+} binding protein troponin-C.

As membrane depolarization spreads along the sarcolemma of cardiomyocytes, it leads to the opening of the voltage-gated calcium channels, $Ca_v1.2$. Ca^{2+} entering the cell binds to the ryanodine receptor RyR2, which is a ligand-gated calcium channel located on the SR. Binding of Ca^{2+} to RyR2 allows calcium channels to open, resulting in a massive release

of Ca^{2+} from the SR into the cytoplasm. This process is known as "calcium-induced calcium release". Ca^{2+} released from the SR binds to troponin-C, which causes the conformational change of the tropomyosin and allows actin-myosin interaction. ATP hydrolysis releases energy that allows the myosin to pull the actin filaments leading to muscle contraction. Binding of ATP to the myosin head leads to its detachment from actin, while ATP hydrolysis leads to rebinding of the myosin head to actin. Then, relaxation takes place when the intracellular Ca^{2+} concentration returns to normal. Most of the intracellular Ca^{2+} is reuptaken by the SR through the SR Ca^{2+}-ATPase (SERCA pump) or it moves out of cells through the Na^{+}/Ca^{2+} exchanger or sarcolemmal Ca^{2+}-ATPase[16].

I.3.6 Electrocardiogram

The electrical activity of the heart can be recorded through electrodes placed on the patient's body. This recording is called an electrocardiogram (ECG). ECG is a non-invasive test that has a key role in the diagnosis of cardiac diseases, like ischemic heart disease and cardiac arrhythmias. ECG provides valuable informations, such as heart rate and regularity, conduction, and chamber sizes and position. These data are obtained through the standard interpretation of the different waves and intervals of the ECG (Figure 7)[17]. These waves represent the sequence of depolarization and repolarization of both the atria and ventricles:

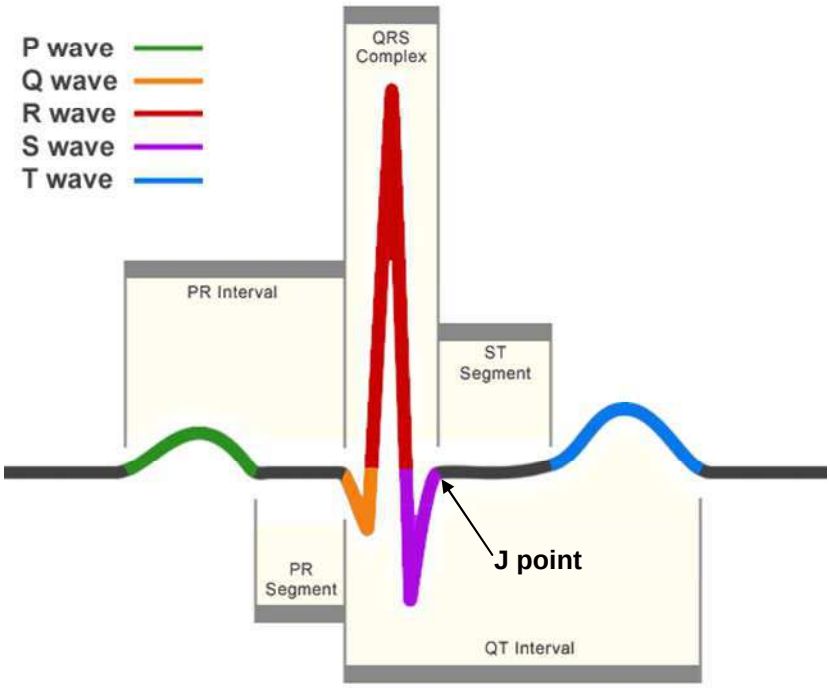

Figure 7: ECG of normal sinus rhythm
Modified from http://catatanmahasiswafk.blogspot.fr/2012/03/skill-lab-pemeriksaan-ekg.html

- P wave: rounded, positive wave that represents atrial depolarization. Usually it is between 80 to 100 ms in duration. We can calculate atrial rate by measuring the time interval between P waves.
- QRS complex: represents ventricular depolarization, it is normally between 60 and 100 ms. Ventricular rate can be calculated by measuring the interval between QRS complexes.
- T wave: represents ventricular repolarization.
- PR interval: is the interval between the beginning of the P wave and the beginning of QRS complex. Normally it is between 120 and 200 ms. It represents the time the electrical signal needs to propagate from the SAN to the AVN. A PR interval longer than 200 ms means there is an AV block.
- ST segment: represents the time during which the whole ventricles are depolarized and is normally isoelectric. An abnormality of ionic currents during this period is most often translated to a ST segment elevation or depression relative to the isoelectric line. To evaluate these shifts, we use the J point, which is the point at which the QRS complex meets the ST segment.

Physiologically, it is located in the extension of the PQ segment, which is used as the baseline in order to look for a shift of J point.

- QT interval: represents the time needed for ventricular depolarization and repolarization, it is approximately equal to the duration of the action potential of ventricular myocytes. The duration of the QT interval varies according to heart rate; it decreases when heart rate increases and vice versa. For this reason, it is better to use the corrected QT interval, which can be calculated according to Bazett's formula, $QTc = QT/\sqrt{RR}$. The normal values are 350 to 450 ms for males, and 360 to 460 ms for females[18]. Short and long QT intervals can be indicative of inherited cardiac arrhythmias called short and long QT syndromes (SQTS and LQTS), respectively.

To record an ECG, an electrode is attached to each of the limbs, and six other electrodes are placed on the chest. With these ten electrodes, twelve leads can be recorded (Figure 8). Each lead represents a view of the electrical activity of the heart from a particular angle across the body. Six limb leads (I, II, III, aVR, aVL, and aVF) view the heart in a vertical plane, and six precordial leads (V1-V6) view the heart in the horizontal plane.

Regarding the anatomical relationships, leads II, III, and aVF view the inferior surface of the heart, leads V1 to V4 view the anterior surface, leads I, aVL, V5, and V6 view the lateral surface.

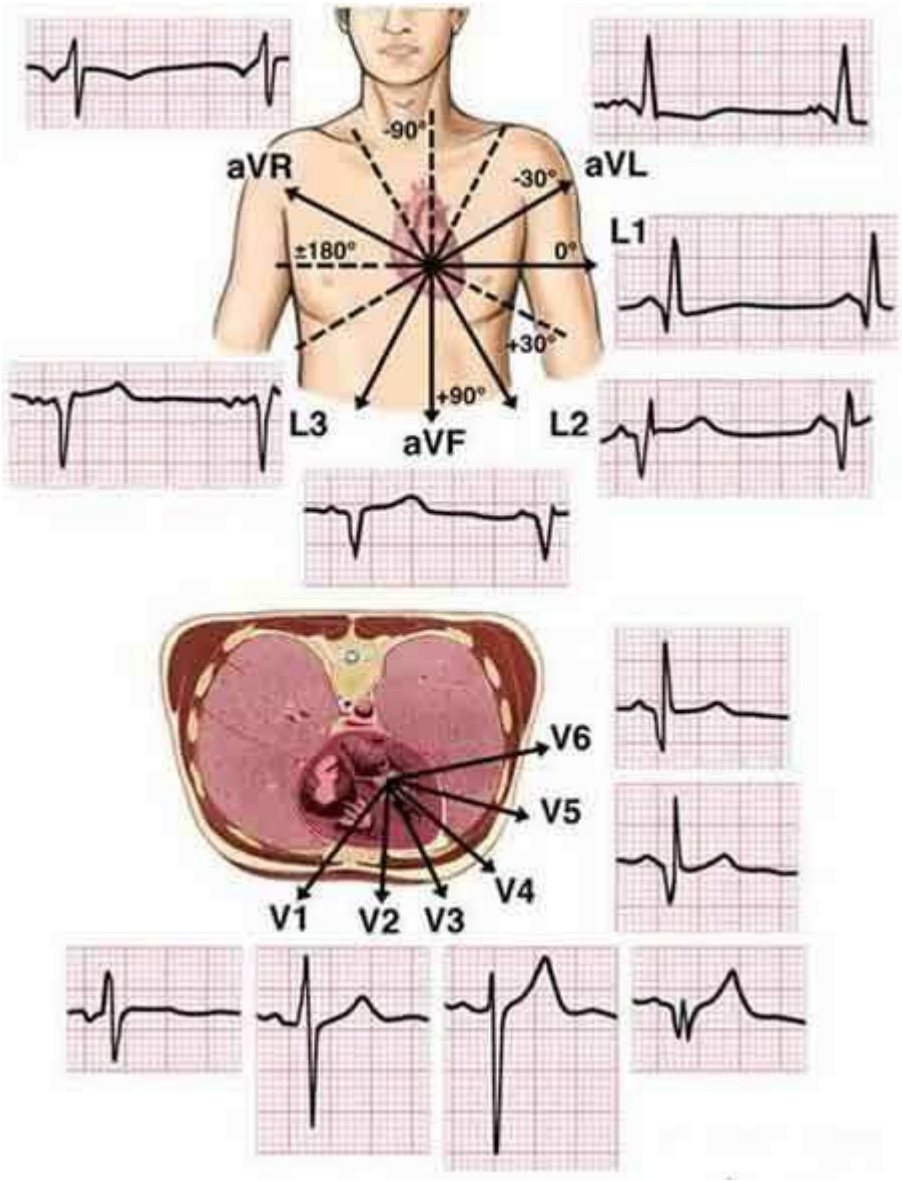

Figure 8: The twelve standard ECG leads
http://www.amperordirect.com/pc/help-ecg-monitor/z-what-is-ecg.html

II. Cardiac arrhythmias

II.1 Mechanisms of cardiac arrhythmias

Any abnormality in the heart rate or in the regularity of heart rhythm is called cardiac arrhythmia. Cardiac arrhythmias can occur in a structurally normal heart as well as in heart diseases. They have a highly variable clinical presentation, but they share common electrophysiological pathways. Three well-known cellular mechanisms are responsible for most of cardiac arrhythmias: automaticity, triggered activity and reentry[19].

II.1.1 Automaticity

Automaticity mechanisms of cardiac arrhythmia can be either due to altered normal automaticity or abnormal automaticity.

In altered normal automaticity, the electrical signal starts in one conductive cell region like the SA or AV nodes with abnormal suppression or enhancement. We can understand the different mechanisms underlying the altered normal automaticity by looking at the AP of nodal cells (Figure 5B). Any factor that changes the maximum diastolic potential, the threshold potential for AP initiation and the rate or slope of phase 4 depolarization, can be responsible for altered impulse initiation. For example, the parasympathetic nervous system decreases heart rate by hyperpolarizing the cells through increasing conductance of K^+ through the G-protein-gated K^+ channel I_{KACh} and decreasing I_f activity[19,20]. In contrast, the sympathetic nervous system increases heart rate by increasing I_f current, enhancing the spontaneous depolarization of phase 4[19].

In abnormal automaticity, atrial and ventricular cardiomyocytes, which normally do not have spontaneous activity, demonstrate automaticity properties. This occurs when the maximum diastolic potential is shifted toward the threshold potential. Many ion currents are involved in this process, resulting in a net inward depolarizing current with decreased K^+ conductance. Premature beats, as well as atrial and ventricular tachycardia are examples of abnormal automaticity related arrhythmias. Increased extracellular K^+ levels and low intracellular pH can cause cardiac arrhythmia through this mechanism[21].

II.1.2 Triggered activity

Triggered activity is defined as impulse initiation caused by an after-depolarization, which is a membrane potential oscillation occuring during or immediately after an AP[22].

Based on the time elapsed from the preceding AP, two types of after-depolarization are present: early after-depolarization (EAD) and delayed after-depolarization (DAD).

EADs occur during phase 2 or 3 of the AP (Figure 9A and B). AP prolongation, favored by lower outward potassium currents or an increase in calcium or sodium inward currents, as well as low heart rate, can all enhance the development of EAD. EAD is the underlying mechanism of arrhythmias seen in patients with LQTS, such as torsade de pointes due to polymorphic ventricular tachycardia (VT)[23].

DADs (Figure 9C) occur during phase 4, due to an increased intracellular Ca^{+} concentration, which mediates the oscillations of membrane potential leading to new AP initiation if they reached the stimulation threshold. Enhanced heart rate is a predisposing factor for DAD development. Digitalis toxicity-induced tachycardia[24] and catecholaminergic polymorphic VT[25] are examples of DAD induced arrhythmias.

II.1.3 Re-entry

The electrical signals in the heart normally propagate in a single direction, from the SAN down to the ventricles. Normally, depolarized cells enter a refractory period, during which they are unable to be re-excited, since most ion channels are inactivated. In re-entry excitation (Figure 10), an area that was not activated during the initial wave of depolarization due to unidirectional block (gray area), can be depolarized by the retrograde signal (blue line). Action potentials exiting the block, could re-excite areas that have already recovered from the refractory period and AP can continue. However, if the AP finds non-excitable tissue, it will end. So, several elements are needed to lead to a re-entry: (1) substrate; myocardial areas that differ in conductivity and refractoriness, (2) unidirectional block to allow conduction propagation in one direction and conduction block in the other (3) slow conduction time to allow recovery from the refractory state of tissue present proximal to the block and (4) an initiating trigger.

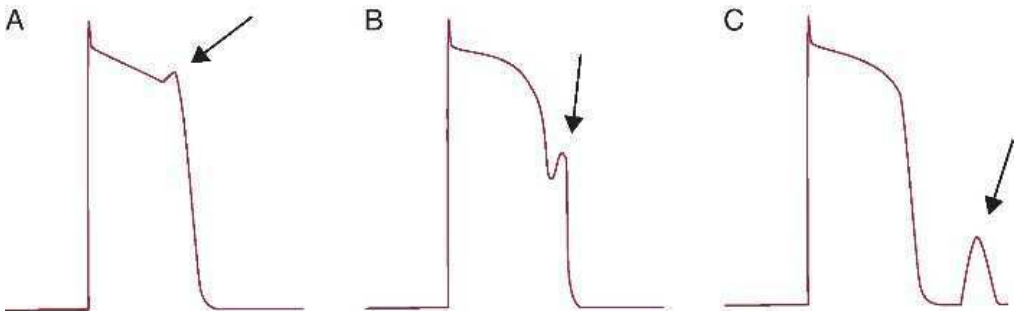

Figure 9: Representation of triggered activity
(A) Phase 2 early after-depolarization. (B) Phase 3 early after-depolarization. (C) Delayed after-depolarization. Gaztanaga L. *et al.* Rev Esp Cardiol (Engl Ed) 2012[19]

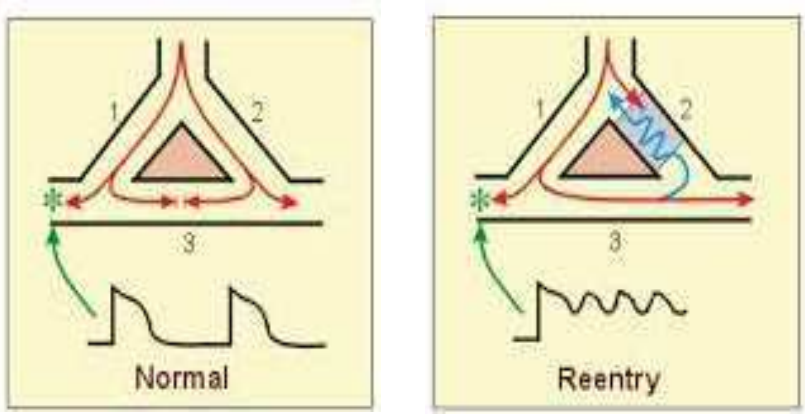

Figure 10: Representation of a re-entry excitation
http://www.cvphysiology.com/Arrhythmias/A008c.htm

II.2 Atrial arrhythmias

Abnormalities in heart rate or rhythm arising from the atrium are called atrial arrhythmias. There are several different types of atrial arrhythmias, which are discussed below.

II.2.1 Supraventricular tachycardia (SVT)

Supraventricular tachycardia is a rapid heart rhythm originating at or above the atrio-ventricular node. There are different types of SVT; here we will discuss those that are the most common.

- **Atrial fibrillation (AF)**

Discussed in chapter II.2.3.

- **Atrial flutter (AFL)**

Atrial flutter is the second most common pathological SVT. It is a macro-reentrant arrhythmia characterized by a regular atrial rhythm of 250-350 bpm, with AVN conduction block, usually 2:1, resulting in a ventricular rate of 140-150 bpm. In the presence of variable AV conduction, the heart rate is irregular. Patients with paroxysmal AFL and rapid ventricular response present with palpitation, dyspnea, chest discomfort, pre-syncope and weakness. There are different types of AFL according to the mechanisms causing the arrhythmia[26]. The most common mechanism is counterclockwise (CCW) right AFL, characterized by circular activation around the tricuspid annulus. The activation wave propagates up over the septal right atrium, and then moves down over the anterolateral right atrium, passing through the tricuspid annulus and the inferior vena cava to again reach the septal right atrium[27] (Figure 11). On the ECG, there are flutter waves with a 'saw-tooth pattern that are negative in inferior leads (II, III, aVF) and positive in V1 (Figure 12). Atrial flutter is more common in men. Advanced age and other medical conditions, like heart failure, chronic pulmonary disease, previous stroke, and myocardial infarction can increase the risk of AFL. The main targets for the treatment of AFL are rate and rhythm control, prevention of stroke, ablation and treatment of the underlying disease[26].

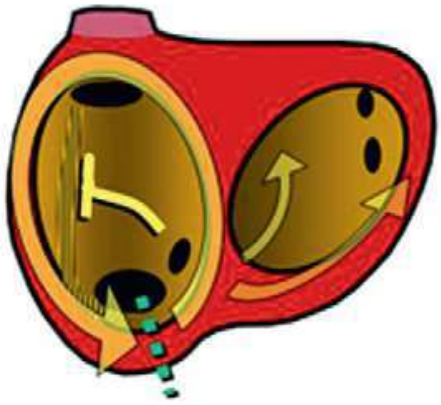

Figure 11: Typical atrial flutter
This left anterior oblique view of the right atrium shows the orifices of the cavae and the coronary sinus and the crista terminalis (vertical strip). The arrows indicate the direction of activation. The green dotted lines mark the critical isthmus of each circuit, the target of ablation. Modified from Garcia-Cosio F. *et al.* Rev Esp Cardiol 2012[27]

Figure 12: ECG signs of atrial flutter
Modified from http://www.dochemp.com/afib.html

- **Atrial tachycardia**

Atrial tachycardia is a focal tachycardia resulting from micro re-entrant circuits or an automatic focus. It is characterized by its occurence in short repetitive bursts as well as warm-up phenomena in which the atrial rate increases slightly over the first 5 to 10 seconds before stabilizing. On ECG, there is a P-wave preceding each QRS complex (Figure13). However, if the rate is very rapid, P-waves may be hidden by QRS complexes.

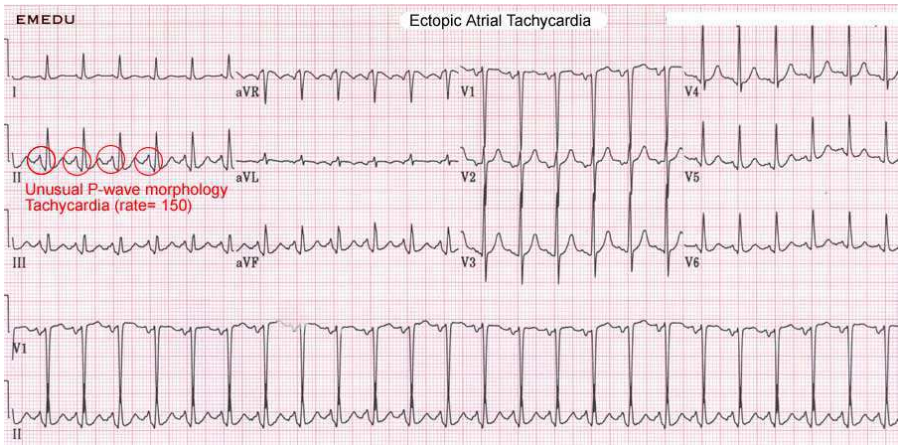

Figure 13: Ectopic atrial tachycardia
http://www.emedu.org/ecg/searchdr.php?diag=SVT

- **Atrio-ventricular nodal re-entrant tachycardia (AVNRT)**

AVNRT is due to a re-entrant loop that involves the AVN and the atrium. It usually affects adult people. In this arrhythmia, AVN has two conduction pathways; both slow and rapid, and the electrical signal leaving the AV node can propagate into anterograde or retrograde directions. In sinus rhythm, the electrical impulse propagates down the fast pathway, enters the distal end of the slow pathway and both impulses cancel each other. However, if premature atrial contraction reaches the AV node during the refractory period of the fast pathway, the impulse will propagate down the slow pathway and when it reaches the end of the slow pathway, the fast pathway will have recovered from the refractory state and impulse may then move retro-gradely through the fast pathway, creating a circuitous movement. In typical AVNRT (slow-fast) the retrograde conduction occurs *via* the fast pathway and the anterograde *via* the slow pathway. Consequently atrial activation appears before, at, or just after the onset of the QRS complex (Figure 14).

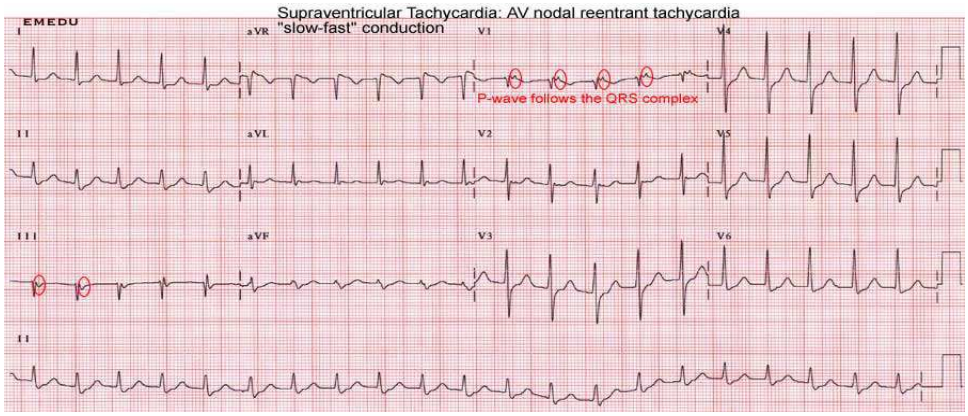

Figure 14: AVNRT
P waves appears at the end of the QRS complex
http://www.emedu.org/ecg/tachycardia.htm

- **Atrio-ventricular reciprocating tachycardia (AVRT)**

Atrio-ventricular reciprocating tachycardia occurs more frequently in pediatric patients due to an accessory pathway reponsible for a direct atrio-ventricular connection. Through this tract, the signal may propagate in anterograde only, retrograde only or in both directions. Patients with tachycardia, and a delta wave on the ECG (initial slurring of the QRS complex), are diagnosed to have Wolff-Parkinson-White syndrome (WPW) (Figure 15).

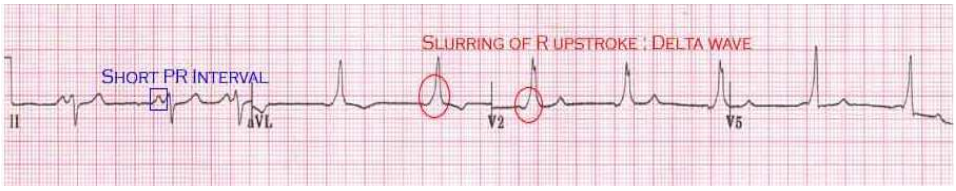

Figure 15: WPW Syndrome
Short PR interval of less than 120 ms, normal P-wave, wide QRS complex, delta wave representing ventricular pre-excitation.
Modified from http://paramedicine101.blogspot.fr/2009/05/wolff-parkinson-white-syndrome.html

II.2.2 Premature atrial contraction (PAC or premature atrial impulses)

PAC occurs when a region of the atria other than the SAN depolarizes before the SAN, leading to premature beats. It is a common and benign arrhythmia seen in stressful conditions, and may occur after caffeine or alcohol intake. On ECG, as the signal in PAC does not start in the SAN, the P-wave has an abnormal shape with longer RR interval after the PAC. QRS is normal as the signal propagates to the ventricles through the AVN (Figure 16). Sometimes the atrial beat is so premature that it reaches the AVN during its refractory time, and as a consequence, the signal does not propagate to the ventricles, leading to the absence of QRS complex after the P-wave.

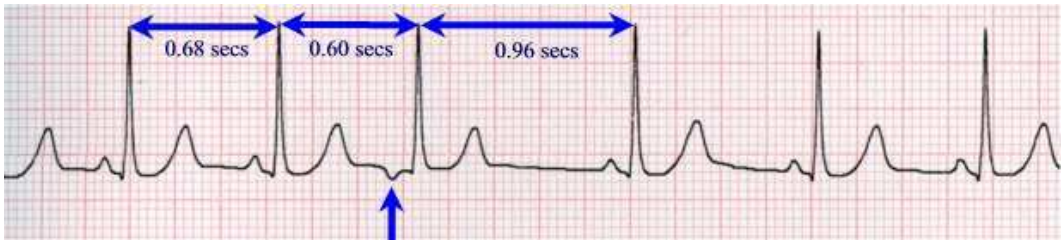

Figure 16: Premature atrial contraction
Abnormal P-wave (arrow), followed by a longer RR interval, QRS complexes are normal.
http://www.crkirk.com/thumbnail/arrhythmias/ectopics.htm

II.2.3 Atrial fibrillation (AF)

Atrial fibrillation (AF) is the most common cardiac arrhythmia, affecting approximately 1-2% of the population[28]. Its prevalence increases with age from 0.5% in those aged 50-59 years to 9.0% in those aged 80-90 years[29]. AF is a tachy-arrhythmia characterized by uncoordinated activity of the atrial muscle leading to irregular heartbeat. This

uncoordinated activity results in reduced ventricular filling and blood stasis in the atria, which can lead to heart failure and thrombembolic stroke. On the ECG, it is characterised by the absence of P wave, fibrillation (f) waves resulting in an oscillating irregular baseline, variable RR intervals, and normal QRS complexes with ventricular rate between 60 to 220 bpm, depending mostly on patient's age and the AVN state (if there is an underlying AV disease or if the patient has received medications that affect AVN conduction) (Figure 17).

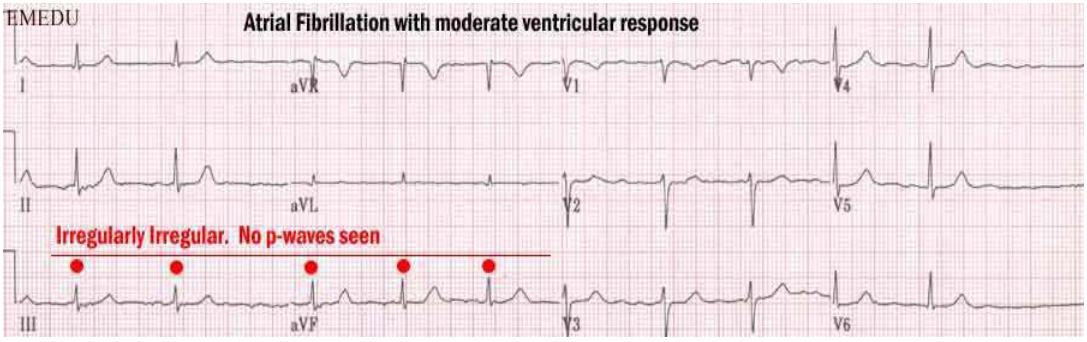

Figure 17: ECG signs of AF
http://www.emedu.org/ecg/oni.php

II.2.3.1 Different types of AF

Based on etiology, AF can be divided into secondary and lone AF. Secondary AF, the most common form, is caused by coexisting medical conditions, cardiac or non-cardiac, such as ischemic heart disease, hypertension, electrolyte depletion, pneumonia, lung cancer and thyrotoxicosis. AF is also common after cardiothoracic operation. In addition, alcohol and caffeine consumption, as well as both physical and emotional stresses can increase AF risk.

Lone AF occurs in younger patients with structurally normal hearts and in the absence of other secondary medical conditions, accounting for 10-30% of AF[30]. It is always a diagnosis of exclusion.

Genetic risk factors, especially mutations in genes encoding ion channels, can also be involved.

The European Society of Cardiology (ESC) issued an AF classification according to episode timing and termination, thus AF can be divided into five types[31]:

- **First diagnosed AF**: A patient presents for the first time with AF regardless of its duration or presence and severity of symptoms.
- **Paroxysmal AF**: AF episode that lasts less than seven days and

terminates spontaneously, usually within 48 hours.

- **Persistent AF**: AF lasts more than seven days or does not terminate spontaneously requiring electrical or pharmalogical cardioversion.
- **Long-standing persistent AF**: AF that has lasted one or more years before rhythm control is decided.
- **Permanent AF**: The presence of AF is accepted by the patient and the physician, and as such, no further rhythm control interventions are carried out.

II.2.3.2 Symptoms of AF

Atrial fibrillation has a wide variety of clinical presentations, ranging from asymptomatic to patients presenting with symptoms of AF complications such as brain stroke, heart failure, or cardiovascular collapse. However, the most common symptoms are palpitations, dyspnea, fatigue, lightheadedness, and chest pain. Since these symptoms are not specific, diagnosis of AF cannot only be made on the clinical presentation.

ECG is the gold standard test for the diagnosis of AF (Figure 17). However, a Holter monitor (a portable device for continuously recording ECG for at least 24 hours) may be needed, if the ECG does not demonstrate AF despite a strong suspicion.

II.2.3.3 Management of AF

The first step in the management of AF is the clinical evaluation of the patient's cardiac stability. If the patient is hemodynamically unstable, emergency electrical cardioversion is needed. However, if the patient has a stable clinical condition, then history, physical examination and diagnostic tests should be done in order to determine the potential causes, triggers, and co-morbid conditions.

AF treatment aims to improve symptoms and prevent future complications. Prevention of AF complications through anti-thrombotic therapy, ventricular rate control and treatment of underlying disease may improve the symptoms. However, in some cases rhythm control is also needed. The main approaches for the treatment of AF consist of anticoagulation, rate and rhythm control, treatment of any underlying diseases, and ablation[31,32] (Figure 18).

- **Antithrombotic therapy**

Treatment with antithrombotic drugs depends mainly on the presence or absence of risk factors for developing stroke and thrombo-embolism. There are many score systems that

can be used to assess stroke risk[31]. According to this score system, the choice of anticoagulant will be decided[32].

- **Rate control**

This aims to reduce the heart rate to normal levels without conversion to normal sinus rhythm. Patients with rapid ventricular response are treated with rate control medication in order to have a target ventricular rate between 80-100 bpm at rest in the acute setting. In stable patients, this can be achieved through oral medications like beta-blockers or non-dihydropyridine calcium channel antagonists. If the patient is unstable, intravenous (IV) verapamil, metoprolol, or amiodarone, in the case of severely depressed left ventricular function can be used. In case of slow ventricular response, intravenous atropine can be used, but most patients need urgent cardioversion or temporary pacemaker implantation in the right ventricle. This acute rate control strategy must be followed by a long–term control strategy.

- **Rhythm control**
  - Cardioversion

Cardioversion aims to convert the abnormal heart rhythm to a normal sinus rhythm. It is usually used in a patient who is severely compromised, or with symptoms that did not improve with rate control management. It can be performed by pharmacological or electrical approaches.

Pharmacological cardioversion is initiated by IV bolus administration of anti-arrhythmic drugs. In contrast to electrical cardioversion, pharmacological cardioversion does not require sedation or anaesthesia. However, its success rate is inferior to that of electrical cardioversion.

Direct current cardioversion (DCC) is a medical procedure used to convert cardiac arrhythmia into a normal sinus rhythm using electricity. It relies on the delivery of a high-energy shock through the chest wall to the heart muscle through two electrode pads that are applied to the skin with a general ansethesia. Before doing electrical cardioversion in AF, transesophageal echocardiogram is mandatory in patients having AF> 48h with no adequate anticoagulation over the preceding three weeks, in order to rule out atrial thrombus, since electrical cardioversion enhances showering embolism. The success of the electrical shock treatment can be determined by ECG showing the presence of two or more consecutive P-waves after the shock.

- Maintenance of sinus rhythm

After cardioversion, maintenance of sinus rhythm can be achieved with anti-arrhythmic drugs, like flecainide and others, according to the cardiac status. It is recommended to start with the safer drug, even though it may be less efficacious, before using a more effective one with more side effects. Moreover, the type of medication used depends on the patient's medical background.

➢ Catheter ablation

Catheter ablation is an invasive procedure used to ablate (destroy) the abnormal cardiac tissue causing the arrhythmia. In AF, it is mainly used to ablate the firing spots responsible for triggering activity, or to create lines of electrical block in the atria that interrupt the abnormal electrical circuits, allowing the pacemaker to regain its control of heart beats.

As ablation is an invasive procedure, it is usually reserved for patients who have remained symptomatic despite the use of optimal rate and rhythm control therapy. Before deciding to perform catheter ablation, benefit-risk ratios of ablation must be evaluated. For example, it is usually used in patients with symptomatic paroxysmal AF that is resistant to at least one anti-arrhythmic drug. However, in persistent or long standing persistent AF, or in patients with heart disease, medical therapy is recommended before ablation since the benefit-risk ratio in these cases is not well established.

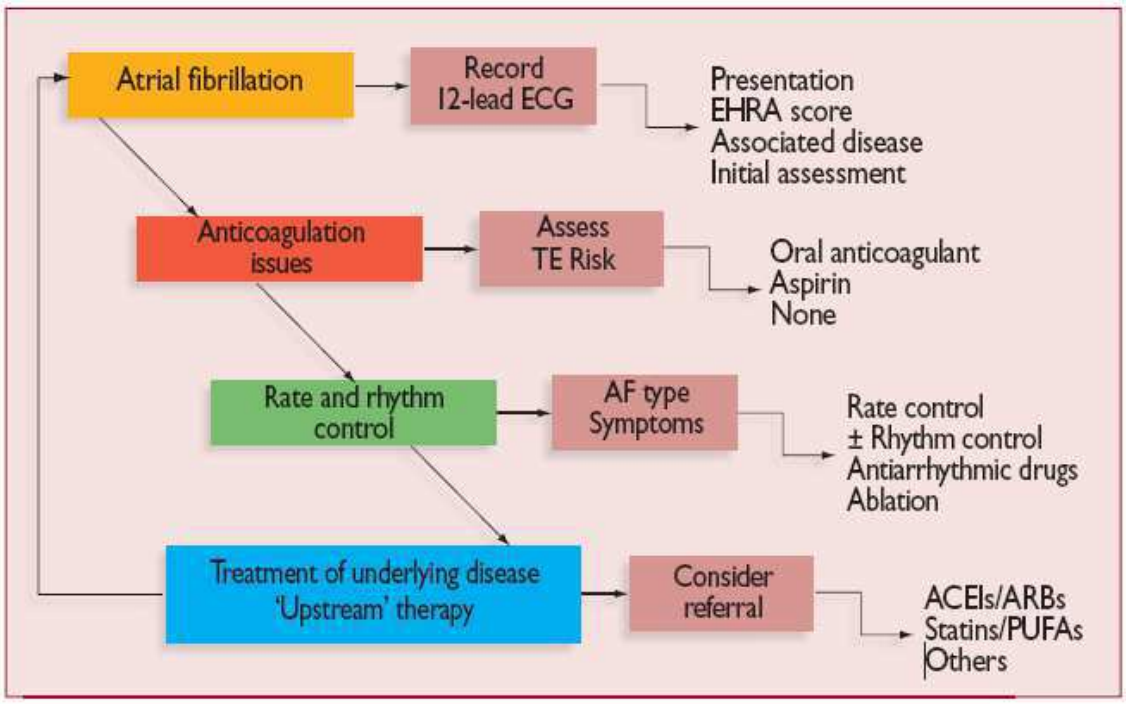

Figure 18: Management cascade for patients with AF

EHRA = European Heart Rhythm Association; ACEI = angiotensin-converting enzyme inhibitor; AF = atrial fibrillation; ARB = angiotensin receptor blocker; PUFA = polyunsaturated fatty acid; TE = thrombo-embolism. Modified from Camm A. J. *et al*. Eur Heart J 2010[31]

II.2.3.4 Mechanisms of AF

AF results from abnormalities in the signaling pathway; where the electrical signal is generated from both the sinus node and multiple random regions in the atrium (Figure 19).

Three classical hypotheses underlie the development of AF: focal activity, single-circuit re-entry and multiple-circuit re-entry[33].

Focal activity results from spontaneous rapid firing of a single or multiple ectopic atrial foci, usually in the left atrium, due to an increase in depolarization, or the presence of after-depolarization. Pulmonary veins account for trigger activity in 85-95% of patients with paroxysmal AF, and other sites, other than the pulmonary veins, appear to be responsible for the rest[34].

Re-entrant arrhythmia circuits arise from differential impulse propagations within atrial tissue, and necessitate the existence of a focal region of conduction block. This block can be either fixed or dynamic. Fixed block can be structural or electrophysiological, like myocardial fibrosis and heterogeneity of ion channels. Dynamic or "functional" factors include membrane-voltage and intracellular Ca^{2+} cycling properties that determine AP duration and conduction velocity.

In addition, according to Coumel's triangle of arrhythmogenesis[35], the mechanism of AF can be explained in terms of substrate, triggers, and modulating factors[36].

Electrical and structural remodeling of the heart is the most prevalent substrate. Electrical remodeling include mechanisms involved in intracellular Ca^{2+} handling, leading to shortened refractory period and enhancement of re-entry. Restoration of sinus rhythm can reverse the electrical remodeling. In structural remodeling, there is a loss of cardiomyocytes, diffuse and patchy fibrosis, and scarring. These structural changes slow the conduction velocity and enhance electrical uncoupling, allowing the genesis of AF. Structural remodeling is irreversible even with the restoration of normal sinus rhythm.

Regarding the triggers, the exact mechanism that underlies the initiation of these firings is unclear. However, enhanced automaticity, after-depolarization and re-entry could be the possible underlying mechanisms. A trigger can then interact with the substrate to generate AF; and modulating factors, such as atrial and pulmonary vein stretch, or hormonal and autonomic nervous factors, may facilitate the initiation or the further development of AF.

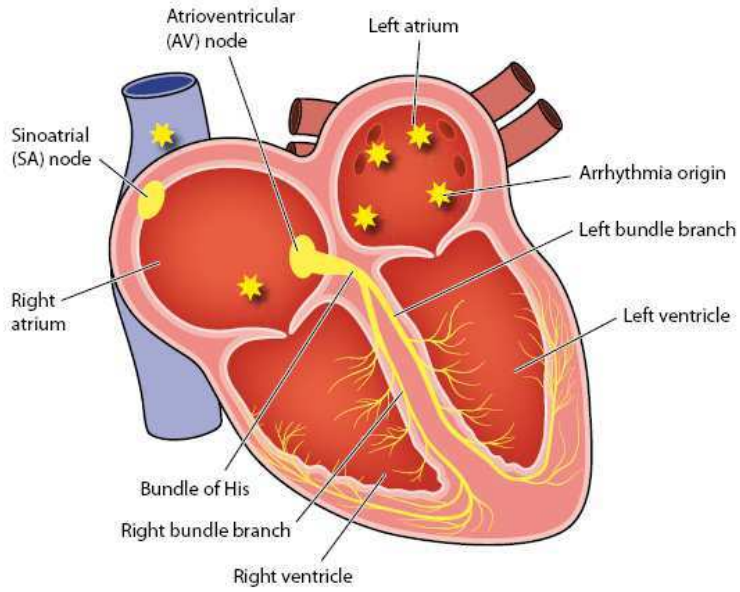

Figure 19: Generation sites of multiple electrical impulses in AF
http://www.educationforhealth.org/data/files/resources/atrial-fibrilliation-part-1-pathophysiology-c-cottrell.pdf

II.2.3.5 Genetics of AF

The majority of AF is sporadic and non-familial, as most cases of AF occur with structural heart disease. Nevertheless, familial forms of AF have been identified. In 1943, the first familial form of AF was reported in three brothers diagnosed with autosomal dominant AF[37]. After that, several studies have confirmed the heritability of AF[38–44]. Familial AF is particularly present in patients with lone AF, where approximately 30% of probands have first degree relatives with AF[38,40,42]. It has been shown that 5% of patients with AF, and 15% of patients with lone AF had a positive family history (one to nine additional relatives affected)[38]. In addition, in the same study four multi-generation families were identified in which AF was transmitted in an autosomal dominant manner[38]. Furthermore, other studies have showed that 38%[40], or 41%[42] of lone AF patients had a first or second degree family member with AF. Moreover, in a prospective cohort study within the Framingham Heart Study, it has been shown that having one parent with AF doubled the risk of predicted AF in the offspring compared to no parental AF. In addition, the risk increased when the parents developed AF before the age of 75 years[39]. In agreement with this study, it has recently been shown that the risk of developing lone AF at a young age, increases with greater numbers of affected relatives and decreasing age at onset of AF in these relatives[45]. All this evidence supports the theory that genetic factors may have a role in AF development.

Rare genetic variants have been identified through either linkage analysis or candidate gene approaches in AF families. Even though these mutations have been identified in two or more family members with lone AF, the penetrance of AF in theses families is highly variable. In addition, in the more common secondary AF, not all patients with secondary risk factors, like hypertension or heart failure, develop AF, suggesting the presence of other modifiers such as single nucleotide polymorphisms (SNPs), which could alter AF susceptibility. Genome-wide association studies (GWAS) have identified a number of SNPs that can increase AF susceptibility.

- **AF loci identified by linkage analysis (Table 1)**

Brugada *et al*. in 1997 discovered the first AF loci on chromosome 10 (10q22-q24) in three different families with autosomal dominant AF[46]. After that, several loci have been identified in familial AF (Table 1). Screening for candidate genes in these loci led to the identification of the first gene *(KCNQ1)* implicated in AF[47], which encodes the α-subuint of the delayed-rectifier cardiac potassium channel (I_{Ks}). This identification led researchers to think that other genes encoding ion channels or subunits and factors that regulate ion channels, could be involved in AF development. Consequently, other genes have been identified by linkage studies and candidate-gene approaches. However, for more than half of the loci, the genes implicated in AF development have not yet been identified (Table 1). In most of these studies, AF has an autosomal dominant inheritance pattern[46–48,52–54], except in one study where AF was inherited in an autosomal recessive manner, occurring during the fetal stage, and associated with neonatal sudden death[49].

OMIM	Locus	Gene	Functional effect
ATFB1	10q22-q24[46]	Unknown	Unknown
		SYNPO2L ?	
ATFB3	11p15.5[47]	*KCNQ1*	Effects on atrial action potential repolarization
ATFB2	6q14-16[48]	Unknown	Unknown
	5p13[49,55]	*NUP155*	Nucleoporin involved in the nuclear pore complex
	10p11-q21[52]	Unknown	Unknown
	5p15[53]	Unknown	Unknown
ATFB6	1p36-p35[54]	*NPPA*	Shortening of the atrial action potential duration

Table 1: Summary of AF-susceptibility loci identified by linkage analysis

- **Monogenic mutations in AF**

Several studies have identified rare variants associated with AF in genes encoding ion channels and accessory subunits, cardiac gap junctions, and signalling molecules. Up to date, AF has been associated with mutations in 25 different genes[56]. Most of these genes encode ion channel subunits involved in cardiac depolarization or repolarization. Functional studies of these mutations showed both gain- and loss-of-function effects, increasing the complexity of AF. Moreover, these rare mutations occur in less than 1% of AF patients[36], suggesting that other rare or common variants, in addition to the environmental factors, could contribute to AF genesis.

- **Ion channel mutations (Table 2)**

- **Mutations in potassium channel genes**

The voltage-gated potassium currents (I_{Ks}, I_{Kr}, I_{Kur}) are involved in the repolarization phase of the atrial AP. Other potassium channels (I_{K1}) are of importance for the control of resting potential. Gain-of-function as well as loss-of-function mutations within potassium channel genes have been identified in AF.

- ***KCNQ1***

The *KCNQ1* gene encodes the pore-forming α subunit, K_vLQT1, of the cardiac I_{Ks}

channel complexes (KCNQ1/KCNE1, KCNQ1/KCNE2 and KCNQ1/KCNE3). They play an important role in repolarization of the cardiac AP. Some gain-of-function mutations have been identified in *KCNQ1* leading to an increase of the I_{Ks} potassium current and a decrease in the atrial AP duration and refractory period. The *KCNQ1* gene represents the first gene historically involved in familial AF. The first mutation, S140G, was identified following linkage of an autosomal dominant persistent AF to the 11p15.5 locus in a Chinese multigenerational family. Functional study of this mutation showed a gain-of-function effect on I_{Ks} potassium current[47]. Since this initial discovery, five other gain-of-function *KCNQ1* mutations have been identified in sporadic or familial cases of AF[57–61].

Loss-of-function of the I_{Ks} potassium current leads to the prolongation of cardiac repolarization and LQTS. Numerous loss-of-function mutations in *KCNQ1* have been identified in LQTS[62,63]. The study of a cohort of LQTS patients showed that 2% of them (especially *KCNQ1*-related LQT1) have early-onset AF (aged less than 50 years) compared to a background prevalence of 0.1%[64]. In addition, it has been shown that some LQT1 mutations can lead to variable mixed clinical pictures of AF and LQTS[65–67].

In addition to *KCNQ1*, mutations in genes encoding the auxiliary subunits (*KCNE1*, *KCNE2*, *KCNE5*) and the atrial natriuretic peptide (*NPPA*), that regulate the I_{Ks} potassium current, have also been identified in patients with AF[54,60,68–70]. Functional studies of these mutations showed gain-of-function effects on the I_{Ks} potassium current.

- ***KCNH2***

The *KCNH2* gene encodes the Kv11.1 α-subunit underlying I_{Kr}, involved in the repolarization phase of cardiac AP. The *KCNH2* gain-of-function mutation N588K has been identified in families with SQTS and AF. Increased I_{Kr} leads to shortening of AP duration and refractoriness, and enhancement of re-entrant arrhythmia[71,72]. In addition, a mutation in the *KCNE3* gene encoding the MiRP2 accessory subunit has been identified in patients with lone AF, and a functional study showed a gain-of-function effect of this mutation on I_{Kr}[73].

- ***KCNA5***

The *KCNA5* gene encodes the $K_v1.5$ subunit responsible for the atrial specific repolarizing current I_{Kur}. Both gain-[74,75] and loss-of-function mutations[75–78] in *KCNA5* have been identified in patients with AF, which further supports the hypothesis that shortening as well as prolongation of the AP duration can increase susceptibility to AF.

- ***KCND3***

The *KCND3* gene encodes the pore-forming K^+ channel subunit $K_V4.3$ that interacts with the K^+ channel-interacting protein (KChIP2) underlying the transient outward K^+ current (I_{to}). Some gain-of-function mutations in the *KCND3* gene have been involved in Brugada syndrome[79,80]. Recently, a new gain-of-function mutation in *KCND3* (A545P) was identified in a proband with early onset persistent AF at the age of 22. The proband did not have Brugada syndrome even after flecainide challenge. Computer simulation showed that the mutant is associated with a reduction of the AP duration[81].

- ***KCNJ2***

The *KCNJ2* gene encodes the Kir2.1 channel protein that underlies the inward rectifier potassium currents $I_{K1.}$ The I_{K1} is mainly involved at the end of the repolarization phase and in the resting membrane potential. In atrial cells, Kir2.1 has lower expression and smaller current density and conductance with shorter opening times compared to the ventricles. These differences lead to a more depolarized resting membrane potential and highly excitable atrial cells[8,9]. As of today, three gain-of-function mutations in *KCNJ2* have been identified in patients with AF[50,82–84]. The increase in I_{KI} accelerates the repolarization phase and the return to resting membrane potential, leading to shortening of AP duration and creation of a favourable substrate for re-entry, a mechanism involved in AF.

- ***KCNJ8***

The *KCNJ8* gene encodes the cardiac K_{ATP} channel Kir6.1 which facilitates a non-voltage-gated inwardly rectifying potassium current, leading to a shortening of the AP duration under conditions of metabolic stress[11]. One gain-of-function mutation has been identified in *KCNJ8* gene in lone AF[85,86].

- ***ABCC9***

The *ABCC9* gene encodes the regulatory SUR2A subunit of the cardiac K_{ATP} channel. One loss-of-function mutation has been identified in a female patient with early-onset adrenergic AF originating from the vein of Marshall[87].

- **Mutations in genes encoding sodium channel subunits**

The *SCN5A* gene encodes the α-subunit of the cardiac sodium channel $Na_v1.5$, which is responsible for the depolarization phase of the cardiac AP. Many mutations in *SCN5A* have

been identified in several arrhythmic cardiac diseases like Brugada syndrome, long QT syndrome, sick sinus syndrome and atrial fibrillation.

In AF, some studies have reported *SCN5A* mutations associated with gain-of-function effects[88,89], loss-of-function effects[51,90–92], or gain- and loss-of-function with increased late sodium current (current that inactivates very slowly or does not inactivate at all, I_{NaL})[93,94].

The M1875T mutation was identified in a Japanese family with autosomal dominant AF[88]. The majority of the patients had a similar clinical picture of palpitation due to PACs, starting in their teens, then progressing to paroxysmal and persistent AF, without QT prolongation[88]. The K1493R mutation was discovered in a woman and her son with lone atrial fibrillation[89]. Both mutations prolonged the time constants of both fast and slow inactivation, and caused positive shift of the steady-state inactivation, suggesting a gain-of-function effect. In addition, the mutant M1875T increased the peak sodium current I_{Na}. Neither of these mutations increased the late sodium current. The gain-of-function of the cardiac sodium channel could lead to repolarization failure, or early after-depolarizations inducing triggered activities. Also, it might increase the conduction velocity and facilitate the maintenance of fibrillation waves. All of these conditions favor the occurrence of AF. In addition, functional study of the K1493R mutant in HL-1 atrial cardiomyocytes showed enhancement of the window current, lower threshold for AP firing, and spontaneous depolarizations, suggesting a cellular hyperexcitability, a phenomenon that can lead to AF[89].

The loss-of-function *SCN5A* mutation D1275N has been reported in two families presenting with atrial arrhythmias (AF, cardiac conduction disease, and sick sinus syndrome) as well as dilated cardiomyopathy[90,91]. This mutation was also found in a third family with atrial arrhythmia and intra-cardiac conduction defects but without prominent ventricular dilatation[51]. Another mutant, N1986K, was identified in a proband with AF, and his father who presented with AF and sick sinus syndrome requiring pacemaker implantation[92]. Both mutations, D1275N and N1986K, have a loss-of-function effect by positive shift of activation and negative shift of steady-state inactivation, respectively.

The third mechanism by which $Na_v1.5$ could play a role in AF is the generation of the late sodium current (I_{NaL}). In a cohort study of patients with early-onset lone AF[93], eight non-synonymous mutations and two rare variants were identified in *SCN5A*; five of these variants and mutations had previously been associated with LQTS. However, all mutation carriers had a normal or borderline QT_c, but some of them showed QT_c interval prolongation after a flecainide challenge, performed to rule out Brugada syndrome. Functional studies of these variants demonstrated electrophysiological parameters of gain- and loss-of-function effects.

Nevertheless, five of them increased I_{NaL}. In another cohort of patients with either lone AF or AF associated with heart disease, variants associated with increased I_{NaL} have also been identified[94]. This high prevalence of long QT variants in patients with AF indicates that I_{NaL} could play a role in the genesis of AF by providing a substrate through AP prolongation, and a trigger by early and delayed after-depolarizations[95,96]. In agreement with this study, patch-clamp experiments performed in isolated right atrial myocytes from patients undergoing heart surgery for permanent AF, showed that permanent AF was associated with decreased $Na_v1.5$ expression and peak I_{Na} density, and that I_{NaL} was significantly greater[97]. In addition, in the ΔKPQ LQTS mouse model, which had a three-fold increased I_{NaL}, prolonged atrial action potentials, EADs and triggered activity were found[95]. Since EADs and triggered activity in ΔKPQ mice atria were due to enhanced I_{NaL}, ranolazine, a selective I_{NaL} blocker, suppressed EADs and triggered activity in ΔKPQ hearts[95].

In the heart, the α-subunit $Na_v1.5$ interacts with β-auxiliary subunits that modulate I_{Na}. Mutations in genes encoding these subunits (*SCN1B*, *SCN2B*, and *SCN3B*) have also been identified in patients with AF[98–102]. These mutations decrease the I_{Na} current, which further supports the implication of the loss of sodium current in the pathogenesis of AF.

- **Non-ion channel mutations**

In addition to mutations in ion channel genes, mutations in other genes encoding gap-junction proteins (*GJA1*[103], *GJA5*[104–107]) and transcription factors (*GATA4*[108–111] *and GATA6*[112–114]) involved in cardiac development have been identified in patients with AF[56].

Despite the fact that many genes have already been involved in AF, such rare variants are present in less than 1% of patients with AF[36], and cannot explain all the heritability aspects of AF. Nevertheless, identification of these mutations gives new insights into the genetic aspects of the disease, and the underlying mechanisms of AF caused by these genetic variations.

OMIM	Genes	Chromosome	Protein	Current	Functional consequences
ATFB 3	*KCNQ1*	11p15	K_vLQT1	I_{Ks}	Gain-of-function effect on I_{Ks} current[57–61]
	KCNE1	21q22.12	minK	I_{Ks}	Gain-of-function effect on I_{Ks} current[68]
ATFB 4	*KCNE2*	21q22	MiRP1	I_{Ks}	Gain-of-function effect on I_{Ks} current[69]
	KCNE5	Xq22.3	MiRP4	I_{Ks}	Gain-of-function effect on I_{Ks} current[70]
ATFB 6	*NPPA*	1p36-p35	ANP	I_{Ks}	Gain-of-function effect on I_{Ks} current[54,60]
	KCNH2	7q36.1	K_v11.1	I_{Kr}	Gain-of-function effect on I_{Kr} current[71,72]
	KCNE3	11q13.4	MiRP2	I_{Kr}	Gain-of-function effect on $I_{Kr\ and}$ I_{to} currents[73]
ATFB 7	*KCNA5*	12p13	K_v1.5	I_{Kur}	Gain-of-function effect on I_{Kur} crrent[74,75] Loss-of-function effect on I_{Kur} current[75–78]
	KCND3	1p13.2	K_v4.3	I_{to}	Gain-of-function effect on I_{to} current[81]
ATFB 9	*KCNJ2*	17q23-q24	Kir2.1	I_{K1}	Gain-of-function effect on I_{K1} current[50,82–84]
	KCNJ8	12p11.23	Kir6.1	I_{KATP}	Gain-of-function effect on I_{KATP} current[85,86]
ATFB 12	*ABCC9*	12p12.1	SUR2A	I_{KATP}	Loss-of-function effect on I_{KATP} current[87]
ATFB 10	*SCN5A*	3p21	Na_v1.5	I_{Na}	Gain-of-function effect on I_{Na} current [88,89,94] Loss-of-function effect on I_{Na} current[51,90–92] Mixed functional effect on I_{Na} current[93]
ATFB 13	*SCN1B*	19q13.1	ß1	I_{Na}	Loss-of-function effect on I_{Na} current[98–100]
ATFB 14	*SCN2B*	11q23	ß2	I_{Na}	Loss-of-function effect on I_{Na} current[98]
	SCN3B	11q23.3	ß3	I_{Na}	Loss-of-function effect on I_{Na} current[101,102]

Table 2: Different ion channel genes involved in AF

❖ Polymorphisms associated with non-familial AF (Table 3)

Single-nucleotide polymorphisms (SNPs) represent the most common type of inherited genetic variations. Genome-wide and candidate gene association studies have identified SNPs that could modulate disease susceptibility and physiological traits such as PR interval and QRS duration. Most of the identified SNPs are located in non-coding regions of the genome, and some of them can affect gene transcription by modulating regulatory factors, such as cis-regulatory elements and transcription factors. Nevertheless, most SNPs should only be considered as genetic markers of a region of interest (locus), putatively co-inherited with nearby functional SNPs (in linkage disequilibrium). In addition, some SNPs, especially those that are nonsynonymous, could directly alter protein functions.

GWAS performed in general AF populations led to the identification of variants that could contribute to AF susceptibility. In 2007, the first GWAS performed in three European and one Chinese populations showed that two variants on chromosome 4q25 (rs2200733, rs10033464) were linked to AF[115]. Association of these variants with AF was stronger in younger patients and in those with lone AF, but was also significant in older patients. These two variants were confirmed by several other studies, especially the rs2200733[116–119]. In a recent meta-analysis study, an additional SNP, rs6817105, at the same locus was associated with AF with the highest score[120]. The closest gene to this locus is the transcription factor *PITX2* which plays an important role in the determination of cardiac right-left asymmetry[121–123]. *PITX2* suppresses the formation of a left-atrial sinus node and plays an important role in the formation of the pulmonary vein myocardium[124,125]. These variants may dysregulate *PITX2* expression, leading to an abnormal structure or function of the left atrium and pulmonary veins predisposing to AF. GWAS allowed the identification of several other loci linked to AF[120,126–130]. The variants in these loci are not only in genes encoding ion channels (*KCNN3*[128], *HCN4*[120]), but also near or within genes involved in cardiopulmonary development (*PRRX1*) and signal transduction (*CAV1*)[120]. Moreover, in general populations, multiple loci modulating the PR interval length have been identified by GWAS, and some of them were found to be associated with AF[129,130]. However, most of these loci have not been confirmed by the recent metanalysis in AF[120]. Nevertheless, these studies suggest that studying the intermediate phenotype of AF, as PR interval duration[131], may help in the identification of new variants linked to AF.

Candidate gene association studies in AF patients identified a variety of SNPs that may affect AF susceptibility[132]. These polymorphisms are located in genes encoding cardiac ion channels (Table 3), and regulatory proteins (*NPPA*[133], *SLN*[134], *eNOS*[135,136], Table 3), a gap

junction protein (*GJA5*[137,138]), circulatory hormones (*ACE*, *AGT*[139,140,136,141–143]), an inflammatory mediator (*interleukin-6*[144]), matrix metalloproteinases (*MMP2*[145], *MMP9*[146]) and others[132].

Functional studies of some of these variants highlight a probable link between these SNPs and AF. The polymorphism E145D (rs12621643, minor allele frequency 33.6%) in the *KCNE4* gene, which encodes the β-subunit (MiRP3) of the K_vLQT1 potassium channel, was associated with AF in the Chinese population[147]. This variant showed a gain-of-function effect on the I_{Ks} potassium current[148]. Study of the G38S polymorphism (rs1805127, minor allele frequency 33.1) in *KCNE1* encoding the β subunit (minK) of K_vLQT1, and the incidence of AF showed that the presence of the G variant increased the risk of developing AF. Whereas, when having two GG alleles, the risk increased further[135,149,150]. In contrast to *KCNE4* E145D, the G allele of *KCNE1* G38S reduced the I_{Ks} current, due to decreased K_vLQT1 membrane expression, and computer simulations demonstrated atrial AP prolongation, especially in the presence of a reduced repolarization reserve, and the occurrence of early afterdepolarization under specific conditions[151]. However, variants identified by the candidate gene association studies were not reported by the recent meta-analysis study[120].

How these common genetic variants, or their combination with other factors, determine AF susceptibility remain to be investigated. The molecular pathways underlying AF could be the same in both sporadic and familial AF. Future association studies in large cohorts will be helpful in identifying new SNPs, especially those with a strong effect but which may have been missed due to their low allele frequencies, or specific haplotypes in which multiple SNPs are inherited in blocks, in order to have a thorough understanding of the genetic aspects of AF.

OMIM	SNP	Locus	Gene	SNP location relative to closest gene	Functional effect
ATBF5	rs2200733[115–119]	4q25	*PITX2*	Intergenic	Right-left cardiac asymmetry, development of pulmonary vein myocardium
	rs17042171[127]				
	rs10033464[115,117]				
	rs6817105[120]				
	rs6843082[128]				
	rs17570669[119]				
	rs3853445[119]				
ATBF8	rs7193343[126]	16q22	*ZFHX3*	Intronic	Unknown
	rs2106261[120,127,152]				
	rs251253[130]	5q34	*NKX2-5*	Intergenic	Cardiac development, especially pulmonary veins and sinus node
	rs13376333[128]	1q21	*KCNN3*	Intronic	Calcium-activated potassium channel involved in atrial repolarization
	rs 6666258[120]				
	rs3903239[120]	1q24	*PRRX1*	Intergenic	Development of great vessels
	rs3807989[129,130,120]	7q31	*CAV1*	Intronic	Atrial signal transduction protein
	rs10821415[120]	9q22	*C9ORF3*	Intronic	Unknown
	rs10824026[120]	10q22	*SYNPO2L*	Intergenic	Cardiac protein that localizes to the Z disc
	rs1152591[120]	14q23	*SYNE2*	Intronic	Structural protein of the cardiac sarcomere
	rs7164883[120]	15q24	*HCN4*	Intronic	Ion channel (I_f) involved in cardiac pacemaking
	rs1805123*, K897T[153]	7q36 .1	*KCNH2*	Exonic	Potassium channel involved in repolarization
	rs1805120*, F513F[154]				
ATFB10	rs1805124*, H558R[155]	3p21	*SCN5A*	Exonic	Sodium channel involved in depolarization

rs11708996[130]			Intronic	
rs6800541[130]	3p22.2	*SCN10A*	Intronic	Sodium channel involved in depolarization?
rs6590357[*], S57S[156]	11q24	*KCNJ5*	Exonic	Potassium channel involved in repolarization
rs7118824[*], L270L[156]				
rs7118833[*], H278H[156]				
rs1805127[*], G38S[135,149–151]	21q22.12	*KCNE1*	Exonic	Auxiliary subunit that modifies potassium current
rs12621643[*], E145D[147,148]	2q36.1	*KCNE4*	Exonic	Auxiliary subunit that modifies potassium current
rs17003955[*], P33S[157]	Xq22.3	*KCNE5*	Exonic	Auxiliary subunit that modifies potassium current

Table 3: SNPs associated with AF

* Identified by candidate gene associations studies

II.3 Bradyarrhythmias and conduction blocks

Bradyarrhythmias are defined as a heart rate below 60 bpm, and can be divided into two major categories depending on the site of conduction abnormalities: sinus node dysfunction (SND) and atrio-ventricular (AV) block. Sinus bradycardia is a physiological condition predominantly caused by increased vagal tone; it is commonly seen in athletes, or in young people at rest and during sleep. In addition, it can be caused by drugs such as beta-blockers and calcium-channel blockers. Persistent symptomatic sinus bradycardia with heart rate below 40 bpm is a pathological condition and usually represents the sick sinus syndrome that will be discussed later. On ECG, P-waves and QRS complexes are normal, but the heart rate is very slow (Figure 20).

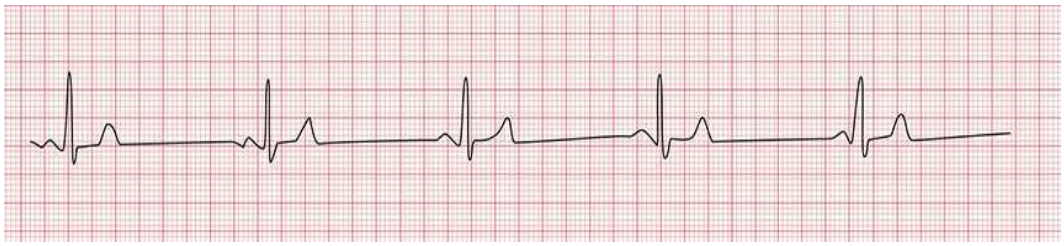

Figure 20: Sinus bradycardia
Normal P-waves and QRS complexes with a heart rate of 37 bpm.
http://rrapid.leeds.ac.uk/ebook/05-circulation-06.html

Atrio-ventricular conduction block is characterized by a delay or failure of conduction of the atrial impulses to the ventricles. According to ECG criteria, it is divided into first-, second- and third-degree (complete) block. In addition, depending on the intracardiac electrophysiological recoding, AV block can be further differentiated into supra-, intra-, or infra-Hisian block.

- **First-degree AV block (Figure 21A)**

First-degree AV block corresponds to a conduction delay of atrial impulses to the ventricles, characterized by constant abnormal prolongation of the PR interval on ECG (PR > 0.2 s) with every P-wave normally followed by a QRS complex (Figure 21A). The conduction delay may occur within the atrium, AV node (the most common), or the His-Purkinje system. Patients with first degree AV block are usually asymptomatic. However, patients may become symptomatic when there is a severe prolongation of PR interval, or during exercise as the heart rate increases but the PR interval does not shorten accordingly.

- **Second-degree AV block (Figure 21B&C)**

Failure of conduction of some atrial impulses to the ventricles results in second degree AV block. According to the ECG criteria, it is divided into two types: type I (Mobitz I or Wenckebach) and type II (Mobitz II).

In Mobitz I (Figure 21B) there is a progressive prolongation of the PR interval (indicated by arrows) before the occurrence of a non-conducted P-wave. The first conducted P-wave after the non-conducted one has the shortest PR interval. In Mobitz II (Figure 21C) there is a constant PR interval before and after the non-conducted P-wave.

- **Third-degree or complete heart block (Figure 21D and E)**

Third-degree or complete heart block corresponds to a failure of conduction of each atrial impulse to the ventricles, resulting in complete AV dissociation with a higher atrial rate than ventricular one. It may be congenital or acquired, with either the AV node, bundle of His, or the right and left bundle branches as the sites of block. Having a narrow QRS complex (Figure 21D) with ventricular escape rhythm of 40-60 bpm indicates that the block is located at the AVN level, which is usually the case in congenital AV-block. However, wide QRS complex (Figure 21E) and/ or a ventricular rate of 20 to 40 bpm point out a block in the His-Purkinje system, which is often seen in acquired AV blocks.

Acquired AV block may be due to extrinsic causes such as drugs, electrolyte disturbances and others, or intrinsic causes like ischemic, inflammatory or infectious heart diseases[158]. However, in approximately 50% of AV block cases, idiopathic progressive degenerative fibrosis of the cardiac conduction system, named as Lenègre or Lev disease, is the leading cause[158]. The treatment of choice in patients with AV block is permanent cardiac pacing. Indication for cardiac pacing depends on the type and location of the AV block, symptoms, and concurrent diseases.

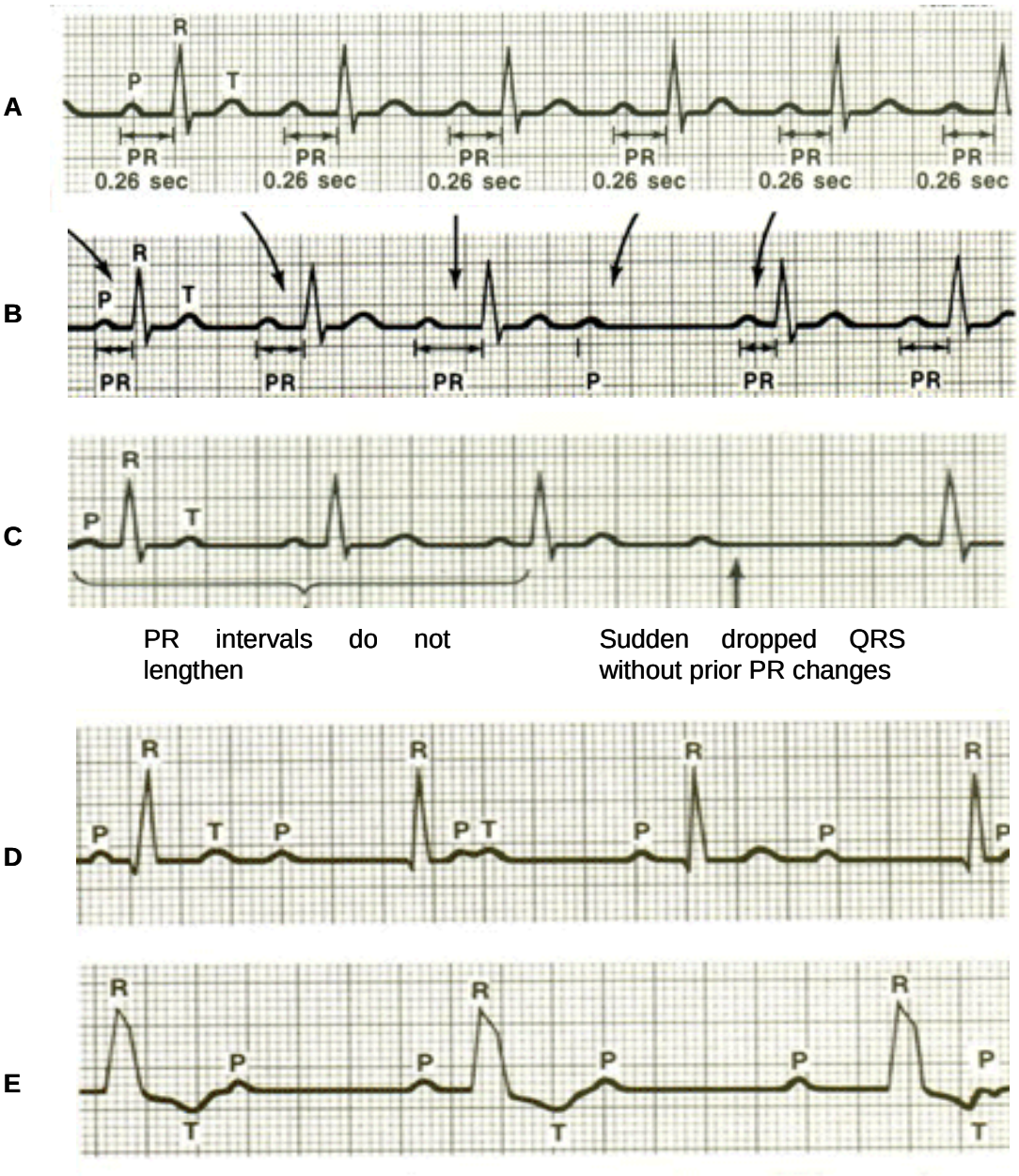

Figure 21: AV conduction blocks
(A) First-degree AV block. (B and C) Mobitz I and Mobitz II second-degree AV blocks. (D and E) narrow and wide QRS complex third degree AV blocks.
Modified from http://www.unm.edu/~lkravitz/EKG/avblocks.html

II.3.1 Sick sinus syndrome (SSS)

SSS is characterized by abnormalities in the SAN impulse formation and propagation leading to atrial rates that are inadequate for physiological requirements. These abnormalities may include sinus bradycardia, sinus arrest, sinoatrial exit block, and chronotropic incompetence. SSS can be caused by an intrinsic disease of the sinus node, or by extrinsic causes[158]. SSS occurs more frequently in the elderly with a peak incidence in the seventh and eighth decades of life[159], the idiopathic degenerative fibrosis of nodal tissue being the main

cause[160]. However, it can occur in fetuses, infants, and children[161–164], especially after cardiac surgery for congenital heart disease. SSS may also occur in young adults without structural abnormalities, and present a familial form, suggesting that genetic factors could be involved in the genesis of the SND[163,165–168].

II.3.1.1 Automaticity of SAN

The sinus node was discovered in 1907 by Keith and Flack while examining human heart histology[169]. Early on, it was described as a small condense area of tissue in the right atrium, where the superior vena cava enters the atrium[170,171], but further studies showed that the SAN is more diffuse, and extends down the inferolateral aspect of the crista terminalis in a cigar shape[172]. In addition, Chandler *et al* identified in 2009 a paranodal area which has a molecular architecture intermediate between the SAN and atrial muscles[173]. It could facilitate the exit of the AP from the SAN into the atrial muscle. The SAN is the natural pacemaker of the heart since it generates impulses faster than other areas of the heart with pacemaker potential. Pacemaker activity of the SAN relies mainly on the spontaneous depolarisation that occurs during diastole (pacemaker potential). SAN Automaticity has been modelled as two clocks[174–176], the membrane voltage clock and the calcium clock (Figure 22). The membrane voltage clock represents the net disequilibrium between the decay of outward potassium currents and the activation of inward currents. The calcium clock contributes to SAN automaticity through Ca^{2+} release from the ER, which can activate the Na^{+}-Ca^{2+} exchanger, generating an inward depolarizing current.

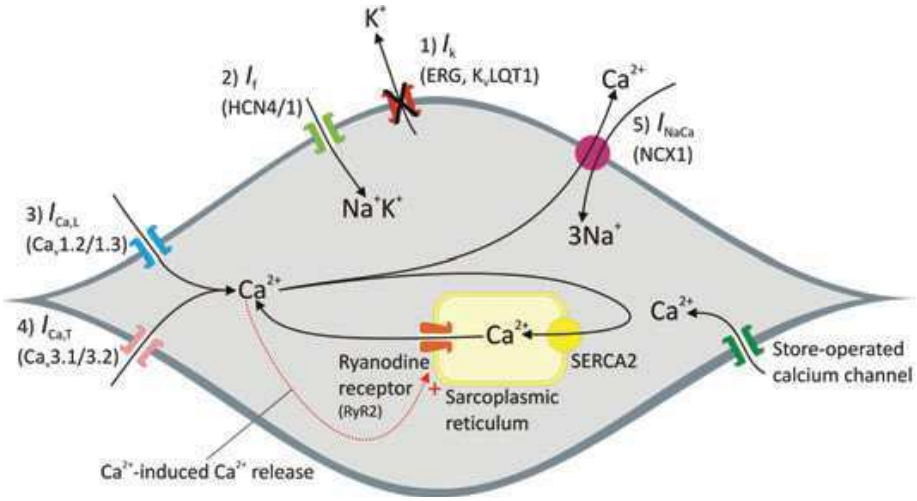

Figure 22: Five ionic currents involved in SAN pacemaking
A SAN myocyte is shown. Membrane clock: during the pacemaker potential, there is a voltage-dependent decay of outward currents (I_K or outward rectifier K^+ current; 1) and a voltage-dependent activation of at least three inward currents, I_f (funny current; 2), $I_{Ca,L}$ (L-type Ca^{2+} current; 3) and $I_{Ca,T}$ (T-type Ca^{2+} current; 4). Ca^{2+} clock: during the final phase of the pacemaker potential, there is an activation of inward I_{NaCa} (Na^+-Ca^{2+} exchange current; 5) in response to a spontaneous release of Ca^{2+} from the sarcoplasmic reticulum *via* the ryanodine receptor (RyR2). Because the Na^+-Ca^{2+} exchanger exchanges one intracellular Ca^{2+} ion for three extracellular Na^+ ions, it is electrogenic and generates an inward current (I_{NaCa}) on removing Ca^{2+} from the cell. Ca^{2+} release from the sarcoplasmic reticulum also occurs as a result of Ca^{2+}-induced Ca^{2+} release in response to Ca^{2+} entry into the cell *via* $I_{Ca,L}$ and $I_{Ca,T}$. The sarcoplasmic reticulum is replenished with Ca^{2+} by reuptake of Ca^{2+} into the sarcoplasmic reticulum *via* SERCA2 (Sarco/Endoplasmic Reticulum Ca^{2+} ATPase). Store-operated Ca^{2+} channels (SOCC) at the cell surface membrane may also help to replenish the sarcoplasmic reticulum with Ca^{2+}. Monfredi O. *et al.* Pacing Clin Electrophysiol 2010[163]

Normally, AP is initiated in a small area of the node called the leading pacemaker site, also known as the center of SAN. Then, it is conducted to atrial muscle through the transitional and peripheral region, where cells are larger and more organized[177]. The leading pacemaker site is not static and can be shifted in response to external factors such as sympathetic and parasympathetic stimulation[177]. The AP is slow and small in the center of the SAN compared to its periphery and the surrounding atrial cells. Differences in ion channels and gap junction expression between the SAN and atrial cells account for the automaticity of the SAN and the shape of nodal AP (Figure 23).

➢ Outward currents

While Kir2.1 underlies the I_{K1} current responsible for the stable resting membrane potential in atrial and ventricular cells, it is absent in nodal cells[173,178]. This leads to an unstable resting membrane potential, and is responsible for the automaticity of nodal cells. During AP, the delayed rectifier potassium channels underlying I_{Ks} and I_{Kr} are activated to account for the repolarization phase, and the decay of these channels allows the inward currents to depolarize the cells. So, it is believed that I_K decay accounts for the earliest part of the pacemaker potential[163,179] (Figure 23).

➢ Inward currents

❖ The funny current

The hyperpolarization-activated or funny current I_f is the major determinant of diastolic depolarization in the SAN. The hyperpolarization-activated cyclic nucleotide–gated channels (HCN) are responsible for the I_f current; there are four HCN channels encoded by different genes (*HCN1-HCN4*). HCN1 and HCN4 are the predominant cardiac isoforms that are present mainly in the human SAN[173]. The HCN channels have unique characteristics including permeability to K^+ and Na^+, activation at hyperpolarized membrane potential and modulation by cAMP. These properties make them ideal for modulating pacemaker potential not only during normal rhythm generation but also during heart regulation by the autonomic nervous systems[180]. The importance of I_f in pacemaker activity is supported by HCN4 mutations associated with SSS that will be discussed below.

❖ Sodium and calcium currents

Early studies have suggested that $Na_v1.5$ plays a minor role in the depolarization phase of the SAN, since the maximum diastolic potential (MDP) is moderately negative, and the SAN has a long diastolic depolarization phase, and as such, most sodium channels are inactivated[179]. Later on, several studies have showed the importance of $Na_v1.5$ in modulating the AP in SAN pacemaker cells, and *SCN5A* mutations have been reported in patients with inherited form of SSS.

Studies on the human SAN showed that the $Na_v1.5$ channel was absent from the center of the SAN, but was present in the periphery, at the junction with atrial cells[173,178]. A large inward current with I_{Na} characteristics was recorded in human SAN cells[181]. Despite that most Na^+ channels may reside in the inactivated state in SAN cells, it was argued that I_{Na} may contribute to human SAN pacemaker activity, and that the atrium exerts an effective

hyperpolarizing load on the periphery of the SAN, thereby bringing the peripheral cells to a more hyperpolarized potential where not all Na^+ channels are steady-state inactivated (window current)[181]. Consequently, the AP upstroke is slow in the center of the SAN, and it is the L-type Ca^{2+} current $I_{Ca,L}$ that is responsible for the depolarization phase. In contrast to atrial and ventricular cells, where the $Ca_v1.2$ channel is the major isoform contributing to $I_{Ca,L}$, nodal cells express $Ca_v1.3$[173] which has a more negative threshold potential than $Ca_v1.2$[163], a feature that makes this channel more appropriate for pacemaker activity, as it is activated earlier in the pacemaker AP. Blocking $I_{Ca,L}$ abolishes AP generation in the center of the SAN, while blocking $Na_v1.5$ slows pacemaker activity at the periphery. This evidence suggests that the presence of $Na_v1.5$ at the periphery is important to provide sufficient inward current for atrial muscle stimulation, resulting in AP conduction out of the nodal cells[178]. In addition to the sodium and L-type Ca^{2+} currents, the T-type Ca^{2+} current, $I_{Ca,T}$, may contribute to the generation of the pacemaker potential of the SAN, mainly the last two thirds of diastolic depolarization (Figure 23)[178].

Moreover, the Na^+-Ca^{2+} exchanger contributes to pacemaker activity elicitated by outward movement of Ca^{2+} during diastole, generating an inward current. It has been suggested that the Na^+-Ca^{2+} exchanger accounts for the last exponential phase of the pacemaker potential[163].

- **Gap junctions**

The electrical coupling in the center of the SAN is weak, mainly because of low connexin expression (Cx43 and Cx40). Instead, Cx45, which forms small conductance channels, is expressed in the center. However, electrical coupling increases at the periphery of the SAN with the expression of Cx43 and Cx40. This organisation of connexin favours the exit of the electrical signal from the node center through the periphery, but at the same time protects the cells in the center from the inhibitory hyperpolarizing influence of atrial muscles[163,173,182].

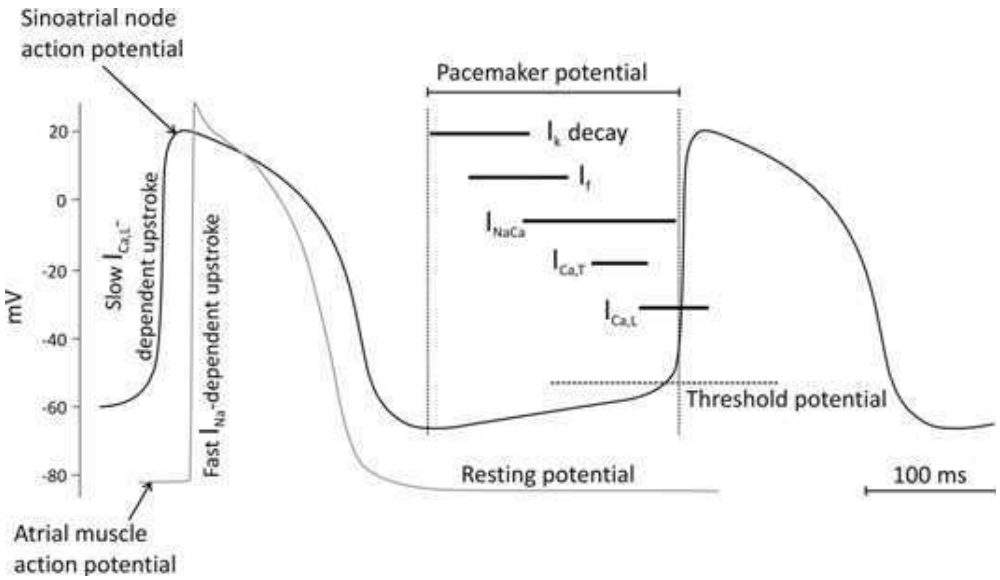

Figure 23: Typical APs recorded from atrial muscle (light gray) and the center of the SAN (black)
The temporal contributions of the main ionic currents to the pacemaker potential are shown by the black bars. Monfredi O. *et al*. Pacing Clin Electrophysiol 2010[163].

II.3.1.2 Genetics of SSS

As the automaticity of the SAN has been modelled as membrane voltage and calcium clocks, it is not surprising that mutations affecting the membrane voltage clock (*SCN5A* and *HCN4*, Table 4 and 5), the calcium clock (*RYR2* and *CASQ2*)[183–185], or both of them (*ANKB*)[186] have been identified in patients with SND. Mutations affecting the membrane voltage clock are discussed below.

➢ SSS and *SCN5A* genetic mutations

Both loss- and gain-of-function mutations in the *SCN5A* gene have been identified in patients with SSS. In 2003, Benson *et al* screened the *SCN5A* gene in a series of ten pediatric patients with congenital SSS treated with pacemaker implantation[187]. In this pioneering study, four cases were diagnosed *in utero*, where SSS was associated with congenital heart defects such as aortic and pulmonary valve stenosis, and no *SCN5A* mutations were found. For the six other patients, SSS was diagnosed between two and nine years of age, in the absence of heart disease, and transmitted as an autosomal recessive trait with complete penetrance. *SCN5A* molecular analysis led to the discovery of compound heterozygous mutations in five patients from three different families. The three probands exhibited the following compound heterozygous mutations: G1408R-P1298L, T220I-R1623X, and delF1617-R1632H.

Functional studies showed that G1408R and R1623X expressed alone produced no current, and the others showed mild to severe channel dysfunction. Each patient harbored one non-functional or severe mutation on an allele, in combination with a milder mutation on the other allele. Interestingly, the subjects who carried only one of these mutations were either asymptomatic, or experienced latent cardiac conduction system disease, such as first degree AV block. However, previous studies have reported that two of these mutations, G1408R and delF1617, led to BrS or conduction abnormalities (G1408R[188]), and long QT syndrome (delF1617[189]), suggesting the role of additional factors in the phenotypical expression of these diseases. Later on, familial SSS was widely studied, and several *SCN5A* loss-of-function mutations have been identified[91,188–197] (Table 4). These mutations lead to no or reduced I_{Na}, due to non-functional channel or altered biophysical properties. As shown in Table 4, some of these mutations are associated with mixed clinical pictures. Studies of several mutations (T220I, P1298L, delF1617, and E161K) in a two-dimensional model of intact SAN-atrium tissue showed that these mutations slowed down pacemaking and compromised AP conduction across the SAN-atrium, leading to possible sinus arrest or SAN exit block. These abnormalities are likely to be exacerbated by vagal nerve activity, and this may account for a high risk of cardiac arrest in SSS patients at night, when vagal activity is prominent[198]. Recently, other mutations in *SCN5A* gene have been identified in patients with SSS without functional studies. The compound heterozygous mutations A735V/D1792N[199], D349N/D1790N[200], and the frame shift mutation F1775Lfs*15[201], all are new mutations, except A735V which was previously reported in BrS[193].

A mouse model with a null mutation in the *SCN5A* gene further confirmed the role of the sodium current in pacemaker function and the contribution of *SCN5A* mutations in the pathophysiology of SSS. The homozygous *SCN5A*$^{-/-}$ mice died *in utero* and showed severe defects in ventricular morphogenesis[202]. However, heterozygous mice had a normal survival rate but presented with a number of electrophysiological abnormalities, including impaired atrio-ventricular conduction, delayed intramyocardial conduction, increased ventricular refractoriness, and ventricular tachycardia with characteristics of re-entrant excitation[202]. Telemetric ECG studies and isolated hearts showed sinus bradycardia, slowed SA conduction, and sino-atrial exit block[203]. These findings directly implicate the role of sodium current in the conduction of AP in the SAN as well as between the SAN and the surrounding atrial cells, and are in line with the *SCN5A* loss-of-function mutations identified in patients with SSS.

Bradycardia and sinus pause have also been reported in LQTS patients with *SCN5A* mutations (LQT3)[204–213] (Table 4). In most of the LQT3 mutations, incomplete or slowed

channel inactivation induces a small persistent inward sodium current, which accounts for the delay in the repolarization and the prolongation of the QT interval. As shown in Table 4, most LQT3 mutations associated with sinus node abnormalities induce both a persistent sodium current and a negative shift of inactivation. In order to determine if these alterations may account for the sinus bradycardia and the sinus pause seen in LQT3 patients, Veldkamp *et al*[211] studied the 1795inD mutation identified in a family with a mixed clinical picture of sinus bradycardia, CCD, LQTS and BrS, in a SAN AP model. This model shows that the 10-mv negative shift of inactivation decreased the sinus rate by decreasing the diastolic depolarization rate, and the persistent current decreased sinus rate by AP prolongation despite the simultaneous slight increase in diastolic depolarization rate. However, the combination of persistent current (1% to 2%) and the shift of inactivation led to a 10% decrease in sinus rate and abolished the slight increase in the depolarization rate seen with persistent current alone.

Mutations	Channel characteristics	Current characteristics	Phenotype	References
E161K	Loss-of-function	Reduced current density, positive shift in activation	SSS, BrS, LQT	Smits *et al*., 2005[190]
T187I	Non-functional	No current	SSS, BrS	Makiyama *et al*., 2005[191]
T220I	Loss-of-function	Reduced current density, negative shift in inactivation	SSS	Benson *et al*., 2003[187]
			DCM, AF, heart block	Olson *et al*., 2005[91]
R367H	Non-functional	No current	Atrial standstill, BrS	Takehara *et al*., 2004[192]
			SUNDS	Vatta *et al*., 2002[193]
G514C	Loss-of-function / gain-of-function	Positive shift in activation reducing I_{Na}. Destabilized inactivation tending to increase I_{Na}	CCD, bradycardia	Tan *et al*., 2001[194]
R878C	Non-functional	No current	SSS	Zhang *et al*., 2008[195]
D1275N	Loss-of-function	Positive shift in activation, fast recovery	SSS, DCM, PCCD	Olson *et al*., 2005[91]
			Atrial stand still with connexin SNP	Groenewegen *et al*., 2003[196]
P1298L	Loss-of-function	Reduced current density, negative shift in inactivation	SSS	Benson *et al*., 2003[187]
G1408R	Non-functional	No current	SSS	Benson *et al*., 2003[187]
			BrS or CCD	Kyndt *et al*., 2001[188]
W1421X	Non-functional	No current (predicted)	SSS	Niu *et al*., 2006[197]
K1578fs/52	Non-functional	No current	SSS, BrS on provocation	Makiyama *et al*., 2005[191]
delF1617	Loss-of-function	Reduced current density, negative in shift inactivation	SSS	Benson *et al*., 2003[187]
			LQT	Splawski *et al*., 2000[189]

R1623X	Non-functional	No current	SSS	Benson *et al*., 2003[187]
			SSS, BrS	Makiyama *et al*., 2005[191]
R1632H	Loss-of-function	Negative shift in inactivation, slow recovery from inactivation	SSS	Benson *et al*., 2003[187]
R121W	Non-functional	No current	SSS, atrial flutter, episodes of VT, PCCD	Holst *et al.*, 2009[214]
L212P	Loss-of-function / gain-of-function	Negative shifts in activation and inactivation, delayed recovery from inactivation	Atrial standstill only with connexin SNP	Makita *et al*., 2005[215]
ΔK1500	Loss-of-function / gain-of-function	Negative shift and reduced slope of inactivation, positive shift of activation and increased late current	LQT, BrS, PCCD; sinus pauses	Grant *et al*., 2002[204]
delKPQ 1505–1507	Gain-of-Function	Sustained inward current during membrane depolarization. Mutant channels fluctuate between normal and non-inactivating gating modes	LQT, Sinus bradycardia; LQT, BrS, PCCD	Bennett *et al*., 1995[205] Grant *et al*., 2002[204] Wang *et al*., 1995[206]
V1763M	Gain-of-function	Persistent tetrodotoxin-sensitive but lidocaine-resistant current. Positive shift of the inactivation curve, steeper activation curve. Faster recovery from inactivation	Sinus bradycardia/ tachycardia; LQT	Chang *et al*., 2004[207]
E1784K	Gain-of-Function	Small residual steady-state current throughout prolonged depolarization. Negative shift in inactivation. 7.5-fold increase in flecainide affinity in resting-state channels	LQT, sinus bradycardia with occasional sinus pauses LQT, BrS, sinus node dysfunction	Wei *et al*., 1999[208] Makita *et al*., 2008[209]
1795insD	Gain-of-Function	Negative shift in voltage-dependence of inactivation;	Sinus bradycardia,	Bezzina *et al*., 1999[210]

		persistent inward currents	CCD, LQT and BrS	Veldkamp *et al*., 2003[211]
D1790G	Gain-of-Function	Negative shift in inactivation, but no D1790G-induced sustained inward current	LQT, sinus arrest	Abriel *et al*., 2000[212] Benhorin *et al*., 2000[213]
L1821fs/10	Loss-of-function/gain-of-function	Reduced current density, negative in shift inactivation, increased late current	SSS, CCD, VT	Tan *et al*., 2007[216]
A1924T	Gain-of-function	Negative shift of activation	Atrial standstill Brs	Lopez *et al*., 2011[217] Rook *et al*., 1999[218]

Table 4: Na^+ channel mutations associated with sinus node dysfunction

Modified from Lei M. *et al.* Prog Biophys Mol Biol 2008[219]

- **SSS and *HCN4* genetic mutations**

Six *HCN4* mutations have been identified in patients with SSS (Table 5), all of which are loss-of-function mutations. The decrease in I_f is due to multiple mechanisms like altered biophysical properties[220–224], trafficking defects[222,225], synthesis defects[222,223], and decreased sensitivity of the channel to cyclic adenosine monophosphate (cAMP)[220]. In addition, two mutations have dominant-negative effect on the WT channels[220,225]. These mutations are associated with variable clinical manifestations such as asymptomatic sinus bradycardia[221,222], syncope with QT prolongation and torsade de pointes[225], symptomatic sinus bradycardia with normal chronotropic and exercise capacity[223], or syncope with intermittent AF and chronotropic incompetence[220]. One mutation was reported in sporadic cases[220], while the others were familial and transmitted in an autosomal dominant way[221–223]. Recently, the mutation K530N was identified in a family which developed tachycardia–bradycardia syndrome and persistent AF in an age-dependent manner, indicating that the dysfunction in the f-channel may contribute to the development of atrial arrhythmias[224].

Mutation	Channel characteristics	Current characteristics	Phenotype
P544fsX30 (HCN4 573X)[220]	Loss-of-function	Negative shift of activation at long activation protocol, insensitive to increased cAMP, dominant-negative on WT	Patient with symptomatic sinus bradycardia, intermittent AF, chronotropic incompetence
D553N[225]	Loss-of-function	Reduced I_f current caused by decreased surface expression of the channel, dominant-negative on WT	Patient with sinus node dysfunction, QT prolongation, PVT, torsade de pointes, AD
S672R[221]	Loss-of-function	Negative shift of activation, faster deactivation, no change of cAMP-induced channel activation	Familial with asymptomatic bradycardia, AD
G480R[222]	Loss-of-function	Reduced I_f current, slow and negative shift of activation	Familial with asymptomatic bradycardia, normal exercise capacity, AD
A485V[223]	Loss-of-function	Drastic decreased in I_f, negative shift of activation	Familial with symptomatic bradycardia, AD
K530N[224]	Loss-of-function	Negative shift of inactivation at the heterozygous state	Familial with tachycardia–bradycardia syndrome and persistent AF in an age-dependent fashion, AD

Table 5: *HCN4* mutations associated with SSS syndrome

AD = autosomal dominant.

II.4 Ventricular arrhythmias

➢ Premature ventricular contractions (PVC)

Like PACs, PVCs are ectopic impulses occuring when a region of the ventricle depolarizes leading to premature beats. PVCs are usually a benign arrhythmia relatively frequent in healthy persons, but they can be caused by cardiac or noncardiac diseases. Prognosis depends on the morphology and frequency of PVCs, as well as on the type and severity of the associated heart diseases. In general, polymorphic PVCs have poorer prognosis than those that are monomorphic, since they can be transformed into ventricular tachycardia and fibrillation. On ECG, PVC is characterized by an abnormally wide QRS complex, abnormal T wave, and an absence of the P wave followed by a compensatory pause (Figure 24).

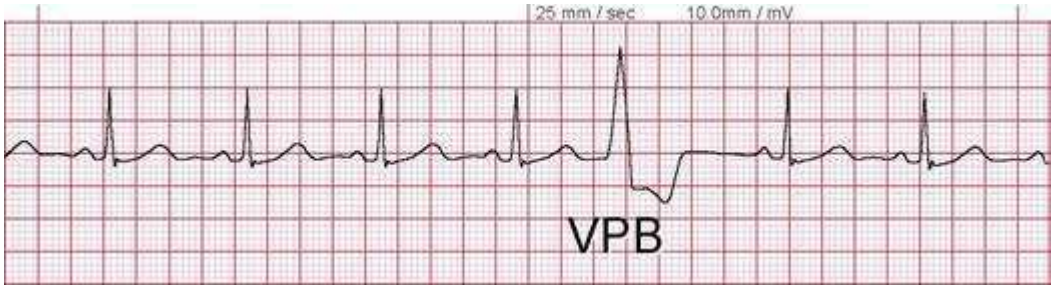

Figure 24: Premature ventricular contraction
VPB: ventricular premature beat.
http://www.medicine-on-line.com/html/ecg/e0001en_files/08.htm

➢ Ventricular tachycardia (VT)

VT is a rapid heart beating entity originating in the ventricles, occuring with or without structural heart disease. Reentry is the main cause of such arrhythmia. On ECG, it is demonstrated by atrio-ventricular dissociation with a rapid ventricular rate, and wide QRS complexes (QRS > 120 ms) (Figure 25).

According to QRS morphology, VT is divided into monomorphic or polymorphic forms. In monomorphic VT, ventricular activation starts either in a single focus, or due to a re-entrant circuit caused by a stable substrate. On ECG, QRS complexes have the same form. However, in polymorphic VT, they have different forms indicating an alteration in ventricular activating sites. Polymorphic VT is more dangerous since it can be transformed into ventricular fibrillation.

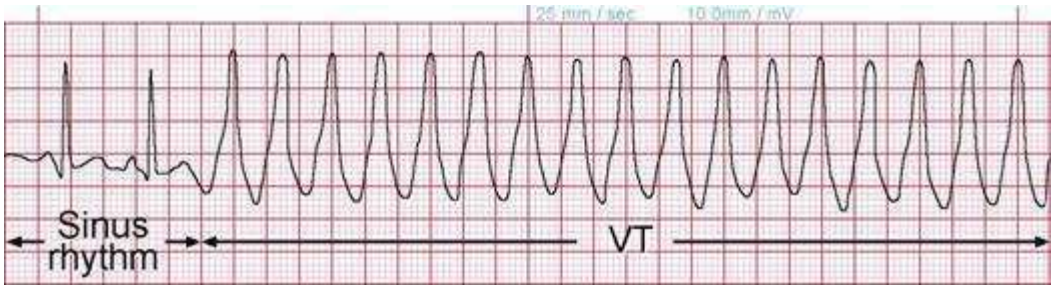

Figure 25: Ventricular tachycardia
http://www.medicine-on-line.com/html/ecg/e0001en.htm

- **Ventricular fibrillation (VF)**

VF is the major cause of sudden cardiac death. It is charaterized by a rapid asynchronous fluttering ventricular contraction without effective blood ejection, leading to severe hypotension, syncope, and sudden death within a few minutes if left untreated. On ECG, VF is recognised by its irregular disorganised oscillations without QRS-complexes (Figure 26).

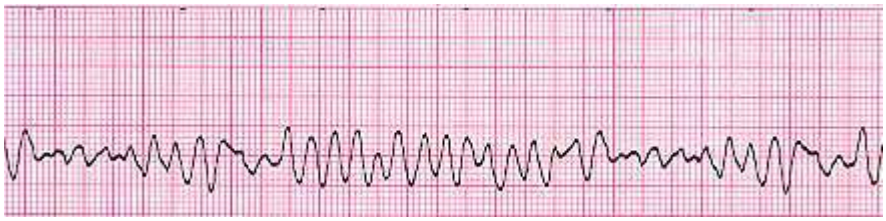

Figure 26: Ventricular fibrillation
http://cardiac.northbayhealthcarenursing.com/ventricular-fibrillation.html

- **Torsade de pointes (TdP)**

TdP is a stereotyped polymorphic ventricular tachycardia, usually associated with LQTS, with a 2- to 3-fold increased frequency in females compared to males[226]. Transmural dispersion of depolarization with EAD as a common tigger is the underlying mechanism of TdP. On ECG, it is characterized by fluctuating amplitude and twisting of QRS complexes around the isoelectric line (Figure 27). In most circumstances, TdP terminates spontaneously, however degeneration into VF may occur resulting in sudden death.

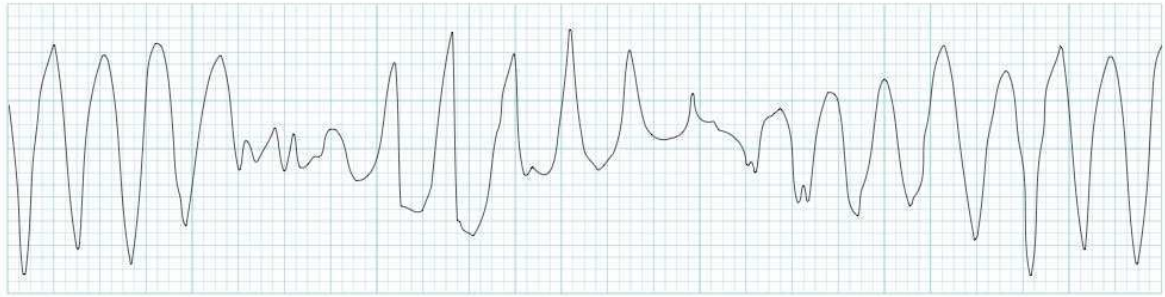

Figure 27: Torsade de pointes
http://lifeinthefastlane.com/ecg-library/tdp/

- **Hereditary ventricular arrhythmias**

Hereditary ventricular arrhythmias are rare diseases associated with a high risk of sudden cardiac death, especially in young patients. Seventy percent of them are pure electrical diseases (ion channel diseases), while 30% are caused by arrhythmogenic structural heart diseases[227]. Long QT syndrome (LQTS), short QT syndrome (SQTS), catecholaminergic polymorphic ventricular tachycardia (CPVT), and Brugada syndrome (BrS) represent the most common primary hereditary ventricular arrhythmias. They are mainly caused by mutations in the genes encoding ion channel and regulatory proteins involved in the generation of the cardiac action potential (Figure 28). They are associated with incomplete penetrance, and variable expressivity[228].

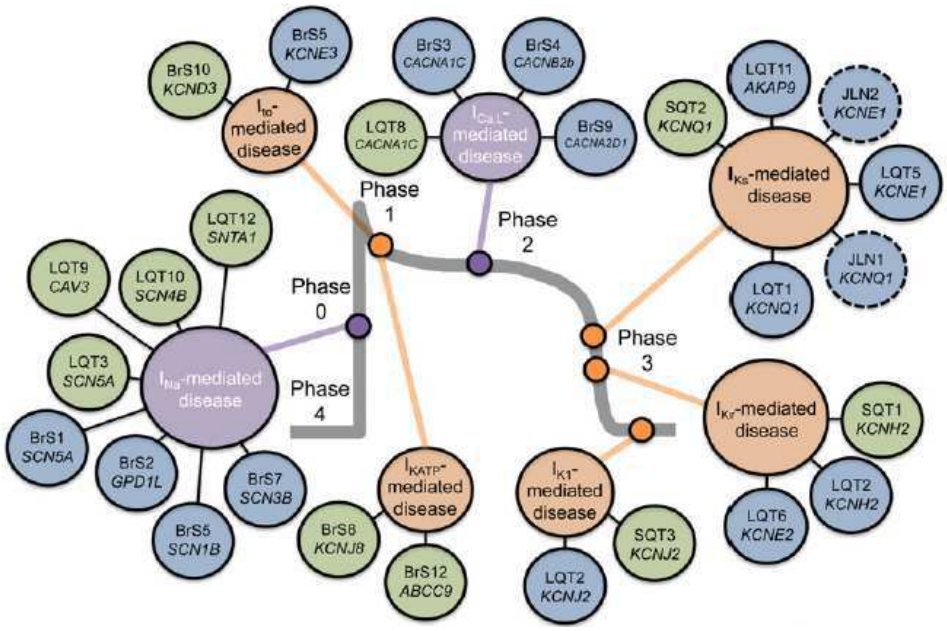

Figure 28: Ion channels involved in hereditary cardiac arrhythmias
Blue and green circles represent loss- and gain-of-function mutations. Solid and dashed lines indicate autosomal dominant and recessive inheritance. Modified from Giudicessi J. R. *et al.* Transl Res 2013[228]

- **Long QT syndrome (LQTS)**

LQTS is a heterogeneous group of hereditary disorders characterized by abnormal prolongation of the QT interval on the ECG (QTc≥450 ms in males and QTc≥460 ms in females), with an increased risk of life-threatening ventricular arrhythmias, like torsade de pointes (TdP), ventricular tachycardia, and ventricular fibrillation; conditions that can lead to sudden death[229]. Currently, mutations in 15 genes encoding ion channel proteins and their partners have been reported in LQTS. These mutations enhance the depolarizing currents (I_{Na}, I_{Ca-L}) or diminish the repolarizing currents (I_{Ks}, I_{Kr}, I_{K1}). The most common genes involved in LQTS are *KCNQ1* (LQT1), *KCNH2* (LQT2), and *SCN5A* (LQT3), and mutations in these genes account for approximately 60-75% of genotype-positive LQTS patients[229]. According to the presence of extracardiac manifestations, six different subtypes of LQTS are distinguished:

1. The autosomal dominant Romano-Ward syndrome is the most common LQTS. It is not associated with extracardiac manifestations.
2. The rare autosomal recessive Jervell and Lange-Nielsen syndrome (JLNS), characterized by the presence of bilateral sensorineural deafness in addition to severe QT prolongation, it is mainly caused by homozygous or

compound heterozygous loss-of-function mutations in *KCNQ1*[230,231] (JLNS1) or *KCNE1*[232,233] (JLNS2).

3. Timothy syndrome (TS) is an extremely rare multisystem disorder, which manifests by the presence of variable degrees of autism spectrum disorder, syndactyly, and severe cardiac arrhythmias[234]. It is caused by some specific loss-of-function missense mutations in the *CACNA1C* gene[235].
4. The Andersen-Tawil syndrome (ATS) is another rare multisystem disorder with mild QT prolongation and moderate risk of life-threatening ventricular arrhythmia. Patients with ATS have variable dysmorphic physical features (low-set ears, micrognathia, and clinodactyly), and periodic paralysis as extracardiac manifestations. It is caused by loss-of-function mutations in the *KCNJ2* gene[236].
5. The ankyrin-B syndrome (ABS) is caused by mutations in the *ANK2* gene encoding the adaptor protein ankyrin B. Patients have QT prolongation, sick sinus syndrome and episodic atrial fibrillation[237].
6. The recurrent infantile cardiac arrest syndrome is a recent multisystem form of LQTS caused by mutations in the genes encoding the Ca^{+} binding protein, calmodulin. It is characterized by severe QT prolongation, 2:1 atrio-ventricular block, neurodevelopmental delay, seizures, and recurrent cardiac arrest during early infancy[238].

The main treatment for LQTS is beta-blockers. In some cases, an implantable cardioverter defibrillator (ICD) may be needed. In addition, patients with LQTS should avoid all medications that cause prolongation of QT interval. The list of such drugs is available on the following Website (www.qtdrugs.org).

- **Catecholaminergic polymorphic ventricular tachycardia (CPVT)**

CPVT is a rare disease characterized by normal ECG at rest with adrenergic-mediated polymorphic ventricular tachyarrhythmias during effort or emotional stress, and with a high mortality rate of up to 50% in severe untreated cases up to the age of 20 years[239,240]. It is mainly caused by mutations in genes involved in calcium homeostasis, the cardiac ryanodine receptor gene (*RYR2*, autosomal dominant)[241], and the gene encoding the cardiac calsequestrin (*CASQ2*, autosomal recessive)[185,242,243]. Recently, mutations in the transmembrane sarcoplasmic reticulum protein triadin (*TRDN*, autosomal recessive)[244], another protein involved in calcium homeostasis, have been reported. These mutations

increase the cytosolic Ca^{2+} concentration, leading to delayed after-depolarizations that trigger arrhythmias. Beta-blockers are the mainstay of treatment for CPVT, and in certain cases ICD can be used.

- **Short QT syndrome (SQTS)**

SQTS is a hereditary disease described for the first time in 2000[245], characterized by short QT interval (QTc<320 ms) with syncope and unexplained atrial or ventricular arrhythmia (atrial fibrillation, polymorphic ventricular tachycardia, and ventricular fibrillation) that could lead to sudden death[246,247]. In contrast to LQTS, SQTS is a very rare disease caused by gain-of-function mutations in the genes *KCNH2* (SQT1), *KCNQ1* (SQT2), and *KCNJ2* (SQT3)[63] affecting the potassium repolarizing currents (I_{Kr}, I_{Ks}, I_{K1}). Treatment options are limited; ICD can be used in cases with a high risk of sudden death.

II.4.1 Brugada syndrome (BrS)

Brugada syndrome is an autosomal inherited cardiac channelopathy with incomplete penetrance[228]. It is characterized by a structurally normal heart with a typical ST segment elevation in the right precordial leads of the ECG[248]. The Brugada brothers, in 1992, were the first to describe BrS as a clinical entity[249]. Patients with BrS have an increased risk of sudden cardiac death by ventricular fibrillation[250].

II.4.1.1 Epidemiology

As the ECG pattern of BrS can be intermittent, often concealed and dependent on ECG lead position, it is difficult to ascertain the true prevalence of BrS in the general population. It has been estimated that the prevalence of a Brugada type 1 ECG pattern is approximately 0.05%, with a mean age of sudden death of 41±15 years[250]. However, this prevalence varies worldwide with the highest prevalence in Asia, followed by Europe and the United States[251]. Despite the fact that BrS is generally considered to be an autosomal dominant disease, its prevalence is up to 10 fold higher in men than women with increased severity[252,253]. BrS typically occurs in adulthood with mean age of diagnosis between 40 and 45 years[250], an age at which most arrhythmic events happen, mainly during sleep or at rest[252–255]. However, BrS can occur in children[250,256]. According to the consensus document, BrS represents 4% of all sudden deaths and at least 20% of sudden deaths in patients with structurally normal hearts[250]. In addition, in 2002, BrS and sudden unexplained nocturnal death syndrome (SUNDS) have been identified as the same entity[193]. SUNDS, which has the same ECG manifestation as BrS, is the most common cause of death in the young healthy Asian population (usually male) during sleep, highly present in Thailand, Japan, the Philippines and Cambodia[193,257,258]. Besides, some mutations in the BrS-related genes have been identified in sudden infant death syndrome (SIDS), an unexplained sudden death of an infant usually during sleep in the first year of life[259,260,80,100].

II.4.1.2 Electrocardiographic characteristics

ECG abnormalities represent important criteria in the diagnosis of BrS. There are three different ECG patterns, however only type-1 ECG is diagnostic (Figure 29):

1. Type 1 is characterized by an ST-segment elevation equal to or greater than 2 mm in one or more right precordial leads V1, V2, positioned in the 2nd, 3rd or 4th intercostal

space. The ST-segment elevation has a coved type appearance and is followed by a negative T-wave. This ECG pattern can be observed spontaneously or after the administration of sodium channel blockers like flecainide and ajmaline, and it represents the gold standard in BrS diagnosis.

2. Type 2 has an ST-segment elevation equal to, or greater than 1 mm, followed by positive or biphasic T-wave with saddleback appearance.
3. Type 3 has an ST-segment elevation of less than 1mm of saddleback type, coved type or both. Type 2 and 3 ECG patterns are not diagnostic of BrS.

Signs of conduction abnormalities, like prolonged P wave duration and PR intervals, and right bundle branch block, are often seen in BrS ECGs, especially in patients with *SCN5A* mutations[261–264].

Importantly, through patient examination including personal and family history, ECG, echocardiography and coronary angiography, other causes of ST-segment elevation should be carefully ruled out, such as myocardial ischemia or infarction, structural cardiac abnormalities and arrhythmogenic right ventricular cardiomyopathy (ARVC).

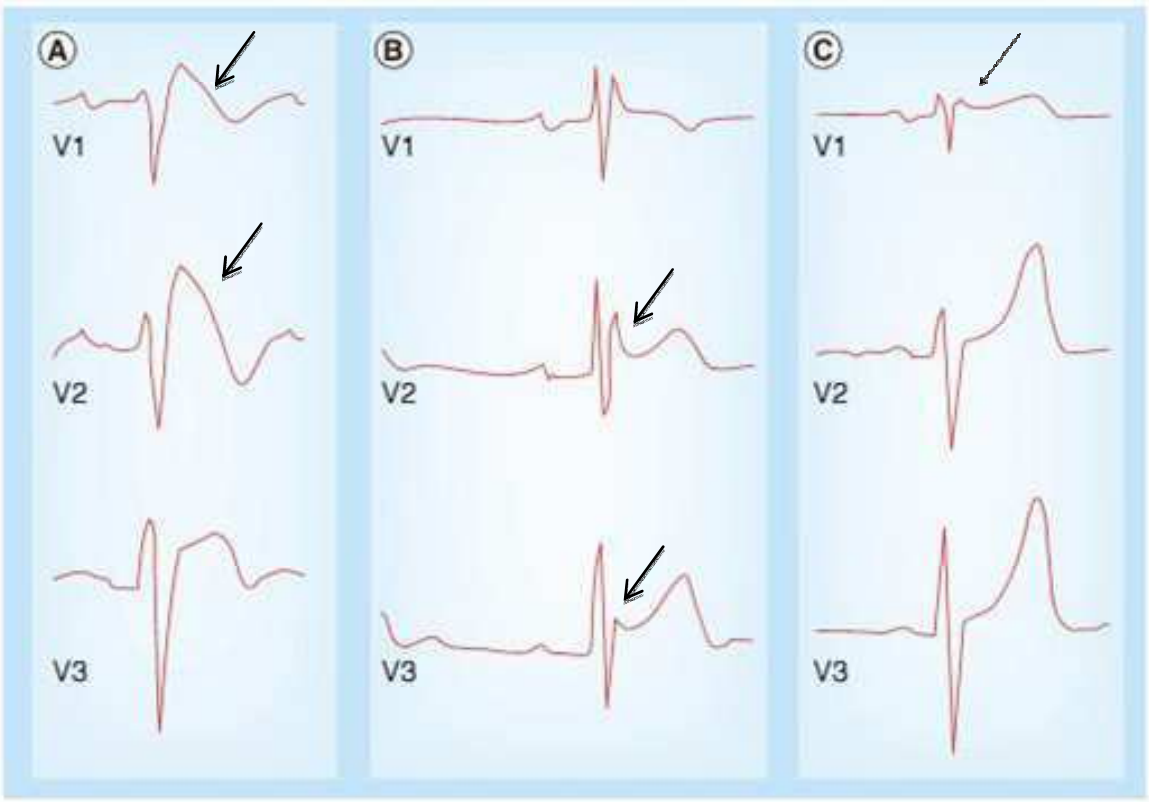

Figure 29: Examples of Brugada type 1, 2, and 3 ECG patterns
(A) Brugada type 1 (coved) in leads V1 and V2 (arrows); (B) Brugada type 2 (saddleback) in leads V2 and V3 (arrows); (C) Brugada type 3 in lead V1. Modified from Li and Behr. Future Cardiology 2013[248]

II.4.1.3 The pathophysiology of BrS

Two main hypotheses have been reported to explain the pathophysiology of BrS: the repolarization and the depolarization hypotheses.

- **Repolarization hypothesis**

Yan and Antzelevitch first proposed the repolarization hypothesis in 1999 based on results from an arterially perfused wedge preparation of the canine right ventricle[265]. In accordance to this hypothesis, there is a net enhancement of the repolarizing current at the end of phase one of the action potential that leads to the augmentation of the AP notch in the right ventricular epicardium.

In normal heart, there is a gradient expression of the transient outward potassium (I_{to}) channels through the ventricular wall, which are highly expressed in the epicardium compared to the endocardium[12,266–269], mainly in the right ventricle[270]. This gradient accounts for the

notch and dome morphology during phase 1 of cardiac AP of the epicardium (Figure 30A). In BrS, reduction of the inward depolarizing currents, I_{Na} or I_{CaL}, or enhancement of the repolarizing potassium current I_{to}, by mutations in the genes encoding these ion channels, increases the net repolarizing currents, and leads to an enhancement of the right ventricular notch and exaggeration of the transmural voltage gradient manifested by the elevation of the ST-segment on the ECG (Figure 30B). If the repolarization of the epicardium precedes that of the myocardium and endocardium, the T wave is positive resulting in a saddleback morphology on the ECG (Figure 30B). If the enhancement of the notch is accompanied by epicardial action potential prolongation, the myocardium and the endocardium will repolarize before the epicardium, reversing the transmural gradient and leading to the inversion of the T-wave and the elevation of coved ST-segment, the typical ECG features seen in BrS (Figure 30C). Further enhancement in the net repolarizing currents could lead to loss of the AP dome in some but not all epicardial cells and not in the endocardium (Figure 30D). This dispersion of repolarization within the epicardium and also transmurally, creates an arrhythmic substrate that may cause phase-2 re-entry triggering polymorphic ventricular tachycardia and ventricular fibrillation (Figure 30E)[271,272]. In human, simultaneous recording of monophasic AP from the epicardium and endocardium in patients with BrS showed spike-and-dome morphology in the epicardial sites, which was absent in the endocardium and in control patients [273].

The repolarization hypothesis is in agreement with the predominant occurrence of BrS in males, since in animals, a higher I_{to} expression is seen in males compared to females[274]. Moreover, higher testosterone levels are found in male patients with BrS compared to controls[275], and disappearance of typical BrS-ECG after castration has been reported[276]. Recent unpublished data by Antzelevitch and collaborators in human induced pluripotent stem cell-derived cardiomyocytes, showed that testosterone increases the expression of I_{to} in these cardiomyocytes by augmenting the Kv4.3 mRNA expression[277]. In addition, Song *et al* showed that the estrogen hormone inhibits the Kv4.3 expression and trafficking in the myometrium of pregnant rats[278].

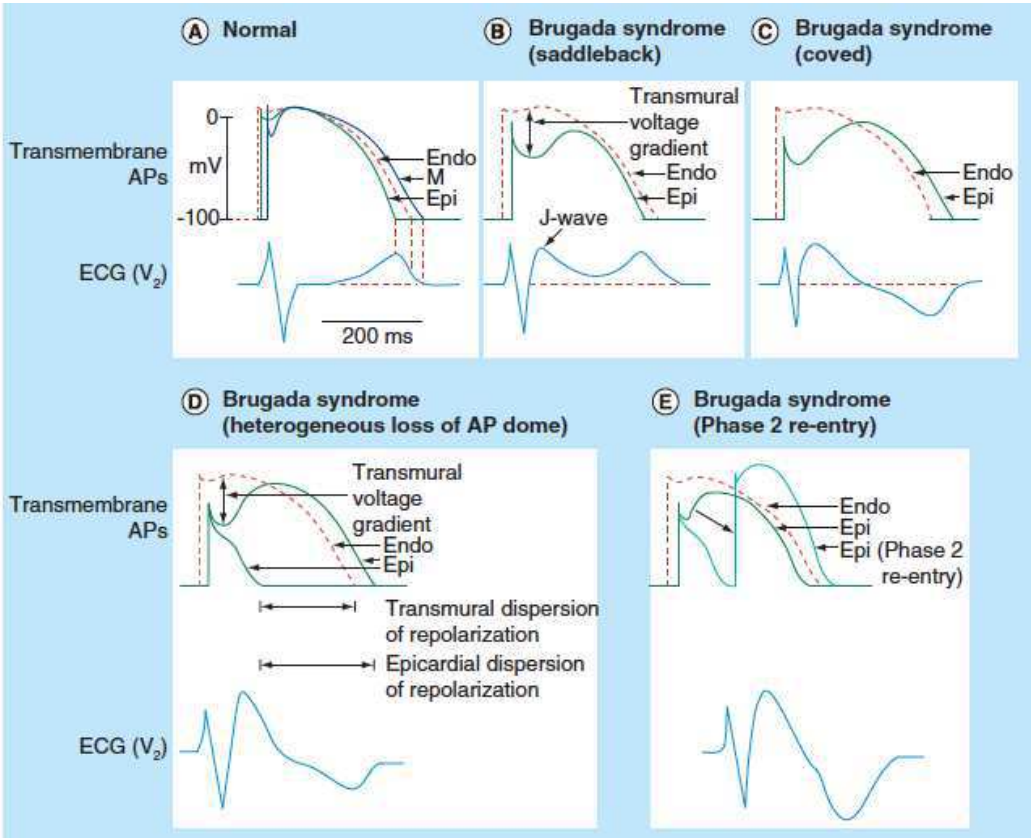

Figure 30: The repolarization hypothesis
(A) Normal transmembrane APs showing a prominent phase 1 notch in epicardium (Epi) and M cells (M) due to a high I_{to} channel expression. (B) Reduction in I_{Na} channel function increases phase 1 notch leading to a steep transmural voltage gradient, inscribing an elevated J-wave on the surface ECG. (C) Prolongation of epicardial repolarization results in a negative T-wave on the surface ECG. (D) Further reduction in I_{Na} leads to loss of the AP dome in some epicardial cells but not others, leading to transmural and epicardial dispersion of repolarization. (E) Phase 2 re-entry leads to short coupled extrasystoles, triggering ventricular fibrillation. AP: Action potential; Endo: Endocardial. Modified from Li and Behr. Future Cardiol 2013[248]

- **Depolarization hypothesis**

Another hypothesis was proposed by Nagase *et al* in 2002, based on the conduction delay observed in the right ventricular outflow tract (RVOT)[279]. During depolarization, the right ventricle is depolarized before the RVOT, resulting in an electrical gradient from the more positive right ventricle to the RVOT (Figure 31C and D), which leads to an ST-segment elevation on ECG. As the depolarization of the RVOT is delayed, this electrical gradient is reversed during the repolarization of the right ventricle, resulting in a negative T-wave on the ECG (Figure 30E and F). Loss-of-function mutations in the cardiac sodium channel $Na_v1.5$, which underlies the depolarization phase of the cardiac AP, could enhance the conduction delay. Premature beats arising in the border zone between early and delayed depolarization

could cause a re-entry circuit, leading to VT/VF[272]. The depolarization hypothesis is consistent with several ECG signs of conduction delay seen in BrS, including longer P-wave, PQ and QRS intervals[280,281]. Moreover, Doppler echocardiography[282] and epicardial mapping studies[283] in BrS support this hypothesis by demonstrating delay in right ventricular contraction, and delayed depolarization over the RVOT epicardium, respectively. Finally, study of an explanted heart of a BrS patient carrying an *SCN5A* mutation showed evidences of right ventricular hypertrophy, fibrosis with fatty infiltration and conduction delay, which were more prominent in the RVOT [284].

The depolarization hypothesis challenges the concept that BrS is a pure channelopathy without structural heart disease. In addition to the fibrosis and hypertrophy seen in the explanted heart of a BrS patient, other structural abnormalities were reported such as myocarditis, apoptosis, fibrofatty replacement of the RV free wall with RV enlargement, dilatation and RVOT enlargement[285,286].

From all evidence mentioned above, we conclude that BrS is not just a monofactorial disease. Each of the above hypotheses alone cannot completely explain the disease, and it is certainly possible that BrS is a disease with multiple mechanisms.

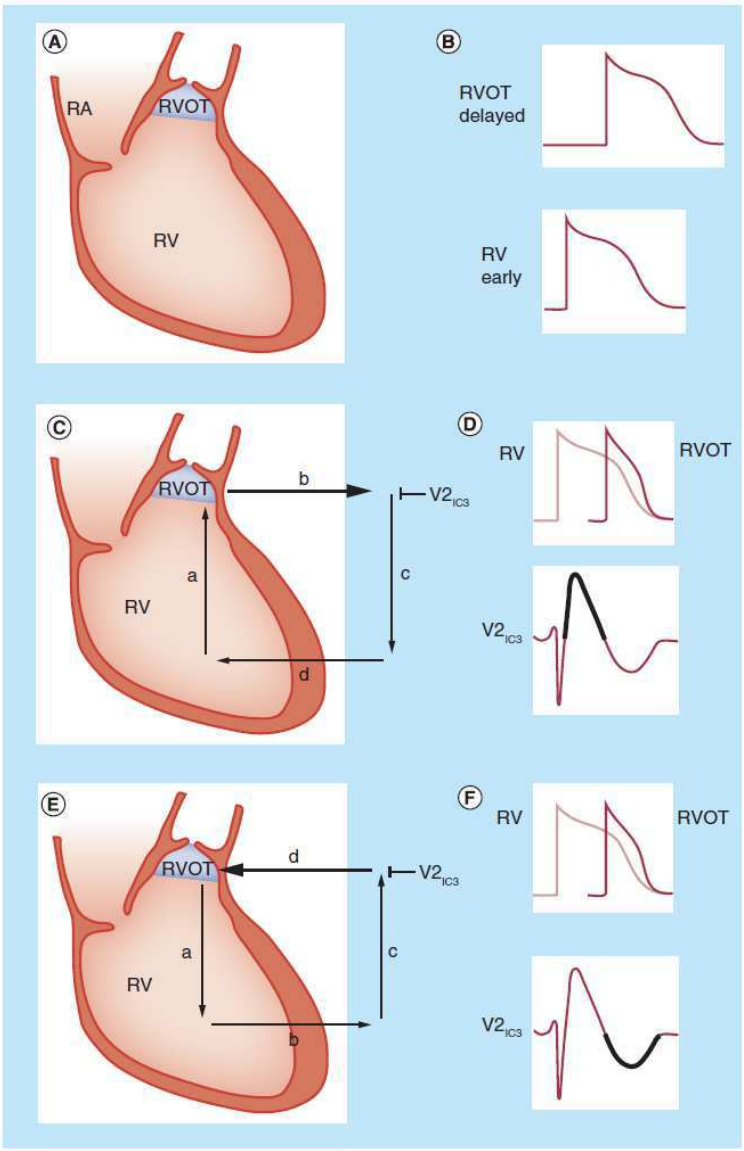

Figure 31: The depolarization hypothesis
(A and B) Conduction delay in RVOT versus RV. (C and D) The electrical gradient between RV and RVOT results in an ST-segment elevation in V2 in the high intercostal lead configuration. (E and F) Delayed repolarization of the RVOT reverses electrical gradient from the RVOT to the RV leading to negative T-waves on the surface ECG. RA: Right atrium; RV: Right ventricle; RVOT: Right ventricular outflow tract; V2IC3: Surface ECG lead V2 in the third intercostal space. Modified from Li and Behr. Future Cardiol 2013[248]

II.4.1.4 Diagnosis of BrS

According to the second consensus report in 2005[250], the diagnostic criteria for BrS were strict, and required the presence of a type 1 ECG pattern either occurring spontaneously or following the administration of a sodium channel blocker, in two or more right precordial leads, with at least one of the following clinical criteria:

- Documented VF/polymorphic VT
- Family history of sudden cardiac death (SCD) in members <45 years old
- Type 1 ECG in family members
- Inducible VT/VF with programmed electrical stimulation
- Syncope or nocturnal agonal respiration

However, according to the recent consensus statement in 2013[287], these criteria have since been changed, and a BrS diagnosis now only requires the presence of a type 1 ECG pattern, spontaneously or following the administration of a sodium channel blocker, in at least one right precordial lead (V1,V2), positioned in 2nd, 3rd, or 4th intercostal space.

For type 2 and 3 ECG patterns; the appearance of these ECG changes in one or more right precordial leads V1, V2, positioned in 2nd, 3rd, or 4th intercostal spaces under baseline conduction, with conversion to type 1 after using sodium channel blockers is considered diagnostic for BrS.

II.4.1.5 BrS treatment

- **Implantable cardioverter defibrillator (ICD)**

According to the most recent consensus Report[287], an ICD is the only effective treatment to prevent sudden death in patients with BrS.

According to this report, an ICD:

- is recommended for BrS patients who are survivors of a cardiac arrest and/or have documented spontaneous sustained VT with or without syncope.
- can be useful in patients with a spontaneous diagnostic type 1 ECG with history of syncope, which could be related to ventricular arrhythmias.
- may be considered in BrS patients with inducible VF.
- is not indicated in asymptomatic BrS patients with a drug induced type 1 ECG and on the basis of a family history of sudden cardiac death alone.

- **Drug therapy**

Until now, limited support is present for the use of medication in the treatment of BrS, since there is a shortage in large randomized studies on the effectiveness of proposed drugs in these patients. However, based on the cellular mechanisms responsible for the Brugada phenotype, drugs that reduce I_{to} or enhance I_{CaL} could be therapeutic options for BrS. The most studied medication in BrS is quinidine, which blocks the I_{to} and I_{Kr} potassium currents. It has shown efficacy in the treatment of electrical storm and in the prevention of spontaneous or induced ventricular arrhythmias. Some studies suggest that it can be used with an ICD or as an alternative, especially in patients who are asymptomatic but experience drug-induced arrhythmias[288–294]. The problem with this medication is the high rate of side effects like diarrhoea, and thrombocytopenia[291]. Isoproterenol, which increases I_{CaL}, is another medication that has been used in treating an electrical storm[295]. Other medications have also been evaluated for their efficacy in BrS treatment[296].

- **Ablation**

Endocardial ablation of ventricular ectopic beats (mainly in the RVOT), which trigger VF, has been effective in treating VF storms[297–300]. However, as ablation is an invasive procedure, it is usually used after the failure of other therapies. According to the recent consensus report[287], catheter ablation may be considered in BrS patients with a history of arrhythmic storms or repeated appropriate ICD shocks[287].

Recently, another approach for ablation has been reported by Nademanee *el al* [301]who showed that the ablation of the region of conduction delay in the right ventricle, mainly the anterior aspect of RVOT epicardium, in nine patients with recurrent episodes of VF leads to VF suppression and normalization of the ECG patterns in 8/9 patients after two years of follow-up.

- **Additional recommendations**

Patients with BrS should avoid all medications that could induce a type 1 ECG pattern and/or ventricular arrhythmia, such as psychotropic drugs, antihistamines and anaesthetics. The list of these drugs is available on the following website (www.brugadadrugs.org)[302].

II.4.1.6 Genetics of BrS

BrS is an autosomal dominant disease with incomplete penetrance and variable expression. It is considered as a channelopathy since, until now, 19 genes encoding ion channel and ion-channel regulatory proteins have been associated with BrS[303–305] (Table 6). However, mutations in these genes have been identified in less than 30% of affected individuals[250,306].

Mutations in the *SCN5A* gene is the most common genotype, accounting for approximately 18 to 30% of the BrS cases[250], with a higher frequency in familial than in sporadic cases[307]. The first mutations were identified by a candidate-gene approach in 1998 in families with idiopathic VF[308]. Since then, an increasing number of *SCN5A* mutations have been reported, and up to now there are nearly 300 published *SCN5A* mutations[306]. The reported mutations include missense, nonsense, frame-shift, splice-site, and in-frame deletion/insertion mutations. Functional studies of some of these mutations in heterologous systems showed loss-of-function effects on the sodium current by different mechanisms including[309]:

- Decreased surface expression of $Na_v1.5$ protein due to:
  - Retention and premature degradation of the mutant proteins by the ER quality control system[310–314].
  - Failure of the mutant to interact with β-subunits or regulatory proteins like ankyrin-G[315], SAP97[316], syntrophin[316], and FHF1[317], all which have an important role in stabilising channel expression at the surface as well as targeting $Na_v1.5$ to special domains in cardiomyocytes. Here, mutations may be in the *SCN5A* gene, like the mutation E1053K[315] that abolishes the interaction with ankyrin-G, or in the genes encoding regulatory proteins, as the mutation Q7R[317] in *FGF12,* which reduces the binding of FHF1 to $Na_v1.5$.
- Expression of non-functional channels[188,318]

  Some mutant channels have a normal membrane expression but they conduct either very small or no sodium currents, as the mutations are located in the channel pore.

- Altered gating properties[210,319–324]

  Delayed activation (activation at more positive potential), earlier inactivation (inactivation at more negative potential), faster inactivation, enhanced slow inactivation and delayed recovery from inactivation, all lead to decreased I_{Na}.

Autosomal transmission of *SCN5A* mutations is not always observed. This is not only due to partial penetrance, but also to the fact that some BrS patients do not carry the familial mutation, suggesting another genetic origin. Indeed, in a study of 13 large families carrying *SCN5A* mutations[263], type-1 Brugada ECG pattern was not observed even after drug challenge in nearly half of the mutation carriers. However, it was seen following drug challenge in five mutation-negative patients, and spontaneously in three others. In the same study, mutation carriers were found to have longer PR intervals and QRS durations than non-carriers, consistent with other studies[261,262,264], suggesting that mutant channels have loss-of-function effects but do not cause BrS. These findings suggest that the simple model of autosomal dominant inheritance of BrS cannot completely explain the disease, and *SCN5A* mutations alone are sometimes not sufficient to induce the disease (although most mutation carriers have conduction problems indicating the loss-of-function effects of these mutations), but they may act as factors favouring BrS in the presence of a specific genetic background. Moreover, the existence of genotype-negative BrS patients indicates that other unknown rare or common genetic variants could play a role in the disease, and that negative genetic testing cannot exclude the disease.

In addition to *SCN5A*, mutations in the genes encoding the β-subunits and the regulatory proteins of $Na_v1.5$ have been involved in BrS, and all lead to $Na_v1.5$ loss-of-function effects (Table 6). Moreover, loss-of-function mutations in the gene encoding the components of L-type calcium channels (*CACNA1C*, *CACNB2B* and *CACNA2D1*) and private gain-of-function mutations in the outward potassium current have also been reported (Table 6). However, these mutations are rare, and account for less than 1% of all the BrS cases.

Although several genes have been reported in BrS, mutations in these genes cannot completely explain the disease phenotype. Meanwhile, other factors like genetic modifiers, drugs, gender and imbalance in autonomic tone could influence the BrS phenotype. Moreover, the presence of structural heart disease in some cases of BrS has challenged the concept that BrS is a pure channelopathy. So, it is likely that genetic susceptibility along with other modulating factors lead to BrS, in combination but probably not in isolation.

OMIM	Gene	Locus	Protein	Current	Functional effects	Reference
BrS1	*SCN5A*	3p21	$Na_v1.5$	I_{Na}	Loss-of-function	Chen *et al*., 1998[308]
BrS2	*GPD1-L*	3p22.3	GPD1L	I_{Na}	Loss-of-function	London *et al*., 2007[325]
BrS3	*CACNA1C*	12p13.3	$Ca_v1.2$	$I_{Ca\text{-}L}$	Loss-of-function	Antzelevitch *et al*., 2007[326]
BrS4	*CACNB2*	10p12	$Ca_vß2$	I_{Ca}	Loss-of-function	Antzelevitch *et al*., 2007[326]
BrS5	*SCN1B*	19q13.1	$Na_vß1$	I_{Na}	Loss-of-function	Watanabe *et al*., 2008[327]
BrS6	*KCNE3*	11q13-14	MiRP2	I_{to}	Gain-of-function	Delpón *et al*., 2008[328]
BrS7	*SCN3B*	11q23.3	$Na_vß3$	I_{Na}	Loss-of-function	Hu *et al*., 2009[329]
BrS8	*HCN4*	15q24.1	HCN4	I_f	Loss-of-function	Ueda *et al*., 2009[*330]
	KCNH2	7q36.1	hERG1	I_{Kr}	Gain-of-function	Itoh *et al*., 2009[331]; Verkerk *et al*., 2005[*332]
	KCNJ8	12p11.23	Kir6.1	I_{KATP}	Gain-of-function	Medeiros-Domingo *et al*., 2010[86]
	CACNA2D1	7q21-q22	$Ca_vα2δ$-1	$I_{Ca\text{-}L}$	Not available	Burashnikov *et al*., 2010[333]
	RANGRF	17p13.1	MOG1	I_{Na}	Loss-of-function	Kattygnarath *et al*., 2011[334]
	KCNE5	Xq22.3	MiRP4	I_{to}	Gain-of-function	Ohno *et al*., 2011[*335]
	KCND3	1p13.3	$K_v4.3$	I_{to}	Gain-of-function	Giudicessi *et al*., 2011[336]
	SLMAP	3p14.3	SLMAP	I_{Na}	Loss-of-function	Ishikawa *et al*., 2012[337]
	TRMP4	19q13.3	TRMP4	NSC_{Ca}	Both	Liu *et al*., 2013[338]
	SCN2B	11q23	$Na_vß2$	I_{Na}	Loss-of-function	Riuró *et al*., 2013[339]
	FGF12	3q28	FHF1	I_{Na}	Loss-of-function	Hennessey *et al*., 2013[304]
	PKP2	12p11	PKP2	I_{Na}	Loss-of-function	Cerrone *et al*., 2013[305]

Table 6: Mutations in genes associated with Brugada syndrome
* May act as modifier factors**.** Modified from Nielsen M. W. *et al*. Front Physiol 2013[303]

II.4.1.7 Conduction abnormalities in patients with BrS

The presence of conduction abnormalities, specifically right bundle branch block (RBBB), were involved in the early definition of BrS, in association with the persistent ST segment elevation in the right precordial leads[249]. However, in the consensus reports of 2002[340], 2005[250], and recently 2013[287], ST elevation is the only maintained diagnostic ECG criterion of BrS. Nevertheless, several studies have shown that patients with BrS have various conduction abnormalities at different levels of the conduction system[261–264].

A recent multicentric study by Maury *et al*[264] including 325 BrS patients showed that only 21% of patients did not have any conduction abnormality on the ECG. The majority of patients had various conduction abnormalities including increased P-wave duration, first degree AV block, right bundle branch block, fascicular block, and prolongation of His-ventricular (HV) interval, occurring separately or in various combinations in the same patient. These abnormalities were more frequent when a BrS-ECG type 1 pattern was induced by a class 1 drug. Moreover, several studies showed that BrS patients carrying *SCN5A* mutations have longer PR intervals and QRS durations than non-carriers, suggesting that these ECG abnormalities may be used to predict the presence of *SCN5A* mutations[261–264]. These ECG abnormalities could also be used in the future for risk stratification of patients, since some of them have been linked to specific outcomes. Such abnormalities include life-threatening ventricular arrhythmias with QRS prolongation[341–343], SD in women with longer PR interval[344], and SD and/or ICD therapy with a first degree AVB[264].

These conduction abnormalities are similar to those seen in the Lenègre disease[158,309], a progressive cardiac conduction disease (PCCD), which is characterized by progressive prolongation of the conduction parameters (P wave, PR interval, QRS) and right or left bundle branch block. PCCD may result in complete heart block leading to syncope or sudden death, but is not associated with ventricular arrhythmias. It is most often caused by fibrosis affecting the cardiac conduction system. In the heritable form, loss-of-function mutations in the *SCN5A* gene or $Na_v1.5$ regulatory proteins have been reported[188,327,345,346]. These mutations reduce I_{Na} by the same mechanisms mentioned previously for BrS. However some of these mutations cause PCCD alone or PCCD with BrS (overlap syndrome), indicating that the I_{Na} reduction is sufficient to cause conduction abnormalities either in PCCD or in BrS. However, in some cases, other factors in addition to I_{Na} loss are required for the development of ST segment elevation, the standard ECG sign of BrS.

The conduction abnormalities observed in Lenègre disease are progressive with age, requiring a pacemaker implantation in the older patients. Similar progressive conduction abnormalities were also reported in some *SCN5A* BrS mutations carriers[262]. Nevertheless, the two diseases remain two distinct clinical entities, as the ST- segment elevation and the life-threatening ventricular arrhythmias, two main BrS features, are absent in PCCD.

III. The cardiac sodium channel $Na_v1.5$

The cardiac sodium channel forms a large protein complex in the cardiomyocyte sarcolemma. The main pore-forming $Na_v1.5$ α-subunit is responsible for the large inward sodium current (I_{Na}) underlying the depolarization phase of the cardiac action potential. The $Na_v1.5$ α-subunit is a glycosylated protein of 2016 amino acids. It has four homologous domains (I–IV), each consisting of six transmembrane α-helical segments (S1-S6), with N- and C-terminal cytoplasmic domains (Figure 32A). The four domains are connected to each other by cytoplasmic linkers, while the transmembrane segments are linked to each other by alternating extracellular and cytoplasmic loops (P-loops). The folding of the four domains enables the formation of the ion-conducting pore, which is lined by the extracellular loops between the S5 and S6 segments (Figure 32B), that determine the selectivity for Na^+. The S4 segments of domains I to IV are positively charged, and act as a voltage sensor to trigger channel activation. Depolarization of the cardiomyocytes by electrical stimuli leads to outward movement of the S4 segments, allowing the channel to activate and thus the opening of the pore. Channel activation is rapid compared to channel inactivation, allowing the channel to open for a short period of time[347].

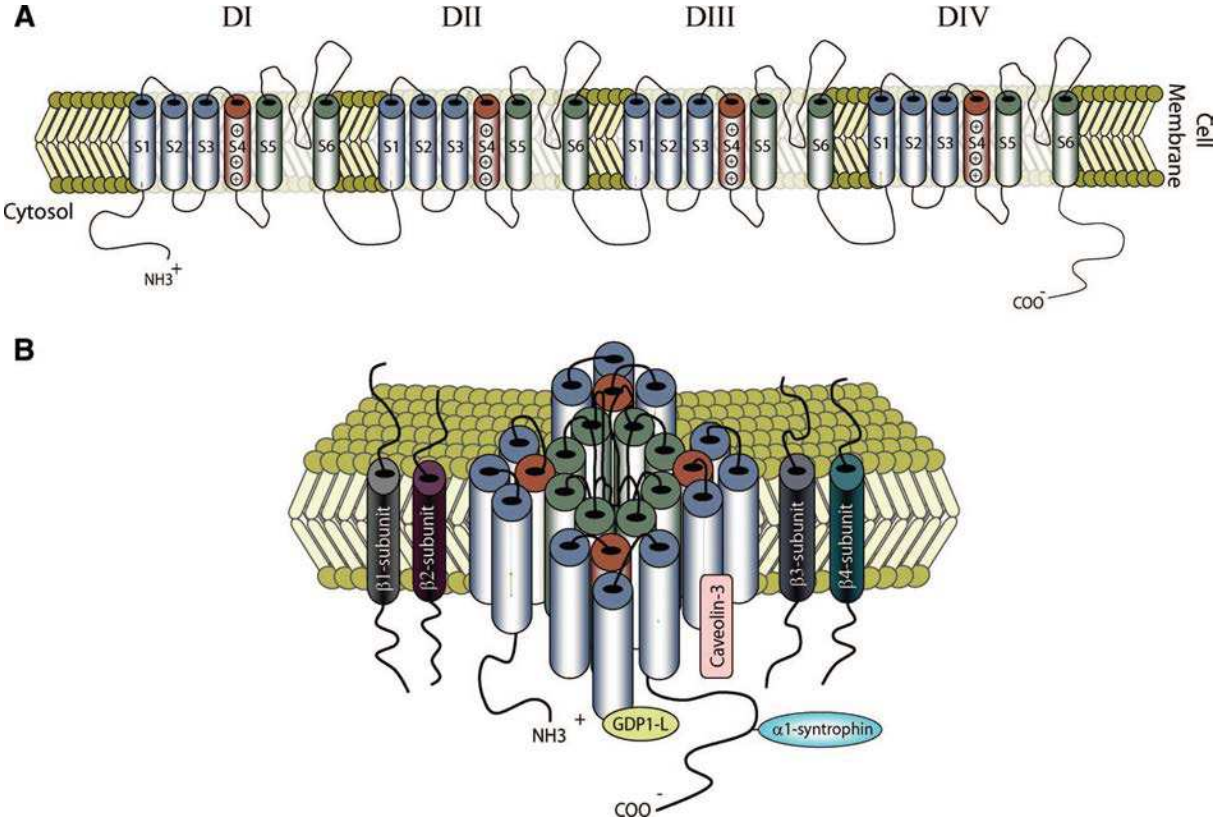

Figure 32: Schematic presentation of the $Na_v1.5$ α-subunit
Modified from Wilde and Brugada, Circ Res 2011[348]

III.1 Conformational changes of $Na_v1.5$ during channel activation and inactivation

Depending on the variations of the membrane potential, the sodium channel can have three conformational states (closed, open, and inactivated). The transition between these states relies on the status of the activation and inactivation gates (Figure 33).

- Closed but capable of opening. In this state only the activation gate is closed.
- Open allowing the entrance of Na^+. In this state both activation and inactivation gates are opened.
- Closed and not able to open. In this state only the inactivation gate is closed.

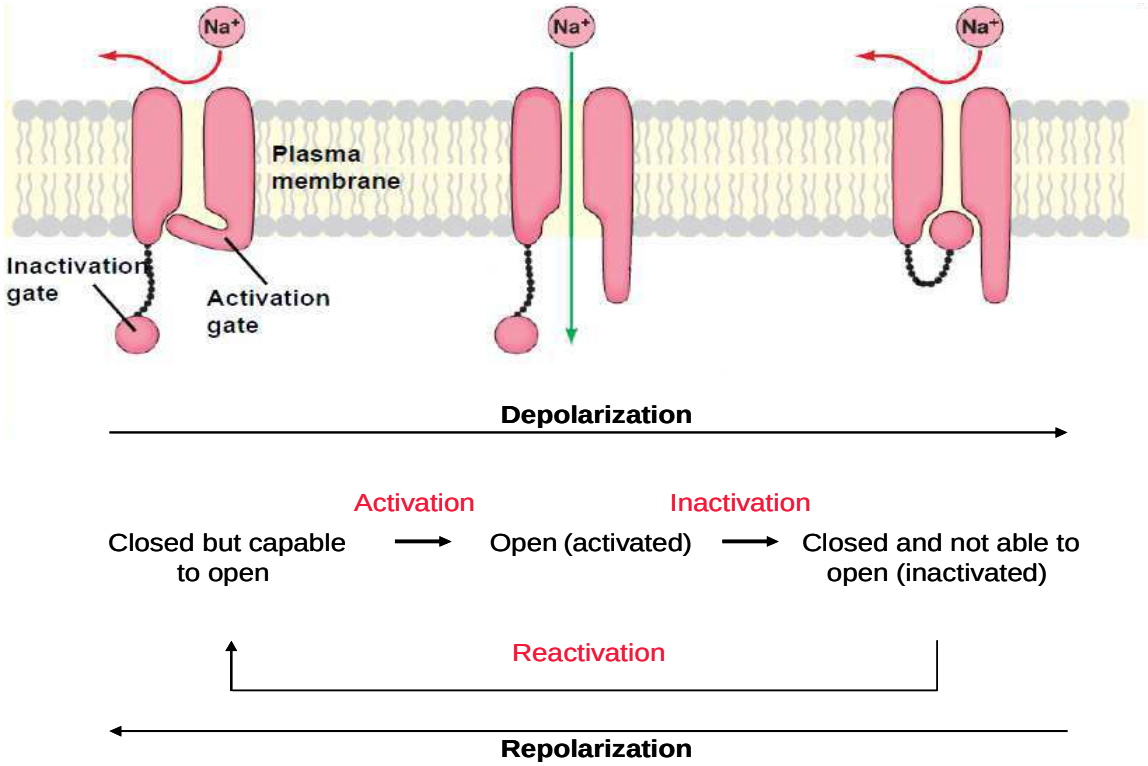

Figure 33: Conformational changes of $Na_v1.5$
Modified from
http://test.classconnection.s3.amazonaws.com/11/flashcards/399011/png/na_channel.png

At the resting membrane potential, the sodium channels are closed but able to open. Upon depolarization by electrical stimuli, conformational changes of the channels permit transition to the open state. Maintenance of depolarization leads to the activation of all the $Na_v1.5$ channels (at around -20mV). Further depolarization results in rapid inactivation through the closure of the inactivation gate. Most channels are inactivated at the end of the action potential upstroke (Phase 0). However, during the plateau phase, a small fraction of channels remain available, and may reopen resulting in late sodium current (I_{NaL}). Under normal conditions, I_{NaL} is very small compared to Peak $I_{Na,}$ with no impact on the AP shape. However, it is of great importance in type III LQTS where *SCN5A* mutations increase I_{NaL}. Then, during Phase 4, channels will progressively return back to their resting state, this transition is called reactivation.

Inactivation of the sodium channel involves two distinguishable kinetic processes, the slow and fast inactivation. Fast inactivation takes place by a ball-and-chain mechanism, in which the inactivaion particle formed by the hydrophobic triplet amino acids, the IFM-motif (isoleucine 1485, phenylalanine 1486, and methionine 1487), located in the cytoplasmic

linker between domains III and IV (IFM), binds to its docking sites, including the linkers between the segments S4 and S5 in domains III and IV, and the cytoplasmic end of the S6 segment in domain IV, which together form the inactivation gate[349]. Fast inactivation is linked to activation. It is thought that the outward movement of the voltage sensors during activation leads to the exposure of the docking sites, allowing their interaction with inactivation particles. Thus the S4 segments could be a part of both the activation and inactivation processes. Moreover, the cytoplasmic C-terminal domain, particularly the proximal structural region, has a role in the inactivation process as it stabilizes the closed state, preventing channel re-opening[350].

Under prolonged depolarization, sodium channels enter into the slow inactivation state; a more stable nonconducting state from which channels need more time to reactivate, compared to the fast inactivation. In addition, the molecular mechanism underlying slow inactivation is less well understood, and it does not require the inactivation particle (the linker III-IV). However, it was proposed that conformational changes in the S5-S6 P-loops, which form the channel pore, could underlie this process[347].

III.2 Expression and localization of $Na_v1.5$ in the cardiomyocytes

After synthesis in the ER, $Na_v1.5$ α-subunits undergo post-translational modification. They are anchored to the cytoskeleton and possibly stored in the subcellular compartments, before being finally targeted to the membrane to carry out their function. Then, from the membrane, they are internalized into endocytic vesicles and degraded. However, little is known about the the detailed processes underlying the synthesis and trafficking of $Na_v1.5$ α-subunits.

Despite the fact that $Na_v1.5$ α-subunits alone can act as voltage-gated sodium channels, it has been demonstrated that these channels are part of multiprotein complexes that modulate biological and/or biophysical properties of the channels. Immunocytochemical studies in cardiomyocytes have shown the presence of the $Na_v1.5$ α-subunit at the intercalated discs, lateral membranes, and T-tubules[351–353]. At these sites, the $Na_v1.5$ α-subunit interacts with various proteins, creating different protein complexes that are localized to specific regions of the cell membrane. According to the localization of these complexes, two distinct functional pools of $Na_v1.5$ channels are present, one at the lateral membranes and the other at intercalated discs[354,355] (Figure 34). At the lateral membrane, $Na_v1.5$ interacts with the syntrophin-dystrophin complex, whereas at the intercalated discs, it interacts with the synapse-associated protein 97 (SAP97). These partner proteins will be discussed later in

detail. These two pools are not only different in their composition, but also in their biophysical properties. Macropatch studies have showed that sodium channels at the lateral membranes have decreased peak sodium current density with a negative shift of steady-state inactivation, and slower recovery from inactivation, compared to channels located at the intercalated discs[356]. A possible third pool of $Na_v1.5$ may also be present at the T-tubules[355]. The exact role of these pools in the (patho)-physiology of cardiomyocytes remains to be elucidated, and future studies are needed to explore their functional roles.

In addition to these distinct pools, $Na_v1.5$ shows heterogeneous expression across the ventricular wall, with a transmural gradient increasing from the epicardium toward the endocardium[7,357].

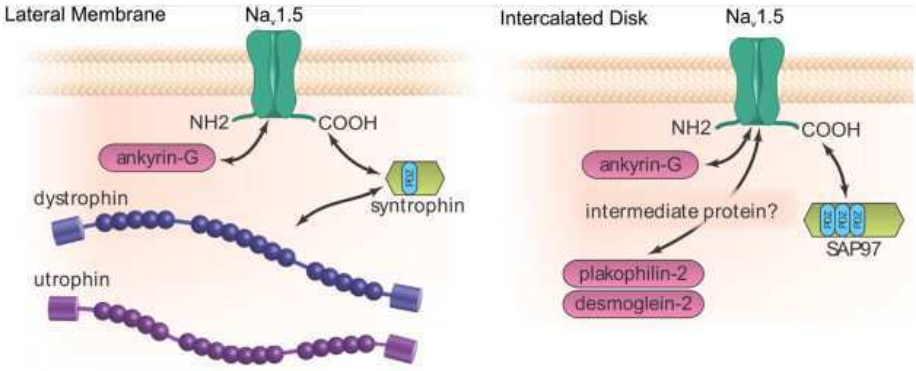

Figure 34: Representative schematic of the $Na_V1.5$ multiple pools model
Shy D. *et al*. Biochim Biophys Acta 2013[355]

III.3 Functional and clinical relevance of $Na_v1.5$-interacting proteins

$Na_v1.5$ is a part of a protein complex which includes a number of partners that regulate the function, membrane expression and the subcellular localization of $Na_v1.5$[354,355] (Figure 35). Mutations in the genes encoding several of these partner proteins have been linked to inherited cardiac arrhythmias, which further highlights the importance of these proteins in the (patho)-physiology of the heart. According to their functions, the partners of $Na_v1.5$ could be divided into (1) anchoring or adaptor proteins that play a role in the trafficking and subcellular localization of the channel, (2) enzymes that interact with and modify channel structure, such as protein kinases and ubiquitin ligases, and (3) proteins that modulate the biophysical properties of the channel[354].

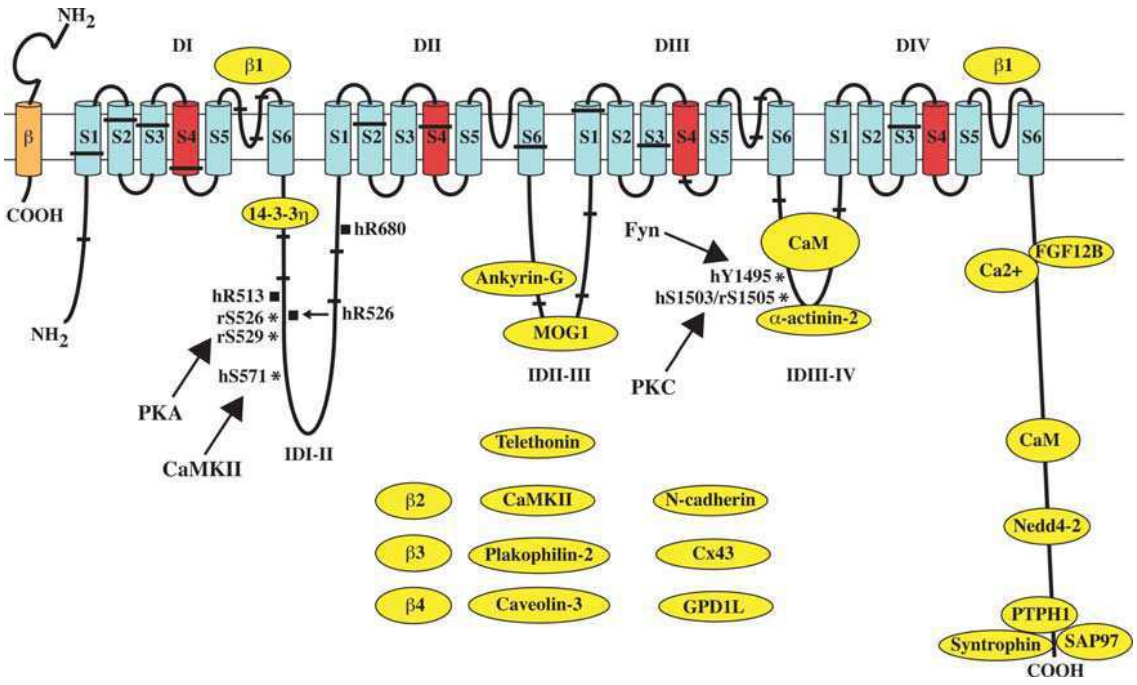

Figure 35: Schematic representation of $Na_v1.5$ and its modulating proteins
Rook M B. *et al*. Cardiovasc Res 2012[358]

III.3.1 Regulation of $Na_v1.5$ by beta subunits (Navβ)

Navβ subunits are single-segment transmembrane proteins with extracellular N-terminal, and intracellular C-terminal domains[359]. In humans, there are four types of Navβ (Navβ1-Navβ4) encoded by four genes, *SCN1B* to *SCN4B*. All are expressed in the heart[7,102]. In cardiomyocytes, Navβ subunits are mainly localized at the T-tubules/Z-lines, and intercalated discs[352,360,361].

Navβ subunits associate with the $Na_v1.5$ α-subunit and modulate its subcellular localization, surface expression as well as its biophysiological properties. Moreover, Navβ subunits play a role in the adhesion of $Na_v1.5$ to the cytoskeletal proteins and extracellular matrix, and in the recruitment of enzymes, signalling molecules, and cytoskeletal adaptor proteins[359]. However, current data concerning the effects of Navβ subunits on $Na_v1.5$ are sometimes contradictory, probably owing to the various models used, or to differences in experimental conditions. In addition, the specific site(s) of interaction between Navβ subunits and $Na_v1.5$ remains unknown.

Until now, several mutations in the β-subunits have been reported in different hereditary cardiac arrhythmias, supporting the role of Navβ in normal cardiac electrical activity. Such arrhythmias include cardiac conduction diseases (CCD) (*SCN1B*[327]), AF (*SCN1B*[98,99], *SCN2B*[98], *SCN3B*[101,102]), BrS (*SCN1B*[99,100,327], *SCN2B*[339], *SCN3B*[329,362]), idiopathic ventricular fibrillation (IVF) (*SCN3B*[363]), and LQTS (*SCN4B*[364]). All of these mutations associated with CCD, BrS, IVF, and AF have a loss-of-function effect on I_{Na}, which is a typical mechanism underlying this kind of *SCN5A* channelopathy. In contrast, the mutation in Navβ4 increases the late sodium current, the same effect as reported for *SCN5A* mutations linked to type III LQTS.

Most of these mutations are localized within the extracellular N-terminal region of the β-subunits, suggesting the importance of this region in the interaction with and regulation of $Na_v1.5$.

- **Navβ1**

The *SCN1B* gene encodes two splice variants, called β1 and β1B, both expressed in the human heart[7,365]. The β1B subunit does not contain the transmembrane domain, and is a secreted protein[366,367]. The Navβ1 transcript is highly expressed in the human heart compared to Navβ2 and Navβ3 subunits, with two-fold expression in the atrium compared to the ventricles[7]. Moreover, higher expression of Navβ1 transcript in the endocardium than the

epicardium has been observed[7]. The β1-subunit co-immunoprecipitates with $Na_v1.5$[360], and co-localizes with it within the ER[368], suggesting a role for the β1-subunit in the transport of $Na_v1.5$ to the membrane. Several studies suggested that the interaction between Navβ1 and $Na_v1.5$ could occur at several sites, between the extracellular domain of β1 and the extracellular loops S5-S6 of DI, DIV[369,370], but also between the carboxyl termini of the two subunits[371,372].

In cardiomyocytes, phosphorylation of the amino acid tyrosine 181 in the C-terminal domain of the β1-subunit determines its subcellular localization. The phosphorylated β1-subunits co-localize with $Na_v1.5$, connexin-43 and N-cadherin at the intercalated discs, whereas the non-phosphorylated subunits are present at the T-tubules[361].

The effects of the β1-subunit on $Na_v1.5$ in heterologous expression systems are variable, depending on the cellular model used. However, most studies have demonstrated an increase in peak I_{Na} density[373–376], positive shift of steady-state inactivation[360,376,377], and decreased I_{NaL}[377,378].

In contradiction, in dissociated *SCN1B*-null cardiomyocytes[379], increased peak I_{Na} and I_{NaL} have been observed, with slowed repolarization. These results are consistent with the observed increase in mRNA and $Na_v1.5$ protein expression, and the prolonged QTc interval and slow heart rate seen in this model. However, no change in $Na_v1.5$ gating properties was observed. In addition to its cardiac features, this model has neurological abnormalities like ataxic gate and seizures, resulting from the dysregulation of the neuronal sodium channels ($Na_v1.1$, 1.3, 1.6)[380].

Discrepancies between the results obtained in the heterologous systems and in the animal model highlight the limitations of the two approaches, and suggest that the heterologous systems may not be the ideal model to mimic the physiological environment of the channels in cardiomyocytes, especially considering the existence of multiple partners.

Mutations in the *SCN1B* gene have been reported in patients with CCD[327], BrS[99,100,327], or AF[98,99]. Co-expression of all these mutant β1-subunits with $Na_v1.5$ in heterologous systems showed decreased peak I_{Na} compared to the co-expression with the WT β1-subunit, suggesting a role for β1-subunits in sarcolemmal expression of $Na_v1.5$. These results are consistent with the I_{Na} reduction observed for all BrS and CCD *SCN5A* mutations, and some *SCN5A* mutations linked to AF.

- **Navβ2**

The Navβ2 subunit co-immunoprecipitates and co-localizes with $Na_v1.5$ at the intercalated discs in cardiomyocytes [352,360]. The Navβ2 subunit is present in human heart, but at lower levels compared to Navβ1[7]. The functional effects of Navβ2 are variable. In several studies, co-expression of Navβ2 with $Na_v1.5$ had no effect on the sodium current[360,368,381], while in one study the modulation of $Na_v1.5$ by Navβ2 depended on the sialylation status of Navβ2[382]. When completely sialylated, Navβ2 caused a negative shift of activation of $Na_v1.5$. Mutations in the *SCN2B* gene have been reported in patients with AF[98] or BrS[339]. The BrS mutation is a C-terminal mutation that decreased the peak I_{Na} by decreasing the surface expression of $Na_v1.5$, without affecting its gating properties[339]. The AF mutations are located in the extracellular N-terminal domain and are also associated with decreased I_{Na} peak but with a positive shift in steady-state-activation[98]. Since the Navβ2 subunits do not co-localize with $Na_v1.5$ in the ER[368], the reduced peak I_{Na} density and surface expression of $Na_v1.5$ with the Navβ2 mutants suggest a role for Navβ2 in the stability of $Na_v1.5$ at the membrane.

- **Navβ3**

Like the other Navβ subunits, there is a discrepancy in the functional effects of Navβ3 on $Na_v1.5$, depending on the expression systems utilized. In Xenopus oocytes, Navβ3 increased the peak I_{Na} density, caused a positive shift of steady-state inactivation, and enhanced the recovery from inactivation[374]. However, co-expression of Navβ3 in CHO and HEK cells showed no effect on the peak I_{Na}, with negative shift of steady-state inactivation [363,378], decreased the late current, and slowed recovery from inactivation in CHO cells[378]. *SCN3B* knockout mice showed results that are concordant with those observed in Xenopus oocytes. The isolated cardiomyocytes from these mice present with decreased peak I_{Na} density and negative shift of steady-state inactivation[383].

Mutations in Navβ3 have been reported in BrS[329,362], IVF[363], SIDS[384] and AF[101,102]. Most of these mutations are located in the extracellular amino terminus of Navβ3, and all lead to decreased I_{Na} density, with alteration in gating properties for some mutations. Moreover, a reduced surface expression of $Na_v1.5$ induced by the Navβ3 mutants has been found[329,362,363]. These results implicate a role for Navβ3 in the regulation of surface expression and the gating properties of Nav1.5, as well as the importance of its N-terminal domain in these functions.

- **Navβ4**

The Navβ4 subunit co-immunoprecipitates with $Na_v1.5$[364]. Co-expression of the Navβ4 subunit with $Na_v1.5$ does not modify the peak I_{Na}, but leads to a negative shift in the steady-state inactivation[364,384]. The contribution of Navβ4 in cardiac diseases was revealed by the identification of *SCN4B* mutations linked to LQTS[364], and SIDS[384].

The first *SCN4B* mutation (L179F) is located in the transmembrane domain of the Navβ4 subunit, and was identified in a family with LQTS and a history of unexpected and unexplained sudden death[364]. Another C-terminal *SCN4B* mutation (S206L) was linked to SIDS[384]. Co-expression of these mutants with $Na_v1.5$ in HEK293 cells resulted in an increase in I_{NaL} with a positive shift in the steady-state inactivation[364,384]. Adenovirus infection of adult rat ventricular myocytes with the mutant S206L confirmed the results obtained in HEK293 cells[384]. The S206L infected cardiomyocytes displayed increased I_{NaL} with longer AP duration compared to WT infected cardiomyocytes[384]. These results are consistent with the underlying mechanism of LQTS.

III.3.2 Anchoring-adaptor proteins

- **α1-Syntrophin**

The cardiac sodium channel $Na_v1.5$ is a part of the dystrophin multiprotein complex[385]. It has been shown by pull-down studies that $Na_v1.5$ interacts with dystrophin and utrophin by the adaptor protein syntrophin[386,387]. This interaction occurs *via* the three last C-terminal amino acids of $Na_v1.5$, Serine-Isoleucine-Valine, which form the PDZ binding motif of $Na_v1.5$[386] (Figure 35). The dystrophin-syntrophin-$Na_v1.5$ complex is mainly localized at the lateral membrane of cardiomyocytes (Figure 34)[353]. In the cardiomyocytes of dystrophin-deficient mice, both total $Na_v1.5$ protein expression and sodium current were decreased[386]. Moreover, immunostaining studies showed reduced lateral membrane expression of $Na_v1.5$, without affecting the $Na_v1.5$ expression at the intercalated discs[353]. These loss-of-function effects on $Na_v1.5$ are in line with the conduction defect seen in this model, demonstrated by the prolongation of the QRS complex[386]. Recently, J. S. Rougier *et al* demonstrated that the reduction in total protein expression is due to a proteosomal degradation of $Na_v1.5$[388]. Interestingly, in the heart of dystrophin-deficient mice, increased expression of utrophin was observed, suggesting a compensating mechanism. Moreover, mice lacking both dystrophin and utrophin showed more pronounced loss-of-function effects of $Na_v1.5$ compared to dystrophin deficient mice[387].

The importance of the interaction between $Na_v1.5$ and syntrophin is further emphasized by the identification of LQTS mutations (LQT12) in the *SNTA1* gene encoding α1-syntrophin. These mutations increased peak I_{Na} and I_{NaL}[389,390].

- **SAP97**

SAP97 (Synapse Associated Protein 97) is one of the MAGUK proteins (Membrane-Associated Guanylate Kinase) that are characterized by the presence of multiple domains for protein-protein interactions including PDZ domains[391]. MAGUK proteins have an important role in the organization of several ion channels through the formation of multi-protein complexes. MAGUK proteins are involved in the targeting, trafficking and localisation of ion channels in the brain[392] and in the heart[353,393–396].

In cardiomyocytes, SAP97 and ZO-1 (zonula occludens) are the major MAGUK proteins[394]. Petitprez *et al* have demonstrated that the PDZ domains of SAP97 interact with the PDZ binding motif of $Na_v1.5$, and that $Na_v1.5$ and SAP97 are co-localized at the intercalated discs of cardiomyocytes, but not at the lateral membrane like the syntrophin-dystrophin complex[353] (Figure 34). Silencing of SAP97 leads to decreased surface expression of $Na_v1.5$ and I_{Na} current in HEK cells and cardiomyocytes, suggesting a role for SAP97 in the regulation of $Na_v1.5$ surface expression[353].

Moreover, SAP97 interacts with the $K_v4.2/3$[393] (I_{to} current), $K_v1.5$[394,395] (I_{kur} current), and Kir2.x[396] potassium channels. These interactions enhance channel expression at the plasma membrane of cardiomyocytes.

Recently, our team has identified mutations in the *DLG1* gene encoding SAP97 in BrS patients. Functional studies of these mutations showed loss-of-function effects on I_{Na} current, and gain-of-function effects on I_{to} current, resulting in a net increased repolarizing current, a mechanism that underlies BrS (Kattygnarath *et al*, unpublished data). These results, along with the fact that multiple channels interact with SAP97, suggest that $Na_v1.5$ is part of multichannel protein complexes, and that SAP97 is a key partner in the formation of these complexes, regulating the targeting of ion channels to specific compartments in cardiomyocytes. Moreover, SAP97 becomes a new susceptibility gene for BrS.

- **Ankyrin-G**

Ankyrins are membrane-cytoskeleton adaptor proteins that anchor membrane proteins to the actin and spectrin cytoskeleton. There are three ankyrin genes (*ANK1*, *ANK2*, and *ANK3)*, encoding three different ankyrin proteins (ankyrin-R, ankyrin-B and ankyrin-G).

Ankyrin-B and ankyrin-G are present in the heart[397]. Mutations in the *ANK2* gene have been linked to LQT4[237]. Nevertheless, there is no data suggesting a direct regulation of $Na_v1.5$ by ankyrin-B. However, there is a direct interaction between ankyrin-G and the ankyrin-binding motif in the cytoplasmic linker II-III of $Na_v1.5$[315,398,399]. In cardiomyocytes, ankyrin-G colocalizes with $Na_v1.5$ at intercalated discs and in T-tubules[315]. A mutation in the ankyrin-G binding-motif of $Na_v1.5$ (E1053K) has been identified in a patient with BrS[315]. E1053K abolishes the $Na_v1.5$-ankyrin-G interaction, and disrupts the localization of $Na_v1.5$ at the cardiomyocyte membrane[315].

Silencing of ankyrin-G in cardiomyocytes leads to a decrease in total and surface $Na_v1.5$ expression, localization of $Na_v1.5$ in the perinuclear region, and a decrease of total I_{Na}[399]. So far, no mutations in the *ANK3* gene have been reported.

- **MOG1**

The *RANGFR* gene encodes MOG1 (multicopy of suppressor gsp1), a small protein of 28-kDa. High mRNA levels of this ubiquitously expressed gene was observed in cardiac tissue. This protein plays a role in nuclear protein trafficking *via* its interacion with GTP binding nuclear protein Ran[400]. By yeast two-hybrid assays, Wu *et al* demonstrated that MOG1 is a partner of $Na_v1.5$[401]. The interaction between MOG1 and $Na_v1.5$ was further confirmed by *in vitro* pull-down assays, and by co-immunoprecipitation studies in both HEK293 and cardiac cells. MOG1 interacts with the linker II-III of $Na_v1.5$ (Figure 35), and the two proteins colocalize at the intercalated discs of cardiomyocytes. Over-expression of MOG1 in neonatal cardiomyocytes, or co-expression of MOG1 with $Na_v1.5$ in HEK293 cells increases the I_{Na} density. The increased current density is due to enhanced surface expression of $Na_v1.5$. Recently, the MOG1 mutation E83D was reported in a patient with a history of syncope and cardiac arrest, who displayed a type 1 BrS ECG pattern after resuscitation[402]. In HEK293 cells stably expressing $Na_v1.5$, expression of E83D mutant alone or with WT MOG1 failed to increase the peak I_{Na} density, suggesting a loss-of-function effect of the mutant on $Na_v1.5$ and a dominant-negative effect on the WT MOG1. Immunostaining studies of adult rat cardiomyocytes transfected with the mutant MOG1 showed decreased surface expression of $Na_v1.5$ compared to the WT, indicating abnormal trafficking of the channel.

- **α-Actinin-2**

Four α-actinin isoforms are encoded by four distinct genes; they are members of the F-actin cross-linking protein family which includes spectrin and dystrophin. These proteins are

involved in many physiological functions, including binding of the transmembrane proteins to the actin filament network. α-Actinin-2 interacts with the linker III-IV of $Na_v1.5$, and increases the I_{Na} density in a heterologous expression system by enhancing the surface expression of $Na_v1.5$, without affecting the biophysical properties of the channel. Immunostaining studies on human ventricular cardiomyocytes showed that α-actinin-2 colocalizes with $Na_v1.5$ at the sarcomeric Z-lines[403]. Thus, α-actinin-2 could stabilize $Na_v1.5$ channels at specific cellular membrane compartments by its direct interaction with the channels or through other α-actinin-2-associated proteins.

III.3.3 Enzymes interacting with and modifying the channel

- **Ubiquitin-protein ligases of the Nedd4/Nedd4-like family**

The ubiquitin-protein ligase enzymes (E3s enzymes) covalently link ubiquitin, a small protein of 76 amino acids, to target proteins. Ubiquitination of membranous proteins leads to their internalization, then to their degradation by the lysosome or proteasome systems, or to their de-ubiquitination by specific proteases and recycling back to the membrane[404]. The Nedd4/Nedd4-like proteins are a family of nine different enzymes, where Nedd4-2 is the isoform with the highest expression level in human heart[405].

The Nedd4-like ligases bind specifically to the PY motif (proline, tyrosine (xPPxY)) in the C-terminal domain of $Na_v1.5$[406–408], as well as those motifs in other cardiac ion channels[405,408,409]. By yeast-two hybrid and GST-pulldown[407], it has been demonstrated that the ubiquitin-protein ligase Nedd4-2, a member of Nedd4/Nedd4-like family, binds to $Na_v1.5$. Nedd4-2 and $Na_v1.5$ co-expression leads to channel internalisation without affecting total $Na_v1.5$ protein expression, and decreased I_{Na} current[406–408]. Moreover, it has been shown that under basal conditions, a fraction of $Na_v1.5$ channels is ubiquitinated, both in HEK293 cells and in mouse heart[407]. These results suggest that the Nedd4-2 ligase modulates the surface expression of $Na_v1.5$, however, the exact mechanism underlying this modulation remains to be elucidated.

- **$Ca2^+$/calmodulin-dependent protein kinase II (CaMKII)**

CaMKII is a serine/threonine protein kinase, which has an important role in intracellular Ca^{+2} signaling, by transducing the increased intracellular Ca^{+2} into multiple proteins phosphorylation, including the cardiac ion channels[410]. $Na_v1.5$ is regulated by CaMKII, which co-immunoprecipitates with and phosphorylates $Na_v1.5$, resulting in

alteration of its gating properties[411,412]. However, the results concerning CaMKII effects on $Na_v1.5$ are conflicting. It has been shown that adenovirus-mediated over-expression of CaMKIIδc, the prominent cardiac isoform, in rabbit ventricular cardiomyocytes led to a negative shift of steady-state inactivation, enhanced intermediate inactivation and slow recovery from inactivation, and increased late I_{Na}[411]. Another study showed that the inhibition of CaMKII in rat ventricular myocytes by KN93, a selective antagonist of CaMKII, has the same effects, with a decreased late current[412]. This discrepancy may be due to differences in expression systems, procedures or protein isoforms used in different studies. It has been recently shown that CaMKIIδc interacts with the linker I-II of $Na_v1.5$, and phosphorylates the serine S516 and threonine T594 residues[413].

- **Protein tyrosine kinase Fyn and protein tyrosine phosphatase PTPH1**

The tyrosine kinase Fyn, which belongs to Src family tyrosine kinase, phosphorylates the tyrosine Y1495 located in the linker III-IV, beside the IFM-motif involved in $Na_v1.5$ inactivation[414] (Figure 35). Phosphorylation of Y1495 leads to a positive shift in the steady-state inactivation, and enhanced recovery from inactivation. However the site of interaction of tyrosine kinase Fyn on $Na_v1.5$ is unknown. Tyrosine phosphatase PTPH1 interacts directly with $Na_v1.5$ *via* the PDZ domain[415]. In HEK293 cells, co-expression of PTPH1 leads to negative shift of steady-state inactivation, this effect depending on the integrity of the SIV motif of $Na_v1.5$[415]. The effect of PTPH1 on $Na_v1.5$ is opposite to that of the tyrosine kinase Fyn, suggesting that the balance between tyrosine kinases (such as Fyn) and phosphatases (such as PTPH1), may regulate the degree of $Na_v1.5$ phosphorylation, and by this way the channel inactivation.

III.3.4 Proteins that modulate the biophysiological properties of $Na_v1.5$ upon binding

- **Calmodulin (CaM)**

The C-terminal domain of $Na_v1.5$ has an IQ motif (IQxxxRxxxxR), which forms the binding motif of the CaM, a ubiquitous Ca^{+2}–sensing protein that has a role in several cellular processes[416–418]. CaM interacts also with the linker III-IV of Nav1.5[419,420] (Figure 35). However, there is a discrepancy in the functional effects of CaM on $Na_v1.5$. Steady-state inactivation and entry into slow inactivation have been shown to be either decreased, increased, or not changed[416,417,419–421]. Another study showed that CaM results in negative

shift of the voltage dependence of activation without affecting the inactivation[422]. It has been proposed that, at basal Ca^{+2} concentration, CaM binds to the IQ motif of $Na_v1.5$. When the Ca^{+2} level increases, the CaM binds to Ca^{+2}, resulting in CaM conformational changes that weaken the interaction between CaM and the IQ motif. The dissociated CaM can then bind to CaMKII or to the other CaM binding domain in the linker III-IV[423]. The interaction with the linker III-IV will inhibit channel inactivation[419,420]. Moreover, when CaM is released, the IQ motif can interact with EF-hand Ca^{+2} binding domain located in the proximal C-terminal region of $Na_v1.5$, and this interaction enhances the affinity of EF domain to Ca^{+2} [423].

- **Telethonin**

Telethonin is a small sarcomeric protein shown to be a partner of $Na_v1.5$ by immunofluorescence and co-immunoprecipitation studies in mouse heart tissue, but its interaction site on the channel remains unknown[424]. Telethonin is mainly expressed in striated muscles[425], but expression in smooth muscles of the gastrointestinal tract was also observed[424]. Mutations in the *TCAP* gene, encoding telethonin, have been reported in limb girdle muscular dystrophy (LGMD2G) and hypertrophic and dilated cardiomyopathies[426,427]. Another mutation in *TCAP*, R76C, was found in a patient with intestinal pseudo-obstruction[424]. In the human gastrointestinal tract, $Na_v1.5$ is expressed in the smooth muscle cells and in the interstitial cells of Cajal (ICC)[428], which generate active pacemaker currents responsible for smooth muscle contraction. Interestingly, expression of the R76C mutant with the $Na_v1.5$ channel in a heterologous expression system caused a negative shift of the voltage-dependent activation and increased the window sodium current. Moreover, silencing of telethonin in HEK293 cells stably expressing $Na_v1.5$, led to a positive shift in voltage-dependent activation of I_{Na}[424], suggesting that the R76C mutation enhances the effect of telethonin on $Na_v1.5$[424]. However, no cardiac phenotype was observed in the patient carrying the R76C mutation.

- **Glycerol phosphate dehydrogenase 1-like protein (GPD1L)**

The GPD1L, encoded by the *GPD1L* gene, is homologous to glycerol phosphate dehydrogenase (GPD1) that catalyzes the reversible conversion of glycerol-3-phosphate (G3P) to dihydroxyacetone phosphate (DHAP), however the function of GPD1L is unknown. This gene on chromosome 3p24 has been linked to BrS by linkage analysis in a large multigenerational family, and a mutation cosegregating with a BrS phenotype in this family has been identified[429,430]. Since then, mutations in *GPD1L* have been reported in subjects

from a cohort with SIDS[431]. Functional analysis of these mutations showed a loss-of-function effect on $Na_v1.5$, by decreasing I_{Na} through the reduction of $Na_v1.5$ surface expression. Two more recent studies have demonstrated that the modulation of I_{Na} by GPD1L occurs *via* the protein kinase C (PKC)[432,433]. In HEK293 cells, when co-expressing the GPD1L mutant and $Na_v1.5$, the decrease in the surface expression of $Na_v1.5$ and in I_{Na} was dependent on the phosphorylation of serine 1503 by PKC[432], a process already known to decrease I_{Na} [434]. In addition, it has been shown that there is an interaction between $Na_v1.5$ and GPD1L, and that the mutations did not affect this interaction, but the enzymatic activity of GPD1L[432]. However, the site of interaction of GPD1L on $Na_v1.5$ remains unknown. Another study showed that the reduction of I_{Na} caused by the mutant GDP1L can be reproduced by adding an activator of PKC or NADH, and inhibited by an inhibitor of PKC or of NAD^+ [433]. The phosphorylation of the channel by the PKC/GPD1L could thus constitute a link between the metabolic state of the cell and its excitability by modulating the sodium current.

- **14-3-3η protein**

The 14-3-3 dimeric cytosolic adaptor proteins interact with a wide variety of other proteins and are involved in the regulation of cell signaling pathways and ion channels[435]. An interaction between the 14-3-3η channel and $Na_v1.5$ was revealed by yeast two-hybrid assay and confirmed by co-immunoprecipitation studies[436]. This protein binds to the cytoplasmic loop DI-DII of $Na_v1.5$ (Figure 35) and co-localizes with $Na_v1.5$ at the intercalated discs of cardiomyocytes. Co-expression of 14-3-3η with $Na_v1.5$ in COS cells led to a negative shift in steady-state inactivation and slowed recovery from inactivation. However, the peak current density was not affected. These results indicate that 14-3-3η could alter the biophysical properties of $Na_v1.5$ but not its trafficking, at least in COS cells[436]. Different isoforms of the 14-3-3 protein family are present in the heart, thus further studies are needed to define the exact role of these cardiac isoforms and their possible implication in heart diseases[436].

- **Plakophilin-2 and desmoglein-2**

Plakophilin-2 and desmoglein-2 are desmosomal cardiac proteins encoded by the genes *PKP2* and *DSG2*, respectively. The association of plakophilin-2 with the $Na_v1.5$ channel was demonstrated by GST-pulldown assay and co-immunoprecipitation studies[437]. Immunostaining analysis showed co-localization of the two proteins at the intercalated discs of cardiomyocytes. Silencing of plakophilin-2 by shRNA in adult rat cardiomyocytes significantly decreased the sodium current density, negatively shifted the steady-state

inactivation, increased the time needed for the recovery from inactivation of $Na_v1.5$, and slowed the action potential propagation[437]. These results were confirmed in the heterozygous knockout mouse model of *PKP2*, where isolated ventricular cardiomyocytes showed a decrease in the sodium current and an accelerated inactivation of $Na_v1.5$[438]. Mutations in *PKP2* have been reported in arrhythmogenic right ventricular cardiomyopathy (ARVC)[439]. Recently, mutations in *PKP2* have been identified in patients with BrS[305]. In the HL-1 derived cardiac cell line, knockdown of *PKP2* led to decreased I_{Na} and decreased localization of $Na_v1.5$ at the intercalated discs. Transfection of PKP2-deficient HL-1 cells with WT PKP2, but not the mutants, restores the functional defects of $Na_v1.5$[305]. The same rescue experiment was performed in human induced pluripotent stem cell cardiomyocytes from an ARVC patient with a homozygous loss-of-function *PKP2* mutation[305]. These results confirm the role of PKP2 in the regulation of $Na_v1.5$, and add a new candidate gene to the list of BrS genes.

Regarding desmoglein-2, a recent study by Rizzo *et al* showed an interaction between desmoglein-2 and $Na_v1.5$ by co-immunoprecipitation studies performed in mouse heart lysate[440]. Mutations in *DSG2* also cause ARVC[439]. Using a mouse model of ARVC over-expressing the mutant desmoglein-2 N271S, reduced I_{Na} was observed in cardiomyocytes without changes in biophysical properties[440].

The site(s) of interaction of these desmosomal proteins on $Na_v1.5$ is (are) still unknown, and the role of these proteins in the targeting or maintenance of channels in the desmosomes remains unclear. Nevertheless, these results indicate that the presence of plakophilin-2 and desmoglein-2 at the intercalated discs are necessary for the proper function of $Na_v1.5$.

- **Caveolin-3**

The function of $Na_v1.5$ is regulated by β-adrenergic stimulation. Stimulation of the β-adrenergic receptor by isoproterenol increases I_{Na}. It has been proposed that this increase in I_{Na} is due to two mechanisms: one is protein kinase A-dependent (PKA-dependent), the other is PKA-independent.

PKA stimulation induces phosphorylation of the serine at the position 526 and 529 in the linker I-II of $Na_v1.5$[441–443] (Figure 35). In addition to these phosphorylation sites, the linker I-II has three ER specific retention motifs (RXR) that could interact with ER chaperon proteins preventing the trafficking of $Na_v1.5$. Elimination of these various motifs either reduces or abolishes the effect of PKA on $Na_v1.5$. This suggests that the phosphorylation of $Na_v1.5$ by the PKA and the presence of these motifs are required for the PKA effects, and that

phosphorylation could hide these retention motifs and allow the transport of $Na_v1.5$ to the membrane[444].

Isoproterenol is also able to increase I_{Na} in the presence of a PKA inhibitor[445]. The time needed for this effect is short (less than 10 minutes), and the effect is reversible upon washing of the β-agonist, suggesting that $Na_v1.5$ proteins could be in a storage compartment and could be released following adrenergic stimulation. Then, it was suggested that caveolae could underlie this PKA-independent mechanism[446]. Caveolae are small invaginations of the plasma membrane, rich in several proteins, including ion channels, and play an important role in cell signaling, protein trafficking and cholesterol homeostasis[447]. Caveolin proteins represent important components of caveolae, and caveolin-3 is the main caveolin expressed in cardiac myocytes[447]. It has been shown that caveolin-3 co-immunoprecipitates with $Na_v1.5$ in rat cardiac tissue[446] and in HEK293 cell lysates[448], but its site of interaction on $Na_v1.5$ remains unknown. Immunostaining studies demonstated co-localization of $Na_v1.5$ and caveolin-3 at the membrane of rat[446] and human cardiomyocytes[448]. Along with $Na_v1.5$, the α-subunit of the stimulatory heterotrimeric G-protein ($G\alpha_s$) is localized in the caveolar membrane[446]. The effect of $G\alpha_s$ on $Na_v1.5$ mimics β-adrenergic stimulation. Thus, it has been proposed that $Na_v1.5$ could be stored in the caveolae, and that activation of $G\alpha_s$ by adrenergic stimulation leads to the opening of the caveolae, resulting in increased expression of $Na_v1.5$ at the membrane. The inhibition of β-adrenergic effects on $Na_v1.5$ expression by a caveolin-3 antibody, supports this hypothesis[446].

Mutations in the *CAV3* gene, encoding caveolin-3, have been reported in patients with LQTS[448] and SIDS[449]. Functional studies of these mutations showed increased late current, which is in accordance with the phenotypes.

- **Fibroblast growth factor homologous factors (FHFs)**

The fibroblast growth factor homologous factors (FHF) constitute a subset of the fibroblast growth factor (FGF) family, however they are unable to stimulate the FGF receptors, and lack the N-terminal secretion signal sequences. Consequently, they are not secreted, but remain intracellular, and bind to the C-terminal domain of the voltage-gated sodium channels (VGSCs), and to islet-brain-2 (IB2), the neuronal mitogen activated protein (MAP) kinase scaffold protein[450]. The genes encoding the four FHFs (FHF1 to FHF4*)* are officially named *FGF12*, *FGF13*, *FGF11*, *FGF14*, respectively. They are mainly expressed in excitable cells, especially in the nervous system, and to a lesser extent in the heart[450]. Each FHF has multiple isoforms resulting from alternative promoter usage and 5′ alternative

splicing, leading to 10 FHF isoforms in humans that differ in the amino-terminal region[451] (Figure 36). Each isoform has N-terminal, core, and C-terminal regions (Figure 36). The core and the C-terminal regions of FHFs show high degrees of similarity between the various FHFs. In heterologous expression systems, differences in the localization of the two A and B isoforms have been observed. The A isoforms mainly have a nuclear localization, while the B isoforms are cytoplasmic and nuclear[451]. This is due to the presence of a nuclear localization signal in the A isoforms[452](Figure 36).

- **Interaction of FHF with the C-terminal domain of the VGSCs**

A yeast-two-hybrid screen for partners of $Na_v1.9$ was the first to demonstrate that FHF1B interacts with the C-terminal domain of $Na_v1.9$, a sodium channel expressed in nociceptive neurons[453]. Then further studies have showed that FHF1A, FHF1B, FHF2A, and FHF3A interact with the cardiac sodium channel $Na_v1.5$[454–456], FHF2B with the neuronal sodium channel $Na_v1.6$[457], and other FHFs with other VGSCs[455].

The exact interaction site of of FHF1B on $Na_v1.5$ is debated, located either in the proximal (amino acids 1773–1832)[454], or in the proximal and the distal parts of $Na_v1.5$ C-terminus (amino acids 1773–1908)[456]. Moreover, differences in the effects of FHF1B on $Na_v1.5$ were also observed[454,456]. In HEK293 cells, co-expression of FHF1B with $Na_v1.5$ leads to a negative shift of steady-state inactivation[454], or a positive shift of the steady-state inactivation of $Na_v1.5$[456].

Crystal structure of FHF2A demonstrates a conserved surface on the FHF core domain involved in the binding of VGSCs to the FHFs[455]. Thirteen residues at different positions in the protein sequence, conserved among the different FHF isoforms but not in FGF, constitute the VGSC binding site (Figure 36)[455]. Moreover, the alternatively spliced N-termini of FHFs have been excluded as binding sites with VGSCs, since the truncation of the N-terminal region of FHF isoforms FHF2A, FHF3A and FHF4B does not affect their interaction with the VGSCs[455]. Recent study has showed that the human *FGF12* polymorphism rs17852067 (P149Q), which is located in the core region but not in the previously reported binding sites to $Na_v1.5$, could also modulate the interaction of FHFs with the VGSCs[456], suggesting that multiple FHF sites could be involved in the VGSC interaction.

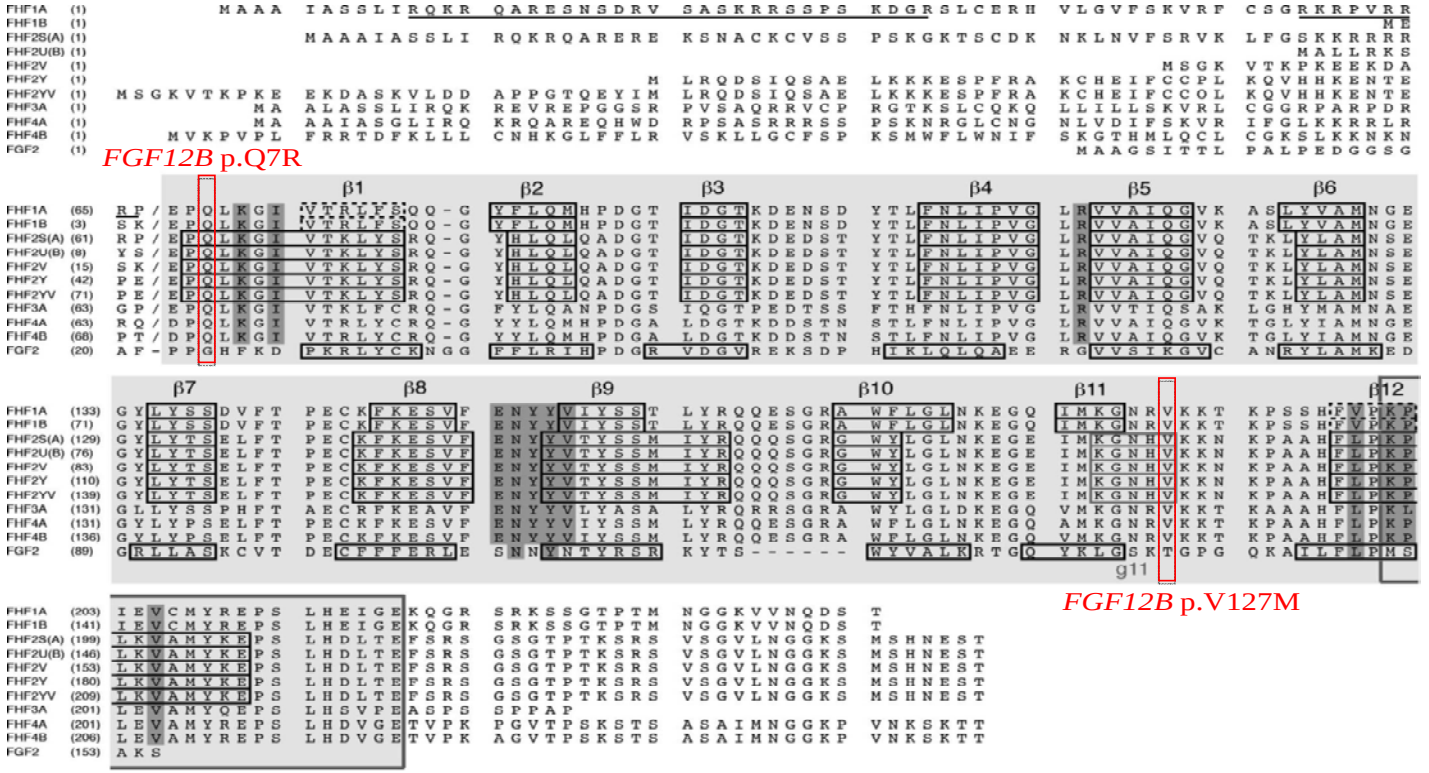

Figure 36: Structure-based sequence alignment of the 10 human FHF isoforms

For comparison, the sequence of fibroblast growth factor FGF2 is included in the alignment. Secondary structure elements (β1-β12, g11) are indicated above and below alignments, and residues containing these elements for known secondary structures are boxed. β1 and β12 strands of FHF1 are indicated by dashed boxes. A slash in each sequence marks the junction between alternatively spliced N-terminal region and FHF homology core region. The FHF homology core region is shaded in light gray, and the 18-residue-long C-terminal extension not shared with FGFs is indicated by a box drawn around the sequences. Residues of the FHF homology region engaged in channel binding are shaded in darker gray. Underlined residues in the FHF1A isoform indicate the nuclear localization sequences. p.Q7R: *FGF12B* BrS mutation identified by Hennessey J A. *et al*[304]. p.V127M: *FGF12B* variant identified in a BrS patient in our laboratory. Modified from Goetz R. *et al*. J Biol Chem 2009[455].

o Expression of the FHF isoforms in the heart

The cardiac expression of the different FHF isoforms was relatively unknown, until a recent study by GS Pitt's group[458], showing that *FGF13* is the most expressed FHF in adult mouse ventricular myocytes. By a quantitative reverse-transcriptase polymerase chain reaction (qPCR), using isoform-specific primers, they demonstrated that *FGF13-VY* is highly expressed in adult mouse cardiomyocytes. The *FGF13-V* and *FGF13-Y* isoforms are expressed at low levels, the other isoforms nearly undetectable (Figure 37A). However, at the protein level, only FHF2 (most probably FHF2-VY) could be detected. Very recent results from the same group[304], using qPCR on RNA from nonfailing human ventricular tissue, showed that in the human heart, *FGF12-B* is the main isoform, whereas *FGF12-A* was nearly undetectable (Figure 37B). The *FFG13-Y* and/or *FGF13-VY* (qPCR was unable to distinguish between these two isoforms) were the second most highly expressed isoforms (Figure 37B).

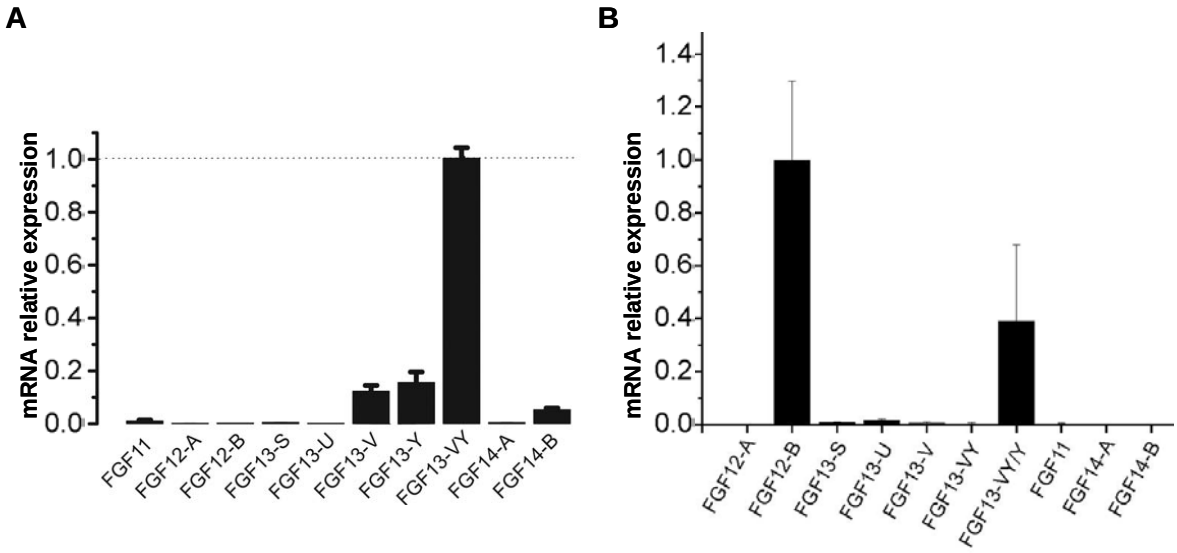

Figure 37: Relative mRNA expression of FHF isoforms in mouse (A) and human (B) cardiomyocytes
Modified from Wang C. *et al*. Circ Res 2011[458], and Hennessey J A. *et al*. Heart Rhythm 2013[304]

o The role of FHF in regulating $Na_v1.5$ channel function

In adult mouse cardiomyocytes, $Na_v1.5$ co-immunoprecipitated with FHF2, and co-localization of both proteins was observed at the lateral membrane and intercalated discs[458]. Silencing of *FGF13* in rat and mouse ventricular myocytes led to reduced peak I_{Na}, a negative shift of steady-state inactivation[304,458], and delayed recovery from inactivation of $Na_v1.5$[458]. Cell surface biotinylation of isolated cardiomyocytes showed decreased surface expression of $Na_v1.5$[458], accounting for the decreased I_{Na}, along with the altered biophysical properties.

However, silencing of *FGF13* does not affect the mRNA level or total protein expression of $Na_v1.5$, suggesting a role of FHF in the trafficking of $Na_v1.5$. Silencing of *FGF13* in neonatal rat ventricular myocyte monolayers showed a slowed conduction velocity compared to control myocytes. The reduced I_{Na} and delayed recovery from inactivation of $Na_v1.5$ could explain the conduction abnormality[458].

In addition to $Na_v1.5$, it has been shown that FHF2 regulates the L-type, voltage-gated Ca^{2+} channel ($Ca_v1.2$)[459]. *FGF13* knockdown decreases the Ca^{2+} current density with alteration in the localization of the α_{1C}, the $Ca_v1.2$ pore-forming subunit. FHF2 modulates the targeting of α_{1C} to the T-tubules[459], possibly through the protein junctophilin-2, a protein involved in the juxtaposing of the tubular $Ca_v1.2$ to the sarcoplasmic reticulum RyR2[460]. Silencing of *FGF13* leads to decreased surface expression of α_{1C} and decreased Ca^{2+} current density, without affecting the biophysical properties[459]. Moreover, decreased Ca^{2+} release from the sarcoplasmic reticulum was also observed. Measured action potentials from *FGF13* silencing adult rat ventricular cardiomyocytes showed decreased AP peak amplitude, with shortening of AP half-width, consistent with the loss-of-function effects on both $Na_v1.5$ and $Ca_v1.2$[459].

- **FHF genetics**

The role of the FHFs has been mainly studied in the nervous system, as the FHFs are highly expressed in the central and peripheral nervous systems[452], and several loss-of-function mutations have been identified in the *FGF14* gene in spinocerebellar ataxia 27 (SCA27), a hereditary neurodegenerative disease[461–464]. Functional studies of the first *FGF14* mutation identified in SCA27, F145S, in rat hippocampal neurons showed decreased neurological sodium current density, reduced Na^+ channels localization at the axon initial segment, and decreased neuronal excitability in a dominant-negative way[464]. A mouse model lacking *FGF14* showed an ataxia phenotype, which is in line with decreased Na^+ channel function and decreased neuronal excitability[465]. Moreover, it has been shown that double knockdown of both *FGF12* and *FGF14* leads to a severe ataxia phenotype[466].

The role of FHFs in heart disease is less well known, however, a very recent study reported a mutation in *FGF12-B* (Figure 36) in a patient with BrS[304]. The missense mutation Q7R was identified in a 61 years old male patient who had a suspicious ECG of BrS type during flecainide treatment for AF. Flecainide test to unmask BrS induced type 1 ECG pattern of BrS. The mutant Q7R has a reduced binding affinity for the C-terminal domain of $Na_v1.5$

compared to the WT. However, it does not affect the interaction of FHF1B with the junctophilin-2. In order to study the effects of this mutation on the sodium and calcium currents in the native environment where all the partners of $Na_v1.5$ are present, an *FGF13* shRNA strategy was used to supress the endogenous *FGF13* of adult rat cardiomyocytes. Then, *FGF13* was replaced by a WT or mutant *FGF12-B* human variant. In this system, knockdown of *FGF13* decreased the sodium and calcium current densities, with mislocalization of the $Ca_v1.2$, and negative shift of steady-state inactivation of $Na_v1.5$, in harmony with previous studies[458,459]. Replacement of *FGF13* by WT or mutant *FGF12-B* restored the calcium current density and the localization of $Ca_v1.2$. However, only the WT *FGF12-B* was able to restore I_{Na} and the negative shift of steady-state inactivation of $Na_v1.5$[304]. These results suggest that *FFG12-B*, the highly expressed FHF isoform in the human heart, is a new candidate gene in BrS. *FGF12-B* mutations could lead to BrS by affecting the sodium channel without perturbing the calcium channel, and vice versa. However, *FGF12-B* mutations affecting both the calcium and sodium channels could also be present.

THESIS OBJECTIVES

Mutations in *SCN5A*, the gene encoding the $Na_v1.5$ α-subunit, have been implicated in many inherited cardiac arrhythmias, which were firstly considered as separate clinical entities with distinct phenotypes. However, a wide spectrum of mixed disease phenotypes was recently reported in *SCN5A*-related arrhythmias, referred to as "overlap syndromes" of cardiac sodium channelopathy. In addition to their variable expression, they are characterized by incomplete penetrance. The reasons behind these two features remain unknown, but this suggests that other genetic and environmental factors, combined with specific altered biophysical properties of a given *SCN5A* mutation could play an important role in the modulation of the clinical phenotype. The main aim of my thesis work was to study such modulating factors. Moreover, since no mutation was found in 75% of BrS patients, I aimed to identify a new candidate gene in BrS.

The detailed objectives of my thesis work were around the following two axes:

1. By the functional characterization of two *SCN5A* mutations, and the screening analysis of common polymorphisms associated with AF and BrS in *SCN5A* mutation carriers, I tried to demonstrate how the specific alteration of the biophysical properties of a given mutation, combined with the genetic background of mutation carriers, could modulate the clinical picture.
2. By candidate gene approach in a group of patients with BrS, I searched for new mutations in a gene encoding a partner of $Na_v1.5$.

To carry out this project, I used several methodological approaches including different techniques of biochemical analysis and molecular biology, transfection in heterologous expression systems, and genotyping.

These methods, in addition to patch-clamp analysis, allowed us to demonstrate the involvement of three factors in modulating the phenotypic expression caused by *SCN5A* mutations: the interaction between the $Na_v1.5$ α-subunits (article 1), the mutant biophysical defects associated with the differences in the electrical properties between the atrial and ventricular cardiomyocytes, and the genetic background of the patients (article 2).

MATERIALS & METHODS

I. Functional studies

I.1 Expression vectors and site-directed mutagenesis

The plasmids used in our study are expression vectors designed for mammalian systems. Plasmids pcDNA3.1-SCN5A (no tag) and pcDNA3.1-GFP-SCN5A (N-terminal-GFP) were gifts from Dr H. Abriel (Bern, Switzerland). Plasmids pGFP-N3-SCN5A (C-terminal-GFP) and pRcCMV-FLAG-SCN5A (N-terminal-FLAG) were gifts from Dr F. Le Bouffant (Nantes, France) and Dr N. Makita (Nagasaki, Japan), respectively. The plasmid pcDNA3.1-HA-SCN5A (HA-WT) was a gift from Dr P. Mohler (Columbus, OH, USA). The plasmid pGFP-N3-SCN5A-ΔNter (C-terminal-GFP) was generated in our team by removing the first 381 nucleotides of *SCN5A* (127 amino acids), and replacing the residue 128 by a methionine. We created the plasmid pNter-IRES2-mRFP1 by cloning the sequence of the first 132 amino acids of $Na_v1.5$ into the pIRES2-mRFP1 vector carrying the red fluorescent protein (RFP) reporter gene. All plasmids contained the hH1a isoform of *SCN5A*. The plasmid pIRES2-acGFP1-FHF1B (C-terminal His_6-tag) was a gift from Dr G. S. Pitt (Durham NC, USA). Plasmid pcDNA3-CD4-KKXX was a gift from J. Mérot (Nantes, France). This plasmid was designed to express the CD4 protein carrying the ER retention KKXX.

- **Site-directed mutagenesis**

$Na_v1.5$ mutants R104W, R104K, R121W, R878C, R1860Gfs*12 and L1821fs*10, and FHF1B mutant V127M were prepared using the QuikChange II XL Site-Directed Mutagenesis Kit (Stratagene, USA) according to the manufacturer's instructions and were verified by sequencing. The principle of this technique is to introduce a mutation into the gene encoding the protein of interest. Briefly, each wild-type plasmid was amplified by PCR in its entirety with a pair of primers bearing the desired mutation in their center. Then the PCR products were subjected to enzymatic digestion with *Dpn*I. This endonuclease enzyme is specific for methylated DNA, and is used to digest the parental WT DNA template, which is methylated due to its production in bacteria, leaving only the newly PCR-synthesized mutated plasmid (not methylated). The primers used for each mutagenesis are listed in Table 7.

Primer	Sequence*	Length (nt)
SCN5A-R104W-F	GCAAGACCATCTTC**T**GGTTCAGTGCCACC	29
SCN5A-R104W-R	GTGGCACTGAACC**A**GAAGATGGTCTTGCC	29
SCN5A-R104K-F	GGCAAGACCATCTTC**AA**GTTCAGTGCCACCAAC	33
SCN5A-R104K-R	GTTGGTGGCACTGAAC**TT**GAAGATGGTCTTGCC	33
SCN5A-R121W-F	CCTTCCACCCCATC**T**GGAGAGCGGCTGTG	29
SCN5A-R121W-R	CACAGCCGCTCTCC**A**GATGGGGTGGAAGG	29
SCN5A-R878C-F	TCAGGCCTGCTGCCT**T**GCTGGCACATGATG	30
SCN5A-R878C-R	CATCATGTGCCAGCA**A**GGCAGCACGCCTGA	30
SCN5A-R1860Gfs*12-F	CTTTGCCTTCACCAAA**A**GGGTCCTGGGG	27
SCN5A-R1860Gfs*12-R	CCCCAGGACCC**T**TTTGGTGAAGGCAAAG	27
SCN5A-L1821fs*10-F	TTGCCGATGCCCTG**TCTG**AGCCACTCCGTAT	27
SCN5A-L1821fs*10-R	ATACGGAGTGGCT**CAGA**CAGGGCATCGGCAA	27
FGF12B-V127M -F	ATGAAGGGGAACAGA**A**TGAAGAAAACCAAGCC	32
FGF12B-V127M -R	GGCTTGGTTTTCTTCA**T**TCTGTTCCCCTTCAT	32

Table 7: Forward (-F) and reverse (-R) primers used for site-directed mutagenesis

*Mutated nucleotides are bolded, enlarged and in red; deleted nucleotides are in blue.

- **Bacterial transformation**

The newly synthesized mutated plasmids were transformed into the XL10-Gold strain of *E. coli*. The DNA was added to the competent bacterial cells and incubated on ice for 30 min. Bacteria were then transformed by a heat shock for 30 sec at 42°C. After 500 µL super optimal broth (SOC) medium was added to the bacteria, they were grown for 1h at 37°C with shaking at 225 rpm. This outgrowth step allows the bacteria to generate the antibiotic resistance proteins encoded on the plasmid backbone. The transformation mixture was then spread onto agar plates containing the appropriate antibiotic and cultured overnight at 37°C. Only the bacteria that received the plasmid were able to grow and form colonies. The following day, five colonies were selected and grown overnight at 37°C with 225 rpm shaking in liquid lysogeny broth (LB) medium containing the selection antibiotic.

- **Plasmid extraction**

From this bacterial culture, the extraction of the plasmid was carried out using the PureLink® Quick Plasmid Miniprep Kit (Life Technologies, USA). Bacterial cells were lysed using an alkaline/SDS procedure and the lysate was then applied to a silica membrane column that selectively binds the DNA. The plasmid was then eluted in water, and sequenced over the entire gene of interest, in order to verify the presence of the desired mutation and to ensure that no other mutation was inserted.

I.2 Heterologous expression systems and cell culture

The cell line HEK293 (Human Embryonic Kidney) was used as the main heterologous expression system for patch-clamp and biochemical analysis. Indeed, these cells are human and they do not express endogenous sodium channels. HEK cells were cultured in DMEM medium (Gibco, Life Technologies, USA) containing 10% fetal calf serum (FCS), 50 IU/ml penicillin, and 50 µg/ml streptomycin at 37°C in an incubator with 5% CO2. We also used a stable HEK293 cell line expressing the cardiac sodium channel $Na_v1.5$, which was a gift from Dr H. Abriel (Bern, Switzerland). This cell line was maintained in the same culture medium as previously described above, but also complemented with 25 g/ml of the selective antibiotic Zeocin (Life Technologies) in order to select for cells expressing the gene of interest. Cells were not kept in culture for more than 20 passages to maintain homogeneity of the results.

I.3 Transient transfection of HEK293 cells

The day before transfection, cells were plated into 6-well plates for patch-clamp analysis or into T25 flasks (25 cm^2) for biochemical analysis. When the cells reached 70-80% confluence, they were transfected using the cationic lipofectant JetPEI® (Polyplus Transfection, USA) according to the manufacturer's recommendations. The amounts of transfected plasmids are specified in each article. For patch-clamp recordings, 24h after transfection, cells were rinsed with phosphate buffered saline (PBS; Life Technologies), detached using 200 µl Trypsin-EDTA per well, resuspended in fresh medium and re-plated at a lower density on 35-mm petri dishes (suitable for the patch-clamp set up) to obtain single cells the next day. Biochemical analyses were performed 36 h after transfection.

In order to inhibit proteasome activity, cells were incubated with 1 µM of MG132, which is a specific, reversible and cell-permeable inhibitor of the 26S proteasome subunit, or with 0.1 % dimethyl sulfoxide (DMSO) as a control for 24 h before protein extraction.

I.4 Biochemical analysis

I.4.1 Total protein extraction

Forty-eight hours after transfection, HEK293 cells were washed twice with PBS and lysed in a RIPA lysis buffer (50 mM Tris pH 7.5, 500 mM NaCl, 1% NP40, 0.1% SDS, 0.5% deoxycholate), and complete protease inhibitor cocktail (Roche, Germany) for 1 h at 4°C with rotation. The soluble fractions from two subsequent 4°C 30-min 14 000 *g* centrifugations were then used for the experiments. To load each lane of the SDS-PAGE with equivalent amounts of total proteins, the protein concentration of each lysate was measured in duplicate by the Bradford assay using a BSA (Bovine Serum Albumin) standard curve.

I.4.2 Cell surface biotinylation

Cell surface biotinylation is a powerful tool designed to study cell surface protein expression. Biotin is a small vitamin efficiently reacting with primary amino groups to form stable amide bonds, and is subsequently used as a marker of labeled molecules. Since biotin has a small size, it does not disrupt the properties of the target molecule. Binding of biotin to primary amino groups is conferred by its ester group N-hydroxysuccinimide (NHS). Several different NHS esters of biotin are available, such as the Sulfo-NHS ester reagent that we used in our experiments (Figure 38). Since it is a water-soluble molecule, biotinylation experiments can be performed in the absence of organic solvents. In addition, as it is a charged molecule, thus unable to cross biological membranes, only primary amines present on the cell surface will be biotinylated. To purify the biotinylated proteins, we used neutravidin agarose resins. Neutravidin is a deglycosylated form of avidin, which is a tetramer with a strong affinity to biotin. The interaction between biotin and avidin represents one of the strongest existing non-covalent bonds. Finally, to elute the biotinylated proteins from the neutravidin resins, the biotin intramolecular disulfide bridge is reduced by Dithiothreitol (DTT) (Figure 39).

Forty-eight hours after transfection with WT or mutant constructs, HEK293 cells were washed twice with ice-cold PBS and incubated for 60 min at 4°C with PBS containing 1.5 mg/mL of EZ Link Sulfo-NHS-SS-Biotin (Pierce, USA). Plates were washed twice and then incubated for 10 min at 4°C with PBS with 100 mM glycine to quench unlinked biotin, and washed twice with PBS. Cells were then lysed for 1 h at 4°C with the lysis buffer described in the previous paragraph. After centrifugation at 14 000 *g* for 30 min at 4°C, supernatants were incubated with immobilized neutravidin beads (Pierce, USA) overnight at 4°C and pelleted by

centrifugation at 14 000 *g* for 1 min at 4°C. After three washes with lysis buffer, the biotinylated proteins were eluted with the Laemmli sample buffer complemented with 50 mM DTT at 37°C for 30 min. Biotinylated proteins were then analyzed by western blot. Glyceraldehyde 3-phosphate dehydrogenase (GAPDH) was used as a negative control of biotinylation, and transferrin receptor (TfnR), as a positive control.

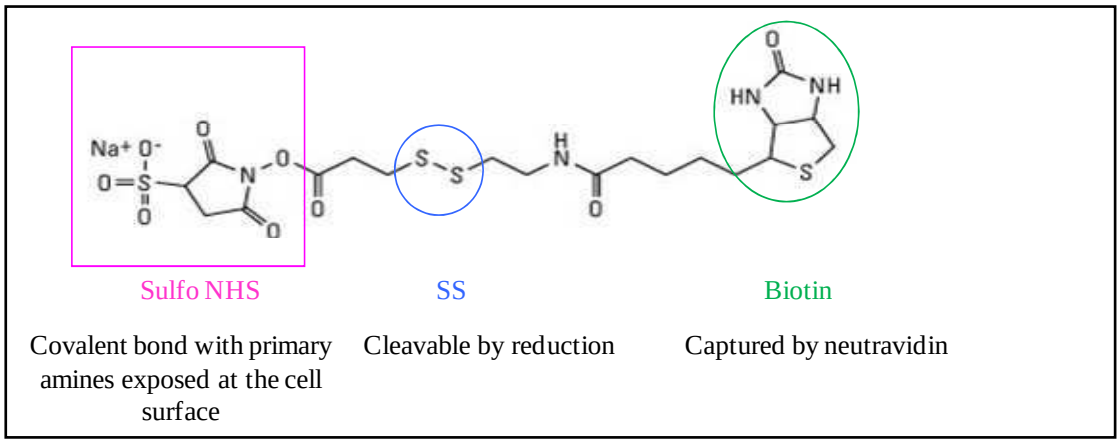

Figure 38: Structure of the EZ-Link™ SULFO-NHS-SS-Biotin
Modified from http://www.piercenet.com/product/ez-link-sulfo-nhs-ss-biotin-biotinylation-kits

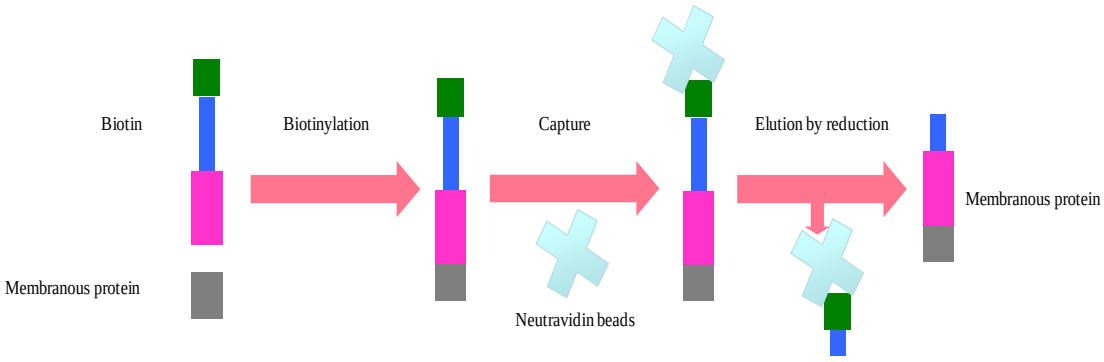

Figure 39: Principle of cell surface protein biotinylation

I.4.3 Immunoprecipitation

This technique aims to purify a protein of interest and its partners from a cell lysate. The total cell lysate containing the protein X is incubated with magnetic beads (Dynal, Norway) on which has been adsorbed an anti-X antibody allowing the specific precipitation of the protein X and its partners if X is part of a protein complex (Figure 40).

Forty-eight hours after transfection, HEK293 cells were washed with PBS and lysed in a specific lysis buffer (150 mM NaCl, 50 mM Tris-HCl, pH 7.5, 1% Triton, and complete

protease inhibitor cocktail). Cell pellets were pipetted up and down 20 times, flushed 20 times through a 22-gauge needle, incubated on a rotating wheel for 1 h at 4°C, and finally centrifuged for 10 min at 16 000 g. Magnetic beads were washed twice with PBS-tween 0.02%, incubated with the antibody against the protein of interest for 2 h at room temperature, washed twice again with PBS-tween 0.02%, and incubated with the pre-cleared lysates. Samples were incubated overnight at 4°C on a rotating wheel. After washing the beads four times with PBS-tween 0.02%, proteins were eluted with the Laemmli sample buffer at 37°C for 30 min with agitation, and analyzed by western blot.

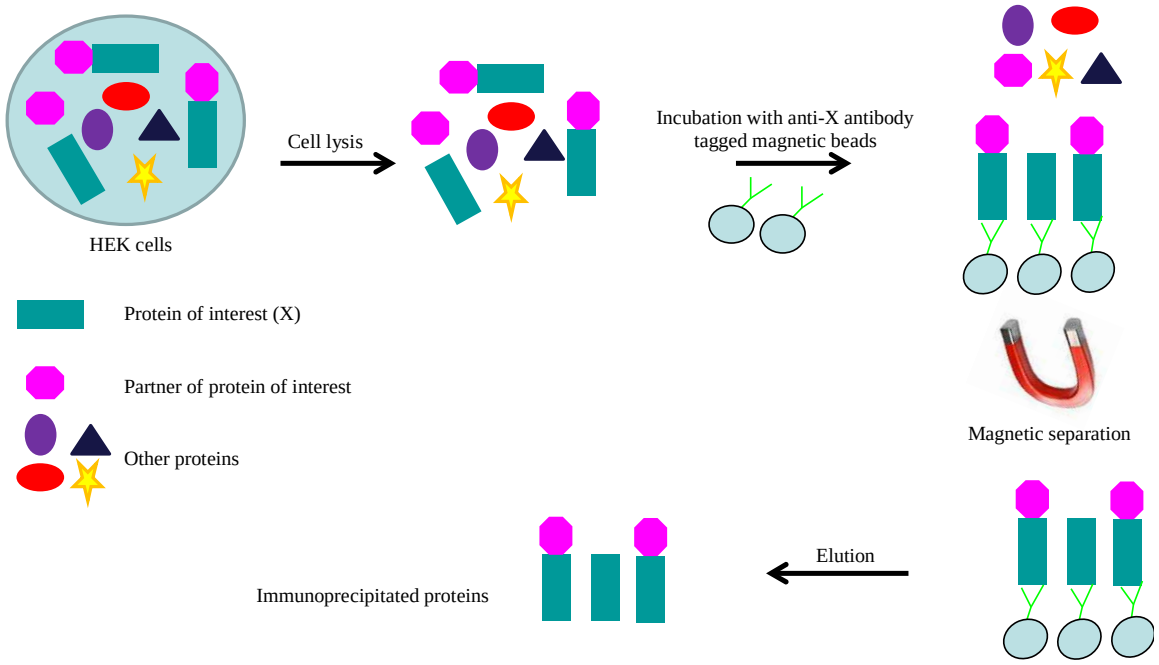

Figure 40: Principle of the immunoprecipitation technique

I.4.4 Western blot

After migration on a SDS-PAGE gel (8-16%), proteins were transferred to a nitrocellulose membrane (Life Technologies, USA) at a constant voltage of 36 V for 2 h. Aspecific sites of fixation were blocked by incubation of the membrane with 5% skim milk in PBS-Tween 0.1% for 1 h. The membrane was then incubated overnight with primary antibodies at 4°C diluted in block. The different antibodies used in our study are listed in Table 8. After three 10 min washes with PBS-Tween 0.1% and one with PBS, the membrane was incubated with infrared IRDye secondary antibodies (LI-COR Biosciences, USA), diluted to 1/10 000 in 5% skim milk in PBS-Tween 0.1%, for 1 h at room temperature and protected from light. After two 10 min washes with PBS-Tween 0.1% and two with PBS,

protein detection was performed using the Odyssey infrared imaging system (LI-COR Biosciences). Signals were quantified using the ImageJ software and normalized to WT levels.

Antibody	Species	Company	Working dilution
GFP	Rabbit	Torrey Pines Biolabs (USA)	1/2000
Flag	Mouse	Sigma (USA)	1/500
GAPDH	Rabbit	Abcam (UK)	1/2000
TfnR	Mouse	Life Technologies (USA)	1/500
6xHistidine	Mouse	QIAGEN (Germany)	1/2000
$Na_v1.5$	Rabbit	Alomone (Israel)	1/100
HA	Rat	Roche (Germany)	1/500

Table 8: Primary antibodies used in western blot

II. Molecular biology

II.1 Total RNA extraction

Total mRNA was extracted from frozen mouse or human hearts using TRIzol (Life technologies, USA) and the Pure link^{TM} RNA mini kit (Life technologies, USA). A small piece of frozen heart was homogenized in 500 µL of TRIzol, incubated 5 min at room temperature while vortexing to allow complete dissociation of nucleoprotein complexes. Then 200 µL of chloroform was added and samples were mixed vigorously by hand for 15 sec and incubated at room temperature for 1-2 min. Lysates were then centrifuged at 15 000 *g* for 10 min at 4°C. This step separates the RNA in the upper aqueous phase, from the DNA and protein in the middle and lower organic phases. RNAs were then precipitated in 70% ethanol and transferred to a spin column. After two washes, RNAs were eluted with RNase-free water.

II.2 RNA reverse transcription

This technique synthesizes complementary strand DNA (cDNA) from an RNA template using an RNA-dependent DNA polymerase (reverse transcriptase). The cDNA contains only the coding sequence of a gene and can be then amplified by PCR.

Here, we reverse-transcribed total RNA using oligo-dT primers, which are short sequences of deoxy-thymine nucleotides that bind to the RNA polyadenylate tail, providing a free 3'-OH end that can be extended by the reverse transcriptase enzyme to create the complementary DNA strand. Then the RNAse enzyme was added to remove the original template mRNA, leaving single stranded cDNA (sscDNA) (Figure 41). This sscDNA could then be converted into a double stranded DNA (dscDNA) by the DNA polymerase.

We used the reverse-transcription kit SuperScript® III First-Strand Synthesis System (Life Technologies, USA). We utilized 1µg of total RNA per 20 µL reaction. At the beginning, we prepared the primer/RNA mix (1µg RNA, 1µL 50 µM Oligo dT, 1µL 10 mM dNTPs, and water to a final volume of 10µL), which was denatured at 65°C for 5 min and then cooled on ice for 1 min. Then we added 10 µL of cDNA synthesis mix (2µL 10X RT buffer, 4µL 25 mM $MgCl_2$, 2µL 0.1 M DTT, 1µL RNAse out, 1µL super script III enzyme) and the reverse transcription reaction was incubated at 50°C for 50 min. We terminated the reaction by heating the sample to 85°C for 5 min. Finally, RNA removal was performed by treating the sample with 1µL of RNase H and by heating to 37°C for 20 min.

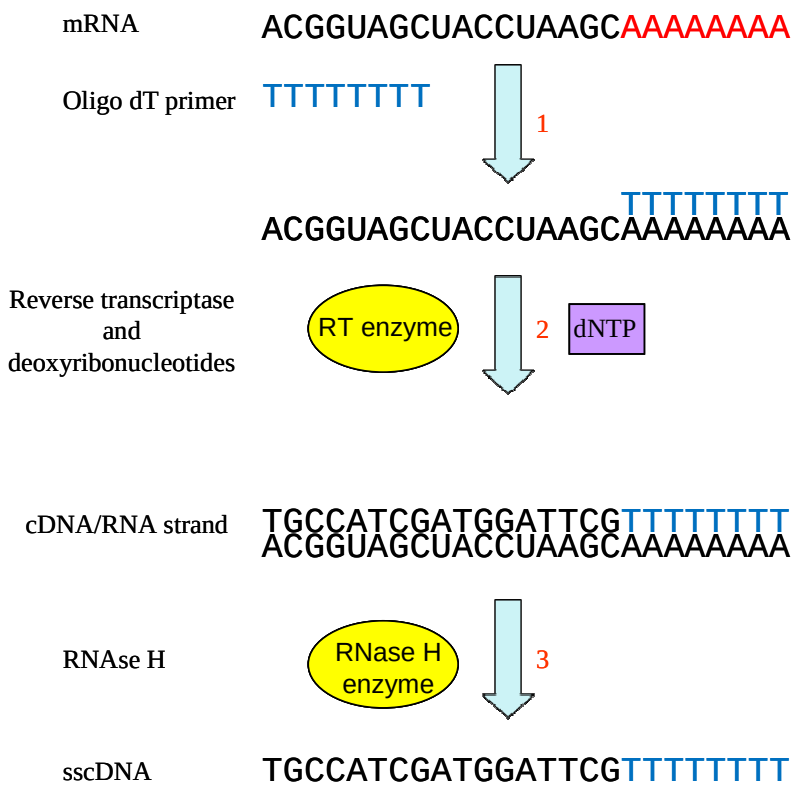

Figure 41: Principle of reverse transcription

II.3 Quantitative real time PCR

The principle of quantitative real time PCR (qPCR) is to detect and quantify a fluorescent reporter whose emission is directly proportional to the amount of amplicon generated during the PCR reaction, and thus to the initial amount of template. It is a quantitative method that gives us an absolute or relative value of the initial amount of template. qPCR is similar to standard PCR, but its key feature is that the amplified DNA is detected as the reaction progresses in real time, in contrast to standard PCR where product detection is performed at the end.

Detection of amplicons by fluorescence is based on the use of the SYBR green DNA-binding dye. This fluorescent compound has a greater emission intensity when it binds to double stranded DNA. Its presence in the reaction mixture does not alter the effectiveness of PCR. Fluorescence measurement is performed at the end of the extension phase when all DNA is synthesized as a double strand (Figure 42). Three phases can be identified in a quantitative PCR reaction. The baseline phase, where the fluorescence intensity is very low. The exponential phase, after a number of cycles, demonstrating the accumulation of PCR products resulted in a measurable variation in the intensity of the emitted fluorescence. The

starting point of the exponential phase is called the threshold cycle (Ct). It corresponds to the number of cycles at which the fluorescence intensity differs from background noise (threshold line), and it is directly related to the amount of matrix originally present in the sample. For example if we have two samples X and Y, and the CtX < CtY, this means that the initial amount of template of X is more than Y (Figure 42). The third and last phase is the plateau phase representing the saturation of the reaction caused by the accumulation of PCR products.

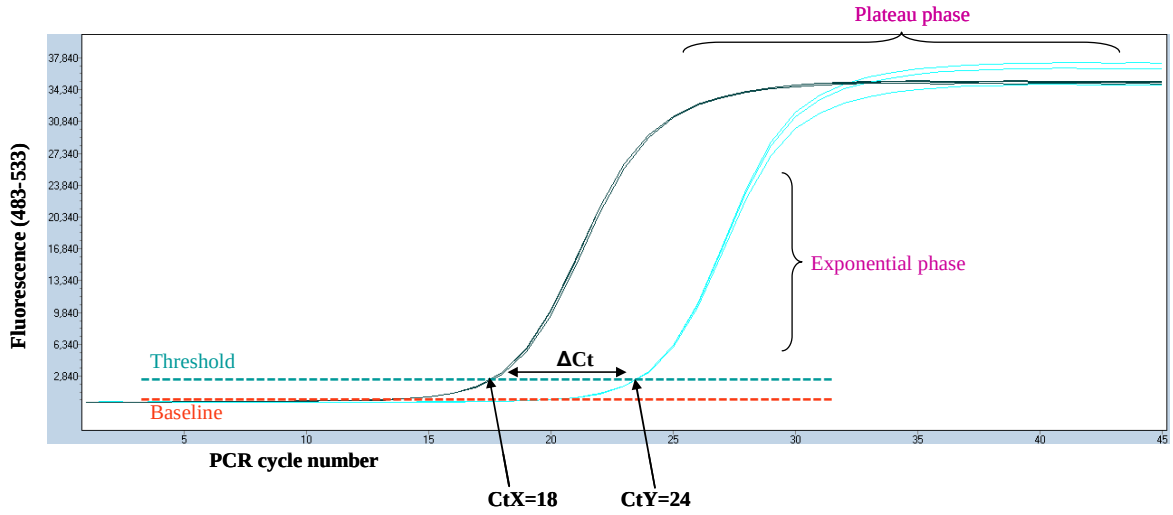

Figure 42: Fluorescence curves detected during PCR amplification

- **Primers used for qPCR**

For our study of the relative expression of the *FGF12* and *FGF13* isoforms in human and mouse hearts, we designed primers located in the homologous region between human and mouse FHF transcripts, as well as primers specific to each isoform. Moreover, in order to selectively amplify the cDNA and not the genomic DNA, primers were designed spanning adjacent exons with large introns in between (Figure 43 and Table 9).

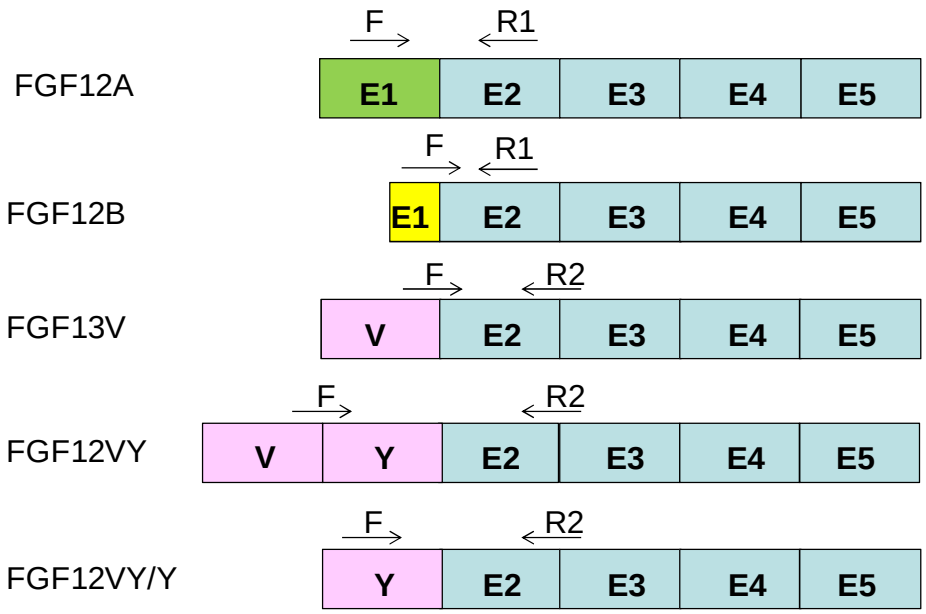

Figure 43: Primers used for the detection of *FGF12* and *FGF13* mRNA transcript levels in adult human and mouse hearts

FHF isoforms	Forward primer (5' – 3')	Reverse primer (5' – 3')	Product length (bp)
FGF12-A	ATAGCCAGCTCCTTGATCC	TAGTCGCTGTTTTCGTCCTT	296
FGF12-B	GGAGAGCAAAGAACCCCAG	TAGTCGCTGTTTTCGTCCTT	120
FGF13-V	GCTTCTAAGGAGCCTCAG	TGAGGTTAAACAGAGTGTAAG	136
FGF13-VY	TGCTTCTAAGGTTCTGGATG	TGAGGTTAAACAGAGTGTAAG	305
FGF13-VY/Y	GTGTCACGAAATCTTCTGCT	TGAGGTTAAACAGAGTGTAAG	191
*RPL32**	GCCCAAGATCGTCAAAAAGA	GTCAATGCCTCTGGGTTT	100

Table 9: qPCR primer pairs used for detecting *FGF12* and *FGF13* transcripts in adult human and mouse hearts

* Ribosomal protein L32 used as a normalizer**.**

- **qPCR**

The cDNA reverse-transcribed from 1 µg of total RNA was used to perform the qPCR. The primer effectiveness was determined by quantitative PCR using a range of successive cDNA dilutions. Quantitative PCR was performed in 96-well plates. Samples were run in triplicate, each well contained 5 µl of total cDNA solution, 1 µl of each sense and antisense 10 µM primer, 10 µl of 2X SYBR Green buffer (LightCycler® 480 DNA SYBR Green I Master, Roche). Negative controls were realized under the same conditions but with

no template. The qPCR was performed using the LightCycler 480 machine (Roche, Germany) with the following PCR program: (i) denaturation 10 min at 95°C, (ii) 45 cycles of amplification (denaturation at 95°C for 10 s, hybridization of primers at 60°C for 20 s, and extension at 72°C for 20 s), (iii) melting step (denaturation at 95°C for 30 s, hybridization at 68°C for 30 s, then the samples were heated gradually (0.06°C/sec) from 65°C to 95°C). This increase in temperature led to dsDNA dissociation (or melting) into single strands, releasing the dye, and causing a change in fluorescence. The result is a melting curve profile characteristic of the amplicon (Figure 44).

To assess the relative expression of FHF isoforms in human and mouse hearts, we calculated the difference between the Ct of each isoform. First of all, to normalize any differences due to the amount of nucleic acids placed in each well, we used the Ct of a reference gene encoding the ribosomal protein L32 (*RPL32*) to calculate the ΔCt = Ct of *RPL32* minus the Ct of each FHF isoform. Then, we calculated the ΔΔCt = ΔCt of each FHF isoform minus the ΔCt of the most highly expressed FHF isoform (*FGF12-B* in human heart, *FGF13-VY* in mouse heart). Then the relative expression of each isoform (Q) was calculated using the formula $Q = 2^{\Delta\Delta Ct}$, where ΔΔCt of the highly expressed isoform is = 0 and Q = 1. The other isoforms have ΔΔCt < 0 and Q < 1, so each FHF isoform was compared to the highly expressed one.

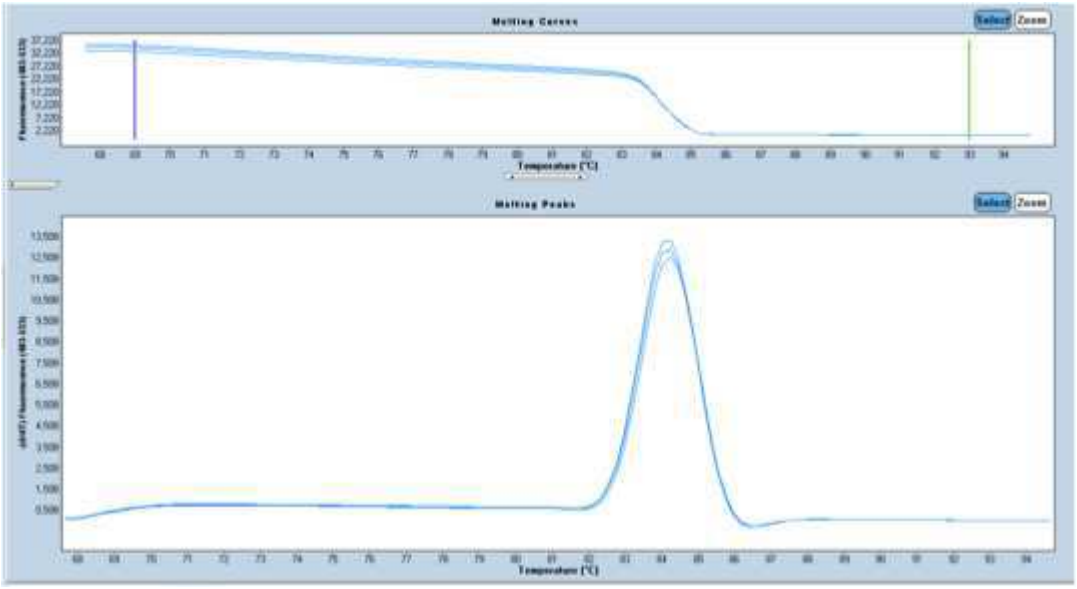

Figure 44: Melting curve of a qPCR

III. Genotyping

Our laboratory has a large collection of DNA from patients with inherited cardiac arrhythmias. For the screening analysis of *FGF12*, 182 BrS probands, without mutations in the *SCN5A, MOG1, DLG1, KCNE3* and *SCN1B* genes, were included in our study. Diagnosis of BrS was based on the accepted criteria of the recent consensus statement in 2013[287]: the presence of a spontaneous type-1 ECG pattern (ST segment elevation ≥2 mm in one or more right precordial leads) spontaneously or following the administration of a sodium channel blocker. Structural heart disease was excluded by echocardiography.

Blood samples were obtained for genetic analyses after signed written informed consent was obtained, and following approval by the local ethics committee of the Pitié-Salpêtrière Hospital. The study was conducted according to the principles of the Helsinki declaration.

III.1 The genomic regions analyzed

All sequences were obtained from the reference databases "NCBI" and "Ensembl genome browser". PCR primers (Table 10) were designed to amplify all exons within their flanking intronic regions (approximately 50 base pairs upstream and downstream).

***FGF12-B* exons**	**Forward primer (5' – 3')**	**Reverse primer (5' – 3')**	**Product length (bp)**
Exon 1	CAATCTGCTGCTGCTCCTAA	CCTTCCTGCCACACTTCC	397
Exon 2	AACACCCAACTCCCAAATAC	CAAGAAGGATAAAGGAAAAGAC	404
Exon 3	CTCCATTTTTCTACCAAGTTC	TACAAAACCTCAAAATAATCCC	372
Exon 4	GTATGATGAATCTTTGTAACCA	GGGCAAGAAGCAGAATTGAT	432
Exon 5	TGACTGAAAGAACTGAAAGAAAA	GGTAAATGGGAAGGAAGGGAA	363

Table 10: Primers used for *FGF12-B* sequencing

III.2 DNA concentration measurement

Before starting the sequence analysis, the concentration and the purity of each genomic DNA sample were evaluated using a spectrophotometer (Nanodrop ®, Thermo Scientific, USA). Nucleic acids have an absorbance wavelength of 260 nm. The DNA concentration is given in ng/µl. The purity of the sample is determined by a 260/280 ratio (DNA/protein). A ratio of ~1.8 is generally accepted as "pure" for DNA.

III.3 Sequence analysis of *FGF12-B*

All *FGF12-B* exons and intronic junctions were amplified by PCR. PCR products were purified using the P100 column (BioRad ®) and the sequencing reaction was realized using the Sanger method with Big Dye Terminator v.3.1 kit (Applied Biosystems ®), followed by a G50 (Sephadex®) purification. The Sanger method depends on the incorporation of chain-terminating dideoxynucleotides by the DNA polymerase during the sequence reaction. The sequence reaction mixture contains the DNA template, forward or reverse primer, DNA polymerase, normal deoxynucleosidetriphosphates (dNTPs), and modified nucleotides (dideoxyNTPs) that terminate DNA strand elongation (Figure 45). These chain-terminating nucleotides do not carry the 3'-OH group needed for the formation of a phosphodiester bond between two nucleotides, causing DNA polymerase to stop the extension of DNA when a ddNTP is incorporated. These ddNTPs are fluorescently labelled to be detected in automated sequencing machines. At the end of the sequencing reaction, fragments of various sizes were generated. They were then separated, according to their size, by migration *via* a 16 capillary 3130 sequencer (Applied biosystems ®, Life technologies, USA). When the fragments pass through the detection sensor, a laser beam excites their fluorescence, which is in turn captured by a camera coupled to a charger that converts this fluorescence into electrical data transferred to the computer in the 3130 Data Collection software (Figure 45). Sequence analysis was then performed using the CodonCode Aligner v3.7.1 software. Each obtained sequence was aligned to the reference sequence. Sequence variants were confirmed by sequencing a second DNA sample from the individual carrying the supposed variant.

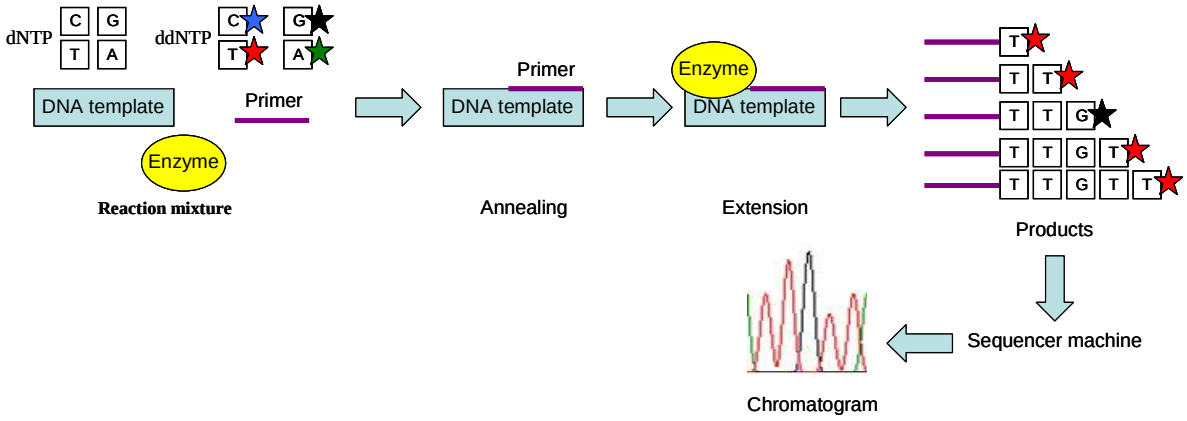

Figure 45: Principle of the Sanger method for sequencing

RESULTS

I. Article 1

Dominant-negative effect of *SCN5A* N-terminal mutations through the interaction of $Na_v1.5$ α-subunits

I.1 Summary of the study

Introduction

Mutations in the *SCN5A* gene account for approximately 25% of BrS cases. The N-terminal mutation R104W was identified in an asymptomatic 33-year-old male patient with spontaneous BrS type 1 ECG pattern. Programmed electrical stimulation in this patient induced sustained ventricular tachycardia degenerating into ventricular fibrillation, and the patient was treated by an implantable cardiac defibrillator. His father, who had a similar ECG pattern, died suddenly during sleep at the age of 61.

Several mutations in the N-terminal domain of $Na_v1.5$ have been reported, however the functional role of this region remains unknown. In this study, we aimed to investigate the role of the N-terminal domain of $Na_v1.5$ on channel function, subcellular localization, and protein expression, by the characterization of the functional effects of the mutant R104W, as well as another N-terminal mutation, R121W, previously published[214,306]. Moreover, we created two constructs: ΔNter, where the N-terminal region was deleted, and Nter, where only the N-terminal region was present.

Methods and Results

Patch-clamp analysis in HEK293 cells transfected with the WT, the mutant channels, R104W, R121W, or the construct ΔNter showed that the two N-terminal mutants and the ΔNter abolished the sodium current. Moreover, co-expression of the N-terminal mutants with the WT channels led to a dominant-negative effect on the WT channels with a positive shift in the activation curve, but not the ΔNter. Immunocytochemical analysis in rat neonatal cardiomyocytes co-transfected with the N-terminal mutants and the CD4 construct carrying the KKXX endoplasmic reticulum (ER) retention motif showed that the N-terminal mutants were retained in the ER, and their expression with the WT led to WT channel retention. In HEK293 cells, total protein extraction and cell surface biotinylation experiments demonstrated that the total and surface protein expression of the N-terminal mutants were reduced compared to the WT. Moreover, treating the cells with MG132, a 26S-subunit ubiquitin-proteasome inhibitor, increased the total protein expression of the mutants,

suggesting the degradation of the mutants by the ubiquitin-proteasome system. However, the ΔNter was slightly degraded and normally adressed to the membrane. The retention of the mutant channels in the ER and their subsequent degradation could explain their loss-of-function effects in the homozygous state, while the retention of the WT in the ER in the presence of the mutant could account for the dominant-negative effect, and suggests a cooperation between the $Na_v1.5$ α-subunits. Co-immunoprecipitation study in HEK293 cells transfected with two different $Na_v1.5$-tag constructs demonstrated that the WT α-subunits interacted with each other, as well as with the mutant R104W. As the mutant was able to inhibit the trafficking of the WT, most probably through the interaction between $Na_v1.5$ α-subunits, we hypothesised that the WT subunits could be able to transport a small part of the mutant subunits with it to the membrane. To test this hypothesis, the N-terminal mutants R104W and R121W were co-transfected with the trafficking-competent but non-functional $Na_v1.5$ mutant, R878C. Patch-clamp analysis showed that the R878C subunits were able to restore a very small sodium current density with a positive shift of the activation curve. This partial rescue confirmed the interaction between the $Na_v1.5$ α-subunits during their transport to the membrane, while the positive shift of activation suggests a possible cooperation between $Na_v1.5$ α-subunits at the membrane. Finally, expression of the Nter with the WT $Na_v1.5$ increased the sodium current density by two-fold compared to the WT.

Discussion

The dominant-negative effect of mutant ion channel subunits on the WT ones has been described mainly for ion channels consisting of multiple α-subunits, like the potassium channels K_vLQT1[467], which form homotetramers, but $Na_v1.5$ α-subunits were not known to oligomerize. Thus, the dominant-negative effect of the N-terminal mutants observed in our study was unexpected, while it has been reported once, for the trafficking-defective mutant L325R[468]. In this study, the authors hypothesized that the mutant channels could exert the dominant-negative effect by affecting the biosynthesis or the trafficking of the WT. In our study, we showed for the first time that an interaction between $Na_v1.5$ α-subunits exists, and that it is not affected by the presence of the mutant R104W. This interaction could underlie the dominant-negative of the mutant. Under normal condition, the WT α-subunits interact with each other, most propably in the ER, and traffic together to the plasma membrane. However, the mutant R104W was retained in the ER and degraded by the ubiquitin-proteasome system, and through the interaction with the WT α-subunits, it retained the WT with it in the ER. Consequently, few WT α-subunits interacting with each other reached the

membrane, accounting for the dominant-negative effect. The mechanism of mutant channel retention remains to be elucidated. It is possible that the N-terminal mutatnts caused conformational changes preventing the proper folding of the $Na_v1.5$ protein, resulting in its degradation by the ER-associated degradation (ERAD) system. In contrast to the trafficking-defective N-terminal mutants, the R878C mutant and the ΔNter-$Na_v1.5$, which were normally expressed at the membrane, did not have dominant-negative effect on the WT. The partial rescue by the trafficking-competent R878C on the N-terminal mutants further supports the cooperation between $Na_v1.5$ α-subunits.

By studying the N-terminal mutants, the ΔNter-$Na_v1.5$ and the Nter, our study highlights the important role of the N-terminal region of $Na_v1.5$. The proper expression of the ΔNter-$Na_v1.5$ at the membrane, with its inability to conduct sodium current suggest that the N-terminal domain is not essential to the trafficking of $Na_v1.5$, but it is important for channel opening. Moreover, the positive shift of activation when the N-terminal mutants were expressed with the WT or with R878C, suggests the involvement of the N-terminal domain in channel activation, and a possible functional cooperation between $Na_v1.5$ α-subunits at the membrane.

From a clinical point of view, the loss-of-function effects of the mutant R104W in the heterozygous state are most probably responsible for the BrS in this patient.

Conclusion

Our study demonstrated for the first time a physical interaction between $Na_v1.5$ α-subunits, likely occuring in the ER, accounting for the dominant-negative effects of the N-terminal mutants, and its partial rescue by the R878C mutant. In addition, our results highlight the role of the N-terminus of $Na_v1.5$ in the channel activation and opening.

I.2 Published article 1

Cardiovascular Research (2012) 96, 53–63
doi:10.1093/cvr/cvs211

Dominant-negative effect of *SCN5A* N-terminal mutations through the interaction of $Na_v1.5$ α-subunits

Jérôme Clatot[1,2], Azza Ziyadeh-Isleem[1,2], Svetlana Maugenre[1,2], Isabelle Denjoy[1,2,3], Haiyan Liu[4], Gilles Dilanian[1,2], Stéphane N. Hatem[1,2], Isabelle Deschênes[4], Alain Coulombe[1,2], Pascale Guicheney[1,2†], and Nathalie Neyroud[1,2*†]

[1]INSERM, UMR_S 956, IFR14, Paris, France; [2]UPMC Univ Paris 06, UMR_S 956, Fondation ICAN, Groupe Hospitalier Pitié-Salpêtrière, Paris, France; [3]Centre de Référence des Maladies Cardiaques Héréditaires, AP-HP, Hôpital Bichat, Paris, France; and [4]Heart and Vascular Research Center, Case Western Reserve University, MetroHealth Campus, Cleveland, OH, USA

Received 6 March 2012; revised 6 June 2012; accepted 21 June 2012; online publish-ahead-of-print 27 June 2012

Time for primary review: 29 days

Aims Brugada syndrome (BrS) is an autosomal-inherited cardiac arrhythmia characterized by an ST-segment elevation in the right precordial leads of the electrocardiogram and an increased risk of syncope and sudden death. *SCN5A*, encoding the cardiac sodium channel $Na_v1.5$, is the main gene involved in BrS. Despite the fact that several mutations have been reported in the N-terminus of $Na_v1.5$, the functional role of this region remains unknown. We aimed to characterize two BrS N-terminal mutations, R104W and R121W, a construct where this region was deleted, ΔNter, and a construct where only this region was present, Nter.

Methods and results Patch-clamp recordings in HEK293 cells demonstrated that R104W, R121W, and ΔNter abolished the sodium current I_{Na}. Moreover, R104W and R121W mutations exerted a strong dominant-negative effect on wild-type (WT) channels. Immunocytochemistry of rat neonatal cardiomyocytes revealed that both mutants were mostly retained in the endoplasmic reticulum and that their co-expression with WT channels led to WT channel retention. Furthermore, co-immunoprecipitation experiments showed that $Na_v1.5$-subunits were interacting with each other, even when mutated, deciphering the mutation dominant-negative effect. Both mutants were mostly degraded by the ubiquitin–proteasome system, while ΔNter was addressed to the membrane, and Nter expression induced a two-fold increase in I_{Na}. In addition, the co-expression of N-terminal mutants with the gating-defective but trafficking-competent R878C-$Na_v1.5$ mutant gave rise to a small I_{Na}.

Conclusion This study reports for the first time the critical role of the $Na_v1.5$ N-terminal region in channel function and the dominant-negative effect of trafficking-defective channels occurring through α-subunit interaction.

Keywords Arrhythmia • Brugada syndrome • $Na_v1.5$ • SCN5A • Sodium

1. Introduction

Brugada syndrome (BrS) is an inherited autosomal-dominant cardiac channelopathy with incomplete penetrance. It is characterized by a structurally normal heart with a typical electrocardiographic (ECG) pattern showing an ST-segment elevation in the right precordial leads (V1–V3) and an increased risk of sudden cardiac death by ventricular fibrillation.[1] Mutations in *SCN5A*, the gene encoding the cardiac voltage-gated sodium channel $Na_v1.5$, have been identified in ~25% of affected individuals[2] and commonly reveal loss-of-function properties reducing the sodium current I_{Na} either by gating abnormalities, trafficking defects, or premature stop codons leading to haploinsufficiency.[3] $Na_v1.5$ constitutes the α-subunit of the cardiac Na^+ channel complex, which includes other transmembrane subunits and intracellular partners that participate in its expression and function.[4] Although $Na_v1.5$ subunits are not known to oligomerize, a dominant-

†These authors contributed equally to this work.

*Corresponding author: Inserm UMRS 956, Université Pierre et Marie Curie Paris 6, 91, boulevard de l'Hôpital, F-75013 Paris, France. Tel: +33 1 40 77 96 49; fax: +33 1 40 77 96 45, Email: nathalie.neyroud@upmc.fr

negative effect of a mutation has been previously reported,[5] and the common polymorphism H558R has been shown to partially restore I_{Na} impaired by mutations when expressed on different constructs,[6,7] suggesting a cooperation between α-subunits.

Several mutations have been identified in the N-terminus of $Na_v1.5$ in patients with BrS or long QT syndrome, but their functional consequences on I_{Na} have not been studied *in vitro*, except for two of them. The non-functional R121W mutant was reported in conduction disease, associated with protein degradation, and the R43Q mutation showed a hyperpolarizing shift of the activation under lidocaine.[8,9] The role of the N-terminal region of $Na_v1.5$ on the trafficking, localization, and regulation of channel function remains largely unknown.

In this study, we characterized two $Na_v1.5$ N-terminal mutations: R104W identified in a BrS patient, R121W which was previously reported,[8] a chimeric channel where the N-terminus of $Na_v1.5$ was deleted, ΔNter, and a construct where only the N-terminus of $Na_v1.5$ was present, Nter. Our results suggest that the N-terminal region of $Na_v1.5$ plays a key role in the cardiac sodium channel function and demonstrate a physical interaction between $Na_v1.5$ α-subunits.

2. Methods

2.1 Patient

The proband was diagnosed with BrS on the basis of a spontaneous type-1 pattern on the 12-lead ECG (ST segment elevation ≥2 mm in one or more right precordial leads) and family history according to the consensus report.[1] Blood samples were obtained after signed written informed consent for genetic analyses and after approval by the local ethics committee of the Pitié-Salpêtrière Hospital. The study was conducted according to the principles of the Helsinki Declaration.

2.2 *SCN5A* mutation analysis

DNA was extracted from peripheral blood leucocytes according to standard procedures. Screening for mutations in the *SCN5A* gene (GenBank accession number NG_008934.1) was performed by genomic DNA amplification of all exons and splice junctions. PCR products were directly sequenced with the Big Dye Terminator v.3.1 kit (Applied Biosystems) on an ABI PRISM 3730 automatic DNA sequencer (Applied Biosystems). Variants and mutations were identified by the visual inspection of the sequence with Seqscape software (Applied Biosystems).

2.3 *SCN5A* cDNA cloning and mutagenesis

Plasmids pcDNA3.1-SCN5A (no tag) and pcDNA3.1-GFP-SCN5A (N-terminal-GFP) were the gifts of Dr H. Abriel (Bern, Switzerland). Plasmids pGFP-N3-SCN5A (C-terminal-GFP) and pRcCMV-FLAG-SCN5A (N-terminal-FLAG) were the gifts of Dr F. Le Bouffant (Nantes, France) and Dr N. Makita (Nagasaki, Japan), respectively. The plasmid pcDNA3.1-HA-SCN5A (HA-WT) was the gift of Dr P. Mohler (Columbus, OH, USA). The plasmid pGFP-N3-SCN5A-ΔNter (C-terminal-GFP) was generated by removing the first 381 nucleotides of *SCN5A* (127 amino acids), and replacing residue 128 by a methionine. The plasmid pNter-IRES2-mRFP1 was created by cloning the sequence of the first 132 amino acids of $Na_v1.5$ in the pIRES2-mRFP1 vector carrying the red fluorescent protein reporter gene. All plasmids contain the hH1a isoform of *SCN5A*. The plasmid pcDNA3-CD4-KKXX and the anti-CD4-KKXX antibody were the gifts of Dr J. Mérot (Nantes, France). This plasmid has been designed to express CD4 carrying the KKXX motif of ER retention. Mutants R104W, R104K, R121W, and R878C in $Na_v1.5$ were prepared using the QuikChange II XL Site-Directed Mutagenesis Kit (Stratagene) according to the manufacturer's instructions and verified by sequencing.

2.4 HEK293 cell culture and transfection

HEK293 cells were maintained in DMEM supplemented with 10% heat-inactivated foetal calf serum and 1% penicillin/streptomycin. HEK293 cells, which do not express endogenous Na_v channels, were transfected with pcDNA3.1-GFP-SCN5A WT or mutants in 35-mm dish well using JET PEI (Polyplus Transfection, New York, USA) according to the manufacturer's instructions. Cells were transfected with a total of 0.6 μg of plasmid per 35 mm dish, to avoid saturating currents. To mimic the heterozygous state of the BrS patient, cells were co-transfected with 0.3 μg of pcDNA3.1-GFP-SCN5A WT and 0.3 μg of each mutant channel plasmid. A HEK293 cell line stably expressing human $Na_v1.5$ (gift of Dr H. Abriel, Bern, Switzerland) was cultured in the presence of 25 μg/mL of zeocin (Invitrogen).

2.5 Electrophysiological recordings

Patch-clamp recordings were carried out in cells transfected with a total of 0.6 μg of plasmid to avoid saturating currents, in the whole-cell configuration at room temperature (22 ± 1°C) as previously reported.[10] Solutions for patch-clamp recordings are described in the Supplementary material online.

Ionic currents were recorded by the whole-cell patch-clamp technique with the amplifier Axopatch 200B, (Axon Instruments, CA, USA). Patch pipettes (Corning Kovar Sealing code 7052, WPI) had resistances of 1.5–2.5 MΩ. Currents were filtered at 5 kHz (−3 dB, 8-pole low-pass Bessel filter) and digitized at 30 kHz (NI PCI-6251, National Instruments, Austin, TX, USA). Data were acquired and analysed with ELPHY® software (G.Sadoc, CNRS, Gif/Yvette, France).

To measure peak I_{Na} amplitude and determine current–voltage relationships (*I/V* curves), currents were elicited by test potentials of 0.2 Hz frequency to −100 to 60 mV by increments of 5 or 10 mV from a holding potential of −120 mV. For the activation-V_m protocol, currents were elicited by 100-ms depolarizing pulses applied at 0.2 Hz from a holding potential of −120 mV, in 5 or 10 mV increments between −100 and +60 mV. The steady-state inactivation-V_m protocol was established from a holding potential of −120 mV and a 2-s conditioning prepulse was applied in 5 or 10 mV increments between −140 and +30 mV, followed by a 50-ms test pulse to −20 mV at 0.2 Hz.

Data for the activation-V_m and steady-state availability-V_m relationship of I_{Na} were fitted to the Boltzmann equation:

$$Y = 1/[\,1 + \exp[-(V_m - V_{1/2})/k]\}\,,$$

where V_m is the membrane potential, $V_{1/2}$ is the half-activation or half-availability potential, and k is the inverse slope factor. For activation-V_m curves, Y represents the relative conductance and k is >0. For availability-V_m curves, Y represents the relative current (I_{Na}/I_{Na}max) and k is <0.

2.6 Rat neonatal cardiomyocyte isolation and transfection

All animals were cared according to the *Guide for the Care and Use of Laboratory Animals* (NIH Publication No. 85–23, revised 1996) and under the supervision of authorized researchers in an approved laboratory (agreement number B75-13-08). Neonate 1-day-old rats were euthanized by decapitation. Their hearts were dissected, digested with collagenase A (Roche Diagnostics, Meylan, France) and incubated in culture medium after 1.5 h pre-plating on 60-mm plastic dishes in order to remove fibroblasts. Non-adherent cells were plated at a density of 4×10^5 cells/well on 35-mm dishes containing glass coverslips coated with 10 mg/mL laminin (Roche Diagnostics) in culture medium DMEM (high glucose/L-glutamine; Gibco ref 41965 039), supplemented with 10% horse serum, 5 FBS, 1% penicillin/streptomycin, cytosine B-D arabinofuranoside 25 mg/mL, and incubated for 24 h (37°C, 5% CO_2). Cells were transfected

in a 1%-CO_2 incubator with 0.6 μg of N-terminal-GFP fused constructs of WT or mutant $Na_v1.5$ using Lipofectamine 2000 (Invitrogen) according to the manufacturer's instructions.

2.7 Immunocytochemistry

Indirect immunofluorescence was performed on rat neonatal cardiomyocytes (RNC) primary culture fixed with methanol for 10 min at −20°C. Cells were then washed twice for 5 min with phosphate buffer saline (PBS), blocked in PBS-5% BSA for 30 min at room temperature. Cells were incubated for 1 h with primary antibodies: rabbit anti-GFP (1:300, Torrey Pines Biolabs) to detect $Na_v1.5$-GFP, mouse anti-Flag (1:300, Stratagene), chicken anti-calreticulin for ER (1:200, Abcam), rabbit anti-giantin for Golgi apparatus (1:1000, Abcam), rabbit anti-Lampl for lysosomes (1:200, Abcam), and rabbit anti-LC3 for proteasome (1:1000, Sigma). Detection was performed after two washes with PBS and 1 h of incubation with secondary antibodies: chicken anti-mouse Alexa Fluor 594, goat anti-rabbit Alexa Fluor 488 (1:1000, Molecular Probes), and the nuclear dye DAPI (1:500, Sigma) diluted in the blocking buffer. Control experiments were performed by omitting the primary antibodies.

2.8 Imaging

Labelled cardiomyocytes were observed with an Olympus epifluorescent microscope (60×). Images were acquired with a CoolSnap camera (Ropper Scientific) and analysed with Metamorph software (Molecular devices) equipped with a 3D-deconvolution module. For each sample, series of consecutive plans were acquired (sectioning step: 0.2 μm).

2.9 Protein extraction

Forty-eight hours after transfection with WT or mutant constructs, HEK293 cells were washed with PBS and lysed in the lysis buffer (50 mM Tris pH 7.5, 500 mM NaCl, 1% NP40, 0.1% SDS, 0.5% deoxycholate, and complete protease inhibitor cocktail from Roche) for 1 h at 4°C on a wheel. The soluble fractions from two subsequent 30 min centrifugations at 14 000 g (4°C) were then used for the experiments. To load each lane of the SDS–PAGE with equivalent amounts of total protein, the protein concentration of each lysate was measured in duplicate by the Bradford assay using a BSA standard curve.

2.10 Biotinylation assay

Forty-eight hours after transfection with WT or mutant constructs, HEK293 cells were washed twice with PBS and biotinylated for 60 min at 4°C using PBS containing 1.5 mg of EZ Link Sulfo-NHS-SS-Biotin (Pierce). Plates were incubated for 10 min at 4°C with PBS-100 mM glycine (to quench unlinked biotin) and washed twice with PBS. Cells were then lysed for 1 h at 4°C with the lysis buffer (composition described in the previous paragraph). After centrifugation at 14 000 g for 30 min (4°C), supernatants were incubated with immobilized neutravidin beads (Pierce) over night at 4°C and pelleted by centrifugation. After three washes with the lysis buffer, the biotinylated proteins were eluted with the Laemmli sample buffer with DTT 2X at 37°C for 30 min. Biotinylated proteins were then analysed by western blot as described below.

2.11 Co-immunoprecipitation

Co-immunoprecipitation experiments were performed as previously described.[11] Briefly, total cell lysates were pre-absorbed with Protein A Dynabeads (Dynal, Norway) for 2 h at 4°C. The unbound extracts were then incubated with Dynabeads Protein A crosslinked to the rat monoclonal anti-HA antibody (clone 3F10, Roche, USA). Western blots were revealed using either the rat monoclonal anti-HA antibody (clone 3F10, Roche, USA) or the mouse monoclonal anti-GFP antibody (Clontech, USA) at 1:1000 dilutions.

2.12 Western blot

Proteins were separated on a 10% acrylamide SDS–PAGE gel, then transferred to a nitrocellulose membrane and incubated with primary antibodies followed by infrared IRDye secondary antibodies (LI-COR Biosciences, USA). Proteins were detected using the Odyssey Infrared Imaging System (LI-COR Biosciences, USA). Signals were quantified using ImageJ software and normalized to WT levels.

2.13 Statistical analysis

Data are presented as means ± SEM. Statistical significance was estimated with SigmaPlot® software by Student's *t*-test or ANOVA, as appropriate. $P < 0.05$ was considered significant.

3. Results

3.1 Identification of a $Na_v1.5$ N-terminal mutation in a BrS patient

The proband (II.1) was an asymptomatic 33-year-old male with a spontaneous BrS type 1 ECG pattern, combining ST-segment elevation and inverted T waves in lead V1, and an incomplete right bundle branch block pattern (PR = 208 ms, QRS = 124 ms) (*Figure 1A* and *B*). Echocardiography, myocardial scintigraphy, and coronary angiography showed small akinetic areas in the right ventricular infundibulum, healthy coronary arteries, and normal left ventricular function. Programmed electrical stimulation induced sustained ventricular tachycardia degenerating into ventricular fibrillation. The patient received an implantable cardiac defibrillator (ICD). No ICD discharge occurred during the 7-year follow-up. His father presented with similar ECG abnormalities (*Figure 1B*) and died suddenly in his sleep at the age of 61.

SCN5A was screened and a variant, c.310 C > T, was identified in exon 3 in the proband, which induces the substitution of the evolutionarily conserved arginine 104 by a tryptophan (p.R104W) (*Figure 1C–E*). This variant was not found in 300 Caucasian controls and neither in the 14 000 alleles of the NHLBI Exome Sequencing Project (Seattle, WA, http://evs.gs.washington.edu/EVS/); it was not transmitted to the proband's healthy offspring and was considered to be a putative mutation responsible for BrS.

3.2 The R104W mutation abolished I_{Na}

Na^+ current was recorded in HEK293 cells 36 h after transfection with WT or R104W constructs. I_{Na} traces and I/V relationships are shown in *Figure 2A* and *B*. Peak current densities and *P*-values are given in *Table 1*. When the R104W mutant channel was expressed alone, no current could be detected. Conditions known to allow some misfolded proteins to escape the ER quality control and reach their final destination,[12,13] were used such as co-expression of R104W with the $Na_v\beta1$ subunit, decrease in cell incubation temperature to 30°C and addition of mexiletine (a class I anti-arrhythmic agent), but none of these restored any I_{Na}.

The substitution of arginine 104 by another positively charged residue, lysine, restored only 12% of the WT current, suggesting that the alterations of channel function critically depend on the R104 residue (see Supplementary material online, *Figure S1*). Interestingly, the $V_{1/2}$ of the R104K activation curve was shifted by +8.6 mV, while inactivation was unaffected.

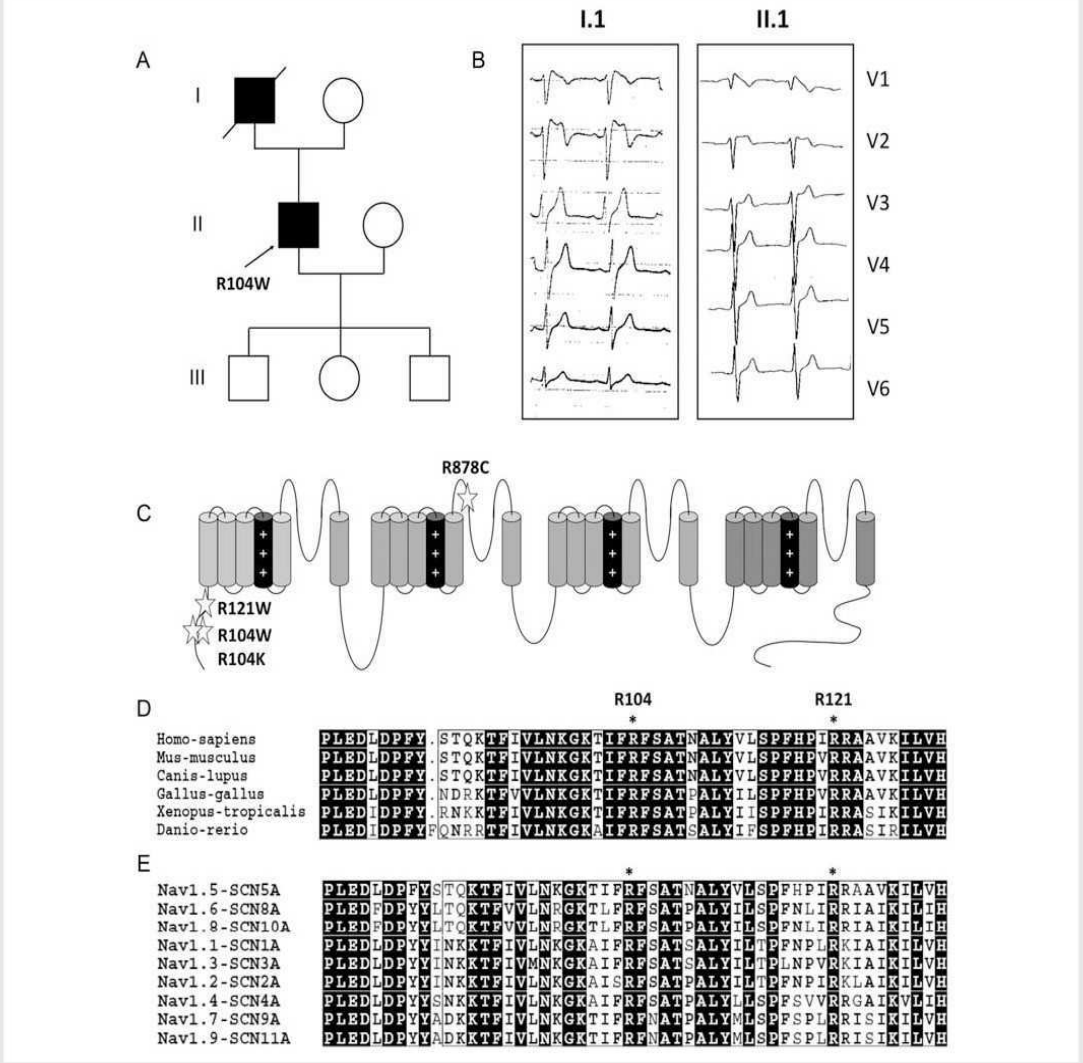

Figure 1 Identification of the R104W *SCN5A* mutation in a patient with BrS. (*A*) Pedigree of the family. The proband (II.1), who carries the mutation, is indicated by an arrow. Squares represent males, circles females, filled symbols affected subjects, and open symbols healthy subjects. (*B*) ECG recordings of precordial leads (V1–V6) of the proband and his father at rest, showing typical type1 BrS pattern. (*C*) Schematic representation of the hNa$_v$1.5 α-subunit. Stars represent the location of mutations characterized in this study. (*D*) Sequences of Na$_v$1.5 N-terminus across species and among voltage-dependent sodium channels (*E*). Conserved amino acids are in boxes. Residues R104 and R121 are indicated by stars. Sequence accession numbers are given in the Supplementary material online.

3.3 Expression in rat neonatal cardiomyocytes

Rat neonatal cardiomyocytes (RNC) transfected with N-terminal-GFP-tagged channel constructs were labelled with an anti-GFP antibody to assess channel location. R104W showed strong perinuclear and intracytoplasmic labelling which was clearly different from WT membrane localization (*Figure 3*). We stained specific sub-cellular compartment proteins, but it is only by cotransfecting RNCs with R104W and CD4 carrying the KKXX motif of ER retention, that we saw an important co-localization of mutant channels and the ER vesicles (*Figure 3*). We compared R104W localization in RNCs to another non-functional N-terminal Na$_v$1.5 mutant, R121W,[8] and observed that, as R104W, R121W was mostly retained in the ER (*Figure 3*). Interestingly, some WT channels were also retained in intracellular compartments when co-expressed in a 1:1 ratio with R104W (*Figure 4*), suggesting a dominant-negative effect of the N-terminal mutant.

3.4 Dominant-negative effect of N-terminal mutants

To test whether N-terminal mutants had a dominant-negative effect on WT channels, we recorded I_{Na} in HEK293 cells co-transfected with the WT channel and R104W or R121W channel in a 1:1 ratio.

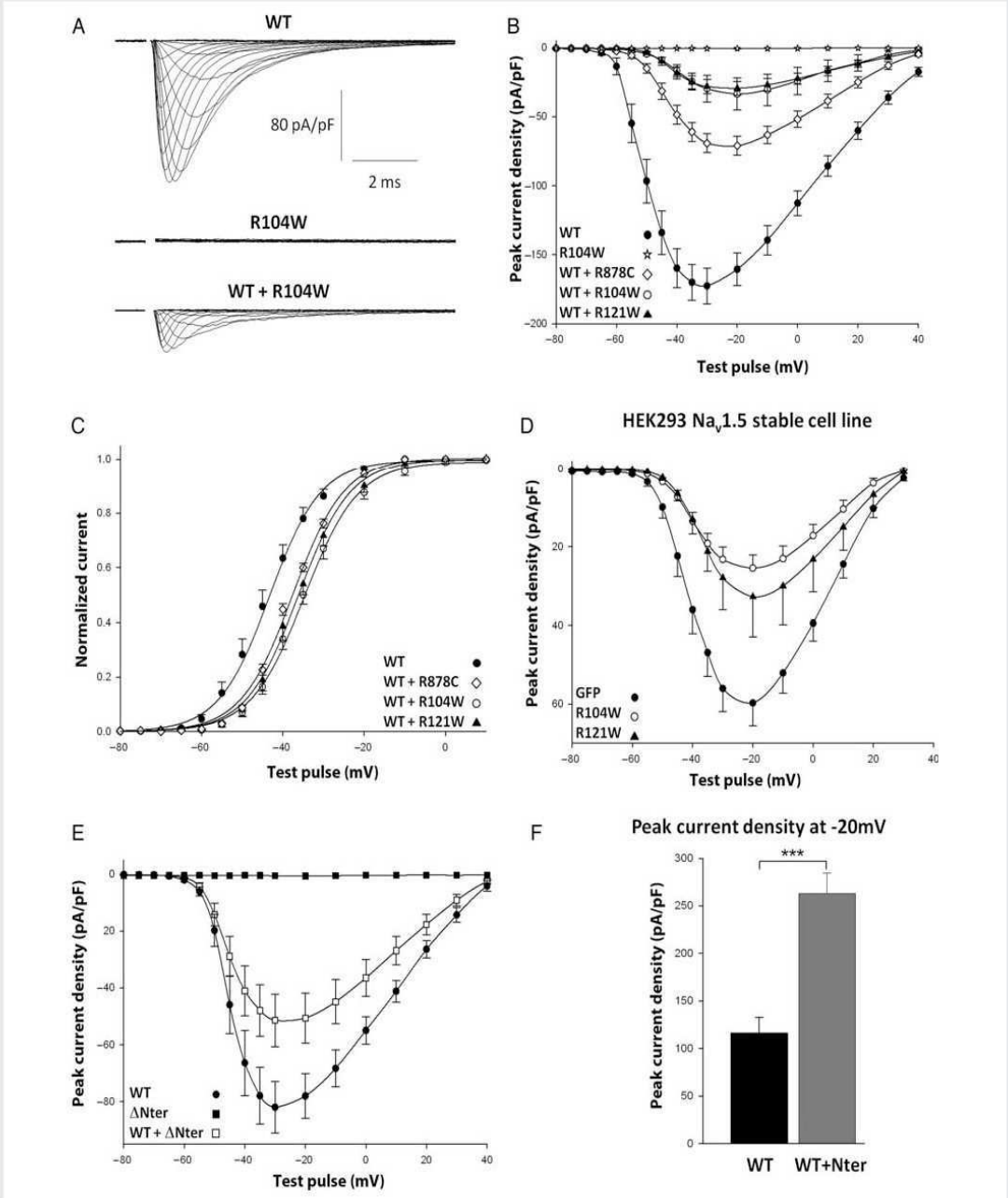

Figure 2 Electrophysiological characterization of $Na_v1.5$ channels. In (*A–D*) panels, the transfected plasmids carry the N-terminal-GFP-tagged $Na_v1.5$. In (*E* and *F*) panels, the GFP is fused to the C-terminus of $Na_v1.5$. Numbers of cells and statistical analysis are indicated in *Table 1*. (*A*) Representative Na^+ current traces of $Na_v1.5$ WT, R104W, and WT+R104W channels. Solid lines indicate the zero current level. (*B*) Current density–voltage relationships in cells co-transfected with WT, R104W, WT + R104W, WT + R121W, or WT + R878C channels. Only R878C did not exert a dominant-negative suppression on WT I_{Na}. (*C*) Activation curves of WT + mutants were shifted to more positive potentials (*D*) Current density–voltage relationships in $Na_v1.5$-stable HEK cells transfected with GFP alone as a control, R104W or R121W mutant channels. Cells were perfused with a 25 mM-Na^+ solution to avoid saturating currents. R104W and R121W significantly decreased I_{Na} when compared with cells transfected with GFP alone (GFP: -59.7 ± 5.8 pA/pF, $n = 17$; R104W: -25.5 ± 3.4 pA/pF, $n = 11$, $P = 0.03$; R121W: -32.8 ± 10.1 pA/pF, $n = 7$, $P = 0.03$). (*E*) Current density–voltage relationships in cells transfected either with WT, ΔNter, or WT + ΔNter. Deletion of the $Na_v1.5$ N-terminus did not exert a dominant-negative effect on WT channels. (*F*) Peak current density at -20 mV of WT channels alone ($n = 10$) or co-expressed with the N-terminal fragment, Nter ($n = 9$; ***$P<0.001$).

Table 1 Biophysical and kinetic properties of WT and mutant I_{Na}

GFP position	Na^+ channels	Peak current density (pA/pF)	P-value	Activation				Inactivation			
				$V_{1/2}$ (mV)	P-value	k (mV)	P-value	$V_{1/2}$ (mV)	P-value	k (mV)	P-value
No GFP	WT	164 ± 27 ($n = 8$)	ns	−42.7 ± 1.2 ($n = 9$)	ns	6.4 ± 0.4	ns	−80.1 ± 0.5 ($n = 11$)	ns	−8.2 ± 0.6	ns
N-term	WT	160 ± 11 ($n = 18$)		−44.2 ± 1.6 ($n = 17$)		6.5 ± 0.3		−81.7 ± 0.6 ($n = 10$)		−8.8 ± 0.5	
	R104W	nd ($n = 15$)		na		na		na		na	
	R121W	nd ($n = 13$)		na		na		na		na	
	R878C	nd ($n = 15$)		na		na		na		na	
	1/2 WT + 1/2 R104W	33.6 ± 11.7 ($n = 10$)	*	−36.5 ± 1.7 ($n = 10$)	*	6.6 ± 0.2	ns	−82.8 ± 0.5 ($n = 9$)	ns	−6.6 ± 0.5	**
	1/2 WT + 1/2 R121W	29.4 ± 5 ($n = 15$)	*	−36.8 ± 1.4 ($n = 13$)	*	6.3 ± 0.2	ns				
	1/2 WT + 1/2 R878C	71.1 ± 6.9 ($n = 17$)	*	−38.3 ± 0.6 ($n = 12$)	***	6.4 ± 0.2	ns				
	1/2 R878C + 1/2 R104W	5.7 ± 1.3 ($n = 9$)		na		na		na			
	1/2 R878C + 1/2 R121W	24.1 ± 4.8 ($n = 5$)		−32.5 ± 1.4 ($n = 5$)	**	5.8 ± 0.2	ns				
C-term	WT	78.3 ± 7.8 ($n = 9$)		−43.5 ± 1.1 ($n = 9$)							
	ΔNter	nd ($n = 13$)		na							
	1/2 WT + 1/2 ΔNter	50.6 ± 8.6 ($n = 13$)	**	−41.6 ± 0.9 ($n = 10$)	ns						

Data are presented as means ± SEM. Peak current density is given at −20 mV.
WT, wild type; nd, not detectable; na, not available because of too small currents; and ns, not significant.
*$P \leq 0.001$, **$P < 0.05$, ***$P \leq 0.005$ compared with N- or C-terminal GFP-tagged WT channel. Note that no difference in biochemical parameters was observed between N-terminal-GFP-tagged channel and not tagged $Na_v1.5$.

This led to a drastic reduction in the peak current densities by ~80% of the WT current density (*Table 1* and *Figure 2B*). In contrast, the co-expression of WT channels and R878C, a trafficking competent but gating-defective mutant[14,15] did not exert a dominant-negative effect, as previously shown[15] (*Table 1* and *Figure 2B*). The N-terminal mutant dominant-negative effect was further confirmed by transfecting a HEK $Na_v1.5$ stable cell line with R104W or R121W (*Figure 2D*).

In cells co-expressing WT and either R104W, R121W, or R878C channels, an unexpected shift of the $V_{1/2}$ of activation to more positive potentials was observed compared with WT alone (*Table 1* and *Figure 2C*). We observed no difference in activation slope factors (*Table 1*). In addition, we observed significant decreases in the fast inactivation time constant of the current and of the fast time constant of recovery from inactivation (see Supplementary material online, *Figure S2*). Voltage-dependent inactivation remained unchanged in cells co-expressing WT and R104W, whereas the slope factor was only slightly increased (*Table 1*).

3.5 $Na_v1.5$ α-subunits interacted with each other

To check whether this dominant-negative effect could be due to an interaction between $Na_v1.5$ α-subunits, we performed co-immunoprecipitation in HEK293 cells transfected with either HA-WT alone, GFP-WT alone, HA-WT + GFP-WT or HA-WT + GFP-R104W (*Figure 5*). $Na_v1.5$ α-subunits tagged with either HA or GFP were used in order to discriminate between the two channels and address whether they interact. When immunoprecipitation was performed with the anti-HA antibody, and western blot revealed with the anti-GFP antibody in cells expressing both HA-WT + GFP-WT or HA-WT + GFP-R104W, a specific band at the expected size was present for both GFP-WT and the GFP-R104W (*Figure 5*, boxed area). This indicates that the HA-WT $Na_v1.5$ α-subunit that was pulled down by the HA antibody, interacted with the GFP-tagged $Na_v1.5$ α-subunit (both, mutant or WT). These results show that an interaction occurs between WT $Na_v1.5$ α-subunits and also between WT and the R104W mutant.

3.6 Deletion of the N-terminus of $Na_v1.5$ abolished I_{Na}

To further characterize the role of the $Na_v1.5$ N-terminal region, we designed a construct where this region was deleted, ΔNter. When expressed alone in HEK293 cells, no current was detected (*Table 1* and *Figure 2E*). In contrast to N-terminal mutants, when ΔNter was co-expressed with WT in a 1:1 ratio, no dominant-negative effect was observed (*Table 1* and *Figure 2E*). In addition, the voltage-dependent activation was unchanged compared with WT, contrasting with the shift observed for co-expression of WT and mutants (*Table 1*).

On the other hand, co-expression of the $Na_v1.5$ N-terminus, Nter, and the full WT channel led to a two-fold increase in I_{Na} density compared with cells expressing WT channels only (*Figure 2F*).

3.7 Degradation of N-terminal mutant channels

Western blots were performed with total transfected HEK293-cell lysates to assess the expression of N-terminal mutants. *Figure 6A* shows a significant decrease in the total protein expression of R104W, R121W, and R104K channels, when compared with WT

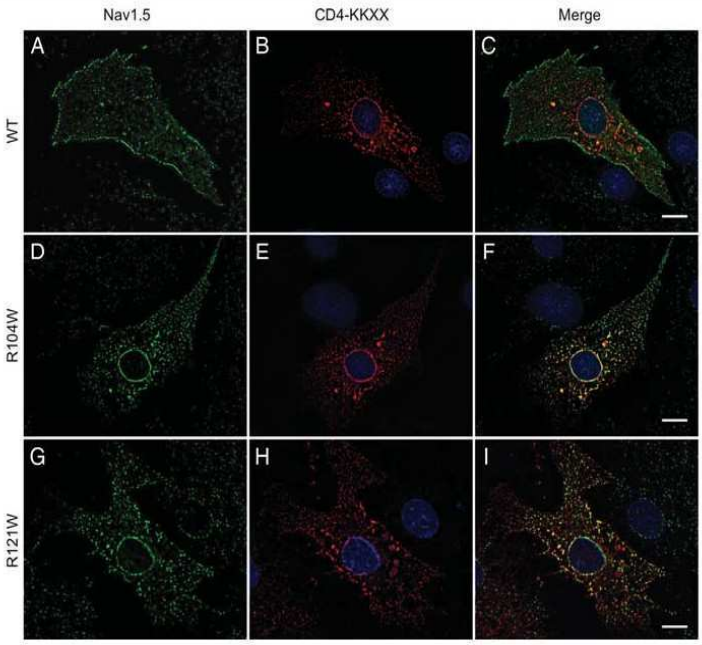

Figure 3 R104W and R121W are mostly retained in the ER in RNC. Three-dimensional deconvolution images of RNC co-transfected with GFP-$Na_v1.5$ (green) and CD4-KKXX (red). Nuclei are stained with DAPI (blue). (*A–C*) $Na_v1.5$ WT, (*D–F*) R104W, and (*G–I*) R121W. Note that in the merged image (*C*) $Na_v1.5$ WT is mostly expressed at the plasma membrane, as opposed to CD4-KKXX, which is retained in the ER. In contrast, N-terminal mutant merged images (*F* and *I*) show numerous internal yellow dots, indicating that $Na_v1.5$ mutants are mostly retained in the ER, similarly to CD4-KKXX. Scale bar: 10 μm.

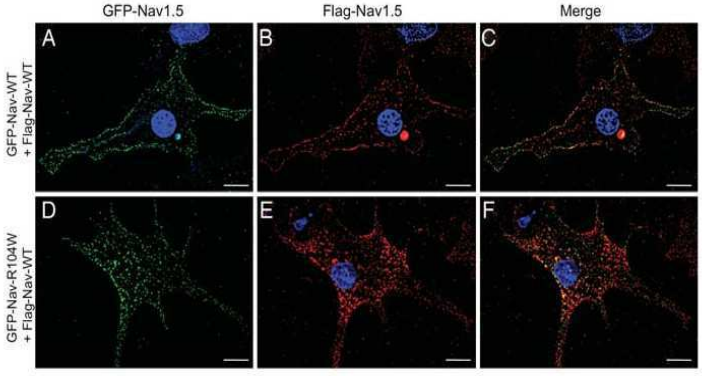

Figure 4 R104W impairs WT channel trafficking in RNC. Three-dimensional deconvolution images of RNCs co-transfected with GFP-$Na_v1.5$ (green) and Flag-$Na_v1.5$ (red). (*A–C*) GFP-$Na_v1.5$-WT + Flag-$Na_v1.5$-WT channels, (*D–F*) GFP-$Na_v1.5$-R104W + Flag-$Na_v1.5$-WT channels. The co-expression of both WT channel constructs exhibits clear membrane staining, whereas the co-expression of WT and R104W mutant shows more intracellular labelling of both channels. Scale bar: 10 μm.

(reduced by 55, 63, and 64%, respectively) or to the R878C mutant. Furthermore, the incubation of cells with the 26S-subunit ubiquitin-proteasome inhibitor, MG132, prevented the degradation of the two N-terminal mutants (*Figure 6B*), without restoring any I_{Na}. To test whether R104W mutant could cause the degradation of WT channels, we co-transfected cells with GFP-tagged and non-tagged channels to distinguish WT from mutant channels. *Figure 6C* shows that WT channels were not degraded in the presence of R104W. To assess whether the N-terminal mutants reached the plasma membrane, we performed cell surface protein biotinylation and showed an important reduction in R104W, R121W, and R104K channel membrane expression compared with WT (reduced by 61, 61, and 91%)

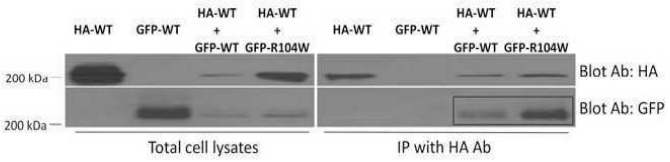

Figure 5 Co-immunoprecipitation of $Na_v1.5$ α-subunits. Co-immunoprecipitation of $Na_v1.5$ α-subunits tagged with either HA or GFP was performed in HEK293 cells. HA-WT, GFP-WT, HA-WT + GFP-WT, or HA-WT + GFP-R104W were transfected as indicated above the lanes. To assess interaction between $Na_v1.5$ α-subunits, the total cell lysates were immunoprecipitated with anti-HA antibody crosslinked to beads. The blots were hybridized with an anti-HA antibody (top gels: blot Ab: HA) or an anti-GFP antibody (bottom gels: blot Ab: GFP). The left side corresponds to the total cell lysates of transfected cells before IP. The right side (IP with HA Ab) corresponds to the elution fractions from beads. The results demonstrated an interaction between $Na_v1.5$ α-subunits, both for WT + WT and WT + mutant (boxed area). These are representative blots from a total of three identical experiments.

or to the R878C mutant (*Figure 6D*). In contrast, ΔNter was slightly degraded (reduced by 21%) but was mostly expressed at the membrane (*Figure 6E*).

Overexpression of N-terminal mutants did not cause reticular stress by the unfolded protein response pathway activation (see Supplementary material online, *Figure S3*).

3.8 Complementation of N-terminal mutants by R878C

In line with the $Na_v1.5$ channel α-subunit cooperation suggested by the dominant-negative effect and the shift of activation, we hypothesized that it might be possible to rescue dominant-negative $Na_v1.5$ mutants by complementation, using the trafficking-competent but non-functional $Na_v1.5$ mutant, R878C. Interestingly, the co-expression of R878C with R104W or R121W in a 1:1 ratio gave rise to small currents of 2 and 8.5% of the WT current, respectively (*Figure 7A* and *B*). It is noteworthy that the $V_{1/2}$ of activation of the current generated by the co-expression of R121W and R878C was more shifted than the $V_{1/2}$ of activation of the current elicited by the co-expression of R121W and WT (*Table 1* and *Figure 7C*). The activation of R104W + R878C was also likely shifted towards positive potentials, but the activation curve could not be reliably determined because of the too small I_{Na} (*Figure 7B*). Altogether, our results showed the complementation of trafficking-defective and non-functional N-terminal mutants by a non-functional but trafficking-competent $Na_v1.5$ mutant.

4. Discussion

Our study highlights for the first time the important role of the N-terminal domain of $Na_v1.5$. We describe several novel findings by the analysis of two mutant channels, R104W and R121W, and two truncated proteins, ΔNter, and the N-terminus fragment. The two mutants and the truncated channel abolished I_{Na}, but only the mutants exerted a dominant-negative effect on WT channels. Unexpectedly, we demonstrated the capacity of R878C, a trafficking-competent but gating-defective mutant, to partially rescue N-terminal mutant function. Finally, we evidenced an interaction between WT $Na_v1.5$ α-subunits, and we showed that this interaction was still present between WT and R104W channels.

We identified the missense $Na_v1.5$ mutation, R104W, in a young asymptomatic patient with a typical type-1 BrS ECG pattern. The R121W mutation has previously been reported in a BrS patient[2] and in a patient with cardiac conduction disease[8] where it was associated with a loss of channel function and protein degradation. Substitution by a tryptophan of these two conserved arginine abolished I_{Na}, as did the truncation of the N-terminus. Other mutations have also been identified in the $Na_v1.5$ N-terminus in BrS and long QT syndrome patients.[2] Altogether, this suggests the importance of this poorly explored domain in the function of $Na_v1.5$.

In our study, missense mutations in the N-terminus of $Na_v1.5$ led to retention and degradation of most of the channels, while the truncation of the N-terminus did not preclude channels to reach the plasma membrane. The mechanism of mutant channel retention remains to be elucidated. It is likely that cells expressing the mutants use ER-associated degradation (ERAD) as a protective mechanism to remove proteins that fail to acquire their native conformation. Indeed, during ERAD, misfolded proteins are moved from the ER to the cytosol and degraded by the ubiquitin–proteasome system.[16] A similar mechanism has already been highlighted with the N-terminal S21P mutant in $Na_v1.6$, which is retained in the Golgi apparatus and further degraded.[17] Most of the ΔNter channel seemed to escape this quality-control pathway, suggesting that the replacement of arginines 104 and 121 by tryptophans caused severe conformational changes of the N-terminus possibly involved in a negative regulatory pathway.

A dominant-negative effect of mutant ion channel subunits has frequently been reported for channels formed by multiple α-subunits, such as K_vLQT1 in long QT syndrome.[18] $Na_v1.5$ α-subunits were not known to interact, therefore, the dominant-negative effect we observed was unexpected, while reported once in studying the trafficking-defective mutation L325R.[5] Here, we highly suggest that the WT cardiac sodium channel α-subunits can interact with each other. Moreover, this interaction, which can be direct or indirect, seems not to be affected by the R104W mutation. This could explain the dominant-negative effect of the missense mutants by an impairment of WT channel trafficking consecutive to the mutant channel retention. Interestingly, several N-terminal mutations in *CACNA1A*, the gene encoding the brain $Ca_v2.1$ channel, whose structure is similar to $Na_v1.5$, induced a dominant-negative effect on WT channels responsible for ataxia,[19,20] leading the authors to postulate

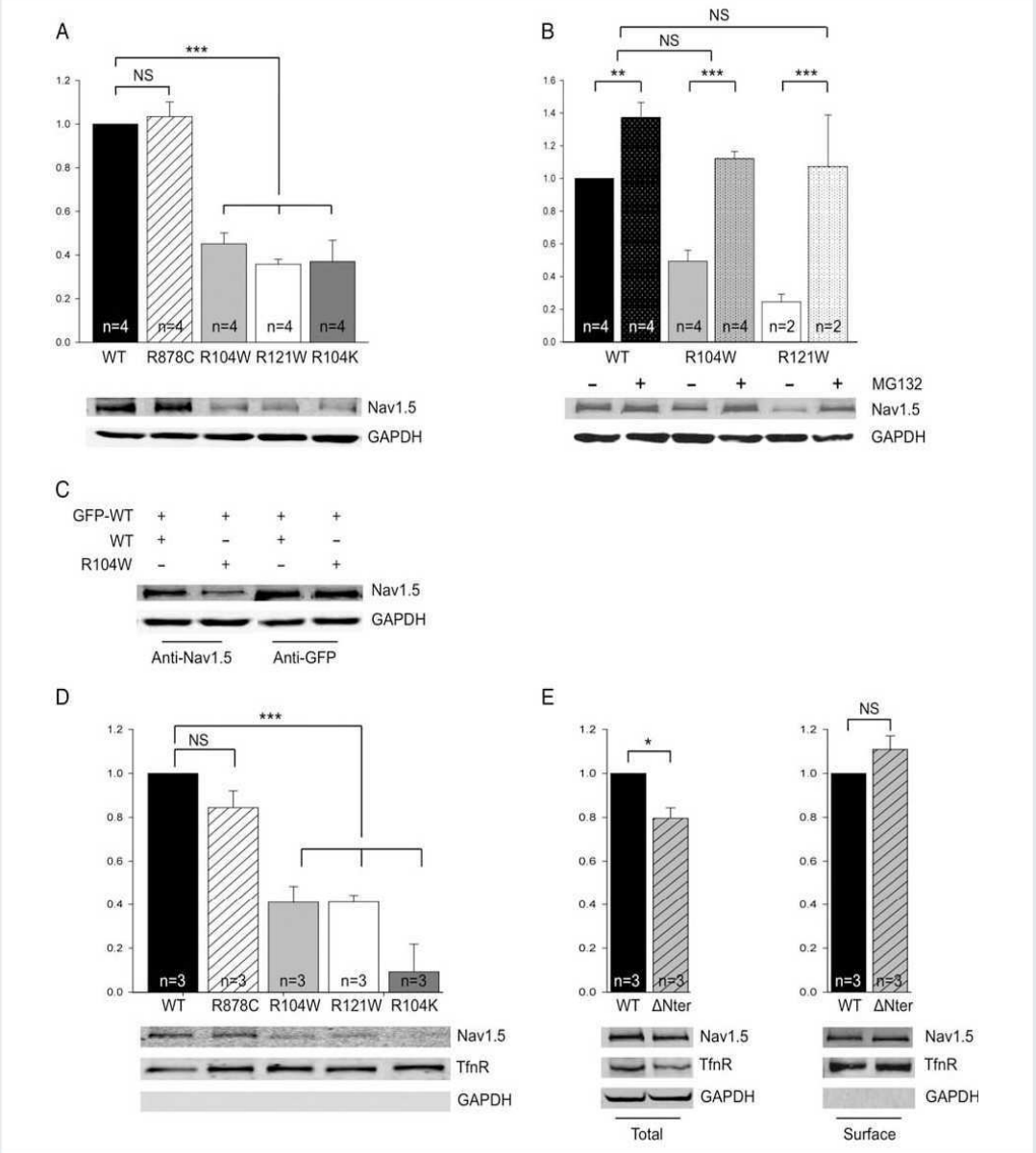

Figure 6 Biochemical analysis. In panels (*A*, *B*, and *D*), cells were transfected with GFP-$Na_v1.5$ and in panel (*E*), with $Na_v1.5$-GFP. NS indicates not significant, $^{**}P = 0.004$ and $^{***}P \leq 0.001$. Data are represented as arbitrary units. Glyceraldehyde 3-phosphate dehydrogenase (GAPDH) was used as total protein loading control. (*A*) Western blots of total cell lysates show that N-terminal mutant protein quantities are significantly lower than WT (*B*) Incubation of transfected cells with MG132 prevented degradation of N-terminal mutants (*C*) Representative western blot of total protein extracted from cells co-transfected with GFP-$Na_v1.5$ WT and the non-tagged $Na_v1.5$ WT or R104W constructs. The anti-$Na_v1.5$ antibody revealed both channels (tagged and non-tagged) and showed a decrease in the total $Na_v1.5$ channel after cotransfection with the mutant. The anti-GFP antibody revealed only the GFP-$Na_v1.5$-WT channels and showed no degradation of GFP-$Na_v1.5$-WT in the presence of the R104W mutant. (*D*) Cell surface biotinylation experiments. Transferrin receptor (TfnR) was used as a biotinylated protein loading control. Note that the surface membrane expression of N-terminal mutants was markedly reduced compared with WT and R878C. (*E*) Western blot of total cell lysates and biotinylation of cells transfected with ΔNter-GFP. ΔNter was slightly degraded compared with WT, while normally expressed at the membrane.

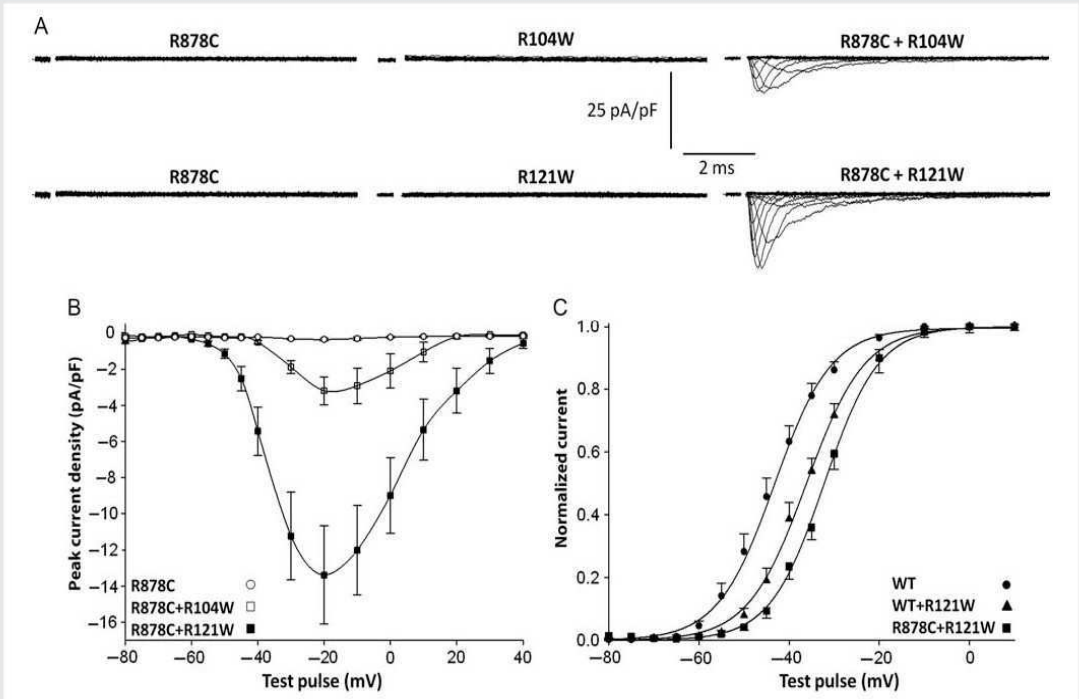

Figure 7 N-terminal mutants are complemented by R878C. (*A*) Representative I_{Na} traces of R878C, R104W, and R121W alone or co-expressed with R878C. Cells were bathed with a 135 mM Na^+ solution because of small I_{Na}. (*B*) I/V relationships of R878C, R878C + R104W, and R878C + R121W channels. R878C was able to restore a small I_{Na} when co-expressed with R104W and R121W mutants (2 and 8.5% of WT I_{Na} density). (*C*) Activation curves of WT, R121W + WT and R121W + R878C channels. Note that the activation was shifted by 7.4 and 11.7 mV compared with WT.

that mutant proteins interfere with either the biosynthesis or the trafficking of WT channels.

These results prompted us to explore the possibility of complementation, a concept studied in the field of CFTR channels.[21–23] Previous reports have demonstrated the rescue of trafficking-defective $Na_v1.5$ mutants by co-expressing the H558R polymorphism in a different construct.[6,7] The mechanisms of this 'complementation phenomenon' remain to be elucidated. We propose that the two N-terminal $Na_v1.5$ mutants studied here are subject to two opposite forces: the first, and the strongest, ensures cell quality control and retains the mutants in the ER impairing WT channel trafficking, whereas the second, through an interaction between α-subunits, drives the mutant channels to the plasma membrane and restores the function of a very small proportion of mutant channels.

Interestingly, our experiments led us to determine the role of the $Na_v1.5$ N-terminus in the function of the channel. Indeed, the co-expression of Nter with the WT channel increased I_{Na} density, suggesting that the presence of the N-terminal fragment enhances WT channel trafficking. This occurs by an unknown mechanism, nevertheless, we can hypothesize that Nter acts as a decoy, allowing more WT channels to bypass a regulatory system and reach the plasma membrane. Moreover, when we truncated the $Na_v1.5$ N-terminus in the ΔNter channel, the channel was correctly addressed to the plasma membrane but was unable to generate any current, suggesting that the N-terminal region is crucial to channel opening. Furthermore, we showed that R104K induced a small I_{Na} with a positive shift of voltage-dependent activation compared with WT channels. Similarly, co-transfection of the N-terminal mutants with either WT or R878C channels led to a positive shift of voltage-dependent activation. Our results are in accordance with a previous study by Lee *et al.*,[24] who demonstrate that the activation of $Na_v1.2$ and $Na_v1.6$ depends on their respective N-terminal sequence. Besides, these results are in concordance with the significant decreases in the fast inactivation time constant of the current and of the fast time constant of recovery from inactivation that we observed in cells co-expressing WT and R104W channels. To our knowledge, the present study is the first to support that the N-terminal part of $Na_v1.5$ can play a role in the kinetics of the cardiac sodium channel. The mechanism by which the presence of the mutants at the plasma membrane affects the kinetics of WT channels remains to be investigated. Nevertheless, these results are consistent with another study showing a tight cooperation in channel gating by double and triple simultaneous openings, suggesting a mechanism of synergy between Na_v channels.[25] We propose that this synergy occurs by interaction between $Na_v1.5$ α-subunits.

From a clinical point of view, the R104W mutation, heterozygous in the BrS patient, should be associated with reduced expression of WT channels in cardiomyocytes, through a pathophysiological mechanism leading to retention and degradation of mutant proteins. In addition, $Na_v1.5$ channels present at the membrane would open at a more

positive membrane potential threshold and inactivate faster (loss of function), so a greater voltage stimulus is needed to achieve the cell depolarization contributing to slow down the action potential propagation. These are mechanisms known to contribute to the patient's BrS phenotype. Extrapolation of our data to patient management remains nevertheless hazardous since many other factors, still unknown, may occur to modulate the $Na_v1.5$ function. However, it is worth noting that such $Na_v1.5$ mutations associated with a reduced number of channels at the membrane, and causing shifts in activation, may lead to more severe consequences than reported mutations leading to haploinsufficiency.

Supplementary material

Supplementary material is available at *Cardiovascular Research* online.

Acknowledgements

We are grateful to Dr Rachel Peat for careful reading of the manuscript, and to the NHLBI GO Exome Sequencing Project.

Conflict of interest: none declared.

Funding

This work was supported by Institut National de la Santé et de la Recherche Médicale (INSERM), the Université Pierre et Marie Curie, the Agence Nationale de la Recherche (ANR-09-GENO-003-CaRNaC), and NIH/NHLBI R01HL094450 (I.D.).

References

1. Antzelevitch C, Brugada P, Borggrefe M, Brugada J, Brugada R, Corrado D *et al.* Brugada syndrome: report of the second consensus conference: endorsed by the heart rhythm society and the european heart rhythm association. *Circulation* 2005; **111**:659–670.
2. Kapplinger JD, Tester DJ, Alders M, Benito B, Berthet M, Brugada J *et al.* An international compendium of mutations in the SCN5A-encoded cardiac sodium channel in patients referred for Brugada syndrome genetic testing. *Heart Rhythm* 2010;**7**: 33–46.
3. Wilde AA, Brugada R. Phenotypical manifestations of mutations in the genes encoding subunits of the cardiac sodium channel. *Circ Res* 2011;**108**:884–897.
4. Abriel H. Cardiac sodium channel Na(v)1.5 and interacting proteins: Physiology and pathophysiology. *J Mol Cell Cardiol* 2010;**48**:2–11.
5. Keller DI, Rougier JS, Kucera JP, Benammar N, Fressart V, Guicheney P *et al.* Brugada syndrome and fever: Genetic and molecular characterization of patients carrying SCN5A mutations. *Cardiovasc Res* 2005;**67**:510–519.
6. Poelzing S, Forleo C, Samodell M, Dudash L, Sorrentino S, Anaclerio M *et al.* SCN5A polymorphism restores trafficking of a Brugada syndrome mutation on a separate gene. *Circulation* 2006;**114**:368–376.
7. Shinlapawittayatorn K, Du XX, Liu H, Ficker E, Kaufman ES, Deschenes I. A common SCN5A polymorphism modulates the biophysical defects of SCN5A mutations. *Heart Rhythm* 2011;**8**:455–462.
8. Holst AG, Liang B, Jespersen T, Bundgaard H, Haunso S, Svendsen JH *et al.* Sick sinus syndrome, progressive cardiac conduction disease, atrial flutter and ventricular tachycardia caused by a novel SCN5A mutation. *Cardiology* 2010;**115**:311–316.
9. Lin MT, Wu MH, Chang CC, Chiu SN, Theriault O, Huang H *et al.* In utero onset of long QT syndrome with atrioventricular block and spontaneous or lidocaine-induced ventricular tachycardia: compound effects of hERG pore region mutation and SCN5A N-terminus variant. *Heart Rhythm* 2008;**5**:1567–1574.
10. Kattygnarath D, Maugenre S, Neyroud N, Balse E, Ichai C, Denjoy I *et al.* Mog1: a new susceptibility gene for Brugada syndrome. *Circ Cardiovasc Genet* 2011;**4**:261–268.
11. Deschenes I, Armoundas AA, Jones SP, Tomaselli GF. Post-transcriptional gene silencing of KChIP2 and Navbeta1 in neonatal rat cardiac myocytes reveals a functional association between Na and ito currents. *J Mol Cell Cardiol* 2008;**45**:336–346.
12. Ulloa-Aguirre A, Janovick JA, Brothers SP, Conn PM. Pharmacologic rescue of conformationally-defective proteins: Implications for the treatment of human disease. *Traffic* 2004;**5**:821–837.
13. Valdivia CR, Tester DJ, Rok BA, Porter CB, Munger TM, Jahangir A *et al.* A trafficking defective, Brugada syndrome-causing SCN5A mutation rescued by drugs. *Cardiovasc Res* 2004;**62**:53–62.
14. Gui J, Wang T, Jones RP, Trump D, Zimmer T, Lei M. Multiple loss-of-function mechanisms contribute to SCN5A-related familial sick sinus syndrome. *PloS One* 2010;**5**:e10985.
15. Zhang Y, Wang T, Ma A, Zhou X, Gui J, Wan H *et al.* Correlations between clinical and physiological consequences of the novel mutation R878C in a highly conserved pore residue in the cardiac Na^+ channel. *Acta Physiol (Oxf)* 2008;**194**:311–323.
16. Brodsky JL, Scott CM. Tipping the delicate balance: defining how proteasome maturation affects the degradation of a substrate for autophagy and endoplasmic reticulum associated degradation (ERAD). *Autophagy* 2007;**3**:623–625.
17. Sharkey LM, Cheng X, Drews V, Buchner DA, Jones JM, Justice MJ *et al.* The ataxia3 mutation in the N-terminal cytoplasmic domain of sodium channel Na(v)1.6 disrupts intracellular trafficking. *J Neurosci* 2009;**29**:2733–2741.
18. Chouabe C, Neyroud N, Guicheney P, Lazdunski M, Romey G, Barhanin J. Properties of KvLQT1 K^+ channel mutations in Romano-Ward and Jervell and Lange-Nielsen inherited cardiac arrhythmias. *Embo J* 1997;**16**:5472–5479.
19. Jouvenceau A, Eunson LH, Spauschus A, Ramesh V, Zuberi SM, Kullmann DM *et al.* Human epilepsy associated with dysfunction of the brain P/Q-type calcium channel. *Lancet* 2001;**358**:801–807.
20. Mezghrani A, Monteil A, Watschinger K, Sinnegger-Brauns MJ, Barrere C, Bourinet E *et al.* A destructive interaction mechanism accounts for dominant-negative effects of misfolded mutants of voltage-gated calcium channels. *J Neurosci* 2008;**28**:4501–4511.
21. Cormet-Boyaka E, Jablonsky M, Naren AP, Jackson PL, Muccio DD, Kirk KL. Rescuing cystic fibrosis transmembrane conductance regulator (CFTR)-processing mutants by transcomplementation. *Proc Natl Acad Sci USA* 2004;**101**:8221–8226.
22. Owsianik G, Cao L, Nilius B. Rescue of functional DeltaF508-CFTR channels by co-expression with truncated CFTR constructs in COS-1 cells. *FEBS Lett* 2003;**554**: 173–178.
23. Villmann C, Oertel J, Ma-Hogemeier ZL, Hollmann M, Sprengel R, Becker K *et al.* Functional complementation of Glra1(spd-ot), a glycine receptor subunit mutant, by independently expressed C-terminal domains. *J Neurosci* 2009;**29**:2440–2452.
24. Lee A, Goldin AL. Role of the amino and carboxy termini in isoform-specific sodium channel variation. *J Physiol* 2008;**586**:3917–3926.
25. Undrovinas AI, Fleidervish IA, Makielski JC. Inward sodium current at resting potentials in single cardiac myocytes induced by the ischemic metabolite lysophosphatidylcholine. *Circ Res* 1992;**71**:1231–1241.

Supplemental methods

SCN5A sequence alignment

SCN5A sequence alignment was performed using the following NCBI accession numbers: Homo sapiens: NP_932173.1, Mus musculus: NP_067519.2, Canis lupus: NP_001002994.1, Gallus gallus: XP_418535.2, Xenopus tropicalis: XP_002932534, Danio rerio: DQ837300.1. (E) Alignment of N-terminal sequences of human voltage-dependent Na^+ channels $Na_v1.1$ to $Na_v1.9$. Sequence alignment was done using the following accession numbers: $Na_v1.1$: NP_001189364.1, $Na_v1.2$: NP_001035233.1, $Na_v1.3$: NP_008853.3, $Na_v1.4$: NP_000325.4, $Na_v1.5$: NP_932173.1, $Na_v1.6$: NP_001171455.1, $Na_v1.7$: NP_002968.1, $Na_v1.8$: NP_006505.2, $Na_v1.9$: NP_054858.2.

Solutions and drugs

Thirty-six hours after transfection, HEK293 cells were trypsinized and seeded to a density that enabled single cells to be identified. Green positive cells were chosen for patch-clamp experiments. Cells were bathed in an extracellular Tyrode solution containing (in mM): 135 NaCl, 4 KCL, 2 $MgCl_2$, 2.5 $CaCl_2$, 1 NaH_2PO_4, 20 glucose, 10 HEPES, pH 7.4 (NaOH). Patch pipette medium was (in mM): 5 NaCl, 140 CsCl, 2 $MgCl_2$, 4 Mg-ATP, 5 EGTA, 10 HEPES, adjusted to pH 4.2 with CsOH. During current recording, cells were perfused with an external solution with reduced Na^+ concentration containing (in mM): 80 NaCl, 50 CsCl, 2 $CaCl_2$, 2.5 $MgCl_2$, 10 HEPES, and 10 glucose, adjusted to pH 7.4 with CsOH. HEK293 $Na_v1.5$-stable cell line perfusion medium contained (in mM): 25 NaCl, 108.5 CsCl, 0.5 $CaCl_2$, 10 HEPES, 10 glucose, 2.5 $MgCl_2$, also adjusted to pH 7.4 with CsOH.

Some HEK293 cells transfected with R104W or R121W mutants were cultured with the class I anti-arrhythmic agent mexiletine at several concentrations (30, 60, 140, 250 or 500 µM) for 24h after transfection. Cells were then returned to their normal buffer 30 min before patch-clamp recordings.

RNA extraction and reverse transcriptase-PCR (RT-PCR)

Forty-eight hours after transfection with WT or mutant channels, selected cells were treated with DTT 500 µM for one hour to induce UPR (Unfolded Protein Response) as a positive control. Total RNA was extracted from DTT-treated and non-treated cells using TRIzol reagent with the PureLink mRNA Mini Kit (Invitrogen, CA, USA). One µg of total mRNA was reverse-transcribed with the SuperScriptIII RT-PCR kit (Invitrogen, CA, USA). PCR was then performed as previously reported using primers XBP1-forward CCTTGTAGTTGAGAACCAGG and XBP1-reverse GGGGCTTGGTATATATGTGG[1].

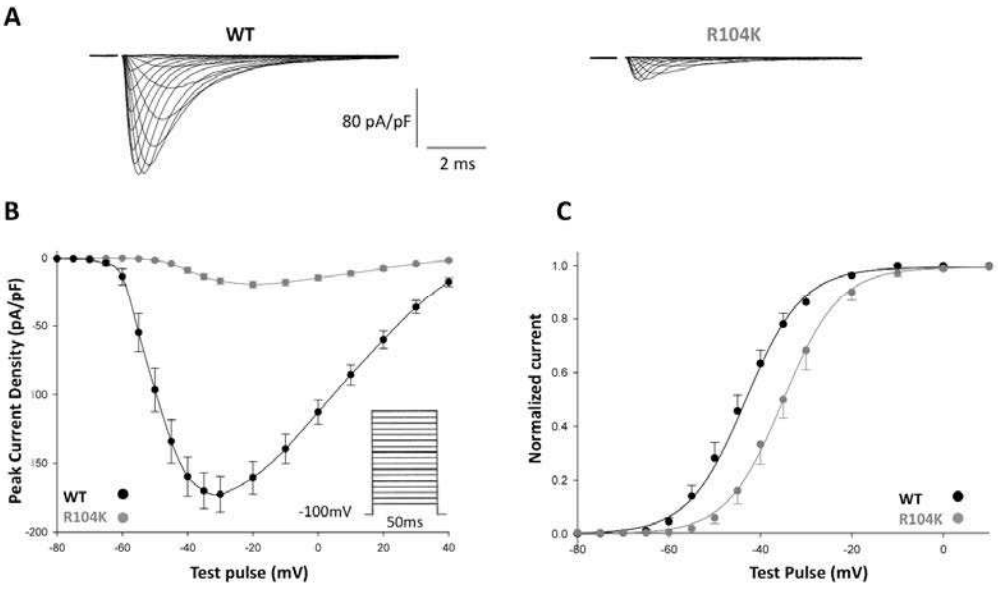

Supplemental Figure 1: Electrophysiological characterization of WT and R104K channels.

To determine whether the absence of the positively charged nature of residue 104 is responsible for the loss of function of the R104W mutant, arginine 104 was replaced by another positive amino acid, lysine. (A) Representative Na^+ current traces of $Na_v1.5$ WT and R104K channels in HEK293 cells transfected with a total of 0.6 µg of plasmid. Solid lines indicate the zero current level. (B) Current density-voltage relationships of WT and R104K channels. R104K gave rise to a small I_{Na} of 12% of WT I_{Na} density (WT: 160±11 pA/pF, n=18 *vs* R104K: 19.4±2.3 pA/pF, n=9, P≤0.001), suggesting that arginine 104 has a more specific role than simply providing a positive charge. (C) V_m-activation relationships of WT and R104K channels. R104K activation was rightward shifted by 8.6 mV compared to WT (WT: -44.2±1.6 mV, n= 17 *vs* R104K: -35.7±2.1 mV, n=8, P≤0.001). R104K $V_{1/2}$ of inactivation was not changed compared to controls (WT: -81.7±0.6 mV, n= 10 *vs* R104K: -79.2±0.6 mV, n=6, ns).

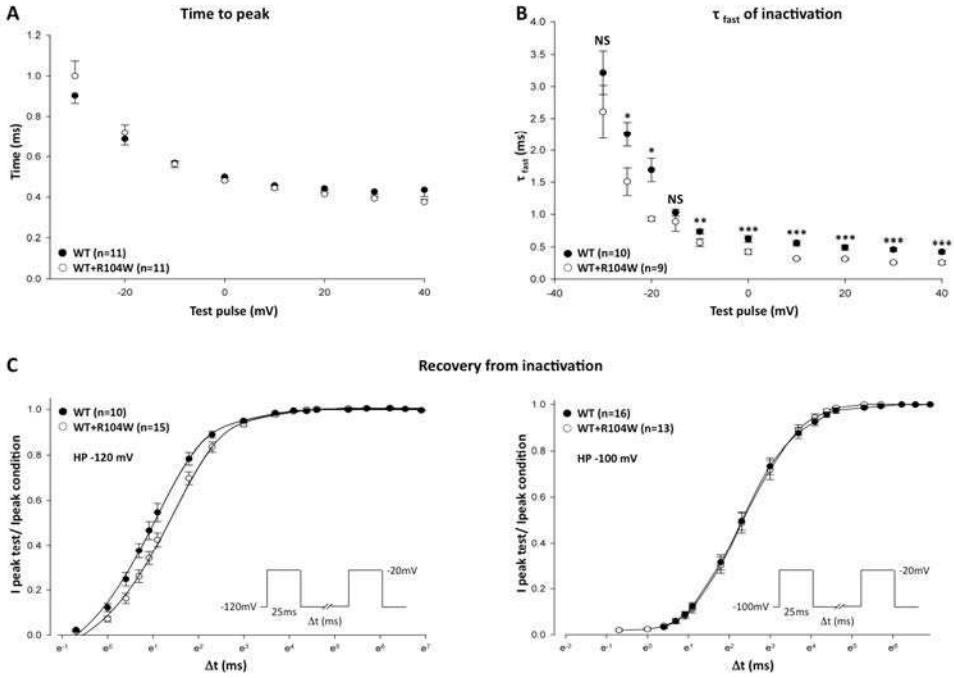

Supplemental Figure 2: Inactivation and recovery from inactivation of WT+R104Wchannels.

A. Kinetics of activation. Time to peak obtained from current traces elicited with the standard I-V protocol, was the time delay between the beginning of the test pulse and the time to reach the current peak. No significant differences were measured in presence of R104W mutant channels compared to WT alone. **B.** Kinetics of inactivation. The fast (τ_f) and slow (τ_s) time constants of inactivation as determined by fitting decaying current curves obtained from the I–V protocol to a double-exponential function. In cells expressing R104W mutant, τ_f of inactivation was faster compared to cells expressing WT alone, while τ_s was unaffected (data not shown). This suggested that the presence of the R104W mutant channel affected inactivation kinetics of WT channels. **C.** Recovery from inactivation of I_{Na} at holding potentials of -120 mV (left panel) or -100 mV (right panel). Test- and conditioning-pulses of 25 ms were separated by the recovery time Δt from 0.5 ms to 1000 ms. Relative currents were calculated as peak I_{Na} elicited by test-pulse versus that elicited by conditioning-pulse, for two different holding potentials: -100 mV and -120 mV. At a holding potential (HP) of -120 mV, τ_{fast} of WT channels was significantly shorter (3.0±0.4 ms (n=10)) than τ_{fast} of WT+R104W channels (4.7±0.5 ms (n=15); $P<0.05$). At a HP of -100 mV, τ_{fast} was not different between WT and WT+R104W channels. τ_{slow} was 43±17 ms, (n=10) for WT, and 60±14 ms, (n=15) for WT+R104W, and were not significantly different. * $P<0.05$, ** $P<0.01$, *** $P<0.001$.

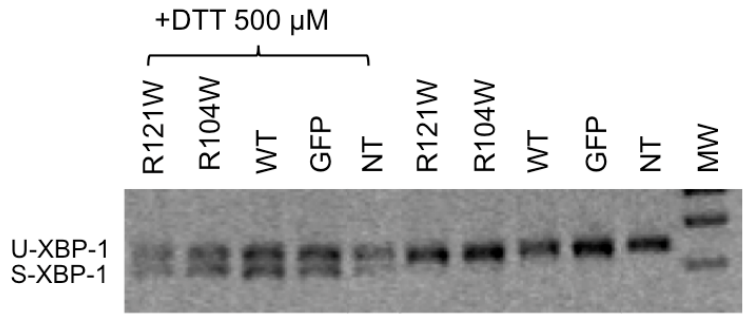

Supplemental Figure 3: RT-PCR of XBP-1 mRNA from HEK293 cells transfected with N-terminal $Na_v1.5$ mutants.
Accumulation of unfolded proteins in the ER can cause reticular stress, and activate signaling pathways including the unfolded protein response (UPR)[2]. UPR activation leads to the XBP-1 mRNA splicing of 26 nucleotides (S-XBP-1) causing a frameshift and the generation of a longer active protein. Analysis of these spliced transcripts is used as a marker of reticular stress[1]. MW indicates molecular weight and NT non-transfected cells. Only cells incubated with DTT, known to induce reticular stress and used as a positive control, contained S-XBP-1 mRNA, suggesting that the mutant Nav1.5 channel transfection does not cause reticular stress by UPR activation.

Supplemental references

1. Yoshida H, Matsui T, Yamamoto A, Okada T, Mori K. XBP1 mRNA is induced by ATF6 and spliced by IRE1 in response to ER stress to produce a highly active transcription factor. *Cell* 2001; **107**:881-891.
2. Brewer JW, Hendershot LM. Building an antibody factory: a job for the unfolded protein response. *Nat Immunol* 2005; **6**:23-29.

I.3 The N-terminal domain is not the site of interaction between $Na_v1.5$ α-subunits

Our previous study demonstrated for the first time that $Na_v1.5$ α-subunits interact with each other. So, our aim was then to search for the site of interaction between $Na_v1.5$ α-subunits. As the N-terminal mutant R104W has a dominant-negative effect on the WT by retaining it in the ER, we thought that the N-terminal domain of $Na_v1.5$ could be the site of interaction between $Na_v1.5$ α-subunits. To test this hypothesis, co-immunoprecipitation studies were performed in HEK293 transfected with either HA-WT + GFP-WT or HA-WT + ΔNter-GFP, and HA-WT alone as a negative control. Immunoprecipitations were performed with the anti-GFP antibody, and western blot revealed with the anti-HA and anti-GFP antibodies. In cells expressing HA-WT + GFP-WT or HA-WT + ΔNter-GFP, a specific band at the expected size of HA-WT was present (Figure 46), indicating that the WT and ΔNter α-subunits interacted with each other. Our results suggest that the interaction between $Na_v1.5$ α-subunits is not N-ter-N-ter. However, we cannot exclude that the interaction could occur for example between the N-terminus and the C-terminus, or between the C-termini. To test this hypothesis further constructs are needed where both N- and C-terminal domains are deleted. In addition, it is possible that the interaction occurs at different sites along the channel, involving the P-loops and the cytoplasmic linkers.

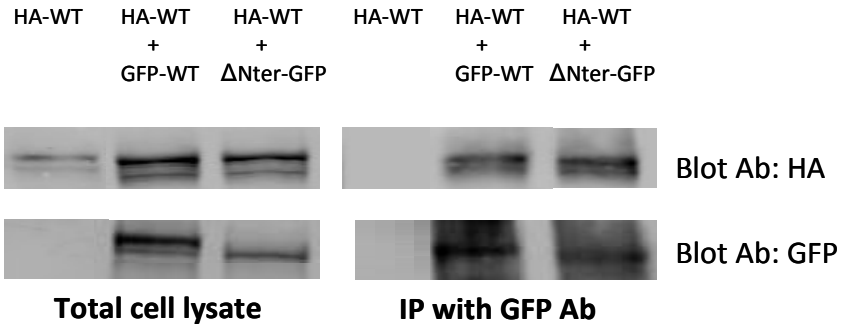

Figure 46: Co-imunoprecipitation study between WT $Na_v1.5$ and ΔNter α-subunits

II. Article 2

A truncating *SCN5A* mutation combined with genetic variability causes sick sinus syndrome and early atrial fibrillation

II.1 Summary of the study

Introduction

Mutations in the *SCN5A* gene encoding the cardiac sodium channel $Na_v1.5$ have been associated with a variety of arrhythmic disorders, highlighting the important role of $Na_v1.5$ channel function in hereditary cardiac arrhythmias. *SCN5A* gain-of-function mutations are linked to LQTS type 3, while loss-of-function mutations induce cardiac conduction abnormalities, BrS, SSS, and some mutations have also been reported in AF. In addition, several *SCN5A* mutations are associated with mixed clinical phenotypes, now known as "overlap syndrome". The mechanisms by which one *SCN5A* mutation leads to variable clinical picture remain unknown, but this suggests the involvement of other factors in modulating the disease phenotypes.

The C-terminal cytoplasmic domain of $Na_v1.5$ plays an important role in the transport and the localization of $Na_v1.5$ at the membrane, through the interaction with several partner proteins involved in channel trafficking, such as SAP97, syntrophin and Nedd4-2. It is also involved in channel inactivation by stabilizing the closed state preventing channel re-opening.

In this study we characterized the C-terminal mutation R1860Gfs*12, which is a frame-shift mutation changing the amino acid arginine at position 1860 into glycine and causing premature termination of $Na_v1.5$ protein at position 1871, resulting in a loss of interaction with several C-terminal-partner proteins. R1860Gfs*12 was identified in a family with a mixed clinical picture of SSS and AF or flutter, and atrioventricular-block. Spontaneous BrS ECG pattern or ventricular arrhythmias were not reported in this family. In addition, ajmaline test in one mutation carrier ruled out BrS but enhanced the conduction abnormalities.

Methods and Results

Patch-clamp analysis of HEK293 transfected with the C-terminal mutant R1860Gfs*12 alone showed that the mutant induced a drastic reduction of I_{Na} density, a positive shift of activation, a negative shift of steady-state inactivation and an increase in persistent current compared to WT. The total protein expression of the mutant was decreased compared to the WT, which was consistent with the reduction in I_{Na} density. In addition,

treating the cells with MG132, a 26S-subunit ubiquitin-proteasome inhibitor, increased the total protein expression of the mutant, suggesting its partial proteasomal degradation. At the heterozygous state, the mutant did not have a dominant-negative effect on the WT channel, but the steady-state inactivation remained importantly left-shifted, and a persistent current was still present. Since the clinical phenotype in this family was mostly atrial, we thought that differences in the electrophysiological properties between atrium and ventricles could be the underlying cause. By measuring I_{Na} of the WT and heterozygous state in HEK293 cells at holding potentials mimicking the resting membrane potentials of atrial or ventricular cardiomyocytes, we showed that the mutant has more pronounced loss-of-function effect at the atrial potential compared to the ventricular one. Moreover, the biophysical properties of Na^+ current for the WT and the heterozygous state were included into a computer model simulation of atrial and ventricular membrane action potentials, which showed that the mutant induced a more marked decrease in AP maximum upstroke velocity, with a marked lengthening of the action potential duration in atrial cells compared to ventricular ones.

Since we demonstrated in our previous study that $Na_v1.5$ α-subunits interact with each other, we tested whether the R1860Gfs*12 truncated mutant still interacted with the WT. By co-immunoprecipitation studies, we showed that the mutant α-subunits interacted with the WT as well as with themselves.

The proband in this family developed the disease at a young age compared to her father and uncle, who carry also the mutation. She had severe SSS requiring the implantation of a pacemaker at 13, and AF at 20. This suggests that the genetic background of the proband could have a role in modulating the disease phenotype. We screened in this family 17 SNPs linked to AF, and we showed that the proband was the only mutation carrier who had one at-risk allele located upstream of *PITX2*, a gene widely associated with AF.

Discussion

The mixed clinical picture caused by a single *SCN5A* mutation raised the possibility of the involvement of other factors in modulating the disease phenotype. In this study, by characterizing the C-terminal truncating mutation R1860Gfs*12, we showed that the differences in the electrophysiological properties between the atrium and ventricles and the altered biophysical properties of the mutant, combined to the genetic background of patients could be some of these factors.

The R1860Gfs *12 is the most distal truncating *SCN5A* mutation identified so far. It is located in the C-terminal region, which has an important role in the channel function through the interaction with many partner proteins[469]. R1860Gfs*12 mutation carriers presented with

a mixed clinical picture, mostly atrial with variable severity (SSS, artial fibrillation or flutter with atrioventricular block).

In the heterozygous state mimicking the heterozygosity of the patients, the altered biophysical properties, mainly the significant negative shift of steady-state inactivation, and the persistent sodium current could explain the clinical phenotype. The increased persistent Na^+ current might cause early after depolarizations (EADs), and delayed after depolarizations (DADs), thereby inducing triggered activities accounting for AF[95,96]. The negative shift of steady-state inactivation combined to the persistent current could be responsible for the SSS and the conduction abnormalities through the reduction of Na^+ channel availability at the normal resting potential of cardiac cells and by the prolongation of the AP[211]. However, these finding cannot explain why the clinical presentation in this family was mostly atrial and why no ventricular arrhythmias were observed. I_{Na} recording in HEK293 cells at holding potential mimicking the constitutively different resting membrane potentials of atrial and ventricular cells, and the computer model stimulation demonstrated a more pronounced effect of the mutant in atrial conditions compared to the ventricular ones, that could explain the prominence of atrial arrhythmias in this family. Indeed, it has been demonstrated that resting membrane potential of atrial cells is more depolarized, and the critical depolarization and current threshold for action potential initiation are smaller in atrial cells than in ventricular cells[470,471], indicating that atrial cells are more readily excitable, and are constitutively more susceptible to develop arrhythmia. These findings suggest that the altered functions of $Na_v1.5$ channel caused by some *SCN5A* mutations, like R1860Gfs*12, could have a greater impact in the atria than in the ventricles, depending on the mutation biophysical properties, and thus predisposing to the development of atrial arrhythmias more readily than to ventricular ones.

By screening 17 SNPs linked to AF, we showed that the proband of this family was the only mutation carrier to carry an AF at-risk allele located upstream of the *PITX2* gene, which encodes a transcription factor involved in the development of the sinus node and the pulmonary vein[124,125]. *PITX2* variants have been widely associated with AF development, mainly early onset AF[115,120]. This association has also been reported to contribute to post-cardiac surgery AF[472] and to recurrence of AF after catheter ablation[473] and cardioversion[474]. In atrial-specific *PITX2* knockout mouse model, reduced mRNA and $Na_v1.5$ protein levels were observed[475]. We hypothesized that that *PITX2* variant could lead to early morphological changes and further loss-of-function of $Na_v1.5$ channels in the proband's atrium compared to her father and uncle, accounting for the occurrence of severe SSS and early onset AF in the proband.

Conclusion

The constitutive differences in the resting membrane potential between atrium and ventricle combined with the altered biophysical properties of $Na_v1.5$, and the genetic background of patients are factors that could modify the phenotype caused by *SCN5A* mutations, and most probably responsible for the predominance of the atrial arrhythmias in these patients carrying the R1860Gfs*12 mutation.

II.2 Article accepted for publication in the Heart Rhythm Journal

A truncating SCN5A mutation combined with genetic variability causes sick sinus syndrome and early atrial fibrillation

Azza Ziyadeh-Isleem, MD [*,1,2], Jérôme Clatot, PhD [*,1,2,3], Sabine Duchatelet, PhD [1,2], Estelle Gandjbakhch, MD, PhD [1,2,4], Isabelle Denjoy, MD [1,2,5], Françoise Hidden-Lucet, MD [1,2,4], Stéphane Hatem, MD, PhD [1,2], Isabelle Deschênes, PhD, FHRS [3], Alain Coulombe, PhD [1,2], Nathalie Neyroud, PhD [‡,1,2], Pascale Guicheney, PharmD, PhD [‡,1,2]

[*,‡] Both authors contributed equally to this work.

Running title: Effects of a $Na_v1.5$ truncating mutation

[1] INSERM, UMR_S1166, Paris, France

[2] Sorbonne Universités, UPMC Univ Paris 06, UMR_S1166, Institute of Cardiometabolism and Nutrition (ICAN), Paris, France

[3] Heart and Vascular Research Center, MetroHealth Campus, Case Western Reserve University, Cleveland, OH, USA

[4] AP-HP, Hôpital Pitié-Salpêtrière, Département de Cardiologie, Paris, France

[5] AP-HP, Hôpital Bichat, Département de Cardiologie, Centre de Référence des Maladies Cardiaques Héréditaires, Paris, France

Acknowledgments: This work was supported by Institut National de la Santé et de la Recherche Médicale (INSERM), the Université Pierre and Marie Curie, the Agence Nationale de la Recherche (ANR-09-GENO-003-CaRNaC, the French Ministry of Health (P.H.R.C. AOR04070, P040411) and NIH R01 (HL094450) (ID).

Word count: 4983 words

None of the authors has conflict of interest.

Correspondence to:
Pascale Guicheney
INSERM, UMR_S1166, Université Pierre & Marie Curie Paris 6
91, boulevard de l'Hôpital, F-75013 Paris, France
Phone: (33) 1 40 77 96 49; Fax: (33) 1 40 77 96 45
Email: pascale.guicheney@upmc.fr

Abstract

Background: Mutations in the *SCN5A* gene, encoding the α-subunit of the cardiac Na^+ channel, $Na_v1.5$, can result in several life-threatening arrhythmias.

Objective: To characterize a distal truncating *SCN5A* mutation, R1860Gfs*12, identified in a family with different phenotypes including sick sinus syndrome (SSS), atrial fibrillation (AF), atrial flutter and atrioventricular-block.

Methods: Patch-clamp and biochemical analysis were performed in HEK293 cells transfected with wild-type (WT) and/or mutant channels.

Results: The mutant channel expressed alone caused a 70% reduction in I_{Na} density compared to WT currents, consistent with its partial proteasomal degradation. It led also to a negative shift of steady-state inactivation and to a persistent current. When mimicking the heterozygous state of the patients by co-expressing WT and R1860Gfs*12 channels, the biophysical properties of I_{Na} were still altered, and the mutant channel α-subunits still interacted with the WT ones. Since the proband developed paroxysmal AF at young age, we screened 17 polymorphisms associated with AF risk in this family, and showed that the proband carries at-risk polymorphisms upstream of *PITX2*, a gene widely associated with AF development. In addition, when mimicking the difference in resting membrane potentials between cardiac atria and ventricles in HEK293 cells, or using computer-model simulation, R1860Gfs*12 induced a more drastic decrease in I_{Na} at the atrial potential.

Conclusion: We have identified a distal truncated *SCN5A* mutant associated with gain- and loss-of-function effects, leading to SSS and atrial arrhythmias. A constitutively higher susceptibility to arrhythmias of atrial tissues and genetic variability could explain the complex phenotype observed in this family.

Keywords

Arrhythmia; Atrial fibrillation; $Na_v1.5$; SCN5A; Sodium; PITX2; Polymorphism; SNP

Abbreviations

AF = atrial fibrillation

AP = action potential

BrS = Brugada syndrome

ECG = electrocardiogram

HP = holding potential

HR = heart rate

I_{Na} = inward sodium current

LQTS = long QT syndrome

SNP = single nucleotide polymorphism

SSS = sick sinus syndrome

TTX = tetrodotoxine

WT = wild type

Introduction

Coordinated activity of multiple ion channels tightly controls generation and propagation of cardiac action potentials (AP)[1]. Mutations in the *SCN5A* gene, encoding the $Na_v1.5$ α-subunit of the cardiac sodium channel, have been involved in numerous inherited cardiac arrhythmias including long QT syndrome (LQTS), Brugada syndrome (BrS), and rare cases of sick sinus syndrome (SSS) and atrial fibrillation (AF)[2]. Atrial arrhythmias are being increasingly diagnosed in patients with BrS (incidence of 6-38%)[3], as well as LQTS[4]. Originally, the various *SCN5A*-related arrhythmias were considered separate clinical entities with distinct phenotypical characteristics. Recently, a wide spectrum of mixed disease phenotypes was reported in these arrhythmias, referred to as overlap syndrome of cardiac Na^+ channelopathy[2]. The reasons why the same *SCN5A* mutation can result in different phenotypes remain unknown, but it raises the possibility that the disease expressivity is influenced by altered biophysical properties and genetic modifiers[5].

In this study, we characterized the $Na_v1.5$ C-terminal truncating mutation R1860Gfs*12 identified in a family presenting with a complex clinical picture of SSS and AF or atrial flutter. Heterologous expression of the mutant channels alone or with wild-type (WT) channels led to a reduction in I_{Na} density, a persistent current and a drastic alteration of the inactivation properties. Interestingly, because of the constitutively different resting membrane potentials in atrial and ventricular tissues, the atrium of the patients might be more susceptible to the altered biophysical properties of the mutant channels and, thus, more prompt to develop arrhythmias. Moreover, the proband carries at-risk polymorphisms upstream of *PITX2*, a gene widely associated with AF development. Altogether, our results could explain the mixed clinical phenotype of this family.

Methods

Patient

Blood samples were obtained after signed written informed consent for genetic analyses and after approval by the local ethics committee. The study was conducted according to the principles of the Helsinki Declaration.

Mutation and SNP analysis

Genomic DNA was isolated from leukocytes according to standard procedures. Screening for mutations was performed by genomic DNA amplification of all exons and splice junctions of several genes responsible for arrhythmias (Supplemental methods). We also genotyped single nucleotide polymorphisms (SNP) associated with AF[6,7] (Supplemental Table 1).

PCR products were directly sequenced with the Big Dye Terminator v.3.1 kit on an ABI PRISM 3730 automatic DNA sequencer (Applied Biosystems). Variants were identified by visual inspection of the sequences with Seqscape software (Applied Biosystems).

SCN5A cDNA cloning and mutagenesis

Plasmids pcDNA3.1-hH1a (no tag) and pcDNA3.1-GFP-hH1a (N-terminal-GFP) were the gift of Dr H. Abriel (Bern, Switzerland). The plasmid pRcCMV-FLAG-SCN5A (N-terminal-FLAG) was the gift of Dr N. Makita (Nagasaki, Japan). All these plasmids contain the hH1a isoform of *SCN5A*. $Na_v1.5$ mutant R1860Gfs*12 was prepared using the QuikChange II XL Site-Directed Mutagenesis Kit (Stratagene) according to the manufacturer's instructions and verified by sequencing. The plasmid pIRES2-acGFP1-FHF1B (C-terminal His_6) was the gift of Dr G. S. Pitt (Durham NC, USA).

HEK293 cell culture and transfection

HEK293 cells were transfected with jetPEI (Polyplus Transfection, New York, USA) according to the manufacturer's instructions. For patch-clamp recordings, HEK293 cells were transfected with pcDNA3.1-GFP-hH1a WT or mutant in 35-mm well dishes, with a total of 0.6 µg of plasmid per 35 mm dish. To mimic the heterozygous state of the patient, cells were co-transfected with 0.3 µg of pcDNA3.1-hH1a (no tag) WT and 0.3 µg of pcDNA3.1-GFP-hH1a mutant. For biochemical analysis, cells were plated in 25-cm² flasks and transfected with 2 µg of pcDNA3.1-GFP-hH1a WT or mutant.

Electrophysiological recordings

Patch-clamp recordings were carried out in the whole-cell configuration at room temperature (~22°C). Solutions for patch-clamp recording are described in the Supplemental methods. Ionic currents were recorded with the amplifier Axopatch 200B (Axon Instruments, CA, USA). Patch pipettes (Corning Kovar Sealing code 7052, WPI) had resistances of 1.5–2.5 MΩ, when filled with pipette medium. Currents were filtered at 10 kHz (-3 dB, 8-pole low-pass Bessel filter) and digitized at 50 kHz (NI PCI-6251, National Instruments, Austin, TX, USA). Data were acquired and analyzed with ELPHY2® software (G. Sadoc, CNRS, Gif/Yvette, France).

Current–voltage relationships (I/V curves) and the steady-state inactivation-V_m protocols were as previously reported[8]. Data for the activation-V_m and steady-state inactivation-V_m relationships of I_{Na} were fitted to the Boltzmann equation as previously reported[8].

The putative involvement of a persistent Na^+ current was assessed by using 100 µM tetrodotoxine (TTX). Currents were elicited by a 500-ms step to -20 mV from a holding potential of -120 mV. The percentage of persistent current was calculated by dividing the TTX-sensitive I_{Na} amplitude determined at the end of the pulse by the peak I_{Na} amplitude obtained before TTX application.

Computer simulations of atrial and ventricular membrane action potentials were performed using Oxsoft Heart Model V. 4.8 as described in the Supplemental methods.

Protein extraction and Western blot

They were performed as previously reported[8]**.** Primary antibodies used were: rabbit anti-GFP (1:2000, Torrey Pines Biolabs, USA), mouse anti-Flag (1:500, Sigma, USA), and rabbit anti-GAPDH (1:2000, Abcam, UK). Total protein signals were firstly normalized to GAPDH levels and then to WT levels.

Co-immunoprecipitation

Co-immunoprecipitation experiments were performed as described in the Supplemental methods. Briefly, total cell lysates were incubated with Dynabeads (Dynal, Norway) crosslinked to anti-GFP antibody (Torrey Pines Biolabs, USA) for 2 h at room temperature. Western blots were revealed using either rabbit anti-GFP (Torrey Pines Biolabs, USA), or mouse anti-Flag (Sigma, USA) antibodies.

Statistical analysis

Data are presented as means ± SEM. Statistical significance was estimated with SigmaPlot® software by Student's t-test or ANOVA, as appropriate. $P < 0.05$ was considered significant.

Results

Identification of a truncating mutation in *SCN5A*

The proband (III.2) was a 26-year-old female diagnosed at 13 with severe SSS associated with severe sinus bradycardia, symptomatic sinus pauses and syncope (Figure 1A and B) which required a pacemaker implantation. At the age of 20, paroxysmal AF was documented in the memories of the pacemaker. She secondarily developed a first degree AV-block (PR = 280 ms, QRS = 80 ms, QTc = 360 ms). Her father (II.2) was diagnosed at 27 with an asymptomatic sinus node dysfunction. At the age of 42, he had one episode of atrial flutter after jogging, and was treated by cardioversion. Moreover, he developed first degree AV-block with left anterior hemi-block (PR = 240 ms, QRS = 80 ms, QTc = 400 ms) (Figures 1A and Ca-b). The proband's uncle (II.1) was diagnosed with SSS which required a pacemaker implantation at 30. None displayed spontaneous Brugada ECG pattern or developed ventricular arrhythmias. The proband's father underwent an ajmaline challenge that excluded BrS ECG pattern (Figure 1Cc-d). It induced bradycardia (40 beats/min), severe prolongation of the PR interval (300 ms) and the QRS complex (240 ms). In addition, sinus node dysfunction with junctional escape rhythm, and supraventricular premature contractions were observed (Supplemental Figure 1). Echocardiograms ruled out structural heart disease except for mild atrial dilatation in the proband's father. The mother and the proband's sister were asymptomatic (Figure 1A).

We sequenced the coding regions of fourteen genes involved in cardiac arrhythmias and identified a unique mutation in *SCN5A,* a deletion of one base pair (A) at the position 5578 in exon 28 (c.5578delA). This deletion induced a frameshift mutation, p.R1860Gfs*12, which changed the amino acid arginine at position 1860 into glycine followed by 10 frame-shifted amino acids before a premature stop codon (Supplemental Figure 2). The proband, her father and uncle carried this mutation, whereas her mother and sister did not (Figure 1A). This variant has never been described and is absent from publicly available databases.

Suspecting the possible contribution of additional genetic factors for AF development, we genotyped the family members for 17 SNPs that alter AF susceptibility (Supplemental Table 1). Interestingly, the proband, who experienced severe SSS and early onset AF, is the only mutation carrier to have one at-risk allele of rs6817105 and rs2200733 located upstream of the *PITX2* gene, which she received from her mother (Figure 1A and Supplemental Table 1). In addition, the father had 2 copies of the protective allele of rs3853445, another SNP

located upstream of the *PITX2* gene, while the proband carried only one copy (Figure 1A and Supplemental Table 1). The multimarker risk score for AF based on combined rs2200733, rs17570669 and rs3853445 genotypes[9] was higher in the proband (1.74) compared to her father (<1) and uncle (<1).

The R1860Gfs*12 mutation produced a loss- and gain-of-function of $Na_v1.5$

Na^+ currents were recorded in HEK293 cells 36 h after transfection with WT or mutant channels. I_{Na} traces and I/V relationships are shown in Figure 2. Peak current densities and *P*-values are given in Table 1. Alone, R1860Gfs*12 showed a drastic reduction of I_{Na} density compared to WT channels (Figure 2A and B). Furthermore, the biophysical characteristics of the C-terminal mutant channels were impaired (Table 1, Figure 2C and D). Indeed, the $V_{1/2}$ of activation for R1860Gfs*12 was shifted by +7.1 mV, and the $V_{1/2}$ of inactivation was shifted by -24.5 mV compared to WT. No change in recovery from inactivation was observed (Supplemental Figure 3). Fast and slow time constants of inactivation (τ_{fast} and τ_{slow}) were significantly increased compared to WT channels (Table 1, Figure 3A-C).

The presence of a TTX-sensitive persistent Na^+ current was assessed using 100 μM TTX (Figure 3D and Supplemental Figure 4). The mutant channel generated a persistent current of 4% of the peak current.

Co-expression of WT and R1860Gfs*12 channels also led to a loss- and gain-of-function of $Na_v1.5$

To mimic the heterozygous state of the patient, cells were co-transfected with the WT channel (no tag) and the R1860Gfs*12 mutant channel (GFP tagged) in a 1:1 ratio. In co-transfected cells, peak current densities were slightly reduced (Figure 2A and B), but not significantly different from the WT alone, as for the $V_{1/2}$ of activation. In contrast, the $V_{1/2}$ of steady-state inactivation remained significantly shifted by -16.6 mV compared to WT (Table 1, Figure 2C and D). Moreover, τ_{fast} and τ_{slow} were significantly increased at the heterozygous state compared to WT alone (Table 1, Figure 3A and B), and the persistent current was still present (Table 1, Figure 3D and Supplemental Figure 4).

Since the steady-state inactivation of the mutant channels alone or co-expressed with WT channels were drastically shifted, we measured I_{Na} successively from a holding potential (HP) of -86 and -83 mV mimicking the ventricular *vs* atrial resting membrane potentials[10,11]. Interestingly, we showed that the 3-mV difference in HPs was sufficient to enhance the reduction of I_{Na} due to the mutation in the atrium compared to the ventricle (Figure 3E).

Indeed, the current reduction was 17% for WT channels, 25% for WT + R1860Gfs*12, and 40% for, R1860Gfs*12 at a HP of -83 *vs* -86 mV.

Differences between WT and heterozygous channel characteristics were included into computer-model simulations of single atrial and ventricular cell membrane action potentials (Supplemental methods). The AP maximum upstroke velocity ($[dV/dt]_{max}$) of the heterozygous state exhibited an important decrease in the atrial (68%) compared to the ventricular myocyte (33%), as well as a marked lengthening of the AP duration in the atria (Figure 4).

The R1860Gfs*12 mutant was partially degraded by the ubiquitin-proteasome system

Western blots of total lysates from transfected HEK293 cells showed a significant decrease of ≈70 % in the total protein expression of the mutant channels when compared to WT, in accordance with the reduction of the current density (Figure 5A). Moreover, incubation of the cells with the 26S-subunit ubiquitin-proteasome inhibitor, MG132, significantly increased the mutant total expression, suggesting a proteasomal degradation of the R1860Gfs*12 mutant (Figure 5A).

The R1860Gfs*12 mutant interacted with WT α-subunits

We have previously demonstrated by co-immunoprecipitation that $Na_v1.5$ α-subunits interact together[8]. To assess if the R1860Gfs*12 truncating mutant still interacted with the WT channel, we performed co-immunoprecipitation in HEK293 cells transfected with either Flag-WT + GFP-WT or Flag-WT + GFP- R1860Gfs*12, and Flag-WT alone as a negative control. Immunoprecipitations were performed with the anti-GFP antibody, and western blot revealed with the anti-Flag antibody. In cells expressing Flag-WT + GFP-WT or Flag-WT + GFP- R1860Gfs*12, a specific band at the expected size of Flag-WT was present (Figure 5B), indicating that the WT and the R1860Gfs*12 truncated α-subunits interacted with each other.

To test whether the R1860Gfs*12 α-subunits could interact with each other, co-immunoprecipitation was performed in HEK293 cells transfected with Flag-R1860Gfs*12 + GFP-R1860Gfs*12. Figure 5B shows that the interaction between truncated α-subunits still occurred. Thus, our results suggested that the last 156 amino acids of the C-terminal domain of $Na_v1.5$ were not essential for the interaction between $Na_v1.5$ α-subunits.

Discussion

We functionally characterized a novel frameshift deletion in *SCN5A* inducing the most distal truncation of the C-terminus of $Na_v1.5$ reported so far, identified in a family with early SSS and atrial arrhythmias. We report that the R1860Gfs*12 mutant showed a loss- and gain-of-function phenotype, which, combined with the variable genetic background of the mutation carriers, may explain the patients' clinical features.

Functional characteristics of R1860Gfs*12 channels

Mutations in *SCN5A* are known to cause various types of arrhythmias including BrS, LQTS, sinus node dysfunction, AF, and overlap syndrome[2]. In general, *SCN5A* mutations leading to a decrease in I_{Na} (loss-of-function) have been associated with conduction slowing and BrS. Gain-of-function mutations in *SCN5A* are typical of LQTS. Nevertheless, numerous reports have shown that a single $Na_v1.5$ mutation may induce various combinations of clinical phenotypes[2]. Here, the R1860Gfs*12 mutant channel expressed alone was mostly degraded, causing a severe reduction in I_{Na} density. Moreover, it induced a 7-mV positive shift of activation, which could delay the action potential, and a dramatic -25 mV shift of the steady-state inactivation, which is likely due to the location of the mutation within a region involved in the inactivation of $Na_v1.5$ and would decrease I_{Na} and affect the action potential velocity. In addition, we showed an inactivation defect delaying the fast and slow inactivation. This loss-of-function phenotype was associated with gain-of-function characteristics since the mutant produced a significant persistent Na^+ current. When co-expressing this mutant with WT channels in order to mimic the heterozygosity of the patients, the steady-state inactivation was also importantly left-shifted, and a persistent current was still present. These parameters have been shown to be a substrate for atrial fibrillation by causing repolarization failure, early after-depolarizations and delayed after-depolarizations[12–14]. Moreover, regarding the important role of $Na_v1.5$ channels in the sino-atrial node function[15,16], the negative shift of inactivation and the persistent current could account for the sinus node dysfunction in this family[17].

We have recently shown that $Na_v1.5$ α-subunits were able to oligomerize, leading to the dominant-negative effect of some BrS *SCN5A* mutations through the retention of WT channels by mutant channels[8]. Here, we showed that the truncated R1860Gfs*12 mutant channels were still interacting with the WT channels. This result suggests that the last 156 amino acids of the C-terminal domain of $Na_v1.5$ are not the main site for α-subunit interaction. In addition, the significant negative shift of the steady-state inactivation in cells

co-expressing mutant and WT channels suggests that $Na_v1.5$ α-subunits also function as oligomers. Alternatively, the C-terminus of $Na_v1.5$ is a site of interactions with several proteins that have important roles, not only in channel function but also in the stabilization of the channels within the plasma membrane[18]. We verified that the truncated R1860Gfs*12 channel did not interact with FHF1B (Supplemental methods, and Supplemental Figure 5). A similar loss of interaction with partners such as SAP97 and syntrophin could contribute to a loss of stability and expression of the truncated channels at the cell membrane[18].

R1860Gfs*12 gain- and loss-of-function features underlie a complex clinical phenotype

Since $Na_v1.5$ channels are expressed in both the atrium and the ventricle, it is unclear why the R1860Gfs*12 mutation carriers showed only atrial but no ventricular arrhythmias. One hypothesis is that the constitutively different electrophysiological properties of atrial and ventricular cells might be an underlying cause. Indeed, it has been shown that the resting membrane potential is more depolarized[10,11], and the I_{Na} density is more important with a negative shift in the steady-state inactivation in the atrium compared to the ventricle[10]. Moreover, atrial cells are more readily excitable than ventricular cells[11]. This suggests that the atrium is constitutively more susceptible to develop arrhythmias than the ventricle. This led us to explore the R1860Gfs*12 mutant current density at the atrial *vs* the ventricular resting membrane potential. Here we showed that a 3-mV difference in resting membrane potentials led to a significant decrease of the peak current by 40% in the atria *vs* the ventricle for the mutant alone, and by 25% when the mutant was co-expressed with WT channels. These results were confirmed by computer-model simulations showing that co-expression of mutant and WT channels led to a more important decrease in the maximum upstroke velocity ($[dV/dt]_{max)}$ in the atrial compared to the ventricular myocytes, as well as a significant increase in the AP duration. Therefore, this *SCN5A* mutation could have different tissue consequences, and could contribute to the predominance of an atrial phenotype in this family.

A very few C-terminal truncating mutations have been identified in $Na_v1.5$[19,20], but their functional consequence have not been studied, except for the C-terminal truncating mutation L1821fs*10. This mutation has been detected in a patient with a complex clinical phenotype of congenital SSS, cardiac conduction disorder with recurrent monomorphic ventricular tachycardia, but no BrS[20]. Functional characterization of this mutant evidenced biophysical properties very similar to the ones of R1860Gfs*12, displaying a gain- and loss-of-function phenotype. Nevertheless, Tan *et al* only reported the absence of a dominant-negative effect of the mutant on the WT channel I_{Na} density[20], while we observed an alteration of the

inactivation biophysical parameters and the presence of a persistent current, when R1860Gfs*12 was co-expressed with WT channels. Altogether, these observations suggest that other parameters, such as additional genetic factors, might influence the clinical expression of the R1860Gfs*12 mutation.

Genetic background of the R1860Gfs*12 mutation carriers

The early occurrence of sinus node dysfunction in the proband at the age of 13 years, followed by atrial fibrillation at 20 was suggestive of a specific genetic background in this patient. Thus, we explored the possibility that polymorphisms associated with AF could modulate the phenotypic expression of the R1860Gfs*12 mutation. Interestingly, the proband is the only mutation carrier who received the *PITX2* at-risk alleles for AF (rs6817105, rs2200733)[6,7]. Furthermore, she received only one *PITX2* protective allele (rs3853445)[9], while her father had 2 copies. The role of the PITX2 transcription factor has been reported in the development of the sinus node and pulmonary vein myocardium[21], which is an important site for AF initiation. Among the numerous variants associated with AF, the 4q25 variants upstream of the *PITX2* gene have the largest effect in early and late AF[6,7]. Reduced PITX2c expression, the main cardiac isoform, was found in AF patients and was shown to induce atrial electrical and structural remodeling in a murine model with a reduction of mRNA and $Na_v1.5$ protein levels[21]. Thus, it is tempting to speculate that the presence of 4q25 variants could induce early atrial morphological changes and further loss of function of $Na_v1.5$ channels in the atrium in the proband, and may thus account for the occurrence of severe SSS with AF at young age compared to her father who had asymptomatic SSS, and her uncle who developed SSS later in his life. Of course, additional factors may also contribute to the clinical phenotypes.

Conclusion

In conclusion, we showed that a C-terminal truncated $Na_v1.5$ α-subunit interacts with WT α-subunits. Their co-expression induced only a mild reduction of the I_{Na} density but a marked shift in inactivation and gave rise to a persistent current, compatible with SSS and AF. The mutant biophysical defects associated with the difference in resting membrane potentials between atrium and ventricle combined with genetic factors might explain the predominantly atrial expression of this mutant. A better knowledge of the functional effects of mutations in *SCN5A* and the genetic background of the mutation carriers should help in the future to explain the large phenotypical variability of the sodium channelopathies.

References

1. Roden DM, Balser JR, George AL Jr, Anderson ME: Cardiac ion channels. Annu. Rev. Physiol. 2002; 64:431–475.
2. Remme CA: Cardiac sodium channelopathy associated with SCN5A mutations: electrophysiological, molecular and genetic aspects. J. Physiol. 2013; 591: 4099–4116.
3. Francis J, Antzelevitch C: Atrial fibrillation and Brugada syndrome. J. Am. Coll. Cardiol. 2008; 51:1149–1153.
4. Johnson JN, Tester DJ, Perry J, Salisbury BA, Reed CR, Ackerman MJ: Prevalence of early-onset atrial fibrillation in congenital long QT syndrome. Heart Rhythm Off. J. Heart Rhythm Soc. 2008; 5:704–709.
5. Scicluna BP, Wilde AAM, Wilde AW, Bezzina CR: The primary arrhythmia syndromes: same mutation, different manifestations. Are we starting to understand why? J. Cardiovasc. Electrophysiol. 2008; 19:445–452.
6. Gudbjartsson DF, Arnar DO, Helgadottir A, et al.: Variants conferring risk of atrial fibrillation on chromosome 4q25. Nature 2007; 448:353–357.
7. Ellinor PT, Lunetta KL, Albert CM, et al.: Meta-analysis identifies six new susceptibility loci for atrial fibrillation. Nat. Genet. 2012; 44:670–675.
8. Clatot J, Ziyadeh-Isleem A, Maugenre S, Denjoy I, Liu H, Dilanian G, Hatem SN, Deschênes I, Coulombe A, Guicheney P, Neyroud N: Dominant-negative effect of SCN5A N-terminal mutations through the interaction of Nav1.5 α-subunits. Cardiovasc. Res. 2012; 96:53–63.
9. Lubitz SA, Sinner MF, Lunetta KL, et al.: Independent susceptibility markers for atrial fibrillation on chromosome 4q25. Circulation 2010; 122:976–984.
10. Burashnikov A, Di Diego JM, Zygmunt AC, Belardinelli L, Antzelevitch C: Atrium-selective sodium channel block as a strategy for suppression of atrial fibrillation: differences in sodium channel inactivation between atria and ventricles and the role of ranolazine. Circulation 2007; 116:1449–1457.
11. Golod DA, Kumar R, Joyner RW: Determinants of action potential initiation in isolated rabbit atrial and ventricular myocytes. Am J Physiol 1998; 274:H1902–13.
12. Lemoine MD, Duverger JE, Naud P, Chartier D, Qi XY, Comtois P, Fabritz L, Kirchhof P, Nattel S: Arrhythmogenic left atrial cellular electrophysiology in a murine genetic long QT syndrome model. Cardiovasc Res 92:67–74.
13. Song Y, Shryock JC, Belardinelli L: An increase of late sodium current induces delayed afterdepolarizations and sustained triggered activity in atrial myocytes. Am J Physiol Heart Circ Physiol 2008; 294:H2031–9.
14. Sossalla S, Kallmeyer B, Wagner S, Mazur M, Maurer U, Toischer K, Schmitto JD, Seipelt R, Schöndube FA, Hasenfuss G, Belardinelli L, Maier LS: Altered Na+ Currents in Atrial Fibrillation: Effects of Ranolazine on Arrhythmias and Contractility in Human Atrial Myocardium. J. Am. Coll. Cardiol. 2010; 55:2330–2342.
15. Dobrzynski H, Boyett MR, Anderson RH: New insights into pacemaker activity: promoting understanding of sick sinus syndrome. Circulation 2007; 115:1921–1932.
16. Lei M, Goddard C, Liu J, et al.: Sinus node dysfunction following targeted disruption of the murine cardiac sodium channel gene Scn5a. J. Physiol. 2005; 567:387–400.
17. Lei M, Huang CL-H, Zhang Y: Genetic Na+ channelopathies and sinus node dysfunction. Prog. Biophys. Mol. Biol. 2008; 98:171–178.
18. Shy D, Gillet L, Abriel H: Cardiac sodium channel Na(V)1.5 distribution in myocytes via interacting proteins: The multiple pool model. Biochim. Biophys. Acta 2013; 1833:886–894.

19. Kapplinger JD, Tester DJ, Alders M, et al.: An international compendium of mutations in the SCN5A-encoded cardiac sodium channel in patients referred for Brugada syndrome genetic testing. Heart Rhythm Off. J. Heart Rhythm Soc. 2010; 7:33–46.
20. Tan B-H, Iturralde-Torres P, Medeiros-Domingo A, Nava S, Tester DJ, Valdivia CR, Tusié-Luna T, Ackerman MJ, Makielski JC: A novel C-terminal truncation SCN5A mutation from a patient with sick sinus syndrome, conduction disorder and ventricular tachycardia. Cardiovasc. Res. 2007; 76:409–417.
21. Franco D, Christoffels VM, Campione M: Homeobox transcription factor Pitx2: The rise of an asymmetry gene in cardiogenesis and arrhythmogenesis. Trends Cardiovasc. Med. 2014; 24:23–31.

Table 1. Biophysical and kinetic properties of I_{Na} from WT and mutant channels

			Activation				Inactivation							
Na^+ channels	Peak current density (pA/pF)	P	$V_{1/2}$ (mV)	P	*k* (mV)	P	$V_{1/2}$ (mV)	P	*k* (mV)	P	τ_f (ms)	P	τ_s (ms)	P
WT	-280.8±22.2 (n=20)		-44.2±1.6 (n=17)		7.0±0.4		-84.5±1.9 (n=12)		-8.1±0.6		0.48±0.02 (n=15)		2.54±0.30 (n=15)	
R1860Gfs*12	-80.3±16.4 (n=13)	***	-37.1±1.4 (n=12)	**	6.1±0.6	ns	-108.1±1.8 (n=8)	***	-6.3±0.4	ns	1.27±0.05 (n=22)	***	9.80±0.80 (n=22)	***
½ WT+ ½ R1860Gfs*12	-237.0±22.5 (n=14)	ns	-40.8±2.0 (n=12)	ns	5.9±0.4	ns	-101.1±1.7 (n=11)	***	-6.3±0.5	ns	0.69±0.05 (n=17)	***	4.55±0.40 (n=17)	***

Data are presented as means ± SEM. Peak current density was calculated at -20 mV. WT indicates wild type, ** P≤0.005, *** P≤0.001 and ns: not significant compared with WT channel. $V_{1/2}$ indicates half activation or inactivation value, *k* inverse slope factor, and τ_f and τ_s: fast and slow time constants of I_{Na} inactivation.

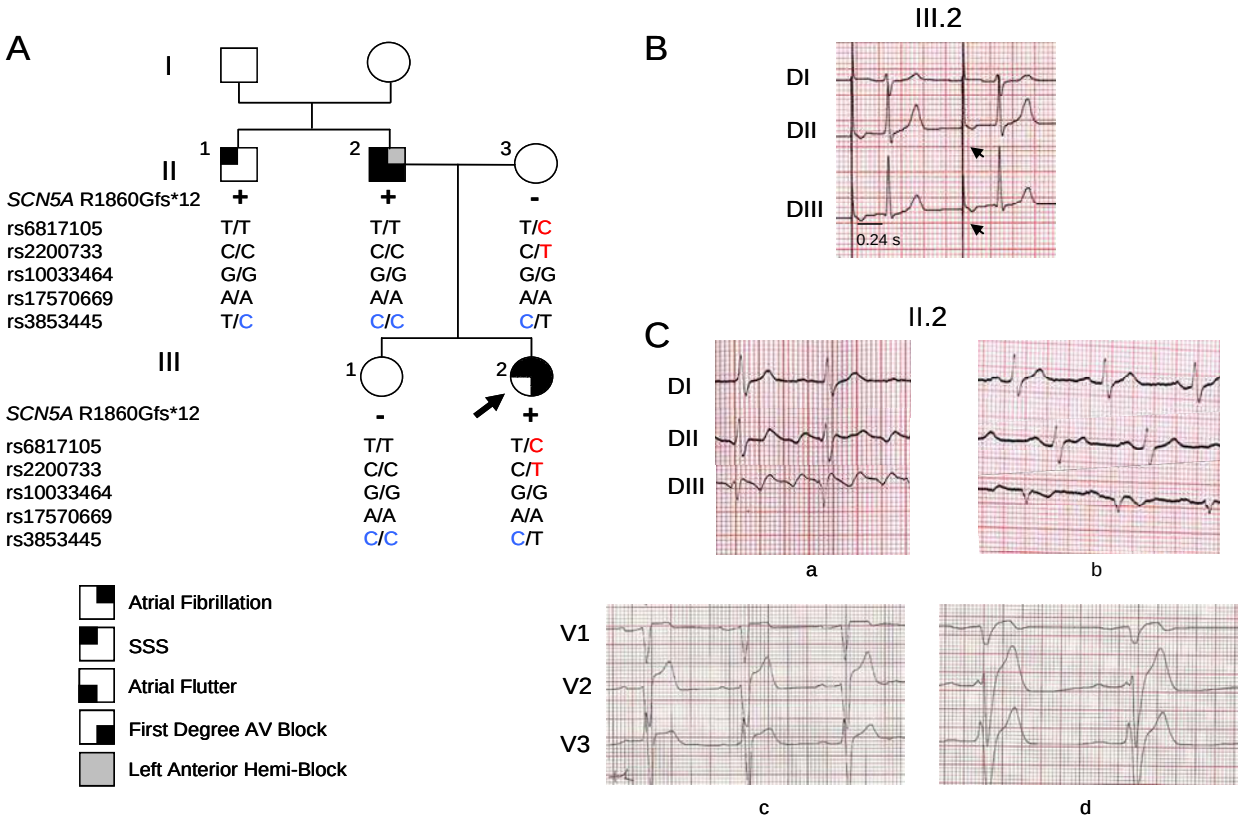

Figure 1: Pedigree and ECG recordings of the family

(A) Pedigree of the family. The proband (III.2) is indicated by an arrow. Squares represent males, circles females, + and - signs, mutation carriers and non-carriers. The haplotypes for 5 SNPs located upstream of the *PITX2* gene are indicated under each subject. At-risk alleles are written in red and protective ones in blue. (B) ECG recordings of the proband. The pacemaker spikes are indicated by arrows. The proband's ECG showed prolongation of the PR interval, a sign of first degree AV block. (C) ECG recordings of the father (II.2) showing the atrial flutter that he developed at 42 (a), and his normal sinus rhythm after cardioversion with left axis deviation (b). (c and d) ECG recordings of II-2 during the ajmaline test (1mg/kg over 5 min) he underwent at 64. At basal condition (c, time 0), the patient has a regular sinus rhythm with a heart rate (HR) of 60 beats/min, a prolongation of the PR interval of 240 ms, and a QRS duration of 120 ms. After the injection of ajmaline (d, time 7 min), bradycardia was observed (HR= 40 beats/min) with a prolongation of the PR interval (300 ms) and of the QRS duration (240 ms), without sign of BrS. Rapid sodium-bicarbonate infusion was then immediately started.

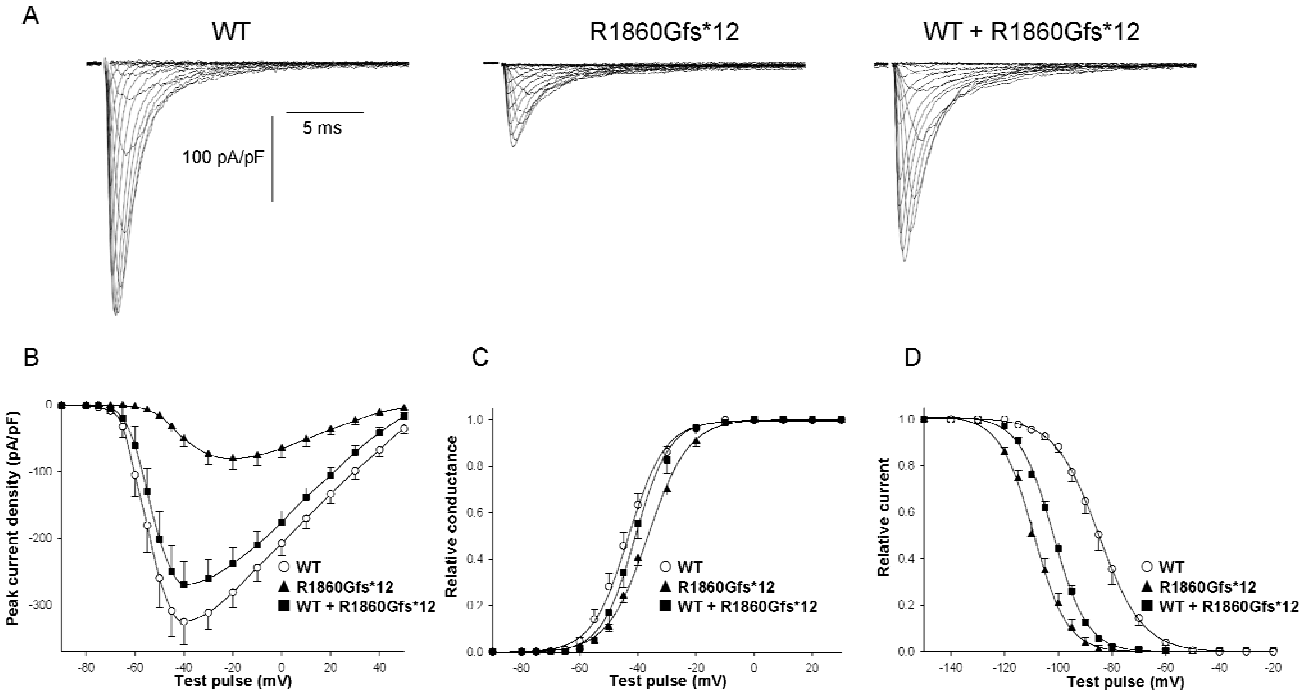

Figure 2: Electrophysiological characterization of $Na_v1.5$ channels (1)
(A) Representative families of Na^+ current traces of WT, R1860Gfs*12 and WT + R1860Gfs*12 channels. (B) Current density-voltage relationships. R1860Gfs*12 current density is significantly reduced compared to WT and WT + R1860Gfs*12 channels. (C) Activation-V_m relationship of R1860Gfs*12 was shifted to more positive potentials compared to WT and WT + R1860Gfs*12 channels. (D) Steady-state inactivation-V_m relationships were shifted towards negative potential for R1860Gfs*12 and WT + R1860Gfs*12 channels compared to WT channels. Numbers of cells and statistical analysis are reported in Table 1.

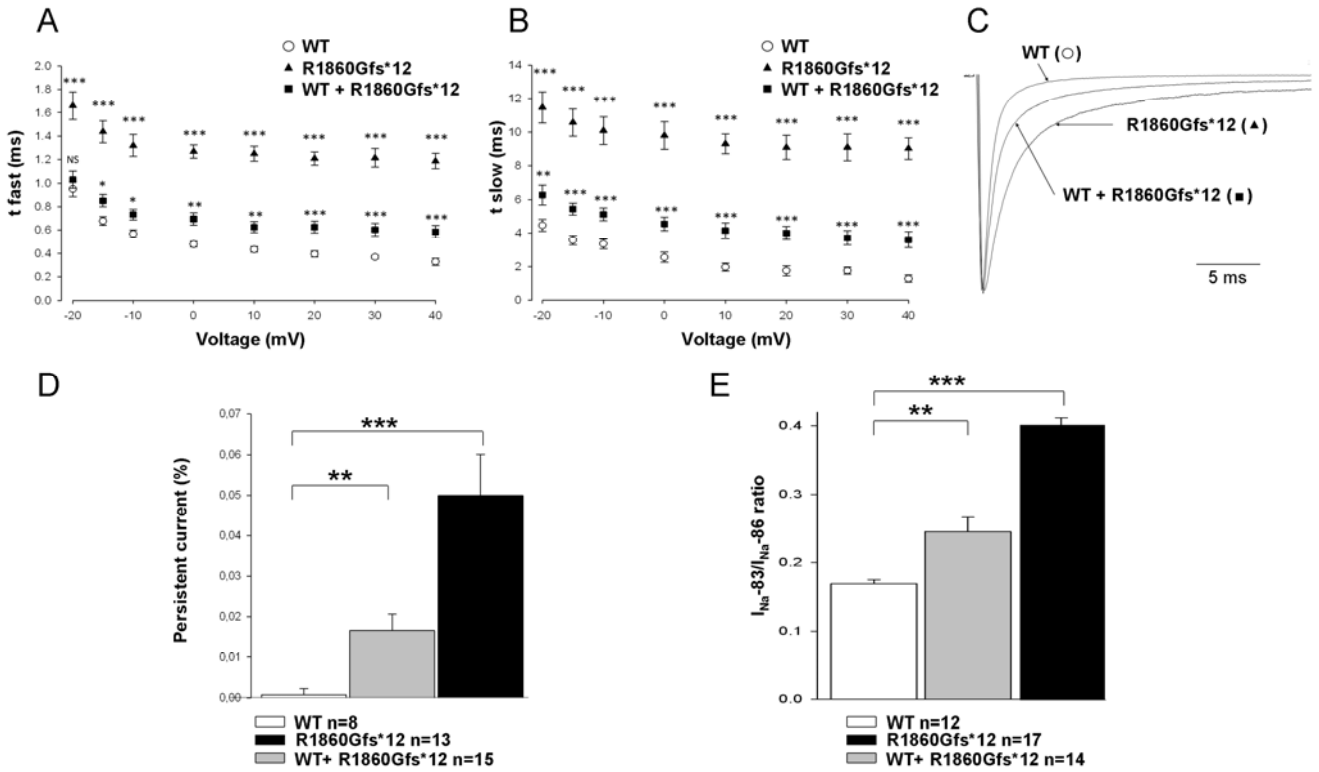

Figure 3: Electrophysiological characterization of $Na_v1.5$ channels (2)

(A) and (B) Fast and slow time constants (τ_f, and τ_s, respectively) for WT, R1860Gfs*12 and WT + R1860Gfs*12 channels were plotted against the test potential. R1860Gfs*12 and WT + R1860Gfs*12 showed an overall slowing of the fast and slow rates of inactivation compared to the WT. (C) Three superimposed representative I_{Na} traces corresponding to the above conditions. The R1860Gfs*12 and the WT + R1860Gfs*12 current traces were normalized to the peak of the WT current (≈ 1200 pA). (D) Ratios of the persistent Na^+ current amplitude (end of pulse) over the peak I_{Na} amplitude for WT, WT + R1860Gfs*12 and R1860Gfs*12 channels, reported in percentage. (E) Ratios of the I_{Na} loss between HPs of -86 and -83 mV for WT, WT+ R1860Gfs*12 and R1860Gfs*12. Peak current density was calculated at -20 mV. * indicates $P \leq 0.05$, ** $P \leq 0.01$, *** $P \leq 0.001$, and n the number of tested cells.

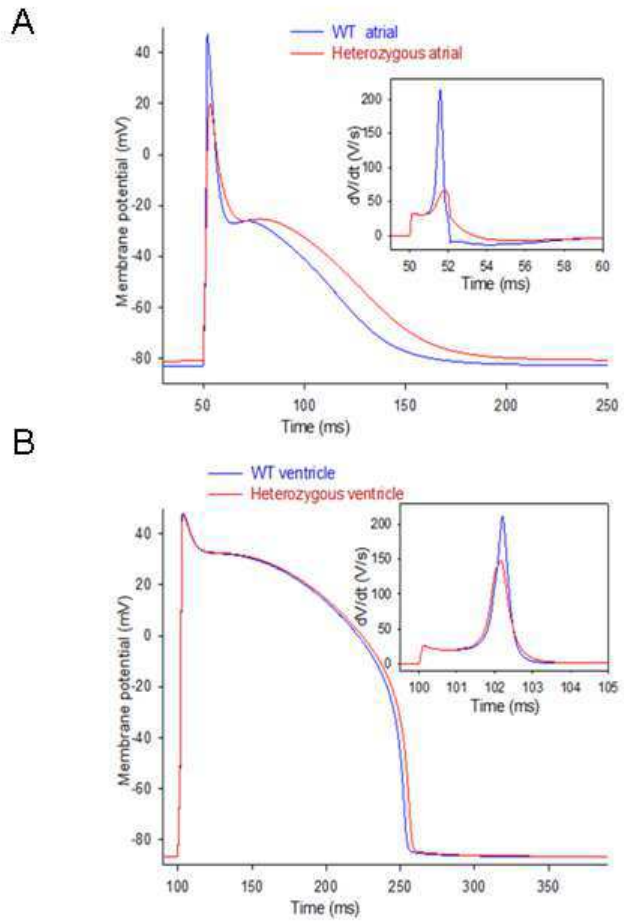

Figure 4: Computer model simulations of single atrial cell and ventricular cell membrane action potentials

Computed AP time courses and expanded time-scale inset exhibiting first time derivatives (dV/dt) of the AP upstroke, in A: atrium and in B: ventricle. Computed dV/dt time courses exhibit a higher decrease in $[dV/dt]_{max}$ for the "heterozygous atrium" condition than for WT (respectively: 68 V/s vs. 212 V/s) whereas the decrease was smaller for "heterozygous ventricle" condition than for WT (respectively: 147 V/s vs. 220 V/s).

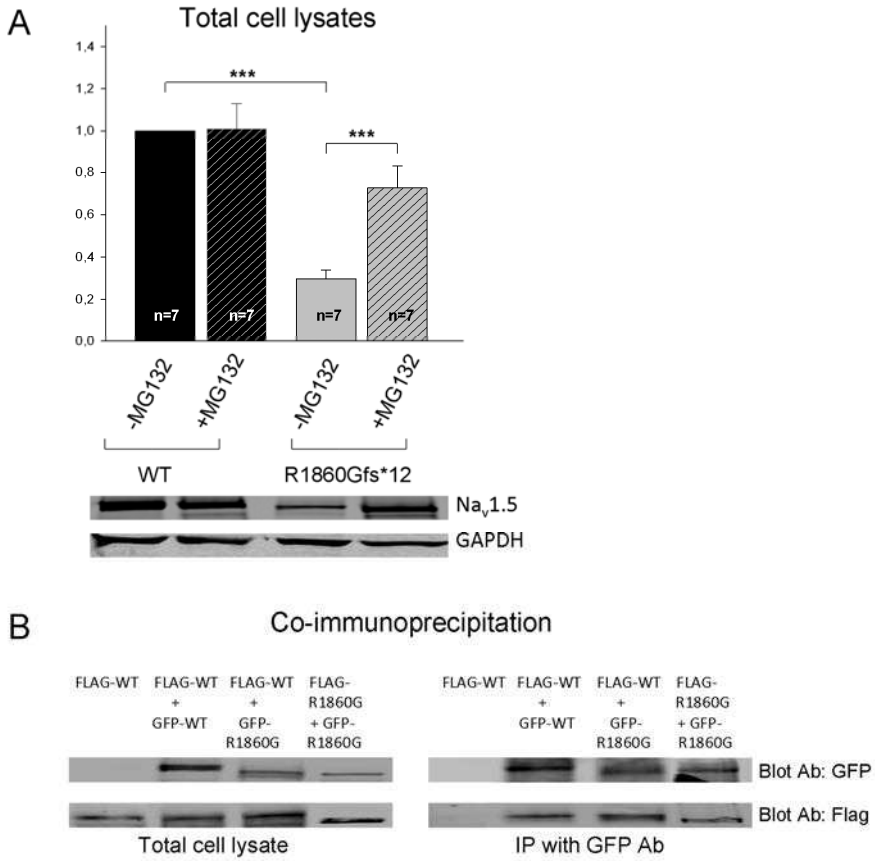

Figure 5: Biochemical analysis
HEK cells were transfected with GFP-$Na_v1.5$ (A) and with GFP-$Na_v1.5$ and/or Flag-$Na_v1.5$ (B). Data are represented as arbitrary units. Glyceraldehyde 3-phosphate dehydrogenase (GAPDH) was used as total protein loading control. (A) Western blots of total cell lysates show that the R1860Gfs*12 protein quantity is significantly lower than the WT. Incubation of transfected cells with MG132 prevented the degradation of the C-terminal mutant; ***$P \leq 0.001$. (B) Co-immunoprecipitation of $Na_v1.5$ α-subunits tagged with either Flag or GFP. Immunoprecipitation was performed with the anti-GFP antibody, and western blot revealed with the anti-Flag antibody. These results demonstrated an interaction between R1860Gfs*12 α-subunits, and between WT and R1860Gfs*12 α-subunits.

Supplemental material

Methods

Genes screened in the proband

Mutational analyses were performed for the following genes: *KCNQ1* (NM_000218), *KCNH2* (NM_000238), *SCN5A* (NM_198056), *KCNE1* (NM_000219), *KCNE2* (NM_172201), *KCNE3* (NM_005472), *KCNE1L* (NM_012282), *NPPA* (NM_006172), *KCNA5* (NM_002234), *KCNJ2* (NM_00891), *GJA5* (NM_005266 and 181703), *SCN1B* (NM_001037 and 199037), *SCN2B* (NM_004588) and *SCN3B* (NM_018400).

Solutions and drugs

Thirty-six hours after transfection, HEK293 cells were trypsinized and seeded to a density that enabled single cells to be identified. Green positive cells were chosen for patch-clamp experiments. Cells were bathed in an extracellular Tyrode solution containing (in mM): 135 NaCl, 4 KCl, 2 $MgCl_2$, 2.5 $CaCl_2$, 1 NaH_2PO_4, 10 HEPES, 20 glucose and adjusted to pH 7.4 with NaOH. Pipette medium was (in mM): 5 NaCl, 140 CsCl, 2 $MgCl_2$, 4 Mg-ATP, 5 EGTA, 10 HEPES, adjusted to pH 7.2 with CsOH. During current recording, cells were perfused with an external solution with reduced Na^+ concentration containing (in mM): 80 NaCl, 50 CsCl, 2 $CaCl_2$, 2.5 $MgCl_2$, 10 HEPES, and 10 glucose, adjusted to pH 7.4 with CsOH.

Computer simulations of membrane action potential

Computer simulations of membrane action potential (AP) were achieved using Oxsoft Heart Model V. 4.8 (written by and available from Pr. Denis Noble, Oxford University; copyright by OXFORD Ltd, UK)[1]. This mathematical modeling software solves the equations developed to model currents associated with ion channels, exchangers and pumps in the heart, and then reconstitute the cellular action potential. We selected it because of its easy commercial availability and because it contains all the parameters needed to verify the importance of the changes in I_{Na} parameters: the fast and background I_{Na} conductances, the shifts of m_∞ and h_∞ -voltage relationships, the time constant of I_{Na} inactivation on the decay of the AP, and the maximum velocity of the AP upstroke, $[dV/dt]_{max}$. We used the built-in models of single atrial cell and ventricle cell APs. Resting membrane potentials (E_r) were

adjusted according to experimental pre-setting holding potentials (-83 mV for atrium and -86 mV for the ventricle) by simply altering the appropriate input in $[K]_o$ as allowed by the model entries. Changes in I_{Na} entries between WT and heterozygous (hetero) currents were incorporated in the built-in parameters and the resulting effects on the computed AP time course and the corresponding upstroke velocity were retrieved. Entry parameters were changed as follows and used for both atrium and ventricle:

$G_{Na\text{-}fast}$ hetero: 0.84 x $G_{Na\text{-}fast}$ WT,

$G_{Na\text{-}background}$ hetero: 1.5 x $G_{Na\text{-}fast}$ WT,

h_∞ (V_m) hetero: -16.5mV shift of h_∞ (V_m) WT

m_∞ (V_m) hetero: -4.0mV shift of m_∞ (V_m) WT

$\tau(V_m)$ hetero: 1.8 x $\tau(V_m)$ WT.

Co-immunoprecipitation

For co-immunoprecipitation of $Na_v1.5$ α-subunits, HEK293 cells were co-transfected with 3 µg of pRcCMV-FLAG-SCN5A WT or mutant and 3 µg of pcDNA3.1-GFP-hH1a WT or mutant in 75-cm² flasks. For co-immunoprecipitation of $Na_v1.5$ and FHF1B, cells were co-transfected with 1.5 µg of pcDNA3.1-GFP-hH1a WT or mutant and 2 µg of pIRES2-acGFP1-FHF1B in 25-cm² flasks. Forty-eight hours after transfection, HEK293 cells were washed with PBS and lysed in lysis buffer (150 mM NaCl, 50 mM Tris-HCl, pH 7.5, 1% Triton, and complete protease inhibitor cocktail from Roche, Germany). Cell pellets were pipetted up and down 20 times, flushed 20 times through a 22-gauge needle, rotated for 1 h at 4°C, and finally centrifuged for 10 min at 16000 g. Magnetic Dynabeads (Dynal, Norway) were washed twice with PBS-tween 0.02%, incubated with the anti-GFP antibody (Torrey Pines Biolabs, USA), or the anti-His_6 antibody (Qiagen, Germany) for 2 h at room temperature, washed twice again with PBS-tween 0.02%, and incubated with the pre-cleared lysates. Samples were rotated overnight at 4°C. After washing the beads 4 times with PBS-tween 0.02%, proteins were eluted with the Laemmli sample buffer at 37°C for 30 minutes under agitation, and analyzed by Western blot.

Figures

Supplemental Figure 1: Sinus node dysfunction during ajmaline test in the proband's father (patient II-2)

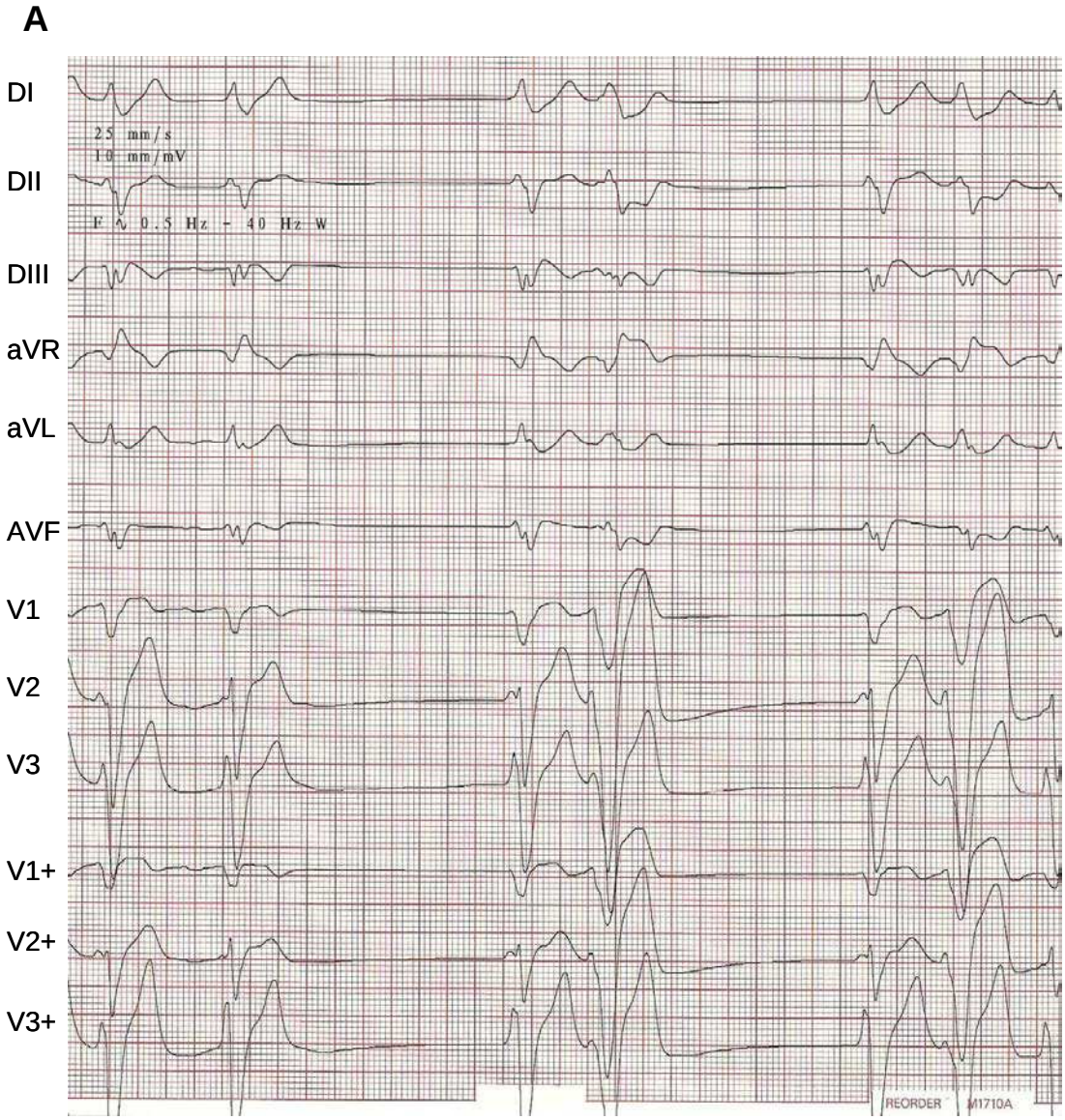

B

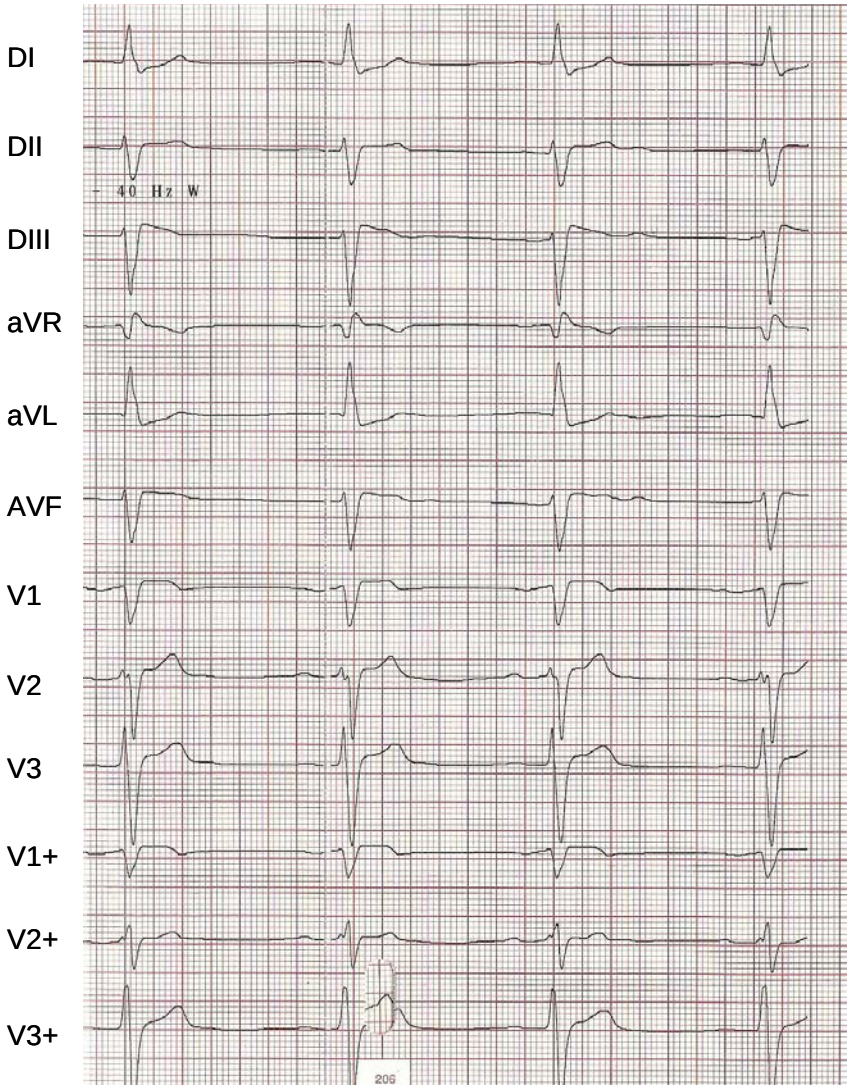

(A) ECG recording of patient II-2 eight minutes after the beginning of ajmaline injection (5 mg/kg over 5 min) shows sinus node dysfunction characterized by the absence of P waves and junctional escape rhythm; and supraventricular premature contractions. (B) Sixteen minutes after the beginning of ajmaline injection, the P waves reappeared, regular sinus rhythm was observed, but a marked bradycardia was still present. V1+, V2+ and V3+ correspond to right precordial leads placed in superior position (3rd intercostal space).

Supplemental Figure 2: Identification of the R1860Gfs*12 mutation

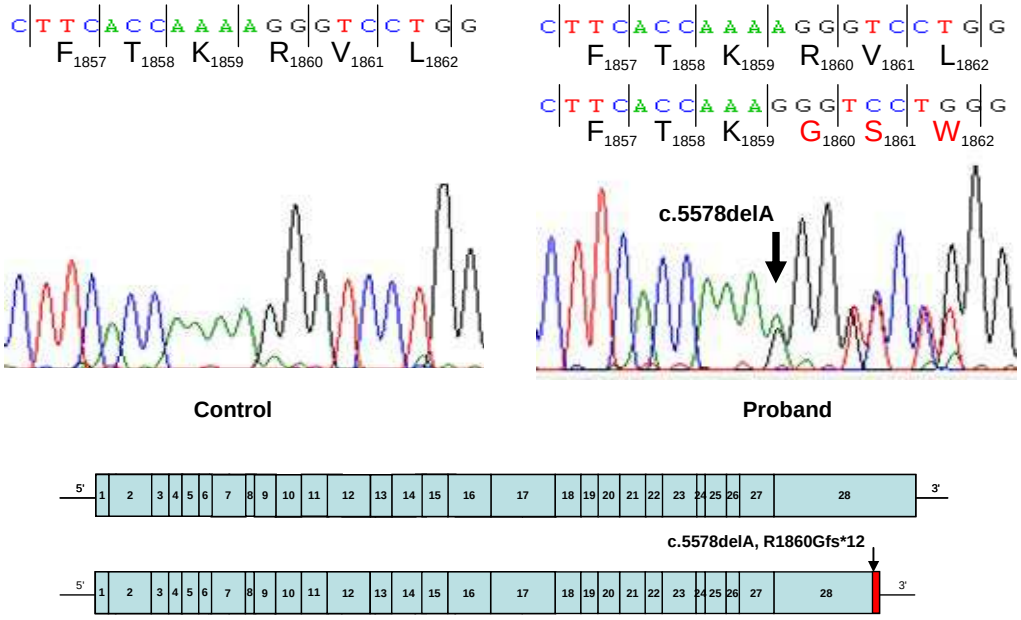

Sequence chromatogram of the proband's genomic DNA showing the deletion of an adenine at position 5578. This frameshift mutation changed the amino acid arginine at position 1860 into glycine and caused premature termination of the protein at position 1871.

Supplemental Figure 3: Recovery from inactivation of I_{Na} at a holding potential of -120 mV

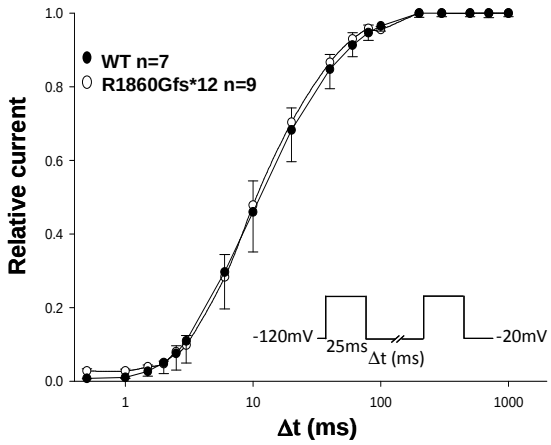

Test- and conditioning-pulses of 25 ms were separated by the recovery time Δt from 0.5 ms to 1000 ms. Relative currents were calculated as peak I_{Na} elicited by test-pulse versus that elicited by

conditioning-pulse. No change in the recovery from inactivation was observed for the mutant compared to the WT.

Supplemental Figure 4: R1860Gfs*12 and WT + R1860Gfs*12 mutant channels were able to generate a TTX-sensitive persistent Na^+ current

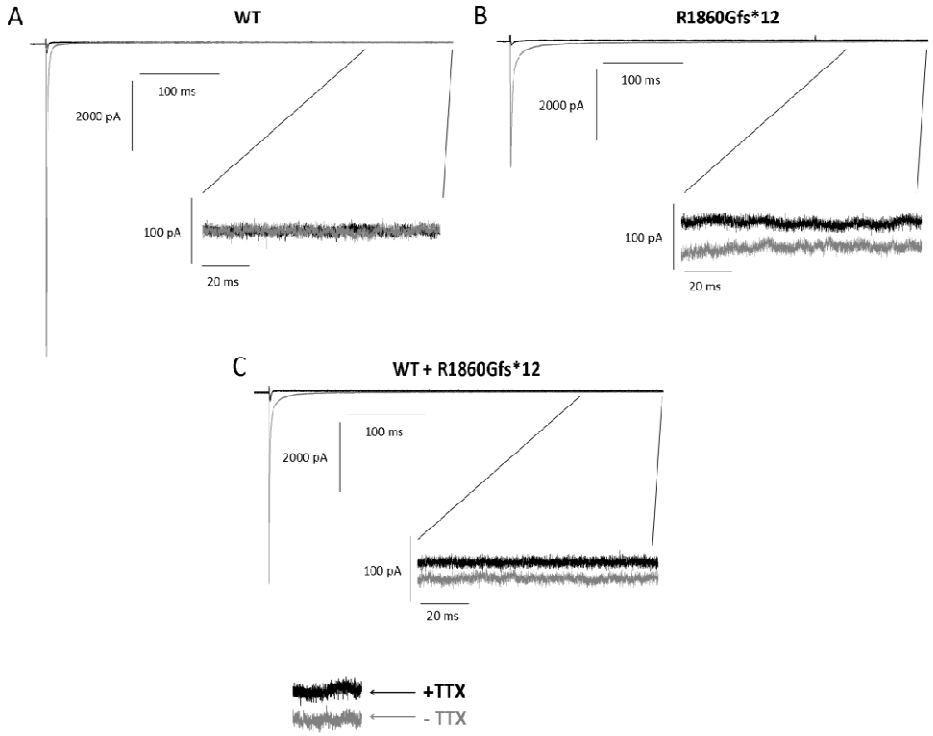

Panels (A), (B) and (C): Representative I_{Na} recordings obtained in the absence and in the presence of 100 µM TTX, generated by WT, R1860Gfs*12 and WT + R1860Gfs*12 channels respectively. For comparison, the peak and late current are shown at different scales. R1860Gfs*12 and the heterozygous WT + R1860Gfs*12 channels exhibited a marked increase in TTX-sensitive persistent current compared to the WT channels.

Supplemental Figure 5: Absence of interaction between the C-terminal mutant R1860Gfs*12 and FHF1B

Several partners interact with the C-terminus of $Na_v1.5$, including the Fibroblast Growth Factor Homologous Factor 1B (FHF1B), which modulates $Na_v1.5$ inactivation. Its interaction site on $Na_v1.5$ was debated [2,3]. It was first reported to be located in the proximal C-terminal domain (amino acids 1773–1832)[2], and later not only in the proximal but also in the distal part of the $Na_v1.5$ C-terminus (amino acids 1773–1908)[3]. By co-immunoprecipitation, we demonstrated that R1860Gfs*12 mutant did not interact with FHF1B, even after increasing the total protein expression of R1860Gfs*12 with the proteasome inhibitor MG132, indicating the involvement of both the proximal and distal parts of $Na_v1.5$ C-terminus in the interaction with FHF1B.

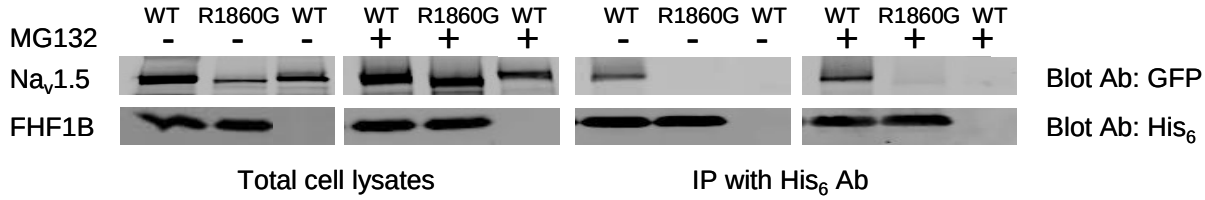

HEK293 cells were transfected with GFP-WT, GFP-WT or GFP-mutant with FHF1B (C-terminal His_6-tag). Cells were treated with or without MG132. Immunoprecipitations were performed with anti-His_6 antibody (Ab), and blots were revealed with the anti-His_6 antibody or with the anti-GFP antibody. The results demonstrated that only the WT channel was precipitated with the FHF1B and not the mutant, even after treating the cells with MG132.

Supplemental Table 1: Genotypes of SNPs associated with atrial fibrillation in the patient's family

Gene	SNP	Location	Major/minor allele	MAF(%)	II1	II2	II3	III1	III2
PITX2	rs6817105[4]	4:111705768	T>C	11.9	T/T	T/T	T/C	T/T	T/C
PITX2	rs2200733[5–9]	4:111710169	C>T	11.5	C/C	C/C	C/T	C/C	C/T
PITX2	rs10033464[5,7,10]	4:111720761	G>T	9.7	G/G	G/G	G/G	G/G	G/G
PITX2	rs17570669[9]	4:111736882	A>T	6.2	A/A	A/A	A/A	A/A	A/A
PITX2	rs3853445[9]	4:111761487	T>C	26.1	T/C	C/C	C/T	C/C	C/T
ZFHX3	rs7193343[11]	16:73029160	C>T	16.4	C/C	C/T	C/C	C/C	C/C
ZFHX3	rs2106261[4,12,13]	16:73051620	C>T	18.1	C/C	C/T	C/C	C/C	C/C
KCNN3	rs13376333[14]	1:154814353	C>T	33.6	C/C	C/C	C/T	C/C	C/C
HCN4	rs7164883[4]	15:73652174	A>G	16.8	A/G	A/A	A/A	A/A	A/A
PRRX1	rs3903239[4]	1:170569317	A>G	44.8	A/G	A/G	A/A	A/A	A/A
SYNE2	rs1152591[4]	14:64680848	G>A	48.7	A/A	G/A	G/A	G/A	A/A
C9orf3	rs10821415[4]	9:97713459	C>A	39.7	A/A	C/A	C/C	C/C	C/C
SYNPO2L	rs10824026[4]	10:75421208	A>G	16.4	A/A	A/A	A/A	A/A	A/A
CAV1	rs3807989[4,15,16]	7:116186241	G>A	42	A/A	A/A	G/G	A/G	A/G
NKX2-5	rs251253[16]	5:172480336	T>C	38.9	T/C	C/C	T/T	C/T	C/T
SCN10A	rs6800541[16]	3:38774832	T>C	42	T/C	T/C	T/T	T/T	C/T
SCN5A	rs11708996[16]	3:38633923	G>C	20	G/C	G/C	G/C	G/G	C/C

Risk alleles are in red and protective alleles in blue. MAF = minor allele frequency in HapMap-CEU.

II.3 Study of the recently BrS-associated SNPs in the family with the R1860Gfs*12 mutation

In the family with the R1860Gfs*12 mutation, in addition to the SNPs linked to AF, we explored the possibility that reported BrS associated SNPs could modulate the phenotypic expression. We screened the three SNPs recently shown to be associated with BrS[476] (Table 11). All R1860Gfs*12 mutation carriers have three risk alleles, while in the pioneer study, most of the BrS patients have two to four risk alleles, and controls have one to three risk alleles. The role of these SNPs remains unclear since 1.5% of European population is expected to carry more than four risk alleles.

SNP	rs11708996	rs10428132	rs9388451
Gene	*SCN5A*	*SCN10A*	*HEY2, NCOA7*
Location	3:38633923	3:38777554	6:126090377
Major/minor allele	G>C	G>T	T>C
MAF(%)	20	42	46.5
Uncle	G/C	G/T	T/C
Father	G/C	G/T	T/C
Mother	G/C	G/G	T/T
Proband	C/C	G/T	T/T
Sister	G/G	G/G	T/C

Table11: BrS associated SNPs in the family with the R1860Gfs*12 *SCN5A* mutation
Risk alleles are in red.

III. Fibroblast Growth Factor Homologous Factor 1B

III.1 The proximal and distal regions of the C-terminal domain of $Na_v1.5$ interacted with FHF1B

The C-terminal domain of $Na_v1.5$ is the site of interaction of several partner proteins regulating channel function. Among these partners is the Fibroblast Growth Factor Homologous Factor 1B (FHF1B), which regulates channel inactivation and surface expression[304,454,456,458]. Recently, the *FGF12* gene encoding FHF1B has been reported as a new candidate in BrS[304]. The site of interaction of FHF1B on $Na_v1.5$ is debated. Liu *et al* showed that FHF1B binds to the C-terminal acid-rich domain (amino acids 1773–1832) of $Na_v1.5$[454], while Wang *et al* reported that both this proximal domain and a more distal region of the C-terminus (amino acids 1773–1908) are required[456]. So we used the R1860Gfs*12 truncated $Na_v1.5$ mutant and another already published L1821fs*10 truncated $Na_v1.5$ channel[216] to test their interaction with FHF1B. According to Liu *et al*, the L1821fs*10 channel should loose its interaction with FHF1B but not the R1860Gfs*12 mutant, while according to Wang *et al*, the two mutants should loose their interaction.

HEK293 cells were transfected with 1.5 µg of pcDNA3.1-GFP-$Na_v1.5$ (N-terminal GFP) WT or mutated with 2 µg of pIRES2-acGFP1-FHF1B (C-terminal His_6-tag), or with pcDNA3.1-GFP-$Na_v1.5$ WT alone as a negative control. Immunoprecipitation was performed as described in the Material and Methods and in Figure 47. Only the WT GFP-$Na_v1.5$ was immunoprecipitated with FHF1B (Figure 47A). Since the two mutants R1860Gfs*12 and L1821fs*10 are partially degraded by the ubiquitin-proteasome system, we checked whether increasing total protein expression with MG132, a 26S-subunit ubiquitin-proteasome inhibitor, could restore the interaction with FHF1B. Immunoprecipitation using anti-His_6 antibody was done after treating the cells with MG132 (Figure 47A). Although we increased total protein expression of the two mutants with MG132, this did not restore the interaction with FHF1B (Figure 47A). Reciprocal co-immunoprecipitation was also performed (Figure 47B). FHF1B protein was successfully precipitated with the WT channels but not with the two mutants.

The loss of interaction of the two mutants with FHF1B confirms the involvement of both the proximal and distal parts of the $Na_v1.5$ C-terminus in the interaction with FHF1B as reported by Wang *et al*[456].

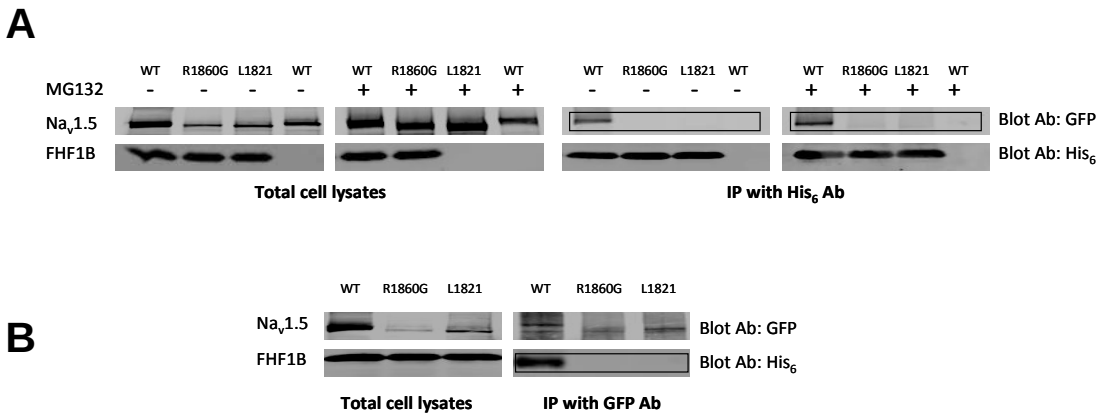

Figure 47: Both proximal and distal regions of $Na_v1.5$ are involved in the interaction with FHF1B

(A) FHF1B was immunoprecipitated using an anti-His_6 antibody, and the bound proteins were then detected by western blot analysis with anti-GFP and anti-His_6 antibodies. Only the WT GFP-$Na_v1.5$ was immunoprecipitated with FHF1B even after increasing the total protein expression of the two mutants with MG132. (B) Reciprocal co-immunoprecipitation performed using the anti-GFP antibody for immunoprecipitation of GFP-$Na_v1.5$, and the anti-His_6 and anti-GFP antibodies for western blot analysis. FHF1B protein was precipitated with the WT channels but not with the two mutants.

III.2 *FGF12-B* is the most highly expressed FHF isoform in the human ventricles

The expression of the different FHF isoforms in the heart was relatively unknown, until a recent study which demonstrated by qPCR that *FGF13-VY* is the most expressed FHF isoform in the adult mouse ventricular myocytes[458], but no study was done at that time in human. So, we aimed to study the expression of FHF isoforms in human and mouse ventricles. RNA extraction from human and mouse ventricles and reverse transcriptase were performed as described in the Material and Methods. Then, we performed qPCR using isoform-specific primers for *FGF12* isoforms A and B, and *FGF13* isoforms VY, VY/Y and V (Table 9 of Material and Methods). Primers are located in the homologous region between human and mouse FHF transcripts. All the data were corrected to a reference gene encoding the ribosomal protein L32 (*RPL32*), and then normalized to *FGF13-VY* in mouse and to *FGF12-B* in human. In the mouse heart *FGF13-VY* was the most highly expressed isoform, *FGF13-V* was expressed at low level, *FGF12-B* was detectable, but *FGF13-Y* and *FGF12-A* were undetectable (Figure 48A). These results are in line with the previous study in mouse heart[458] except that the *FGF13-Y* isoform in our study was undetectable. In the human heart,

FGF12-B was the most highly expressed isoform, *FGF13-VY* was detectable, but *FGF13-Y* and *FGF12-A* were undetectable (Figure 48B). Our results are consistent with a very recent study, that was unpublished at the time we started our work, which showed that *FGF12-B* is most the highly expressed isoform in human heart[304]. In this study, the qPCR was unable to distinguish between the *FGF13-VY* and *FGF13-Y* isoforms, and these isoforms were expressed at approximately 40% of *FGF12-B* in human ventricles. In our study, *FGF13-VY* was detectable but at a very low level compared to *FGF12-B*, while *FGF13-Y* was undetectable.

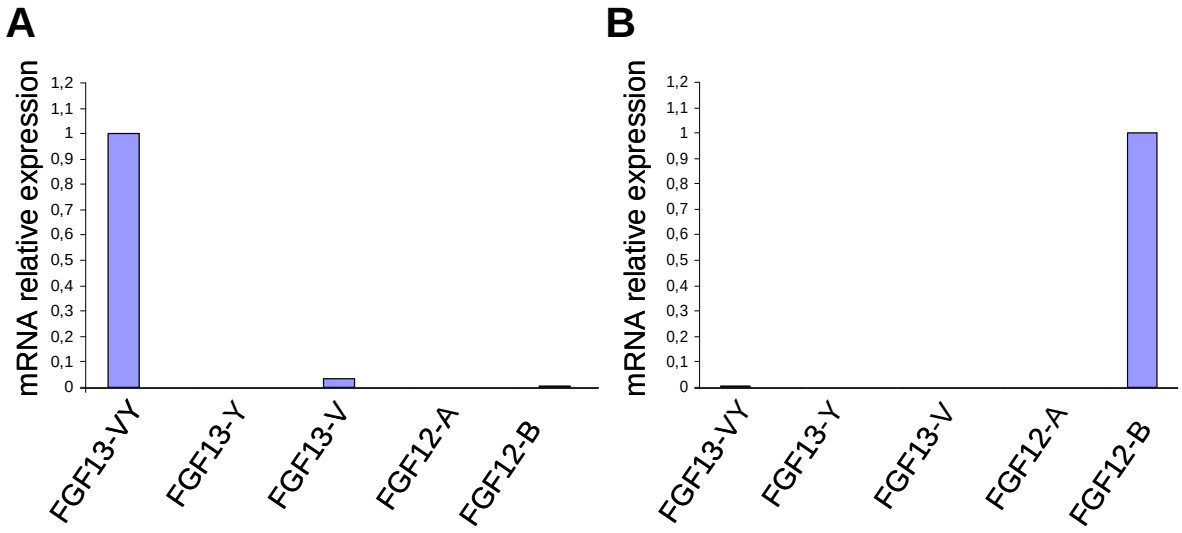

Figure 48: Relative mRNA expression of FHF isoforms in mouse (A) and human (B) ventricular cardiomyocytes
FGF13-VY was the most expressed isoform in mouse heart, while *FGF12-B* was the highly expressed isoform in human heart.
For comparison with the previous studies see Figure 37.

III.3 Screening of *FGF12-B* in patients with BrS

Since no mutation was found in 75% of BrS patients, and FHF1B is a partner of $Na_v1.5$, we screened the *FGF12-B* gene coding for the most highly expressed FHF isoform in human ventricles in a group of BrS patients. Our study population consisted of 182 unrelated patients diagnosed with BrS based on the presence of a spontaneous type-1 ECG pattern (ST segment elevation ≥2 mm in one or more right precordial leads) spontaneously or following the administration of a sodium channel blocker. Structural heart disease was excluded by echocardiography. Informed consent for genetic testing was given by each patient. All probands were negative for mutations in *SCN5A*, *MOG1*, *DLG1*, *KCNE3* and *SCN1B*.

All *FGF12-B* exons and intronic junctions (GenBank accession number NM_004113.5) were amplified by PCR (PCR primers are reported in Table 10 of Material and Methods), and the sequencing reaction was realized using the Sanger method with the Big Dye Terminator v.3.1 kit (Applied Biosystems) as described in the Material and Methods. Sequence analysis was then performed using the CodonCode Aligner v3.7.1 software.

A c.379 G>A transversion in exon 4, predicting a valine-to-methionine substitution at position 127 (p.V127M), was identified in one patient (Figure 36 and 49A). Alignment of the *FGF12* amino acid sequences demonstrated that the valine acid in position 127 is highly conserved across species, and it is also conserved in the human *FGF11*, *FGF13* and *FGF14*, suggesting the importance of this residue (Figure 49B). Moreover, this variant has never been described and is absent from the following publicly available databases:

- http://www.1000genomes.org/ensemble-browser
- http://evs.gs.washington.edu/EVS/
- http://genome.sph.umich.edu/wiki/Exome_Chip_Design

Using the Polymorphism Phenotyping v2 (PolyPhen-2), a programme that predicts the possible impact of a variant on the structure and function of protein, (http://genetics.bwh.harvard.edu/pph2/), the V127M variant is predicted to be probably damaging.

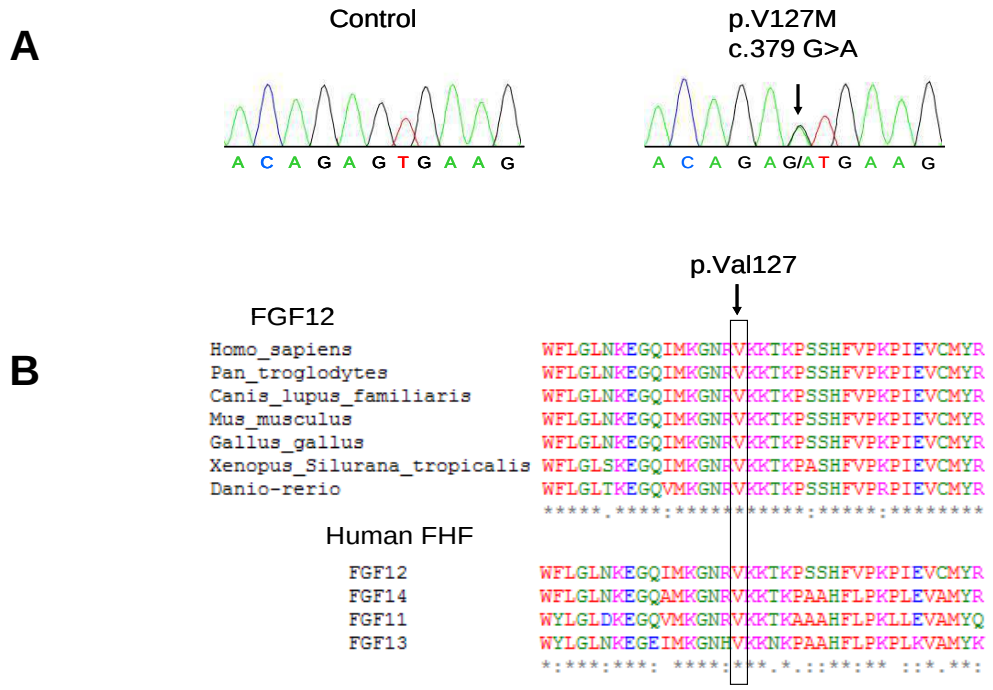

Figure 49: The *FGF12-B* variant p.V127M
(A) DNA sequence chromatogram showing the nucleotide change resulting in a valine (V) to methionine (M) substitution at position 127 compared to control. (B) Conservation of the valine 127 across species and among the human FHFs.

III.4 Preliminary functional study of the variant V127M in *FGF12-B*

The plasmid containing the variant V127M in FGF12-B was prepared by site directed mutagenesis of the WT pIRES2-acGFP1-FGF12-B where the FGF12-B C-terminus was fused to a His_6-tag. Patch-clamp analysis of HEK293 cells stably expressing $Na_v1.5$ transfected with the WT or mutant FGF12-B was performed in our team. In our experiments, expression of the WT FGF12-B did not affect the peak I_{Na} and caused a negative shift of the steady-state inactivation of $Na_v1.5$. However, no difference was observed in the functional effects on the Na^+ current between the WT and the mutant FGF12-B (Figure 50). As the heterologous system does not represent the physiological environment of ventricular cardiomyocytes, and since it was recently reported that the effects of the coexpression of FHFs on $Na_v1.5$ or on the calcium channel $Ca_v1.2$ in HEK293 cells were different than in adult ventricular cardiomyocytes[304], we plan to study the V127M variant in adult rat ventricular cardiomyocytes, where the endogenous *FGF13* is knocked out. These experiments will be performed through a collaboration with the group of Geoffrey Pitt in the USA.

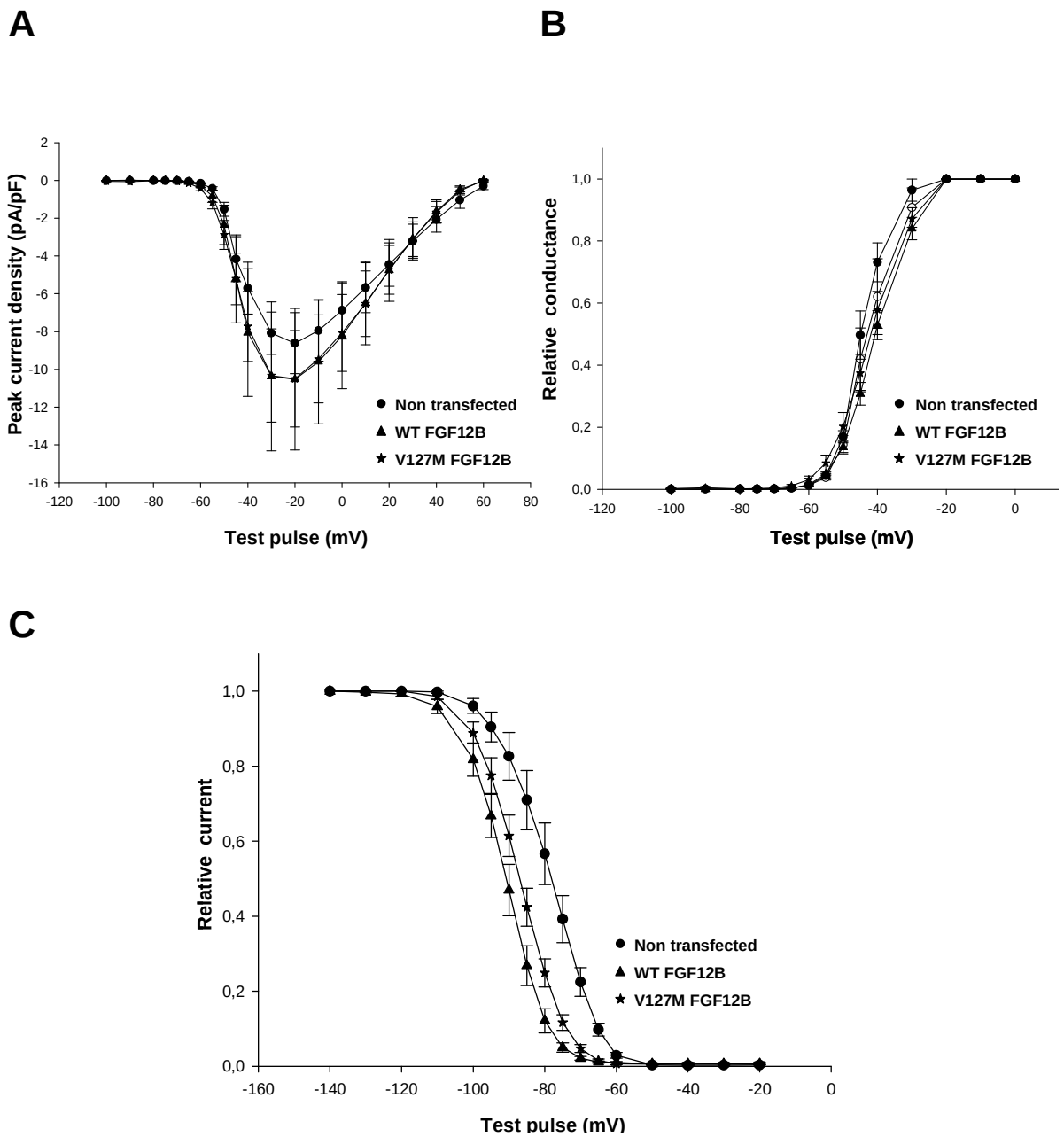

Figure 50: Preliminary functional study of the *FGF12-B* variant V127M
(A) Current density-voltage and (B) activation-Vm relationships in $Na_v1.5$-stable HEK cells not transfected as a control (n = 6), or transfected with either WT (N = 8) or the V127M FGF12-B variant (n = 9). Sodium current density and activation-Vm relationship are not affected by the coexpression of the WT or the V127M FGF12-B variant. (C) Steady-state inactivation-Vm relationships were shifted towards negative potential with both the WT and the V127M FGF12-B variant compared to non-transfected condition. n = number of cells

DISCUSSION

Identification of pathogenic mutations in genes encoding cardiac ion channels in hereditary cardiac arrhythmias (channelopathies) has improved the management of these disorders, and genetic testing has proved its efficacy in the pre-symptomatic identification of mutation carriers and subsequently, their early treatment. However, large variability in the clinical phenotype and incomplete penetrance have been observed in these channelopathies. This renders the identification of mutation carriers who are at risk of developing fatal arrhythmias difficult, and raises the possibility of the involvement of other unknown mechanistic, genetic, and environmental factors in the determination of the phenotypical expression of the disease. Better understanding of these modulatory factors could help in the future to explain the large variability in the phenotype and to improve risk stratification and treatment.

In this thesis work, we addressed *SCN5A* mutations, which are involved in a wide spectrum of disease phenotypes including LQTS, BrS, PCCD, AF, SSS, and dilated cardiomyopathies. Moreover, a mixed clinical picture now known as "overlap syndrome" has been reported in *SCN5A* channelopathies[477]. Currently, a growing number of *SCN5A* variants have been identified, but few of them are characterized by electrophysiological studies. This further complicates the interpretation of genetic testing since some of these variants are benign and may not be the actual cause of the disease.

By characterizing two *SCN5A* mutations, R104W and R1860Gfs*12, we demonstrated three possible mechanisms that could play a role in the determination of the phenotypic expression of *SCN5A* mutations. Moreover, we highlighted the role of the $Na_v1.5$ N-terminal domain in the channel function.

The interaction between $Na_v1.5$ α-subunits

We characterized the N-terminal mutant R104W, which was identified in a BrS patient. Using co-immunoprecipitation studies with two distinct $Na_v1.5$ α-subunit tagged constructs, we demonstrated for the first time that $Na_v1.5$ α-subunits interact with each other, and that this interaction was responsible for the dominant-negative effect of the R104W mutant on the WT channels. When expressed alone, the R104W was retained in the ER, degraded by the ubiquitine-proteasome system, and no I_{Na} was detected. Co-expression of R104W with WT, led to WT retention the in the ER through the interaction between $Na_v1.5$ α-subunits, resulting in a dominant-negative effect. Few *SCN5A* mutations have been studied in conditions mimicking patient heterozygous state, since the large $Na_v1.5$ α-subunits were not thought to oligomerize, contrary to many potassium channels that form

homotetramers[467,478,479]. Nevertheless, a dominant-negative effect caused by a $Na_v1.5$ mutant has been reported once for the trafficking-defective mutant L325R, located in the pore region (loop S5-S6) of domain I[468]. The authors hypothesized that the mutant channels exerted the dominant-negative effect by affecting the trafficking of WT channels. Another recent study has confirmed the interaction between $Na_v1.5$ α-subunits, which is responsible for the dominant-negative effect of the BrS *SCN5A* mutation R1432G[480]. This trafficking-defective mutant is located in the pore region (loop S5-S6) of domain III, and abolished I_{Na}. In the heterozygous state, the mutant decreases WT surface expression, with a resultant dominant-negative effect. In contrast to the R104W N-terminal mutant, both L325R and R1432G mutants were not degraded by the ubiquitin-proteasome system. The dominant-negative effect observed for the three mutations, L325R, R1432G and R104W, is mutation specific and not a generalized mechanism. Indeed, for example we have shown that the trafficking competent but non-functional channels, R878C and ΔN-$Na_v1.5$, do not exert a dominant-negative effect on WT channels.

The three trafficking-defective mutants, L325R, R1432G and R104W, most likely caused the retention of WT channels due to the interaction between $Na_v1.5$ α-subunits. However, the mechanisms underlying the retention of each of these mutants seem to be different. The mutant L325R caused an 80% reduction in I_{Na}, while no I_{Na} was recorded with R1432G and R104W mutants, suggesting that a small part of L325R was able to reach the membrane. In addition, incubating the cells at low temperature or with mexiletine, experimental conditions known to partially rescue some misfolded channels, rescue the mutant L325R[468], but not the R104W and R1432G mutants[310]. Moreover, the N-terminal mutant R104W was degraded by the ubiquitine-proteasome system, but not the two pore mutants L325R[468] and R1432G[480]. These differences suggest that these mutants do not follow the same retention pathway, and that misfolding is not the only cause underlying the intracellular retention. Therefore, further studies are needed to explore the mechanisms underlying this mutant channel retention. We hypothesized that the R104W mutation caused conformational changes in the mutant $Na_v1.5$ protein, which then unmasked an ER retention motif leading to its retention. This hypothesis is in line with our experiments in neonatal rat cardiomyocytes showing a co-localization of the mutant R104W and CD4-KKXX, a construct containing the ER retention motif, KKXX.

Since the trafficking-defective mutant R104W was able to inhibit the trafficking of WT channels, most probably through the interaction between $Na_v1.5$ α-subunits, it is possible that trafficking-competent channels could be able to transport a small amount of the mutant

channels with them to the membrane. By expressing the N-terminal mutants R104W and R121W with the trafficking-competent but non-functional $Na_v1.5$ mutant R878C[195], we showed that the mutant R878C restored a very small I_{Na}. This mechanism of transcomplementation has been previously reported for the cystic fibrosis transmembrane conductance regulator (CFTR), a cAMP-activated chloride channel[481,482]. Interestingly, it has also been demonstrated that the common *SCN5A* polymorphism, H558R, located in the linker I-II, is able to restore the trafficking-defective R282H mutant, located in the pore region (loop S5-S6) of domain I, when it was present in the second allele, but not in the same allele[483]. It is possible that the assembly of the $Na_v1.5$ α-subunits in the ER masks an ER retention signal in the misfolded protein, or it provides an export signal from the ER, as it has been suggested for the CFTR mutant[481,482]. Another possibility is that the interaction between the $Na_v1.5$ α-subunits could stabilize both proteins allowing proper folding. Shinlapawittayatorn *et al*[484] have recently shown that small peptides containing the polymorphism H558R are able to restore the trafficking-defective R282H mutant by promoting proper folding in the ER. Moreover, in the same study, the small peptides were able to restore the trafficking of five out of nine mutant proteins with the mutations located in the pore region of domain 1, but did not have an effect on the WT, suggesting that the peptides specifically restored some mutants. Interestingly, in this study acute expression of the peptides in the intracellular solution during the patch-clamp analysis did not rescue the mutant channels, suggesting that this peptide effect occurs mostly in the ER. In our study, co-expression of the WT $Na_v1.5$ and the $Na_v1.5$ N-terminus, Nter, induced a two-fold increase in I_{Na}. The mechanism underlying this increase in I_{Na} remains unknown. We hypothesize that the Nter could saturate the ER quality control machinery, allowing more WT channels to escape this system and reach the membrane. Other possible explanations are that the Nter occludes the retention signal or provides exit codes, enhancing channel export from the ER or other cellular compartments. Further studies are needed to understand the mechanisms responsible for this increase in I_{Na}. We should invesigate whether the Nter increases the surface expression of the WT, and if it is able to rescue the N-terminal mutant R104W or other trafficking-defective mutants. Moreover, co-immunoprecipitation studies between $Na_v1.5$ α-subunits and the Nter or the small peptides containing the H558R are needed to see if these small peptides interact directly with $Na_v1.5$.

Altogether, these data strongly suggest that the interaction between $Na_v1.5$ α-subunits occurs in the ER before trafficking to the membrane, either impairing or enhancing it. Nevertheless, an interaction at the membrane could also be occuring. The observed positive shift of activation of the N-terminal mutants in the heterozygous state and of the N-terminal

mutants rescued by R878C, as well as the negative shift of steady-state inactivation of the C-terminal mutant R1860Gfs*12 in the heterozygous state, highly suggest that interaction between $Na_v1.5$ α-subunits also exists at the membrane, and that $Na_v1.5$ α-subunits function as oligomers. Our results are in line with a previous study demonstrating double and triple simultaneous openings and closings of the sodium channels, and the authors hypothesized that there is a tight cooperation in channel gating[485]. Interestingly, a recent study has demonstrated that one mutant is able to completely restore the gating defects of the another mutant located in the second allele[486]. The compound heterozygous *SCN5A* mutations, D1690N located in loop S5-S6 of domain IV, and G1748D located in the S6 of domain IV, were identified in a BrS patient[486]. Both mutants are trafficking-defective leading to a severe reduction in I_{Na}, with altered biophysical properties for the G1748D mutant. When expressed with the WT channels, both mutants have a dominant-negative effect on WT channels. Co-expression of D1690N with G1748D, mimicking the heterozygous state of the patient, completely restored the gating defects of G1748D, while it partially restored its trafficking defects.

Detailed aspects of the interaction between $Na_v1.5$ α-subunits remain to be elucidated. In the study of mutant R1432G[480], the authors reported that co-transfection of the β1-subunit with $Na_v1.5$ is essential for the dominant-negative effect, as well as for the interaction between $Na_v1.5$ α-subunits. The experiments in this study were performed in HEK293, the same heterologous system used in our study. Nevertheless, in our study co-transfection with the β1-subunit was not required neither for the interaction between $Na_v1.5$ α-subunits, nor for the dominant-negative effect. We cannot exclude that the interaction between $Na_v1.5$ is mediated by the β1-subunit, since the β1-subunit is endogenously expressed in HEK293 cells[487]. So it remains to be verified if the β1-subunit is needed for the interaction between the α-subunits. Co-immunoprecipitation study in HEK293 cells, where the endogenous β1-subunit is suppressed by RNA interference, or in another heterologous system where β1-subunit is absent are needed to test this hypothesis. However, if the interaction is β1-dependent, it remains unknown why, in the study of the R1432G mutant, the interaction was dependent on the co-expression of the β1 subunits since they are endogenously expressed. A possible explanation is that the mutant R1432G weakens the interaction between $Na_v1.5$ and the β1-subunit and over-expression of the β1-subunit is needed to overcome this problem. However, further studies are needed to better understand the mechanism of interaction between $Na_v1.5$ α-subunits.

The site of $Na_v1.5$ involved in the interaction between $Na_v1.5$ α-subunits needs to be fully defined. Such information would be very useful in order to predict the potential effects of *SCN5A* mutations on this interaction as well as in determining the contribution of this interaction (dominant-negative effect or rescue) to the highly variable clinical manifestations of *SCN5A* mutations. By co-immunoprecipitation studies using the ΔNter construct and the C-terminal truncating R1860Gf*12 mutation, we demonstrated that the N- and C-terminal truncated channels were still able to interact with WT $Na_v1.5$ channels. In addition, the R1860Gfs*12 α-subunits interacted with each other. These results showed that deletion of the N-terminal domain or the distal region of the C-terminal domain did not inhibit the interaction between α-subunits. These data combined with the results of the rescue effect of the small peptides around the H558R polymorphism, and the increase of I_{Na} with the Nter, suggest that multiple sites of $Na_v1.5$ could be involved in this interaction. Further studies are needed to define these interaction sites.

In conclusion, the interaction between $Na_v1.5$ α-subunits is a new concept in the field of sodium channels that were not previously thought to oligomerize. This is a new mechanism that could modulate phenotypic expression, and highlight the importance of heterozygous expression when characterizing *SCN5A* mutations. Nevertheless, the dominant-negative and the rescue effects should be confirmed in cardiomyocytes, where all channel partners are physiologically present. Moreover, the rescue effects of the H558R peptides, and the increased I_{Na} with Nter are interesting findings that should be confirmed *in vivo*. These small peptides may lead to the development of new treatment strategies for the sodium channelopathies. These peptides have the advantage of being small fragments of the target gene, which should reduce the difficulties usually encountered with gene therapy.

The role of the $Na_v1.5$ N-terminal domain in channel function

The role of the $Na_v1.5$ N-terminal domain in channel function was previously largely unknown, even though several N-terminal mutations associated with LQTS, conduction abnormalities or BrS have been reported[306]. By the characterization of the N-terminal mutants R104W, R121W[214,306], and of the two constructs, ΔNter, where the N-terminal region was deleted, and Nter, where only the N-terminal region was present, we highlighted the important role of the $Na_v1.5$ N-terminal domain in channel function. Our results demonstrated that the N-terminal domain is not necessary for the trafficking of $Na_v1.5$ to the membrane, since the ΔNter $Na_v1.5$ was able to reach the membrane. Nevertheless, the missense mutations, R104W

and R121W, led to channel ER retention and their subsequent degradation. Our results suggest that these missense mutations cause severe conformational changes in the channel proteins compared to ΔNter, leading to the retention of the mutant channels by the quality control system, while most of the ΔNter $Na_v1.5$ has escaped from this system and reached the membrane. However, the mechanism of mutant channel retention remains to be clearly defined. It is plausible that cells could use the ERAD system to quickly move the misfolded proteins from the ER to the cytosol, and then degrade them by the ubiquitin-proteasome system[488]. This would prevent the accumulation of misfolded proteins in the ER and the occurrence of reticular stress. This hypothesis correlates with our results showing that treating the transfected cells with MG132, a 26S-subunit ubiquitin-proteasome inhibitor, increased the total expression of the mutants, suggesting that they are degraded by the ubiquitine-proteasome system. Moreover, we reinforced this hypothesis by demonstrating that the mutant proteins did not induce reticular stress in HEK293 cells. Similarly to the $Na_v1.5$ N-terminal mutants, the N-terminal mutant S21P in the neuronal sodium channel $Na_v1.6$ was retained in the Golgi apparatus and degraded[489].

The ΔNter $Na_v1.5$ was expressed at the membrane but was unable to conduct I_{Na}, proposing a role for the N-terminal domain in channel opening, which has not previously been reported. Moreover, the positive shift of activation observed in the heterozygous state and for the small current rescued by R878C, further supports the involvement of the N-terminal domain in channel activation and opening. Our results are in line with recent data from Gutter *et al*[490] characterizing several N-terminal *SCN5A* mutations identified in LQTS and BrS. In this study, the expression of the BrS R104Q mutant in HEK293 results in the absence of I_{Na} similar to the R104W mutant, suggesting an essential role for the amino acid 104 in $Na_v1.5$ channel function. However, expression of R104Q in Xenopus oocytes gives a small I_{Na} with a negative shift of the steady-state inactivation, which decreases channel availability. This difference between the two heterologous systems could be due to differences in the cellular mechanisms between the two models. Interestingly, the other five N-terminal BrS mutants in this study conduct I_{Na} similarly to the WT channel, but with a positive shift of activation for two of them. This positive shift of activation is similar to that observed in our study in the heterozygous state of R104W and in the rescued current. Combined with the fact that the ΔNter construct did not alter the voltage-activation of the WT $Na_v1.5$, this alteration in the activation is most probably due to the N-terminal domain of $Na_v1.5$. Surprisingly, in three of the six BrS mutations, and one of the three LQTS mutations

characterized in this study, no functional defects were observed, which suggests that they may be rare polymorphisms and not disease-causing mutations, and that we should be cautious when interpreting the results of genetic testing. Nevertheless, in this study none of these mutations was studied in the heterozygous state, and other unknown factors may contribute to the disease phenotype.

The C-terminal truncated mutations are associated with a mixed clinical phenotype

The C-terminal domain of $Na_v1.5$, consisting of 243 amino acids, has an important role in regulating channel gating and expression through its interaction with many partner proteins[355]. It has been demonstrated that the C-terminal domain has a proximal structural region consisting of six α-helices and an unstructured distal region[491]. The proximal structural region stabilizes the inactivated state of the channel during prolonged depolarization through a direct physical interaction with the III-IV linker inactivation gate[350]. Interruption of this interaction destabilizes inactivation and increases the chance for the channel to reopen during prolonged depolarization. Few C-terminal $Na_v1.5$ truncating mutations have been reported in BrS (L1786Efs*2, F1808Ifs*3, E1823Hfs*10, and R1860Kfs*13)[306], and in overlap syndrome (L1821fs*10[216] and D1816Vfs*7[492]). Of these mutations, only L1821fs*10 and recently D1816Vfs*7 were functionally characterized.

The R1860Gfs*12 mutation identified here is the most distal truncating mutation in the C-terminus of $Na_v1.5$. Because of its location in the last exon of the *SCN5A* gene, the induced premature stop codon is expected to escape the RNA quality control system and the truncated protein is likely to be present in patient cardiomyocytes. The three family members carrying the R1860Gfs*12 mutation had a mixed clinical picture, mostly atrial (SSS, AF or atrial flutter with atrioventricular conduction block), with variable severity. Similarly to R1860Gf*12, the other two *SCN5A* truncating mutations L1821fs*10[216] and D1816Vfs*7[492] were associated with variable clinical picture and severity. However, the clinical presentation of the R1860Gfs*12 carriers was mostly atrial, while the L1821fs*10 and D1816Vfs*7 carriers presented atrial and ventricular arrhythmias. The proband carrying L1821fs*10 was a 12-year old male with congenital SSS, CCD and recurrent monomorphic VT. A propafenone test was performed to rule out BrS and induced severe prolongation of QRS complexes without ST segment elevation. Other mutation carriers in the same family were either asymptomatic or had some conduction abnormalities. The mutant D1816Vfs*7 was identified in a family where all mutation carriers had PR and QRS intervals prolongation compared to non-carriers. The proband was a 53-year old woman who underwent frequent episodes of

ventricular fibrillation requiring 20 defibrillations over 72 hours. In addition, she had paroxysmal AF, and sinus bradycardia at basal conditions and after a flecainide test, however, no BrS ECG pattern was revealed. Interestingly, a flecainide test performed in one son and two sisters of the proband carrying the same mutation induced a type-1 BrS ECG pattern in the son and one sister, while it was negative in the second sister who had permanent AF. Moreover, other asymptomatic mutation carriers were also present in the family. This high variability in the clinical picture observed with the C-terminal truncating mutations could be due to specific alterations in the sodium current properties. Interestingly, functional studies of these three mutants performed in heterologous systems showed both gain- and loss-of-function effects on $Na_v1.5$.

Gain- and loss-of-function effects of the C-terminal truncating mutations

When expressed in heterologous expression systems (HEK293 or CHO cells), the three truncated mutants display both gain- and loss-of-function effects. They induced a drastic reduction in I_{Na} with a positive shift in the activation curve. The decrease in I_{Na} is most probably due to a decreased surface expression of the mutants, since all these truncated $Na_v1.5$ abolished the sites of interaction with many partner proteins involved in membrane channel stabilization[355]. Moreover, the decrease in I_{Na} is consistent with the results from Cormier *et al* demonstrating that truncation of $Na_v1.5$ distal C-terminus (L1921X truncated construct) reduced current density[491]. In addition, L1821fs*10 and R1860Gfs*12 mutants induced a negative shift of the steady-state inactivation decreasing channel availability, while the mutant D1816Vfs*7 induced a positive shift of the steady-state inactivation and enhanced the recovery from inactivation, effects that would increase channel availability. Moreover, L1821fs*10 and R1860Gfs*12 increased the fast and slow time constants of inactivation and increased I_{NaL}, parameters that were unaffected by the mutant D1816Vfs*7. The observed alteration in the inactivation by the two mutants L1821fs*10 and R1860Gfs*12 is consistent with the involvement of the proximal region of the C-terminus in channel inactivation. It has been demonstrated that truncation of the sixth helix in the proximal region and the distal region of $Na_v1.5$ (S1885X truncated construct) decreased I_{Na}, induced a negative shift of the steady-state inactivation, and increased I_{NaL}[491]. However, it remains unknown why the mutant D1816Vfs*7 had a different effect on the steady-state inactivation with no I_{NaL}. One possibility is that the mutant D1816Vfs*7 could affect the interaction with unknown partner proteins that modulate channel inactivation.

In the heterozygous state, neither of the three truncated mutants had a dominant-negative effect on WT channels. Nevertheless, alteration of the biophysical properties were observed for both D1816Vfs*7 and R1860Gfs*12: positive shift of activation and steady-state inactivation, with enhanced recovery from inactivation for D1816Vfs*7; and significant negative shift of steady-state inactivation, prolonged time constants of inactivation and I_{NaL} for R1860Gfs*12.

The complex functional effects caused by the C-terminal truncating mutations could be responsible for the mixed clinical picture observed, but they do not explain the prominence of atrial arrhythmias in patients carrying the R1860Gfs*12 mutation compared to the other two mutations which caused atrial and ventricular arrhythmias. This led us to hypothesize that the significant negative shift of steady-state inactivation and the presence of I_{NaL} combined with the constitutive difference in the resting membrane potential between atria and ventricles could be responsible for the prominence of atrial arrhythmia in this family. Mimicking this difference in HEK293 cells or using computer-model simulation evidenced more pronounced effects of the mutant R1860Gfs*12 in the atria compared to the ventricles.

The R1860Gfs*12 biophysical defects associated with the constitutive difference in resting membrane potentials between atrium and ventricle might induce a prominence of atrial arrhythmias

It has been shown in both dogs[470] and rabbits[471] that the resting membrane potential of atrial cells is more depolarized than ventricular cells (-83 *vs* -86 mV). In addition, I_{Na} density is more important in atria than in ventricles, with an hyperpolarization of the steady-state inactivation of -16mV[470]. Moreover, the critical depolarization and current thresholds for action potential initiation are smaller in atrial cells than in ventricular cells indicating that atrial cells are more readily excitable than ventricular ones[471]. The impact of some *SCN5A* mutations might thus be greater in the atria than in the ventricles, and may predispose to the development of atrial arrhythmias more readily than to ventricular ones. By measuring I_{Na} in HEK293 cells transfected with the WT and/or the R1860Gfs*12 mutant channels, and maintained at a holding potential mimicking the resting membrane potentials of atrial or ventricular cardiomyocytes, we demonstrated that the mutant induced a more important decrease in I_{Na} at atrial potential compared to ventricular one. Moreover, the fact that the steady-state inactivation of $Na_v1.5$ in the atria is shifted by -16mV compared to the ventricles[470] could exacerbate this loss of current density, since a greater percentage of atrial $Na_v1.5$ channels would be inactivated at a given resting or take-off potential compared to the

ventricular $Na_v1.5$ channels. We confirmed our results by including the biophysical properties of the WT and the heterozygous currents into computer-model simulations of single atrial and ventricular cell membrane action potentials[493]. A marked decrease in AP maximum upstroke velocity ($[dV/dt]_{max}$), representing the maximum speed of depolarization, and a lengthening of the AP duration were observed in the atrial compared to the ventricular myocytes. We hypothesized that the significant shift of steady-state inactivation leads to a severe reduction in channel availability in atrial cardiomyocytes, which are more depolarized compared to the ventricular ones. Compared to the mutant R1860Gfs*12, the D1816Vfs*7 mutation carriers have both atrial and ventricular arrhythmias. The mutant D1816Vfs*7 increased channel availability but it also caused a significant positive shift of activation, which is a major loss-of-function feature, since channels are able to open at more depolarized potentials. We hypothesized that this positive shift of activation in the heterozygous state of the mutant D1816Vfs*7 might lead to a marked loss of I_{Na} in both atrial and ventricular cells. This effect may account for the occurrence of atrial and ventricular arrhythmias compared to the mutant R1860Gfs*12 showing an unaffected channel activation in the heterozygous state. Computer modeling of the D1816Vfs*7 mutation might be needed in order to test our hypothesis. From a clinical point of view, regarding the important role of $Na_v1.5$ channels in the SAN function, the negative shift of steady-state inactivation in the heterozygous state and the persistent current could account for the sinus node dysfunction observed in the family carrying the R186Gfs*12 mutation. Indeed, the SAN AP model showed that the negative shift of steady-state inactivation decreases the sinus rate, by decreasing the diastolic depolarization rate, and the persistent current decreases the sinus rate by AP prolongation despite the simultaneous slight increase in diastolic depolarization rate[211]. However, the combination of a persistent current and a shift of inactivation lead to a decrease in the sinus rate and abolish the slight increase in the depolarization rate seen with persistent current alone. Moreover, an increase in the persistent current above a critical level leads to a plateau oscillation and repolarization failure resulting in sinus pause or arrest[211]. In addition, the association of the prolonged time constant of fast and slow inactivation and the $I_{NaL,}$ might cause repolarization failure, early after-depolarizations (EADs) and delayed after-depolarizations (DADs)[95–97,494], thereby inducing triggering activities accounting for AF. This is supported by a study using isolated atrial myocytes from patients with permanent AF, which showed that permanent AF is associated with significantly greater I_{NaL}, decreased peak I_{Na} density and $Na_v1.5$ expression[97]. In addition, in the study of a cohort of patients with early-onset lone AF, a high prevalence of *SCN5A* mutations previously associated with LQT3 have been identified, all leading to I_{NaL}[93].

However, it is important to emphasize that our study in a heterologous system or using a computer model, like other studies in the field, may not completely reflect what happens in the cardiomyocytes, due to the tissue specific variability of subunits and interacting proteins. Nevertheless, characterization of ion channel mutations in heterologous expression systems provides information about the biophysical phenotypes possibly leading to the clinical symptoms. Further studies are needed in a physiological environment like a mouse model, or human cardiomyocytes, in order to better understand the pathogenic pathway underlying the disease.

A specific biophysical defect of a given *SCN5A* mutation might be able to explain the variability in the clinical expression between different mutations, but it cannot explain the variability in the clinical phenotypes and in the severity of the disease among family members carrying the same mutation. This has drawn our attention to the participation of the patient's genetic background in the modulation of the disease phenotype.

The genetic background of the *SCN5A* mutation carriers could modulate the clinical phenotype

By screening 17 SNPs linked to AF, and 3 SNPs linked to BrS in the family carrying the R1860Gfs*12 mutation, we showed that the proband, who had severe SSS and early onset AF, was the only mutation carrier to have one at-risk allele within the locus 4q25 upstream of the *PITX2* gene. The 4q25 variants have been widely associated with AF development, mainly early onset AF. This association has been replicated in many studies[115–120], and 4q25 variants have also been reported to contribute to post-cardiac surgery AF[472] and to AF recurrence after catheter ablation[473] and cardioversion[474]. These SNPs are located 150-kb upstream the *PITX2* gene. *PITX2* encodes a homeobox transcription factor of the paired type, which has a very important role in the left-right asymmetry[121–123], in the normal development of the sinus node[124] and the pulmonary vein[125], which is an important site for AF initiation[495]. Loss of the *PITX2c* isoform expression in mice can lead to a right atrial isomerization, a failure to suppress the default pathway for sinus node development of the pulmonary myocardium[125,496]. In humans, the *PITX2c* isoform is highly expressed in the left atrium compared to the right atrium and ventricles[497]. It has been demonstrated that patients with sustained AF have decreased atrial *PITX2c* RNA expression compared to patients in sinus rhythm[475]. The *PITX2c*$^{+/-}$ mouse model has no obvious alteration in cardiac morphology, but does display shorter atrial AP duration, and an increased risk to develop inducible AF compared to WT[497]. In this model, a number of cellular and molecular pathways, including

genes related to calcium ion binding, gap and tight junctions and ion channels were altered. In addition, in atrial-specific *PITX2* deficient mice[475], the ECG showed evidence of AVN block and absence of P waves, despite the presence of properly organized SA and AV nodes. Electrophysiological studies showed that the left atrium of this mouse model had more depolarized resting action potential and smaller action potential amplitude. Moreover, both mRNA and protein levels of Kir2.1 and $Na_v1.5$ channels were decreased in the atrial chamber. We hypothesized that the 4q25 variants could modulate the expression of the *PITX*2 gene, inducing early atrial morphological changes and further loss-of-function of $Na_v1.5$ channels in the proband's atrium, accounting for the occurrence of severe SSS with AF at a young age. A recent study by Ritchie *et al*[498] has demonstrated that the 4q25 variants, especially rs2200733 and rs10033464, modified the clinical expression of signaling molecule and ion channel gene mutations associated with familial AF. In this study, seventy subjects in eleven families, in which AF was present in two or more family members, were included. Family members shared an AF causing mutation, and the probands had lone AF. Genotyping of the rs2200733 and rs10033464 SNPs was performed in the seventy subjects. Statistical analysis demonstrated a significant association between the presence of both 4q25 variants and AF mutations in the development of AF. All these data support the hypothesis that 4q25 variants could act as genetic modifiers of the clinical phenotype by modulating the expression of cardiac ion channels. However, there are several questions, which remain to be answered. The first is how these reported variants could alter the expression and/or the function of *PITX2*. Secondly, whether the arrhythmogenic substrate formed by the alteration of *PITX2* expression is established during the embryonic stage[496,499], or during later stages of heart development[497,475]. Moreover, how the 4q25 variants interact with the other AF-associated variants to modulate the phenotypes, and which of these variants has the most important effect in AF development remain to be elucidated. Quantitative PCR of *PITX2* mRNA using human atrial biopsies from patients carrying the 4q25 variants could be useful to test if these variants alter *PITX2* expression.

Modulation of the phenotypic expression of ion channel gene mutations by common genetic variants is a major focus of recent research on the genetics of arrhythmia. Remme *et al* in 2009 have demonstrated that the genetic background can modulate disease severity[500]. By comparing the phenotypic expression of the *SCN5A* mutation 1798insD in two different mouse genetic backgrounds (129P2 and FVB/N), they demonstrated that the 129P2 mice had a more severe phenotype than the FVB/N ones. Recently, GWAS for different diseases and traits have identified common variants (SNPs) that could modulate disease susceptibility.

Since the diagnosis of the disease is often made only when a clinical threshold is exceeded, a large number of predisposing-variant carriers will be present in the healthy control population. GWAS of the intermediate phenotypes, which are traits associated with, or predisposing to specific diseases, have proven their efficacy in identifying modulating variants with greater statistical power. Then, these identified variants can be investigated for their association with the disease. GWAS on ECG parameters in the general population have identified genetic variants modulating QT_c[501–503], PR intervals[129,130], QRS duration[129,504] and heart rate[129,505,506]. These variants are not only located in, or near genes encoding ion channels, but also in or near genes encoding transcription factors. These variants represent good candidates to be investigated for their contribution to specific diseases. Studies such as this are starting to become more popular. Indeed, the common genetic variants in *NOS1AP* modulating the QT interval in the general population were found to modulate the QT interval duration and the risk of arrhythmias in long QT syndrome[507,508]. Variants associated with PR interval prolongation were also found to be associated with AF[129,130].

GWAS have provided a huge number of SNPs that can modulate physiological traits or disease development. However, the major difficulty is to link these variants to specific genes, to detect the true functional variants, and to determine their underlying mechanisms of action. Despite these difficulties, the concept that a combination of rare and common variants contribute to disease development could have a significant impact on the management of the disease, through the identification of patients who are at a high risk to develop disease or to display severe phenotypes.

CONCLUSION

Expression of disease mutations is a complex process where many factors modulate the functional defects caused by a given mutation to lead to a clinical phenotype. In this thesis, we characterized three mechanisms that contribute to the variability of the phenotypes caused by mutations in *SCN5A*: interaction between the $Na_v1.5$ α-subunits, the differences in the constitutive electrical properties between atrial and ventricular cardiomyocytes, and the genetic background of the mutation carriers.

Many aspects of the regulation of the $Na_v1.5$ cardiac sodium channel remain to be elucidated, given the large number of partner proteins interacting with this channel, and our limited knowledge of its *in vivo* regulation. In addition, channel regulation may vary at the cellular level (intercalated discs *vs* lateral membranes), as well as at the tissue level, given differences in the expression of the channel and its partners in specific cardiac tissues (ventricle *vs* atrium *vs* Purkinje fibers, right *vs* left heart, epicardium *vs* endocardium). The classical view of sodium channelopathies, which links a single genetic mutation with a specific disease, does no longer exist. Obviously, the overall effects of any given *SCN5A* mutation should be considered in an integrated system combining the genetic background, the alteration caused by the mutation, and the physiological cardiac environment. Animal models or the new approach of human induced pluripotent stem cell cardiomyocytes could help us to better understand the complexity of the cardiac pathophysiology. Such cardiomyocytes from patients carrying common and/or rare genetic variants would be a useful model to explore how the genetic background of patients combined with the altered biophysical properties of a given ion channel mutation could modulate the disease phenotype.

REFERENCES

1. Deo R, Albert CM. Epidemiology and Genetics of Sudden Cardiac Death. *Circulation*. 2012;125:620–637.
2. Kolder ICRM, Tanck MWT, Bezzina CR. Common genetic variation modulating cardiac ECG parameters and susceptibility to sudden cardiac death. *J Mol Cell Cardiol*. 2012;52:620–629.
3. Cerrone M, Priori SG. Genetics of sudden death: focus on inherited channelopathies. *Eur Heart J*. 2011;32:2109–2118.
4. Song K, Nam Y-J, Luo X, Qi X, Tan W, Huang GN, Acharya A, Smith CL, Tallquist MD, Neilson EG, Hill JA, Bassel-Duby R, Olson EN. Heart repair by reprogramming non-myocytes with cardiac transcription factors. *Nature*. 2012;485:599–604.
5. Souders CA, Bowers SLK, Baudino TA. Cardiac Fibroblast The Renaissance Cell. *Circ Res*. 2009;105:1164–1176.
6. Takeda N, Manabe I. Cellular Interplay between Cardiomyocytes and Nonmyocytes in Cardiac Remodeling. *Int J Inflamm*. 2011;2011:535241.
7. Gaborit N, Bouter SL, Szuts V, Varro A, Escande D, Nattel S, Demolombe S. Regional and tissue specific transcript signatures of ion channel genes in the non-diseased human heart. *J Physiol*. 2007;582:675–693.
8. Schotten U, Verheule S, Kirchhof P, Goette A. Pathophysiological Mechanisms of Atrial Fibrillation: A Translational Appraisal. *Physiol Rev*. 2011;91:265–325.
9. Hatem SN, Coulombe A, Balse E. Specificities of atrial electrophysiology: Clues to a better understanding of cardiac function and the mechanisms of arrhythmias. *J Mol Cell Cardiol*. 2010;48:90–95.
10. Giudicessi JR, Ackerman MJ. Potassium-channel mutations and cardiac arrhythmias--diagnosis and therapy. *Nat Rev Cardiol*. 2012;9:319–332.
11. Nerbonne JM, Kass RS. Molecular Physiology of Cardiac Repolarization. *Physiol Rev*. 2005;85:1205–1253.
12. Näbauer M, Beuckelmann DJ, Überfuhr P, Steinbeck G. Regional Differences in Current Density and Rate-Dependent Properties of the Transient Outward Current in Subepicardial and Subendocardial Myocytes of Human Left Ventricle. *Circulation*. 1996;93:168–177.
13. Michael G, Xiao L, Qi X-Y, Dobrev D, Nattel S. Remodelling of cardiac repolarization: how homeostatic responses can lead to arrhythmogenesis. *Cardiovasc Res*. 2009;81:491–499.
14. Ravens U, Cerbai E. Role of potassium currents in cardiac arrhythmias. *Eur Eur Pacing Arrhythm Card Electrophysiol J Work Groups Card Pacing Arrhythm Card Cell Electrophysiol Eur Soc Cardiol*. 2008;10:1133–1137.
15. Desplantez T, Dupont E, Severs NJ, Weingart R. Gap junction channels and cardiac impulse propagation. *J Membr Biol*. 2007;218:13–28.
16. Greenstein JL, Winslow RL. Integrative Systems Models of Cardiac Excitation–Contraction Coupling. *Circ Res*. 2011;108:70–84.
17. Kligfield P, Gettes LS, Bailey JJ, Childers R, Deal BJ, Hancock EW, van Herpen G, Kors JA, Macfarlane P, Mirvis DM, Pahlm O, Rautaharju P, Wagner GS, American Heart Association Electrocardiography and Arrhythmias Committee, Council on Clinical Cardiology, American College of Cardiology Foundation, Heart Rhythm Society, Josephson M, Mason JW, Okin P, Surawicz B, Wellens H. Recommendations for the standardization and interpretation of the electrocardiogram: part I: The electrocardiogram and its technology: a scientific statement from the American Heart Association Electrocardiography and Arrhythmias Committee, Council on Clinical Cardiology; the American College of Cardiology Foundation; and the Heart Rhythm Society: endorsed by the International Society for Computerized Electrocardiology.

Circulation. 2007;115:1306–1324.
18. Patel C, Yan G-X, Antzelevitch C. Short QT Syndrome: From Bench to Bedside. *Circ Arrhythm Electrophysiol*. 2010;3:401–408.
19. Gaztañaga L, Marchlinski FE, Betensky BP. Mechanisms of Cardiac Arrhythmias. *Rev Esp Cardiol Engl Ed*. 2012;65:174–185.
20. Sakmann B, Noma A, Trautwein W. Acetylcholine activation of single muscarinic K+ channels in isolated pacemaker cells of the mammalian heart. *Nature*. 1983;303:250–253.
21. Parham WA, Mehdirad AA, Biermann KM, Fredman CS. Hyperkalemia Revisited. *Tex Heart Inst J*. 2006;33:40–47.
22. Zipes DP. Mechanisms of Clinical Arrhythmias. *J Cardiovasc Electrophysiol*. 2003;14:902–912.
23. Yan G-X, Wu Y, Liu T, Wang J, Marinchak RA, Kowey PR. Phase 2 Early Afterdepolarization as a Trigger of Polymorphic Ventricular Tachycardia in Acquired Long-QT Syndrome Direct Evidence From Intracellular Recordings in the Intact Left Ventricular Wall. *Circulation*. 2001;103:2851–2856.
24. Antman EM, Smith TW. Digitalis Toxicity. *Annu Rev Med*. 1985;36:357–367.
25. Leenhardt A, Denjoy I, Guicheney P. Catecholaminergic Polymorphic Ventricular Tachycardia. *Circ Arrhythm Electrophysiol*. 2012;5:1044–1052.
26. Lee KW, Yang Y, Scheinman MM, University of Califoirnia-San Francisco, San Francisco, CA, USA. Atrial flutter: a review of its history, mechanisms, clinical features, and current therapy. *Curr Probl Cardiol*. 2005;30:121–167.
27. García-Cosío F, Pastor Fuentes A, Núñez Angulo A. Arrhythmias (IV). Clinical approach to atrial tachycardia and atrial flutter from an understanding of the mechanisms. Electrophysiology based on anatomy. *Rev Esp Cardiol Engl Ed*. 2012;65:363–375.
28. Lemmens R, Hermans S, Nuyens D, Thijs V. Genetics of atrial fibrillation and possible implications for ischemic stroke. *Stroke Res Treat*. 2011;2011:208694.
29. National Collaborating Centre for Chronic Conditions (UK). Atrial Fibrillation: National clinical guideline for management in primary and secondary care [Internet]. London: Royal College of Physicians (UK); 2006 [cited 2013 Jun 29]. Available from: http://www.ncbi.nlm.nih.gov/books/NBK51113/
30. Fuster V, Rydén LE, Cannom DS, Crijns HJ, Curtis AB, Ellenbogen KA, Halperin JL, Kay GN, Le Huezey J-Y, Lowe JE, Olsson SB, Prystowsky EN, Tamargo JL, Wann LS. 2011 ACCF/AHA/HRS Focused Updates Incorporated Into the ACC/AHA/ESC 2006 Guidelines for the Management of Patients With Atrial Fibrillation: A Report of the American College of Cardiology Foundation/American Heart Association Task Force on Practice Guidelines Developed in partnership with the European Society of Cardiology and in collaboration with the European Heart Rhythm Association and the Heart Rhythm Society. *J Am Coll Cardiol*. 2011;57:e101–e198.
31. European Heart Rhythm Association, European Association for Cardio-Thoracic Surgery, Camm AJ, Kirchhof P, Lip GYH, Schotten U, Savelieva I, Ernst S, Van Gelder IC, Al-Attar N, Hindricks G, Prendergast B, Heidbuchel H, Alfieri O, Angelini A, Atar D, Colonna P, De Caterina R, De Sutter J, Goette A, Gorenek B, Heldal M, Hohloser SH, Kolh P, Le Heuzey J-Y, Ponikowski P, Rutten FH. Guidelines for the management of atrial fibrillation: the Task Force for the Management of Atrial Fibrillation of the European Society of Cardiology (ESC). *Eur Heart J*. 2010;31:2369–2429.
32. Camm AJ, Lip GYH, De Caterina R, Savelieva I, Atar D, Hohnloser SH, Hindricks G, Kirchhof P, ESC Committee for Practice Guidelines (CPG), Bax JJ, Baumgartner H,

Ceconi C, Dean V, Deaton C, Fagard R, Funck-Brentano C, Hasdai D, Hoes A, Kirchhof P, Knuuti J, Kolh P, McDonagh T, Moulin C, Popescu BA, Reiner Z, Sechtem U, Sirnes PA, Tendera M, Torbicki A, Vahanian A, Windecker S, Document Reviewers, Vardas P, Al-Attar N, Alfieri O, Angelini A, Blömstrom-Lundqvist C, Colonna P, De Sutter J, Ernst S, Goette A, Gorenek B, Hatala R, Heidbüchel H, Heldal M, Kristensen SD, Kolh P, Le Heuzey J-Y, Mavrakis H, Mont L, Filardi PP, Ponikowski P, Prendergast B, Rutten FH, Schotten U, Van Gelder IC, Verheugt FWA. 2012 focused update of the ESC Guidelines for the management of atrial fibrillation: an update of the 2010 ESC Guidelines for the management of atrial fibrillation. Developed with the special contribution of the European Heart Rhythm Association. *Eur Heart J*. 2012;33:2719–2747.

33. Fatkin D, Otway R, Vandenberg JI. Genes and Atrial Fibrillation A New Look at an Old Problem. *Circulation*. 2007;116:782–792.
34. Lee G, Sanders P, Kalman JM. Catheter ablation of atrial arrhythmias: state of the art. *The Lancet*. 380:1509–1519.
35. Coumel P, Leclercq JF, Leenhardt A. Arrhythmias as predictors of sudden death. *Am Heart J*. 1987;114:929–937.
36. Xiao J, Liang D, Chen Y-H. The genetics of atrial fibrillation: from the bench to the bedside. *Annu Rev Genomics Hum Genet*. 2011;12:73–96.
37. Wolff L. Familial Auricular Fibrillation. *N Engl J Med*. 1943;229:396–398.
38. Darbar D, Herron KJ, Ballew JD, Jahangir A, Gersh BJ, Shen W-K, Hammill SC, Packer DL, Olson TM. Familial atrial fibrillation is a genetically heterogeneous disorder. *J Am Coll Cardiol*. 2003;41:2185–2192.
39. Fox CS PH. PArental atrial fibrillation as a risk factor for atrial fibrillation in offspring. *JAMA*. 2004;291:2851–2855.
40. Ellinor PT, Yoerger DM, Ruskin JN, MacRae CA. Familial aggregation in lone atrial fibrillation. *Hum Genet*. 2005;118:179–184.
41. Arnar DO, Thorvaldsson S, Manolio TA, Thorgeirsson G, Kristjansson K, Hakonarson H, Stefansson K. Familial aggregation of atrial fibrillation in Iceland. *Eur Heart J*. 2006;27:708–712.
42. Marcus GM, Smith LM, Vittinghoff E, Tseng ZH, Badhwar N, Lee BK, Lee RJ, Scheinman MM, Olgin JE. A first-degree family history in lone atrial fibrillation patients. *Heart Rhythm Off J Heart Rhythm Soc*. 2008;5:826–830.
43. Christophersen IE, Ravn LS, Budtz-Joergensen E, Skytthe A, Haunsoe S, Svendsen JH, Christensen K. Familial Aggregation of Atrial Fibrillation A Study in Danish Twins. *Circ Arrhythm Electrophysiol*. 2009;2:378–383.
44. Lubitz SA, Yin X, Fontes JD, Magnani JW, Rienstra M, Pai M, Villalon ML, Vasan RS, Pencina MJ, Levy D, Larson MG, Ellinor PT, Benjamin EJ. Association between Familial Atrial Fibrillation and Risk of New-onset Atrial Fibrillation. *JAMA J Am Med Assoc*. 2010;304:2263–2269.
45. Oyen N, Ranthe MF, Carstensen L, Boyd HA, Olesen MS, Olesen S-P, Wohlfahrt J, Melbye M. Familial aggregation of lone atrial fibrillation in young persons. *J Am Coll Cardiol*. 2012;60:917–921.
46. Brugada R, Tapscott T, Czernuszewicz GZ, Marian AJ, Iglesias A, Mont L, Brugada J, Girona J, Domingo A, Bachinski LL, Roberts R. Identification of a Genetic Locus for Familial Atrial Fibrillation. *N Engl J Med*. 1997;336:905–911.
47. Chen Y-H, Xu S-J, Bendahhou S, Wang X-L, Wang Y, Xu W-Y, Jin H-W, Sun H, Su X-Y, Zhuang Q-N, Yang Y-Q, Li Y-B, Liu Y, Xu H-J, Li X-F, Ma N, Mou C-P, Chen Z, Barhanin J, Huang W. KCNQ1 gain-of-function mutation in familial atrial fibrillation. *Science*. 2003;299:251–254.

48. Ellinor PT, Shin JT, Moore RK, Yoerger DM, MacRae CA. Locus for Atrial Fibrillation Maps to Chromosome 6q14–16. *Circulation*. 2003;107:2880–2883.
49. Oberti C, Wang L, Li L, Dong J, Rao S, Du W, Wang Q. Genome-Wide Linkage Scan Identifies a Novel Genetic Locus on Chromosome 5p13 for Neonatal Atrial Fibrillation Associated With Sudden Death and Variable Cardiomyopathy. *Circulation*. 2004;110:3753–3759.
50. Xia M, Jin Q, Bendahhou S, He Y, Larroque M-M, Chen Y, Zhou Q, Yang Y, Liu Y, Liu B, Zhu Q, Zhou Y, Lin J, Liang B, Li L, Dong X, Pan Z, Wang R, Wan H, Qiu W, Xu W, Eurlings P, Barhanin J, Chen Y. A Kir2.1 gain-of-function mutation underlies familial atrial fibrillation. *Biochem Biophys Res Commun*. 2005;332:1012–1019.
51. Laitinen-Forsblom PJ, Mäkynen P, Mäkynen H, Yli-Mäyry S, Virtanen V, Kontula K, Aalto-Setälä K. SCN5A mutation associated with cardiac conduction defect and atrial arrhythmias. *J Cardiovasc Electrophysiol*. 2006;17:480–485.
52. Volders PGA, Zhu Q, Timmermans C, Eurlings PMH, Su X, Arens YH, Li L, Jongbloed RJ, Xia M, Rodriguez L-M, Chen YH. Mapping a novel locus for familial atrial fibrillation on chromosome 10p11-q21. *Heart Rhythm Off J Heart Rhythm Soc*. 2007;4:469–475.
53. Darbar D, Hardy A, Haines JL, Roden DM. Prolonged Signal-Averaged P-Wave Duration as an Intermediate Phenotype for Familial Atrial Fibrillation. *J Am Coll Cardiol*. 2008;51:1083–1089.
54. Hodgson-Zingman DM, Karst ML, Zingman LV, Heublein DM, Darbar D, Herron KJ, Ballew JD, de Andrade M, Burnett JC Jr, Olson TM. Atrial natriuretic peptide frameshift mutation in familial atrial fibrillation. *N Engl J Med*. 2008;359:158–165.
55. Zhang X, Chen S, Yoo S, Chakrabarti S, Zhang T, Ke T, Oberti C, Yong SL, Fang F, Li L, de la Fuente R, Wang L, Chen Q, Wang QK. Mutation in nuclear pore component NUP155 leads to atrial fibrillation and early sudden cardiac death. *Cell*. 2008;135:1017–1027.
56. Olesen MS, Nielsen MW, Haunsø S, Svendsen JH. Atrial fibrillation: the role of common and rare genetic variants. *Eur J Hum Genet EJHG*. 2014;22:297–306.
57. Hong K, Piper DR, Diaz-Valdecantos A, Brugada J, Oliva A, Burashnikov E, Santos-de-Soto J, Grueso-Montero J, Diaz-Enfante E, Brugada P, Sachse F, Sanguinetti MC, Brugada R. De novo KCNQ1 mutation responsible for atrial fibrillation and short QT syndrome in utero. *Cardiovasc Res*. 2005;68:433–440.
58. Otway R, Vandenberg JI, Guo G, Varghese A, Castro ML, Liu J, Zhao J, Bursill JA, Wyse KR, Crotty H, Baddeley O, Walker B, Kuchar D, Thorburn C, Fatkin D. Stretch-sensitive KCNQ1 mutation A link between genetic and environmental factors in the pathogenesis of atrial fibrillation? *J Am Coll Cardiol*. 2007;49:578–586.
59. Das S, Makino S, Melman YF, Shea MA, Goyal SB, Rosenzweig A, Macrae CA, Ellinor PT. Mutation in the S3 segment of KCNQ1 results in familial lone atrial fibrillation. *Heart Rhythm Off J Heart Rhythm Soc*. 2009;6:1146–1153.
60. Abraham RL, Yang T, Blair M, Roden DM, Darbar D. Augmented potassium current is a shared phenotype for two genetic defects associated with familial atrial fibrillation. *J Mol Cell Cardiol*. 2010;48:181–190.
61. Bartos DC, Anderson JB, Bastiaenen R, Johnson JN, Gollob MH, Tester DJ, Burgess DE, Homfray T, Behr ER, Ackerman MJ, Guicheney P, Delisle BP. A KCNQ1 Mutation Causes a High Penetrance for Familial Atrial Fibrillation. *J Cardiovasc Electrophysiol*. 2013;24:562–569.
62. Herbert E, Trusz-Gluza M, Moric E, Smiłowska-Dzielicka E, Mazurek U, Wilczok T. KCNQ1 gene mutations and the respective genotype-phenotype correlations in the long QT syndrome. *Med Sci Monit Int Med J Exp Clin Res*. 2002;8:RA240–248.

63. Morita H, Wu J, Zipes DP. The QT syndromes: long and short. *Lancet*. 2008;372:750–763.
64. Johnson JN, Tester DJ, Perry J, Salisbury BA, Reed CR, Ackerman MJ. Prevalence of early-onset atrial fibrillation in congenital long QT syndrome. *Heart Rhythm*. 2008;5:704–9.
65. Lundby A, Ravn LS, Svendsen JH, Olesen S-P, Schmitt N. KCNQ1 mutation Q147R is associated with atrial fibrillation and prolonged QT interval. *Heart Rhythm Off J Heart Rhythm Soc*. 2007;4:1532–1541.
66. Bartos DC, Duchatelet S, Burgess DE, Klug D, Denjoy I, Peat R, Lupoglazoff J-M, Fressart V, Berthet M, Ackerman MJ, January CT, Guicheney P, Delisle BP. R231C mutation in KCNQ1 causes long QT syndrome type 1 and familial atrial fibrillation. *Heart Rhythm Off J Heart Rhythm Soc*. 2011;8:48–55.
67. Henrion U, Zumhagen S, Steinke K, Strutz-Seebohm N, Stallmeyer B, Lang F, Schulze-Bahr E, Seebohm G. Overlapping Cardiac Phenotype Associated with a Familial Mutation in the Voltage Sensor of the KCNQ1 Channel. *Cell Physiol Biochem*. 2012;29:809–818.
68. Olesen MS, Bentzen BH, Nielsen JB, Steffensen AB, David J-P, Jabbari J, Jensen HK, Hauns? S, Svendsen JH, Schmitt N. mutations in the potassium channel subunit kcne1 are associated with early onset familial atrial fibrillation. *BMC Med Genet*. 2012;13:24.
69. Yang Y, Xia M, Jin Q, Bendahhou S, Shi J, Chen Y, Liang B, Lin J, Liu Y, Liu B, Zhou Q, Zhang D, Wang R, Ma N, Su X, Niu K, Pei Y, Xu W, Chen Z, Wan H, Cui J, Barhanin J, Chen Y. Identification of a KCNE2 gain-of-function mutation in patients with familial atrial fibrillation. *Am J Hum Genet*. 2004;75:899–905.
70. Ravn LS, Aizawa Y, Pollevick GD, Hofman-Bang J, Cordeiro JM, Dixen U, Jensen G, Wu Y, Burashnikov E, Haunso S, Guerchicoff A, Hu D, Svendsen JH, Christiansen M, Antzelevitch C. Gain of function in IKs secondary to a mutation in KCNE5 associated with atrial fibrillation. *Heart Rhythm Off J Heart Rhythm Soc*. 2008;5:427–435.
71. Hong K, Bjerregaard P, Gussak I, Brugada R. Short QT syndrome and atrial fibrillation caused by mutation in KCNH2. *J Cardiovasc Electrophysiol*. 2005;16:394–396.
72. Brugada R, Hong K, Dumaine R, Cordeiro J, Gaita F, Borggrefe M, Menendez TM, Brugada J, Pollevick GD, Wolpert C, Burashnikov E, Matsuo K, Wu YS, Guerchicoff A, Bianchi F, Giustetto C, Schimpf R, Brugada P, Antzelevitch C. Sudden Death Associated With Short-QT Syndrome Linked to Mutations in HERG. *Circulation*. 2004;109:30–35.
73. Lundby A, Ravn LS, Svendsen JH, Hauns S, Olesen S-P, Schmitt N. KCNE3 mutation V17M identified in a patient with lone atrial fibrillation. *Cell Physiol Biochem Int J Exp Cell Physiol Biochem Pharmacol*. 2008;21:47–54.
74. Mann SA, Otway R, Guo G, Soka M, Karlsdotter L, Trivedi G, Ohanian M, Zodgekar P, Smith RA, Wouters MA, Subbiah R, Walker B, Kuchar D, Sanders P, Griffiths L, Vandenberg JI, Fatkin D. Epistatic Effects of Potassium Channel Variation on Cardiac Repolarization and Atrial Fibrillation Risk. *J Am Coll Cardiol*. 2012;59:1017–1025.
75. Christophersen IE, Olesen MS, Liang B, Andersen MN, Larsen AP, Nielsen JB, Haunsø S, Olesen S-P, Tveit A, Svendsen JH, Schmitt N. Genetic variation in KCNA5: impact on the atrial-specific potassium current IKur in patients with lone atrial fibrillation. *Eur Heart J*. 2013;34:1517–1525.
76. Olson TM, Alekseev AE, Liu XK, Park S, Zingman LV, Bienengraeber M, Sattiraju S, Ballew JD, Jahangir A, Terzic A. Kv1.5 channelopathy due to KCNA5 loss-of-function mutation causes human atrial fibrillation. *Hum Mol Genet*. 2006;15:2185–

2191.
77. Yang Y, Li J, Lin X, Yang Y, Hong K, Wang L, Liu J, Li L, Yan D, Liang D, Xiao J, Jin H, Wu J, Zhang Y, Chen Y-H. Novel KCNA5 loss-of-function mutations responsible for atrial fibrillation. *J Hum Genet*. 2009;54:277–283.
78. Yang T, Yang P, Roden DM, Darbar D. Novel KCNA5 mutation implicates tyrosine kinase signaling in human atrial fibrillation. *Heart Rhythm Off J Heart Rhythm Soc*. 2010;7:1246–1252.
79. Giudicessi JR, Ye D, Tester DJ, Crotti L, Mugione A, Nesterenko VV, Albertson RM, Antzelevitch C, Schwartz PJ, Ackerman MJ. Transient Outward Current (Ito) Gain-of-Function Mutations in the KCND3-Encoded Kv4.3 Potassium Channel and Brugada Syndrome. *Heart Rhythm Off J Heart Rhythm Soc*. 2011;8:1024–1032.
80. Giudicessi JR, Ye D, Kritzberger CJ, Nesterenko VV, Tester DJ, Antzelevitch C, Ackerman MJ. Novel Mutations in the KCND3-Encoded Kv4.3 K+ Channel Associated with Autopsy-Negative Sudden Unexplained Death. *Hum Mutat*. 2012;33:989–997.
81. Olesen MS, Refsgaard L, Holst AG, Larsen AP, Grubb S, Haunsø S, Svendsen JH, Olesen S-P, Schmitt N, Calloe K. A novel KCND3 gain-of-function mutation associated with early-onset of persistent lone atrial fibrillation. *Cardiovasc Res*. 2013;98:488–495.
82. Kharche S, Garratt CJ, Boyett MR, Inada S, Holden AV, Hancox JC, Zhang H. Atrial proarrhythmia due to increased inward rectifier current (I(K1)) arising from KCNJ2 mutation--a simulation study. *Prog Biophys Mol Biol*. 2008;98:186–197.
83. Hattori T, Makiyama T, Akao M, Ehara E, Ohno S, Iguchi M, Nishio Y, Sasaki K, Itoh H, Yokode M, Kita T, Horie M, Kimura T. A novel gain-of-function KCNJ2 mutation associated with short-QT syndrome impairs inward rectification of Kir2.1 currents. *Cardiovasc Res*. 2012;93:666–673.
84. Deo M, Ruan Y, Pandit SV, Shah K, Berenfeld O, Blaufox A, Cerrone M, Noujaim SF, Denegri M, Jalife J, Priori SG. KCNJ2 mutation in short QT syndrome 3 results in atrial fibrillation and ventricular proarrhythmia. *Proc Natl Acad Sci U S A*. 2013;110:4291–4296.
85. Delaney JT, Muhammad R, Blair MA, Kor K, Fish FA, Roden DM, Darbar D. A KCNJ8 mutation associated with early repolarization and atrial fibrillation. *Europace*. 2012;14:1428–1432.
86. Medeiros-Domingo A, Tan B-H, Crotti L, Tester DJ, Eckhardt L, Cuoretti A, Kroboth SL, Song C, Zhou Q, Kopp D, Schwartz PJ, Makielski JC, Ackerman MJ. Gain-of-function mutation S422L in the KCNJ8-encoded cardiac K(ATP) channel Kir6.1 as a pathogenic substrate for J-wave syndromes. *Heart Rhythm Off J Heart Rhythm Soc*. 2010;7:1466–1471.
87. Olson TM, Alekseev AE, Moreau C, Liu XK, Zingman LV, Miki T, Seino S, Asirvatham SJ, Jahangir A, Terzic A. KATP channel mutation confers risk for vein of Marshall adrenergic atrial fibrillation. *Nat Clin Pract Cardiovasc Med*. 2007;4:110–116.
88. Makiyama T, Akao M, Shizuta S, Doi T, Nishiyama K, Oka Y, Ohno S, Nishio Y, Tsuji K, Itoh H, Kimura T, Kita T, Horie M. A novel SCN5A gain-of-function mutation M1875T associated with familial atrial fibrillation. *J Am Coll Cardiol*. 2008;52:1326–34.
89. Li Q, Huang H, Liu G, Lam K, Rutberg J, Green MS, Birnie DH, Lemery R, Chahine M, Gollob MH. Gain-of-function mutation of Nav1.5 in atrial fibrillation enhances cellular excitability and lowers the threshold for action potential firing. *Biochem Biophys Res Commun*. 2009;380:132–7.

90. McNair WP, Ku L, Taylor MRG, Fain PR, Dao D, Wolfel E, Mestroni L, Familial Cardiomyopathy Registry Research Group. SCN5A mutation associated with dilated cardiomyopathy, conduction disorder, and arrhythmia. *Circulation*. 2004;110:2163–2167.
91. Olson TM, Michels VV, Ballew JD, Reyna SP, Karst ML, Herron KJ, Horton SC, Rodeheffer RJ, Anderson JL. Sodium channel mutations and susceptibility to heart failure and atrial fibrillation. *JAMA J Am Med Assoc*. 2005;293:447–454.
92. Ellinor PT, Nam EG, Shea MA, Milan DJ, Ruskin JN, MacRae CA. Cardiac sodium channel mutation in atrial fibrillation. *Heart Rhythm Off J Heart Rhythm Soc*. 2008;5:99–105.
93. Olesen MS, Yuan L, Liang B, Holst AG, Nielsen N, Nielsen JB, Hedley PL, Christiansen M, Olesen S-P, Haunsø S, Schmitt N, Jespersen T, Svendsen JH. High Prevalence of Long QT Syndrome–Associated SCN5A Variants in Patients With Early-Onset Lone Atrial FibrillationClinical Perspective. *Circ Cardiovasc Genet*. 2012;5:450–459.
94. Darbar D, Kannankeril PJ, Donahue BS, Kucera G, Stubblefield T, Haines JL, George AL Jr, Roden DM. Cardiac sodium channel (SCN5A) variants associated with atrial fibrillation. *Circulation*. 2008;117:1927–1935.
95. Lemoine MD, Duverger JE, Naud P, Chartier D, Qi XY, Comtois P, Fabritz L, Kirchhof P, Nattel S. Arrhythmogenic left atrial cellular electrophysiology in a murine genetic long QT syndrome model. *Cardiovasc Res*. 92:67–74.
96. Song Y, Shryock JC, Belardinelli L. An increase of late sodium current induces delayed afterdepolarizations and sustained triggered activity in atrial myocytes. *Am J Physiol Heart Circ Physiol*. 2008;294:H2031–9.
97. Sossalla S, Kallmeyer B, Wagner S, Mazur M, Maurer U, Toischer K, Schmitto JD, Seipelt R, Schöndube FA, Hasenfuss G, Belardinelli L, Maier LS. Altered Na+ Currents in Atrial Fibrillation: Effects of Ranolazine on Arrhythmias and Contractility in Human Atrial Myocardium. *J Am Coll Cardiol*. 2010;55:2330–2342.
98. Watanabe H, Darbar D, Kaiser DW, Jiramongkolchai K, Chopra S, Donahue BS, Kannankeril PJ, Roden DM. Mutations in sodium channel β1- and β2-subunits associated with atrial fibrillation. *Circ Arrhythm Electrophysiol*. 2009;2:268–275.
99. Olesen MS, Holst AG, Svendsen JH, Haunsø S, Tfelt-Hansen J. SCN1Bb R214Q found in 3 patients: 1 with Brugada syndrome and 2 with lone atrial fibrillation. *Heart Rhythm*. 2012;9:770–773.
100. Hu D, Barajas-Martínez H, Medeiros-Domingo A, Crotti L, Veltmann C, Schimpf R, Urrutia J, Alday A, Casis O, Pfeiffer R, Burashnikov E, Caceres G, Tester DJ, Wolpert C, Borggrefe M, Schwartz P, Ackerman MJ, Antzelevitch C. A novel rare variant in SCN1Bb linked to Brugada syndrome and SIDS by combined modulation of Na(v)1.5 and K(v)4.3 channel currents. *Heart Rhythm Off J Heart Rhythm Soc*. 2012;9:760–769.
101. Wang P, Yang Q, Wu X, Yang Y, Shi L, Wang C, Wu G, Xia Y, Yang B, Zhang R, Xu C, Cheng X, Li S, Zhao Y, Fu F, Liao Y, Fang F, Chen Q, Tu X, Wang QK. Functional dominant-negative mutation of sodium channel subunit gene SCN3B associated with atrial fibrillation in a Chinese GeneID population. *Biochem Biophys Res Commun*. 2010;398:98–104.
102. Olesen MS, Jespersen T, Nielsen JB, Liang B, Møller DV, Hedley P, Christiansen M, Varró A, Olesen S-P, Haunsø S, Schmitt N, Svendsen JH. Mutations in sodium channel β-subunit SCN3B are associated with early-onset lone atrial fibrillation. *Cardiovasc Res*. 2011;89:786–793.
103. Thibodeau IL, Xu J, Li Q, Liu G, Lam K, Veinot JP, Birnie DH, Jones DL, Krahn AD,

Lemery R, Nicholson BJ, Gollob MH. Paradigm of genetic mosaicism and lone atrial fibrillation: physiological characterization of a connexin 43-deletion mutant identified from atrial tissue. *Circulation*. 2010;122:236–244.
104. Gollob MH, Jones DL, Krahn AD, Danis L, Gong X-Q, Shao Q, Liu X, Veinot JP, Tang ASL, Stewart AFR, Tesson F, Klein GJ, Yee R, Skanes AC, Guiraudon GM, Ebihara L, Bai D. Somatic mutations in the connexin 40 gene (GJA5) in atrial fibrillation. *N Engl J Med*. 2006;354:2677–2688.
105. Yang Y-Q, Liu X, Zhang X-L, Wang X-H, Tan H-W, Shi H-F, Jiang W-F, Fang W-Y. Novel connexin40 missense mutations in patients with familial atrial fibrillation. *Eur Eur Pacing Arrhythm Card Electrophysiol J Work Groups Card Pacing Arrhythm Card Cell Electrophysiol Eur Soc Cardiol*. 2010;12:1421–1427.
106. Yang Y-Q, Zhang X-L, Wang X-H, Tan H-W, Shi H-F, Jiang W-F, Fang W-Y, Liu X. Connexin40 nonsense mutation in familial atrial fibrillation. *Int J Mol Med*. 2010;26:605–610.
107. Sun Y, Yang Y-Q, Gong X-Q, Wang X-H, Li R-G, Tan H-W, Liu X, Fang W-Y, Bai D. Novel germline GJA5/connexin40 mutations associated with lone atrial fibrillation impair gap junctional intercellular communication. *Hum Mutat*. 2013;34:603–609.
108. Posch MG, Boldt L-H, Polotzki M, Richter S, Rolf S, Perrot A, Dietz R, Ozcelik C, Haverkamp W. Mutations in the cardiac transcription factor GATA4 in patients with lone atrial fibrillation. *Eur J Med Genet*. 2010;53:201–203.
109. Yang Y-Q, Wang M-Y, Zhang X-L, Tan H-W, Shi H-F, Jiang W-F, Wang X-H, Fang W-Y, Liu X. GATA4 loss-of-function mutations in familial atrial fibrillation. *Clin Chim Acta Int J Clin Chem*. 2011;412:1825–1830.
110. Jiang J-Q, Shen F-F, Fang W-Y, Liu X, Yang Y-Q. Novel GATA4 mutations in lone atrial fibrillation. *Int J Mol Med*. 2011;28:1025–1032.
111. Wang J, Sun Y-M, Yang Y-Q. Mutation spectrum of the GATA4 gene in patients with idiopathic atrial fibrillation. *Mol Biol Rep*. 2012;39:8127–8135.
112. Yang Y-Q, Wang X-H, Tan H-W, Jiang W-F, Fang W-Y, Liu X. Prevalence and spectrum of GATA6 mutations associated with familial atrial fibrillation. *Int J Cardiol*. 2012;155:494–496.
113. Yang Y-Q, Li L, Wang J, Zhang X-L, Li R-G, Xu Y-J, Tan H-W, Wang X-H, Jiang J-Q, Fang W-Y, Liu X. GATA6 loss-of-function mutation in atrial fibrillation. *Eur J Med Genet*. 2012;55:520–526.
114. Li J, Liu W-D, Yang Z-L, Yang Y-Q. Novel GATA6 loss-of-function mutation responsible for familial atrial fibrillation. *Int J Mol Med*. 2012;30:783–790.
115. Gudbjartsson DF, Arnar DO, Helgadottir A, Gretarsdottir S, Holm H, Sigurdsson A, Jonasdottir A, Baker A, Thorleifsson G, Kristjansson K, Palsson A, Blondal T, Sulem P, Backman VM, Hardarson GA, Palsdottir E, Helgason A, Sigurjonsdottir R, Sverrisson JT, Kostulas K, Ng MCY, Baum L, So WY, Wong KS, Chan JCN, Furie KL, Greenberg SM, Sale M, Kelly P, MacRae CA, Smith EE, Rosand J, Hillert J, Ma RCW, Ellinor PT, Thorgeirsson G, Gulcher JR, Kong A, Thorsteinsdottir U, Stefansson K. Variants conferring risk of atrial fibrillation on chromosome 4q25. *Nature*. 2007;448:353–357.
116. Viviani Anselmi C, Novelli V, Roncarati R, Malovini A, Bellazzi R, Bronzini R, Marchese G, Condorelli G, Montenero AS, Puca AA. Association of rs2200733 at 4q25 with atrial flutter/fibrillation diseases in an Italian population. *Heart Br Card Soc*. 2008;94:1394–1396.
117. Kääb S, Darbar D, van Noord C, Dupuis J, Pfeufer A, Newton-Cheh C, Schnabel R, Makino S, Sinner MF, Kannankeril PJ, Beckmann BM, Choudry S, Donahue BS, Heeringa J, Perz S, Lunetta KL, Larson MG, Levy D, MacRae CA, Ruskin JN,

Wacker A, Schömig A, Wichmann H-E, Steinbeck G, Meitinger T, Uitterlinden AG, Witteman JCM, Roden DM, Benjamin EJ, Ellinor PT. Large scale replication and meta-analysis of variants on chromosome 4q25 associated with atrial fibrillation. *Eur Heart J*. 2009;30:813–819.

118. Shi L, Li C, Wang C, Xia Y, Wu G, Wang F, Xu C, Wang P, Li X, Wang D, Xiong X, Bai Y, Liu M, Liu J, Ren X, Gao L, Wang B, Zeng Q, Yang B, Ma X, Yang Y, Tu X, Wang QK. Assessment of association of rs2200733 on chromosome 4q25 with atrial fibrillation and ischemic stroke in a Chinese Han population. *Hum Genet*. 2009;126:843–849.
119. Lubitz SA, Sinner MF, Lunetta KL, Makino S, Pfeufer A, Rahman R, Veltman CE, Barnard J, Bis JC, Danik SP, Sonni A, Shea MA, Del Monte F, Perz S, Müller M, Peters A, Greenberg SM, Furie KL, van Noord C, Boerwinkle E, Stricker BHC, Witteman J, Smith JD, Chung MK, Heckbert SR, Benjamin EJ, Rosand J, Arking DE, Alonso A, Kääb S, Ellinor PT. Independent susceptibility markers for atrial fibrillation on chromosome 4q25. *Circulation*. 2010;122:976–984.
120. Ellinor PT, Lunetta KL, Albert CM, Glazer NL, Ritchie MD, Smith AV, Arking DE, Müller-Nurasyid M, Krijthe BP, Lubitz SA, Bis JC, Chung MK, Dörr M, Ozaki K, Roberts JD, Smith JG, Pfeufer A, Sinner MF, Lohman K, Ding J, Smith NL, Smith JD, Rienstra M, Rice KM, Van Wagoner DR, Magnani JW, Wakili R, Clauss S, Rotter JI, Steinbeck G, Launer LJ, Davies RW, Borkovich M, Harris TB, Lin H, Völker U, Völzke H, Milan DJ, Hofman A, Boerwinkle E, Chen LY, Soliman EZ, Voight BF, Li G, Chakravarti A, Kubo M, Tedrow UB, Rose LM, Ridker PM, Conen D, Tsunoda T, Furukawa T, Sotoodehnia N, Xu S, Kamatani N, Levy D, Nakamura Y, Parvez B, Mahida S, Furie KL, Rosand J, Muhammad R, Psaty BM, Meitinger T, Perz S, Wichmann H-E, Witteman JCM, Kao WHL, Kathiresan S, Roden DM, Uitterlinden AG, Rivadeneira F, McKnight B, Sjögren M, Newman AB, Liu Y, Gollob MH, Melander O, Tanaka T, Stricker BHC, Felix SB, Alonso A, Darbar D, Barnard J, Chasman DI, Heckbert SR, Benjamin EJ, Gudnason V, Kääb S. Meta-analysis identifies six new susceptibility loci for atrial fibrillation. *Nat Genet*. 2012;44:670–675.
121. Piedra ME, Icardo JM, Albajar M, Rodriguez-Rey JC, Ros MA. Pitx2 participates in the late phase of the pathway controlling left-right asymmetry. *Cell*. 1998;94:319–324.
122. Logan M, Pagán-Westphal SM, Smith DM, Paganessi L, Tabin CJ. The transcription factor Pitx2 mediates situs-specific morphogenesis in response to left-right asymmetric signals. *Cell*. 1998;94:307–317.
123. Yoshioka H, Meno C, Koshiba K, Sugihara M, Itoh H, Ishimaru Y, Inoue T, Ohuchi H, Semina EV, Murray JC, Hamada H, Noji S. Pitx2, a bicoid-type homeobox gene, is involved in a lefty-signaling pathway in determination of left-right asymmetry. *Cell*. 1998;94:299–305.
124. Mommersteeg MTM, Hoogaars WMH, Prall OWJ, de Gier-de Vries C, Wiese C, Clout DEW, Papaioannou VE, Brown NA, Harvey RP, Moorman AFM, Christoffels VM. Molecular pathway for the localized formation of the sinoatrial node. *Circ Res*. 2007;100:354–362.
125. Mommersteeg MTM, Brown NA, Prall OWJ, de Gier-de Vries C, Harvey RP, Moorman AFM, Christoffels VM. Pitx2c and Nkx2-5 are required for the formation and identity of the pulmonary myocardium. *Circ Res*. 2007;101:902–909.
126. Gudbjartsson DF, Holm H, Gretarsdottir S, Thorleifsson G, Walters GB, Thorgeirsson G, Gulcher J, Mathiesen EB, Njølstad I, Nyrnes A, Wilsgaard T, Hald EM, Hveem K, Stoltenberg C, Kucera G, Stubblefield T, Carter S, Roden D, Ng MCY, Baum L, So WY, Wong KS, Chan JCN, Gieger C, Wichmann H-E, Gschwendtner A, Dichgans M,

Kuhlenbäumer G, Berger K, Ringelstein EB, Bevan S, Markus HS, Kostulas K, Hillert J, Sveinbjörnsdóttir S, Valdimarsson EM, Løchen M-L, Ma RCW, Darbar D, Kong A, Arnar DO, Thorsteinsdottir U, Stefansson K. A sequence variant in ZFHX3 on 16q22 associates with atrial fibrillation and ischemic stroke. *Nat Genet*. 2009;41:876–878.

127. Benjamin EJ, Rice KM, Arking DE, Pfeufer A, van Noord C, Smith AV, Schnabel RB, Bis JC, Boerwinkle E, Sinner MF, Dehghan A, Lubitz SA, D'Agostino RB Sr, Lumley T, Ehret GB, Heeringa J, Aspelund T, Newton-Cheh C, Larson MG, Marciante KD, Soliman EZ, Rivadeneira F, Wang TJ, Eiríksdottir G, Levy D, Psaty BM, Li M, Chamberlain AM, Hofman A, Vasan RS, Harris TB, Rotter JI, Kao WHL, Agarwal SK, Stricker BHC, Wang K, Launer LJ, Smith NL, Chakravarti A, Uitterlinden AG, Wolf PA, Sotoodehnia N, Köttgen A, van Duijn CM, Meitinger T, Mueller M, Perz S, Steinbeck G, Wichmann H-E, Lunetta KL, Heckbert SR, Gudnason V, Alonso A, Kääb S, Ellinor PT, Witteman JCM. Variants in ZFHX3 are associated with atrial fibrillation in individuals of European ancestry. *Nat Genet*. 2009;41:879–881.
128. Ellinor PT, Lunetta KL, Glazer NL, Pfeufer A, Alonso A, Chung MK, Sinner MF, de Bakker PIW, Mueller M, Lubitz SA, Fox E, Darbar D, Smith NL, Smith JD, Schnabel RB, Soliman EZ, Rice KM, Van Wagoner DR, Beckmann B-M, van Noord C, Wang K, Ehret GB, Rotter JI, Hazen SL, Steinbeck G, Smith AV, Launer LJ, Harris TB, Makino S, Nelis M, Milan DJ, Perz S, Esko T, Kottgen A, Moebus S, Newton-Cheh C, Li M, Mohlenkamp S, Wang TJ, Kao WHL, Vasan RS, Nothen MM, MacRae CA, Stricker BHC, Hofman A, Uitterlinden AG, Levy D, Boerwinkle E, Metspalu A, Topol EJ, Chakravarti A, Gudnason V, Psaty BM, Roden DM, Meitinger T, Wichmann H-E, Witteman JCM, Barnard J, Arking DE, Benjamin EJ, Heckbert SR, Kaab S. Common Variants in KCNN3 are Associated with Lone Atrial Fibrillation. *Nat Genet*. 2010;42:240–244.
129. Holm H, Gudbjartsson DF, Arnar DO, Thorleifsson G, Thorgeirsson G, Stefansdottir H, Gudjonsson SA, Jonasdottir A, Mathiesen EB, Njølstad I, Nyrnes A, Wilsgaard T, Hald EM, Hveem K, Stoltenberg C, Løchen M-L, Kong A, Thorsteinsdottir U, Stefansson K. Several common variants modulate heart rate, PR interval and QRS duration. *Nat Genet*. 2010;42:117–122.
130. Pfeufer A, van Noord C, Marciante KD, Arking DE, Larson MG, Smith AV, Tarasov KV, Müller M, Sotoodehnia N, Sinner MF, Verwoert GC, Li M, Kao WHL, Köttgen A, Coresh J, Bis JC, Psaty BM, Rice K, Rotter JI, Rivadeneira F, Hofman A, Kors JA, Stricker BHC, Uitterlinden AG, van Duijn CM, Beckmann BM, Sauter W, Gieger C, Lubitz SA, Newton-Cheh C, Wang TJ, Magnani JW, Schnabel RB, Chung MK, Barnard J, Smith JD, Van Wagoner DR, Vasan RS, Aspelund T, Eiriksdottir G, Harris TB, Launer LJ, Najjar SS, Lakatta E, Schlessinger D, Uda M, Abecasis GR, Müller-Myhsok B, Ehret GB, Boerwinkle E, Chakravarti A, Soliman EZ, Lunetta KL, Perz S, Wichmann H-E, Meitinger T, Levy D, Gudnason V, Ellinor PT, Sanna S, Kääb S, Witteman JCM, Alonso A, Benjamin EJ, Heckbert SR. Genome-wide association study of PR interval. *Nat Genet*. 2010;42:153–159.
131. Cheng S, Keyes MJ, Larson MG, McCabe EL, Newton-Cheh C, Levy D, Benjamin EJ, Vasan RS, Wang TJ. Long-term outcomes in individuals with prolonged PR interval or first-degree atrioventricular block. *JAMA J Am Med Assoc*. 2009;301:2571–2577.
132. Mahida S, Lubitz SA, Rienstra M, Milan DJ, Ellinor PT. Monogenic atrial fibrillation as pathophysiological paradigms. *Cardiovasc Res*. 2011;89:692–700.
133. Ren X, Xu C, Zhan C, Yang Y, Shi L, Wang F, Wang C, Xia Y, Yang B, Wu G, Wang P, Li X, Wang D, Xiong X, Liu J, Liu Y, Liu M, Liu J, Tu X, Wang QK. Identification

of NPPA variants associated with atrial fibrillation in a Chinese GeneID population. *Clin Chim Acta Int J Clin Chem*. 2010;411:481–485.
134. Nyberg MT, Stoevring B, Behr ER, Ravn LS, McKenna WJ, Christiansen M. The variation of the sarcolipin gene (SLN) in atrial fibrillation, long QT syndrome and sudden arrhythmic death syndrome. *Clin Chim Acta*. 2007;375:87–91.
135. Fatini C, Sticchi E, Genuardi M, Sofi F, Gensini F, Gori AM, Lenti M, Michelucci A, Abbate R, Gensini GF. Analysis of minK and eNOS genes as candidate loci for predisposition to non-valvular atrial fibrillation. *Eur Heart J*. 2006;27:1712–1718.
136. Bedi M, McNamara D, London B, Schwartzman D. Genetic susceptibility to atrial fibrillation in patients with congestive heart failure. *Heart Rhythm Off J Heart Rhythm Soc*. 2006;3:808–812.
137. Juang J-M, Chern Y-R, Tsai C-T, Chiang F-T, Lin J-L, Hwang J-J, Hsu K-L, Tseng C-D, Tseng Y-Z, Lai L-P. The association of human connexin 40 genetic polymorphisms with atrial fibrillation. *Int J Cardiol*. 2007;116:107–112.
138. Wirka RC, Gore S, Van Wagoner DR, Arking DE, Lubitz SA, Lunetta KL, Benjamin EJ, Alonso A, Ellinor PT, Barnard J, Chung MK, Smith JD. A common connexin-40 gene promoter variant affects connexin-40 expression in human atria and is associated with atrial fibrillation. *Circ Arrhythm Electrophysiol*. 2011;4:87–93.
139. Gensini F, Padeletti L, Fatini C, Sticchi E, Gensini GF, Michelucci A. Angiotensin-converting enzyme and endothelial nitric oxide synthase polymorphisms in patients with atrial fibrillation. *Pacing Clin Electrophysiol PACE*. 2003;26:295–298.
140. Tsai C-T, Lai L-P, Lin J-L, Chiang F-T, Hwang J-J, Ritchie MD, Moore JH, Hsu K-L, Tseng C-D, Liau C-S, Tseng Y-Z. Renin-angiotensin system gene polymorphisms and atrial fibrillation. *Circulation*. 2004;109:1640–1646.
141. Fatini C, Sticchi E, Gensini F, Gori AM, Marcucci R, Lenti M, Michelucci A, Genuardi M, Abbate R, Gensini GF. Lone and secondary nonvalvular atrial fibrillation: role of a genetic susceptibility. *Int J Cardiol*. 2007;120:59–65.
142. Tsai C-T, Hwang J-J, Chiang F-T, Wang Y-C, Tseng C-D, Tseng Y-Z, Lin J-L. Renin-angiotensin system gene polymorphisms and atrial fibrillation: a regression approach for the detection of gene-gene interactions in a large hospitalized population. *Cardiology*. 2008;111:1–7.
143. Ravn LS, Benn M, Nordestgaard BG, Sethi AA, Agerholm-Larsen B, Jensen GB, Tybjaerg-Hansen A. Angiotensinogen and ACE gene polymorphisms and risk of atrial fibrillation in the general population. *Pharmacogenet Genomics*. 2008;18:525–533.
144. Gaudino M, Andreotti F, Zamparelli R, Di Castelnuovo A, Nasso G, Burzotta F, Iacoviello L, Donati MB, Schiavello R, Maseri A, Possati G. The -174G/C interleukin-6 polymorphism influences postoperative interleukin-6 levels and postoperative atrial fibrillation. Is atrial fibrillation an inflammatory complication? *Circulation*. 2003;108 Suppl 1:II195–199.
145. Kato K, Oguri M, Hibino T, Yajima K, Matsuo H, Segawa T, Watanabe S, Yoshida H, Satoh K, Nozawa Y, Yokoi K, Yamada Y. Genetic factors for lone atrial fibrillation. *Int J Mol Med*. 2007;19:933–939.
146. Gai X, Lan X, Luo Z, Wang F, Liang Y, Zhang H, Zhang W, Hou J, Huang M. Association of MMP-9 gene polymorphisms with atrial fibrillation in hypertensive heart disease patients. *Clin Chim Acta Int J Clin Chem*. 2009;408:105–109.
147. Zeng Z, Tan C, Teng S, Chen J, Su S, Zhou X, Wang F, Zhang S, Gu D, Makielski JC, Pu J. The single nucleotide polymorphisms of I(Ks) potassium channel genes and their association with atrial fibrillation in a Chinese population. *Cardiology*. 2007;108:97–103.
148. Ma K, Li N, Teng S, Zhang Y, Sun Q, Gu D, Pu J. Modulation of KCNQ1 current by

atrial fibrillation-associated KCNE4 (145E/D) gene polymorphism. *Chin Med J (Engl)*. 2007;120:150–154.
149. Lai L-P, Su M-J, Yeh H-M, Lin J-L, Chiang F-T, Hwang J-J, Hsu K-L, Tseng C-D, Lien W-P, Tseng Y-Z, Huang SKS. Association of the human minK gene 38G allele with atrial fibrillation: evidence of possible genetic control on the pathogenesis of atrial fibrillation. *Am Heart J*. 2002;144:485–490.
150. Prystupa A, Dzida G, Myśliński W, Małaj G, Lorenc T. MinK gene polymorphism in the pathogenesis of lone atrial fibrillation. *Kardiol Pol*. 2006;64:1205–1211; discussion 1212–1213.
151. Ehrlich JR, Zicha S, Coutu P, Hébert TE, Nattel S. Atrial fibrillation-associated minK38G/S polymorphism modulates delayed rectifier current and membrane localization. *Cardiovasc Res*. 2005;67:520–528.
152. Li C, Wang F, Yang Y, Fu F, Xu C, Shi L, Li S, Xia Y, Wu G, Cheng X, Liu H, Wang C, Wang P, Hao J, Ke Y, Zhao Y, Liu M, Zhang R, Gao L, Yu B, Zeng Q, Liao Y, Yang B, Tu X, Wang QK. Significant association of SNP rs2106261 in the ZFHX3 gene with atrial fibrillation in a Chinese Han GeneID population. *Hum Genet*. 2011;129:239–246.
153. Sinner MF, Pfeufer A, Akyol M, Beckmann B-M, Hinterseer M, Wacker A, Perz S, Sauter W, Illig T, Näbauer M, Schmitt C, Wichmann H-E, Schömig A, Steinbeck G, Meitinger T, Kääb S. The non-synonymous coding IKr-channel variant KCNH2-K897T is associated with atrial fibrillation: results from a systematic candidate gene-based analysis of KCNH2 (HERG). *Eur Heart J*. 2008;29:907–914.
154. Wang Q-S, Wang X-F, Chen X-D, Yu J-F, Wang J, Sun J, Lu S-B, Shen M-Y, Lu M, Li Y-G, Jin L. Genetic Polymorphism of KCNH2 Confers Predisposition of Acquired Atrial Fibrillation in Chinese. *J Cardiovasc Electrophysiol*. 2009;20:1158–1162.
155. Chen LY, Ballew JD, Herron KJ, Rodeheffer RJ, Olson TM. A common polymorphism in SCN5A is associated with lone atrial fibrillation. *Clin Pharmacol Ther*. 2007;81:35–41.
156. Zhang C, Yuan G-H, Cheng Z-F, Xu M-W, Hou L-F, Wei F-P. The single nucleotide polymorphisms of Kir3.4 gene and their correlation with lone paroxysmal atrial fibrillation in Chinese Han population. *Heart Lung Circ*. 2009;18:257–261.
157. Ravn LS, Hofman-Bang J, Dixen U, Larsen SO, Jensen G, Haunsø S, Svendsen JH, Christiansen M. Relation of 97T polymorphism in KCNE5 to risk of atrial fibrillation. *Am J Cardiol*. 2005;96:405–407.
158. Vogler J, Breithardt G, Eckardt L. Bradyarrhythmias and Conduction Blocks. *Rev Esp Cardiol Engl Ed*. 2012;65:656–667.
159. Epstein AE, DiMarco JP, Ellenbogen KA, Estes NAM 3rd, Freedman RA, Gettes LS, Gillinov AM, Gregoratos G, Hammill SC, Hayes DL, Hlatky MA, Newby LK, Page RL, Schoenfeld MH, Silka MJ, Stevenson LW, Sweeney MO, Tracy CM, Epstein AE, Darbar D, DiMarco JP, Dunbar SB, Estes NAM 3rd, Ferguson TB Jr, Hammill SC, Karasik PE, Link MS, Marine JE, Schoenfeld MH, Shanker AJ, Silka MJ, Stevenson LW, Stevenson WG, Varosy PD, American College of Cardiology Foundation, American Heart Association Task Force on Practice Guidelines, Heart Rhythm Society. 2012 ACCF/AHA/HRS focused update incorporated into the ACCF/AHA/HRS 2008 guidelines for device-based therapy of cardiac rhythm abnormalities: a report of the American College of Cardiology Foundation/American Heart Association Task Force on Practice Guidelines and the Heart Rhythm Society. *J Am Coll Cardiol*. 2013;61:e6–75.
160. Adán V, Crown LA. Diagnosis and treatment of sick sinus syndrome. *Am Fam Physician*. 2003;67:1725–1732.

161. Radford DJ, Izukawa T. Sick sinus syndrome. Symptomatic cases in children. *Arch Dis Child*. 1975;50:879–885.
162. Kugler JD, Gillette PC, Mullins CE, McNamara DG. Sinoatrial conduction in children: an index of sinoatrial node function. *Circulation*. 1979;59:1266–1276.
163. Monfredi O, Dobrzynski H, Mondal T, Boyett MR, Morris GM. The anatomy and physiology of the sinoatrial node--a contemporary review. *Pacing Clin Electrophysiol PACE*. 2010;33:1392–1406.
164. Bravo-Valenzuela NJM. Fetal bradycardia and sinus node dysfunction. *Pediatr Cardiol*. 2013;34:1250–1253.
165. Ector H, Van der Hauwaert LG. Sick sinus syndrome in childhood. *Br Heart J*. 1980;44:684–691.
166. Spellberg RD. Familial sinus node disease. *Chest*. 1971;60:246–251.
167. Ward DE, Ho SY, Shinebourne EA. Familial atrial standstill and inexcitability in childhood. *Am J Cardiol*. 1984;53:965–967.
168. Bharati S, Surawicz B, Vidaillet HJ Jr, Lev M. Familial congenital sinus rhythm anomalies: clinical and pathological correlations. *Pacing Clin Electrophysiol PACE*. 1992;15:1720–1729.
169. Keith A, Flack M. The Form and Nature of the Muscular Connections between the Primary Divisions of the Vertebrate Heart. *J Anat Physiol*. 1907;41:172–189.
170. Truex RC, Smythe MQ, Taylor MJ. Reconstruction of the human sinoatrial node. *Anat Rec*. 1967;159:371–378.
171. JAMES TN. Anatomy of the human sinus node. *Anat Rec*. 1961;141:109–139.
172. Sánchez-Quintana D, Cabrera JA, Farré J, Climent V, Anderson RH, Ho SY. Sinus node revisited in the era of electroanatomical mapping and catheter ablation. *Heart*. 2005;91:189–194.
173. Chandler NJ, Greener ID, Tellez JO, Inada S, Musa H, Molenaar P, Difrancesco D, Baruscotti M, Longhi R, Anderson RH, Billeter R, Sharma V, Sigg DC, Boyett MR, Dobrzynski H. Molecular architecture of the human sinus node: insights into the function of the cardiac pacemaker. *Circulation*. 2009;119:1562–1575.
174. Lakatta EG, Vinogradova T, Lyashkov A, Sirenko S, Zhu W, Ruknudin A, Maltsev VA. The integration of spontaneous intracellular Ca2+ cycling and surface membrane ion channel activation entrains normal automaticity in cells of the heart's pacemaker. *Ann N Y Acad Sci*. 2006;1080:178–206.
175. Maltsev VA, Lakatta EG. Dynamic interactions of an intracellular Ca2+ clock and membrane ion channel clock underlie robust initiation and regulation of cardiac pacemaker function. *Cardiovasc Res*. 2008;77:274–284.
176. Maltsev VA, Lakatta EG. Synergism of coupled subsarcolemmal Ca2+ clocks and sarcolemmal voltage clocks confers robust and flexible pacemaker function in a novel pacemaker cell model. *Am J Physiol Heart Circ Physiol*. 2009;296:H594–615.
177. Boyett MR, Honjo H, Kodama I. The sinoatrial node, a heterogeneous pacemaker structure. *Cardiovasc Res*. 2000;47:658–687.
178. Dobrzynski H, Boyett MR, Anderson RH. New insights into pacemaker activity: promoting understanding of sick sinus syndrome. *Circulation*. 2007;115:1921–1932.
179. Irisawa H, Brown HF, Giles W. Cardiac pacemaking in the sinoatrial node. *Physiol Rev*. 1993;73:197–227.
180. Biel M, Wahl-Schott C, Michalakis S, Zong X. Hyperpolarization-activated cation channels: from genes to function. *Physiol Rev*. 2009;89:847–885.
181. Verkerk AO, Wilders R, van Borren MMGJ, Tan HL. Is sodium current present in human sinoatrial node cells? *Int J Biol Sci*. 2009;5:201–204.
182. Mangoni ME, Nargeot J. Genesis and Regulation of the Heart Automaticity. *Physiol*

Rev. 2008;88:919–982.
183. Postma AV, Denjoy I, Kamblock J, Alders M, Lupoglazoff J-M, Vaksmann G, Dubosq-Bidot L, Sebillon P, Mannens MMAM, Guicheney P, Wilde AAM. Catecholaminergic polymorphic ventricular tachycardia: RYR2 mutations, bradycardia, and follow up of the patients. *J Med Genet*. 2005;42:863–870.
184. Bhuiyan ZA, van den Berg MP, van Tintelen JP, Bink-Boelkens MTE, Wiesfeld ACP, Alders M, Postma AV, van Langen I, Mannens MMAM, Wilde AAM. Expanding spectrum of human RYR2-related disease: new electrocardiographic, structural, and genetic features. *Circulation*. 2007;116:1569–1576.
185. Postma AV, Denjoy I, Hoorntje TM, Lupoglazoff J-M, Da Costa A, Sebillon P, Mannens MMAM, Wilde AAM, Guicheney P. Absence of calsequestrin 2 causes severe forms of catecholaminergic polymorphic ventricular tachycardia. *Circ Res*. 2002;91:e21–26.
186. Le Scouarnec S, Bhasin N, Vieyres C, Hund TJ, Cunha SR, Koval O, Marionneau C, Chen B, Wu Y, Demolombe S, Song L-S, Le Marec H, Probst V, Schott J-J, Anderson ME, Mohler PJ. Dysfunction in ankyrin-B-dependent ion channel and transporter targeting causes human sinus node disease. *Proc Natl Acad Sci U S A*. 2008;105:15617–15622.
187. Benson DW, Wang DW, Dyment M, Knilans TK, Fish FA, Strieper MJ, Rhodes TH, George, A. L. J. Congenital sick sinus syndrome caused by recessive mutations in the cardiac sodium channel gene (SCN5A). *J Clin Invest*. 2003;112:1019–28.
188. Kyndt F, Probst V, Potet F, Demolombe S, Chevallier J-C, Baro I, Moisan J-P, Boisseau P, Schott J-J, Escande D, Marec HL. Novel SCN5A Mutation Leading Either to Isolated Cardiac Conduction Defect or Brugada Syndrome in a Large French Family. *Circulation*. 2001;104:3081–3086.
189. Splawski I, Shen J, Timothy KW, Lehmann MH, Priori S, Robinson JL, Moss AJ, Schwartz PJ, Towbin JA, Vincent GM, Keating MT. Spectrum of mutations in long-QT syndrome genes. KVLQT1, HERG, SCN5A, KCNE1, and KCNE2. *Circulation*. 2000;102:1178–1185.
190. Smits JP, Koopmann TT, Wilders R, Veldkamp MW, Opthof T, Bhuiyan ZA, Mannens MM, Balser JR, Tan HL, Bezzina CR, Wilde AA. A mutation in the human cardiac sodium channel (E161K) contributes to sick sinus syndrome, conduction disease and Brugada syndrome in two families. *J Mol Cell Cardiol*. 2005;38:969–81.
191. Makiyama T, Akao M, Tsuji K, Doi T, Ohno S, Takenaka K, Kobori A, Ninomiya T, Yoshida H, Takano M, Makita N, Yanagisawa F, Higashi Y, Takeyama Y, Kita T, Horie M. High risk for bradyarrhythmic complications in patients with Brugada syndrome caused by SCN5A gene mutations. *J Am Coll Cardiol*. 2005;46:2100–2106.
192. Takehara N, Makita N, Kawabe J, Sato N, Kawamura Y, Kitabatake A, Kikuchi K. A cardiac sodium channel mutation identified in Brugada syndrome associated with atrial standstill. *J Intern Med*. 2004;255:137–142.
193. Vatta M, Dumaine R, Varghese G, Richard TA, Shimizu W, Aihara N, Nademanee K, Brugada R, Brugada J, Veerakul G, Li H, Bowles NE, Brugada P, Antzelevitch C, Towbin JA. Genetic and biophysical basis of sudden unexplained nocturnal death syndrome (SUNDS), a disease allelic to Brugada syndrome. *Hum Mol Genet*. 2002;11:337–345.
194. Tan HL, Bink-Boelkens MT, Bezzina CR, Viswanathan PC, Beaufort-Krol GC, van Tintelen PJ, van den Berg MP, Wilde AA, Balser JR. A sodium-channel mutation causes isolated cardiac conduction disease. *Nature*. 2001;409:1043–7.
195. Zhang Y, Wang T, Ma A, Zhou X, Gui J, Wan H, Shi R, Huang C, Grace AA, Huang CL-H, Trump D, Zhang H, Zimmer T, Lei M. Correlations between clinical and

physiological consequences of the novel mutation R878C in a highly conserved pore residue in the cardiac Na+ channel. *Acta Physiol Oxf Engl*. 2008;194:311–323.
196. Groenewegen WA, Firouzi M, Bezzina CR, Vliex S, van Langen IM, Sandkuijl L, Smits JPP, Hulsbeek M, Rook MB, Jongsma HJ, Wilde AAM. A cardiac sodium channel mutation cosegregates with a rare connexin40 genotype in familial atrial standstill. *Circ Res*. 2003;92:14–22.
197. Niu D-M, Hwang B, Hwang H-W, Wang NH, Wu J-Y, Lee P-C, Chien J-C, Shieh R-C, Chen Y-T. A common SCN5A polymorphism attenuates a severe cardiac phenotype caused by a nonsense SCN5A mutation in a Chinese family with an inherited cardiac conduction defect. *J Med Genet*. 2006;43:817–821.
198. Butters TD, Aslanidi OV, Inada S, Boyett MR, Hancox JC, Lei M, Zhang H. Mechanistic links between Na+ channel (SCN5A) mutations and impaired cardiac pacemaking in sick sinus syndrome. *Circ Res*. 2010;107:126–137.
199. Selly J-B, Boumahni B, Edmar A, Jamal Bey K, Randrianaivo H, Clerici G, Millat G, Caillet D. [Cardiac sinus node dysfunction due to a new mutation of the SCN5A gene]. *Arch Pédiatrie Organe Off Sociéte Fr Pédiatrie*. 2012;19:837–841.
200. Kodama T, Serio A, Disertori M, Bronzetti G, Diegoli M, Narula N, Grasso M, Mazzola S, Arbustini E. Autosomal recessive paediatric sick sinus syndrome associated with novel compound mutations in SCN5A. *Int J Cardiol*. 2013;167:3078–3080.
201. Nakajima S, Makiyama T, Hanazawa K, Kaitani K, Amano M, Hayama Y, Onishi N, Tamaki Y, Miyake M, Tamura T, Kondo H, Motooka M, Izumi C, Nakagawa Y, Horie M. A Novel SCN5A Mutation Demonstrating a Variety of Clinical Phenotypes in Familial Sick Sinus Syndrome. *Intern Med Tokyo Jpn*. 2013;52:1805–1808.
202. Papadatos GA, Wallerstein PMR, Head CEG, Ratcliff R, Brady PA, Benndorf K, Saumarez RC, Trezise AEO, Huang CL-H, Vandenberg JI, Colledge WH, Grace AA. Slowed conduction and ventricular tachycardia after targeted disruption of the cardiac sodium channel gene Scn5a. *Proc Natl Acad Sci U S A*. 2002;99:6210–6215.
203. Lei M, Goddard C, Liu J, Léoni A-L, Royer A, Fung SS-M, Xiao G, Ma A, Zhang H, Charpentier F, Vandenberg JI, Colledge WH, Grace AA, Huang CL-H. Sinus node dysfunction following targeted disruption of the murine cardiac sodium channel gene Scn5a. *J Physiol*. 2005;567:387–400.
204. Grant AO, Carboni MP, Neplioueva V, Starmer CF, Memmi M, Napolitano C, Priori S. Long QT syndrome, Brugada syndrome, and conduction system disease are linked to a single sodium channel mutation. *J Clin Invest*. 2002;110:1201–1209.
205. Bennett PB, Yazawa K, Makita N, George AL Jr. Molecular mechanism for an inherited cardiac arrhythmia. *Nature*. 1995;376:683–685.
206. Wang Q, Shen J, Splawski I, Atkinson D, Li Z, Robinson JL, Moss AJ, Towbin JA, Keating MT. SCN5A mutations associated with an inherited cardiac arrhythmia, long QT syndrome. *Cell*. 1995;80:805–811.
207. Chang C-C, Acharfi S, Wu M-H, Chiang F-T, Wang J-K, Sung T-C, Chahine M. A novel SCN5A mutation manifests as a malignant form of long QT syndrome with perinatal onset of tachycardia/bradycardia. *Cardiovasc Res*. 2004;64:268–278.
208. Wei J, Wang DW, Alings M, Fish F, Wathen M, Roden DM, George AL Jr. Congenital long-QT syndrome caused by a novel mutation in a conserved acidic domain of the cardiac Na+ channel. *Circulation*. 1999;99:3165–3171.
209. Makita N, Behr E, Shimizu W, Horie M, Sunami A, Crotti L, Schulze-Bahr E, Fukuhara S, Mochizuki N, Makiyama T, Itoh H, Christiansen M, McKeown P, Miyamoto K, Kamakura S, Tsutsui H, Schwartz PJ, George AL Jr, Roden DM. The E1784K mutation in SCN5A is associated with mixed clinical phenotype of type 3

long QT syndrome. *J Clin Invest*. 2008;118:2219–2229.
210. Bezzina C, Veldkamp MW, van Den Berg MP, Postma AV, Rook MB, Viersma JW, van Langen IM, Tan-Sindhunata G, Bink-Boelkens MT, van Der Hout AH, Mannens MM, Wilde AA. A single Na(+) channel mutation causing both long-QT and Brugada syndromes. *Circ Res*. 1999;85:1206–13.
211. Veldkamp MW, Wilders R, Baartscheer A, Zegers JG, Bezzina CR, Wilde AAM. Contribution of sodium channel mutations to bradycardia and sinus node dysfunction in LQT3 families. *Circ Res*. 2003;92:976–983.
212. Abriel H, Wehrens XH, Benhorin J, Kerem B, Kass RS. Molecular pharmacology of the sodium channel mutation D1790G linked to the long-QT syndrome. *Circulation*. 2000;102:921–925.
213. Benhorin J, Taub R, Goldmit M, Kerem B, Kass RS, Windman I, Medina A. Effects of flecainide in patients with new SCN5A mutation: mutation-specific therapy for long-QT syndrome? *Circulation*. 2000;101:1698–1706.
214. Holst AG, Liang B, Jespersen T, Bundgaard H, Haunso S, Svendsen JH, Tfelt-Hansen J. Sick sinus syndrome, progressive cardiac conduction disease, atrial flutter and ventricular tachycardia caused by a novel SCN5A mutation. *Cardiology*. 2010;115:311–316.
215. Makita N, Sasaki K, Groenewegen WA, Yokota T, Yokoshiki H, Murakami T, Tsutsui H. Congenital atrial standstill associated with coinheritance of a novel SCN5A mutation and connexin 40 polymorphisms. *Heart Rhythm Off J Heart Rhythm Soc*. 2005;2:1128–1134.
216. Tan B-H, Iturralde-Torres P, Medeiros-Domingo A, Nava S, Tester DJ, Valdivia CR, Tusié-Luna T, Ackerman MJ, Makielski JC. A novel C-terminal truncation SCN5A mutation from a patient with sick sinus syndrome, conduction disorder and ventricular tachycardia. *Cardiovasc Res*. 2007;76:409–417.
217. Lopez KN, Decker JA, Friedman RA, Kim JJ. Homozygous mutation in SCN5A associated with atrial quiescence, recalcitrant arrhythmias, and poor capture thresholds. *Heart Rhythm Off J Heart Rhythm Soc*. 2011;8:471–473.
218. Rook MB, Bezzina Alshinawi C, Groenewegen WA, van Gelder IC, van Ginneken AC, Jongsma HJ, Mannens MM, Wilde AA. Human SCN5A gene mutations alter cardiac sodium channel kinetics and are associated with the Brugada syndrome. *Cardiovasc Res*. 1999;44:507–517.
219. Lei M, Huang CL-H, Zhang Y. Genetic Na+ channelopathies and sinus node dysfunction. *Prog Biophys Mol Biol*. 2008;98:171–178.
220. Schulze-Bahr E, Neu A, Friederich P, Kaupp UB, Breithardt G, Pongs O, Isbrandt D. Pacemaker channel dysfunction in a patient with sinus node disease. *J Clin Invest*. 2003;111:1537–1545.
221. Milanesi R, Baruscotti M, Gnecchi-Ruscone T, DiFrancesco D. Familial sinus bradycardia associated with a mutation in the cardiac pacemaker channel. *N Engl J Med*. 2006;354:151–157.
222. Nof E, Luria D, Brass D, Marek D, Lahat H, Reznik-Wolf H, Pras E, Dascal N, Eldar M, Glikson M. Point mutation in the HCN4 cardiac ion channel pore affecting synthesis, trafficking, and functional expression is associated with familial asymptomatic sinus bradycardia. *Circulation*. 2007;116:463–470.
223. Laish-Farkash A, Glikson M, Brass D, Marek-Yagel D, Pras E, Dascal N, Antzelevitch C, Nof E, Reznik H, Eldar M, Luria D. A novel mutation in the HCN4 gene causes symptomatic sinus bradycardia in Moroccan Jews. *J Cardiovasc Electrophysiol*. 2010;21:1365–1372.
224. Duhme N, Schweizer PA, Thomas D, Becker R, Schröter J, Barends TRM, Schlichting

I, Draguhn A, Bruehl C, Katus HA, Koenen M. Altered HCN4 channel C-linker interaction is associated with familial tachycardia-bradycardia syndrome and atrial fibrillation. *Eur Heart J*. 2013;34:2768–2775.
225. Ueda K, Nakamura K, Hayashi T, Inagaki N, Takahashi M, Arimura T, Morita H, Higashiuesato Y, Hirano Y, Yasunami M, Takishita S, Yamashina A, Ohe T, Sunamori M, Hiraoka M, Kimura A. Functional characterization of a trafficking-defective HCN4 mutation, D553N, associated with cardiac arrhythmia. *J Biol Chem*. 2004;279:27194–27198.
226. Sauer AJ, Newton-Cheh C. Clinical and genetic determinants of torsade de pointes risk. *Circulation*. 2012;125:1684–1694.
227. Beckmann B-M, Pfeufer A, Kääb S. Inherited cardiac arrhythmias: diagnosis, treatment, and prevention. *Dtsch Ärztebl Int*. 2011;108:623–633; quiz 634.
228. Giudicessi JR, Ackerman MJ. Determinants of incomplete penetrance and variable expressivity in heritable cardiac arrhythmia syndromes. *Transl Res*. 2013;161:1–14.
229. Giudicessi JR, Ackerman MJ. Genotype- and Phenotype-Guided Management of Congenital Long QT Syndrome. *Curr Probl Cardiol*. 2013;38:417–455.
230. Splawski I, Timothy KW, Vincent GM, Atkinson DL, Keating MT. Molecular basis of the long-QT syndrome associated with deafness. *N Engl J Med*. 1997;336:1562–1567.
231. Neyroud N, Tesson F, Denjoy I, Leibovici M, Donger C, Barhanin J, Fauré S, Gary F, Coumel P, Petit C, Schwartz K, Guicheney P. A novel mutation in the potassium channel gene KVLQT1 causes the Jervell and Lange-Nielsen cardioauditory syndrome. *Nat Genet*. 1997;15:186–189.
232. Schulze-Bahr E, Wang Q, Wedekind H, Haverkamp W, Chen Q, Sun Y, Rubie C, Hördt M, Towbin JA, Borggrefe M, Assmann G, Qu X, Somberg JC, Breithardt G, Oberti C, Funke H. KCNE1 mutations cause jervell and Lange-Nielsen syndrome. *Nat Genet*. 1997;17:267–268.
233. Duggal P, Vesely MR, Wattanasirichaigoon D, Villafane J, Kaushik V, Beggs AH. Mutation of the gene for IsK associated with both Jervell and Lange-Nielsen and Romano-Ward forms of Long-QT syndrome. *Circulation*. 1998;97:142–146.
234. Splawski I, Timothy KW, Priori SG, Napolitano C, Bloise R. Timothy Syndrome [Internet]. In: Pagon RA, Adam MP, Bird TD, Dolan CR, Fong C-T, Stephens K, editors. GeneReviews™. Seattle (WA): University of Washington, Seattle; 1993 [cited 2013 Nov 21]. Available from: http://www.ncbi.nlm.nih.gov/books/NBK1403/
235. Splawski I, Timothy KW, Sharpe LM, Decher N, Kumar P, Bloise R, Napolitano C, Schwartz PJ, Joseph RM, Condouris K, Tager-Flusberg H, Priori SG, Sanguinetti MC, Keating MT. Ca(V)1.2 calcium channel dysfunction causes a multisystem disorder including arrhythmia and autism. *Cell*. 2004;119:19–31.
236. Tristani-Firouzi M, Jensen JL, Donaldson MR, Sansone V, Meola G, Hahn A, Bendahhou S, Kwiecinski H, Fidzianska A, Plaster N, Fu Y-H, Ptacek LJ, Tawil R. Functional and clinical characterization of KCNJ2 mutations associated with LQT7 (Andersen syndrome). *J Clin Invest*. 2002;110:381–388.
237. Mohler PJ, Schott J-J, Gramolini AO, Dilly KW, Guatimosim S, duBell WH, Song L-S, Haurogné K, Kyndt F, Ali ME, Rogers TB, Lederer WJ, Escande D, Marec HL, Bennett V. Ankyrin-B mutation causes type 4 long-QT cardiac arrhythmia and sudden cardiac death. *Nature*. 2003;421:634–639.
238. Crotti L, Johnson CN, Graf E, De Ferrari GM, Cuneo BF, Ovadia M, Papagiannis J, Feldkamp MD, Rathi SG, Kunic JD, Pedrazzini M, Wieland T, Lichtner P, Beckmann B-M, Clark T, Shaffer C, Benson DW, Kääb S, Meitinger T, Strom TM, Chazin WJ, Schwartz PJ, George AL Jr. Calmodulin mutations associated with recurrent cardiac arrest in infants. *Circulation*. 2013;127:1009–1017.

239. Leenhardt A, Denjoy I, Guicheney P. Catecholaminergic polymorphic ventricular tachycardia. *Circ Arrhythm Electrophysiol*. 2012;5:1044–1052.
240. Van der Werf C, Wilde AAM. Catecholaminergic polymorphic ventricular tachycardia: from bench to bedside. *Heart Br Card Soc*. 2013;99:497–504.
241. Priori SG, Napolitano C, Tiso N, Memmi M, Vignati G, Bloise R, Sorrentino V, Danieli GA. Mutations in the cardiac ryanodine receptor gene (hRyR2) underlie catecholaminergic polymorphic ventricular tachycardia. *Circulation*. 2001;103:196–200.
242. Lahat H, Eldar M, Levy-Nissenbaum E, Bahan T, Friedman E, Khoury A, Lorber A, Kastner DL, Goldman B, Pras E. Autosomal recessive catecholamine- or exercise-induced polymorphic ventricular tachycardia: clinical features and assignment of the disease gene to chromosome 1p13-21. *Circulation*. 2001;103:2822–2827.
243. Lahat H, Pras E, Olender T, Avidan N, Ben-Asher E, Man O, Levy-Nissenbaum E, Khoury A, Lorber A, Goldman B, Lancet D, Eldar M. A missense mutation in a highly conserved region of CASQ2 is associated with autosomal recessive catecholamine-induced polymorphic ventricular tachycardia in Bedouin families from Israel. *Am J Hum Genet*. 2001;69:1378–1384.
244. Roux-Buisson N, Cacheux M, Fourest-Lieuvin A, Fauconnier J, Brocard J, Denjoy I, Durand P, Guicheney P, Kyndt F, Leenhardt A, Le Marec H, Lucet V, Mabo P, Probst V, Monnier N, Ray PF, Santoni E, Trémeaux P, Lacampagne A, Fauré J, Lunardi J, Marty I. Absence of triadin, a protein of the calcium release complex, is responsible for cardiac arrhythmia with sudden death in human. *Hum Mol Genet*. 2012;21:2759–2767.
245. Gussak I, Brugada P, Brugada J, Wright RS, Kopecky SL, Chaitman BR, Bjerregaard P. Idiopathic short QT interval: a new clinical syndrome? *Cardiology*. 2000;94:99–102.
246. Viskin S, Zeltser D, Ish-Shalom M, Katz A, Glikson M, Justo D, Tekes-Manova D, Belhassen B. Is idiopathic ventricular fibrillation a short QT syndrome? Comparison of QT intervals of patients with idiopathic ventricular fibrillation and healthy controls. *Heart Rhythm Off J Heart Rhythm Soc*. 2004;1:587–591.
247. Schimpf R, Wolpert C, Gaita F, Giustetto C, Borggrefe M. Short QT syndrome. *Cardiovasc Res*. 2005;67:357–366.
248. Li A, Behr ER. Brugada syndrome: an update. *Future Cardiol*. 2013;9:253–271.
249. Brugada P, Brugada J. Right bundle branch block, persistent ST segment elevation and sudden cardiac death: a distinct clinical and electrocardiographic syndrome. A multicenter report. *J Am Coll Cardiol*. 1992;20:1391–1396.
250. Antzelevitch C, Brugada P, Borggrefe M, Brugada J, Brugada R, Corrado D, Gussak I, LeMarec H, Nademanee K, Riera ARP, Shimizu W, Schulze-Bahr E, Tan H, Wilde A. Brugada Syndrome: Report of the Second Consensus Conference Endorsed by the Heart Rhythm Society and the European Heart Rhythm Association. *Circulation*. 2005;111:659–670.
251. Mizusawa Y, Wilde AAM. Brugada Syndrome. *Circ Arrhythm Electrophysiol*. 2012;5:606–616.
252. Giustetto C, Drago S, Demarchi PG, Dalmasso P, Bianchi F, Masi AS, Carvalho P, Occhetta E, Rossetti G, Riccardi R, Bertona R, Gaita F, Italian Association of Arrhythmology and Cardiostimulation (AIAC)-Piedmont Section. Risk stratification of the patients with Brugada type electrocardiogram: a community-based prospective study. *Eur Eur Pacing Arrhythm Card Electrophysiol J Work Groups Card Pacing Arrhythm Card Cell Electrophysiol Eur Soc Cardiol*. 2009;11:507–513.
253. Probst V, Veltmann C, Eckardt L, Meregalli PG, Gaita F, Tan HL, Babuty D, Sacher

F, Giustetto C, Schulze-Bahr E, Borggrefe M, Haissaguerre M, Mabo P, Le Marec H, Wolpert C, Wilde AAM. Long-term prognosis of patients diagnosed with Brugada syndrome: Results from the FINGER Brugada Syndrome Registry. *Circulation*. 2010;121:635–643.

254. Brugada J, Brugada R, Brugada P. Determinants of sudden cardiac death in individuals with the electrocardiographic pattern of Brugada syndrome and no previous cardiac arrest. *Circulation*. 2003;108:3092–3096.
255. Eckardt L, Probst V, Smits JPP, Bahr ES, Wolpert C, Schimpf R, Wichter T, Boisseau P, Heinecke A, Breithardt G, Borggrefe M, LeMarec H, Böcker D, Wilde AAM. Long-term prognosis of individuals with right precordial ST-segment-elevation Brugada syndrome. *Circulation*. 2005;111:257–263.
256. Probst V, Denjoy I, Meregalli PG, Amirault J-C, Sacher F, Mansourati J, Babuty D, Villain E, Victor J, Schott J-J, Lupoglazoff J-M, Mabo P, Veltmann C, Jesel L, Chevalier P, Clur S-AB, Haissaguerre M, Wolpert C, Marec HL, Wilde AAM. Clinical Aspects and Prognosis of Brugada Syndrome in Children. *Circulation*. 2007;115:2042–2048.
257. Nademanee K, Veerakul G, Nimmannit S, Chaowakul V, Bhuripanyo K, Likittanasombat K, Tunsanga K, Kuasirikul S, Malasit P, Tansupasawadikul S, Tatsanavivat P. Arrhythmogenic marker for the sudden unexplained death syndrome in Thai men. *Circulation*. 1997;96:2595–2600.
258. Gilbert J, Gold RL, Haffajee CI, Alpert JS. Sudden cardiac death in a southeast Asian immigrant: clinical, electrophysiologic, and biopsy characteristics. *Pacing Clin Electrophysiol PACE*. 1986;9:912–914.
259. Skinner JR, Chung S-K, Montgomery D, McCulley CH, Crawford J, French J, Rees MI. Near-miss SIDS due to Brugada syndrome. *Arch Dis Child*. 2005;90:528–529.
260. Valdivia CR, Ueda K, Ackerman MJ, Makielski JC. GPD1L links redox state to cardiac excitability by PKC-dependent phosphorylation of the sodium channel SCN5A. *Am J Physiol Heart Circ Physiol*. 2009;297:H1446–1452.
261. Smits JPP, Eckardt L, Probst V, Bezzina CR, Schott JJ, Remme CA, Haverkamp W, Breithardt G, Escande D, Schulze-Bahr E, LeMarec H, Wilde AAM. Genotype-phenotype relationship in Brugada syndrome: electrocardiographic features differentiate SCN5A-related patients from non-SCN5A-related patients. *J Am Coll Cardiol*. 2002;40:350–356.
262. Probst V, Allouis M, Sacher F, Pattier S, Babuty D, Mabo P, Mansourati J, Victor J, Nguyen J-M, Schott J-J, Boisseau P, Escande D, Le Marec H. Progressive cardiac conduction defect is the prevailing phenotype in carriers of a Brugada syndrome SCN5A mutation. *J Cardiovasc Electrophysiol*. 2006;17:270–275.
263. Probst V, Wilde AAM, Barc J, Sacher F, Babuty D, Mabo P, Mansourati J, Le Scouarnec S, Kyndt F, Le Caignec C, Guicheney P, Gouas L, Albuisson J, Meregalli PG, Le Marec H, Tan HL, Schott J-J. SCN5A mutations and the role of genetic background in the pathophysiology of Brugada syndrome. *Circ Cardiovasc Genet*. 2009;2:552–557.
264. Maury P, Rollin A, Sacher F, Gourraud J-B, Raczka F, Pasquié J-L, Duparc A, Mondoly P, Cardin C, Delay M, Derval N, Chatel S, Bongard V, Sadron M, Denis A, Davy J-M, Hocini M, Jaïs P, Jesel L, Haïssaguerre M, Probst V. Prevalence and prognostic role of various conduction disturbances in patients with the brugada syndrome. *Am J Cardiol*. 2013;112:1384–1389.
265. Yan GX, Antzelevitch C. Cellular basis for the Brugada syndrome and other mechanisms of arrhythmogenesis associated with ST-segment elevation. *Circulation*. 1999;100:1660–1666.

266. Fedida D, Giles WR. Regional variations in action potentials and transient outward current in myocytes isolated from rabbit left ventricle. *J Physiol*. 1991;442:191–209.
267. Clark RB, Bouchard RA, Salinas-Stefanon E, Sanchez-Chapula J, Giles WR. Heterogeneity of action potential waveforms and potassium currents in rat ventricle. *Cardiovasc Res*. 1993;27:1795–1799.
268. Liu DW, Gintant GA, Antzelevitch C. Ionic bases for electrophysiological distinctions among epicardial, midmyocardial, and endocardial myocytes from the free wall of the canine left ventricle. *Circ Res*. 1993;72:671–687.
269. Wettwer E, Amos GJ, Posival H, Ravens U. Transient outward current in human ventricular myocytes of subepicardial and subendocardial origin. *Circ Res*. 1994;75:473–482.
270. Di Diego JM, Sun ZQ, Antzelevitch C. I(to) and action potential notch are smaller in left vs. right canine ventricular epicardium. *Am J Physiol*. 1996;271:H548–561.
271. Antzelevitch C. Brugada syndrome. *Pacing Clin Electrophysiol PACE*. 2006;29:1130–1159.
272. Meregalli PG, Wilde AAM, Tan HL. Pathophysiological mechanisms of Brugada syndrome: depolarization disorder, repolarization disorder, or more? *Cardiovasc Res*. 2005;67:367–378.
273. Kurita T, Shimizu W, Inagaki M, Suyama K, Taguchi A, Satomi K, Aihara N, Kamakura S, Kobayashi J, Kosakai Y. The electrophysiologic mechanism of ST-segment elevation in Brugada syndrome. *J Am Coll Cardiol*. 2002;40:330–334.
274. Di Diego JM, Cordeiro JM, Goodrow RJ, Fish JM, Zygmunt AC, Pérez GJ, Scornik FS, Antzelevitch C. Ionic and cellular basis for the predominance of the Brugada syndrome phenotype in males. *Circulation*. 2002;106:2004–2011.
275. Shimizu W, Matsuo K, Kokubo Y, Satomi K, Kurita T, Noda T, Nagaya N, Suyama K, Aihara N, Kamakura S, Inamoto N, Akahoshi M, Tomoike H. Sex hormone and gender difference--role of testosterone on male predominance in Brugada syndrome. *J Cardiovasc Electrophysiol*. 2007;18:415–421.
276. Matsuo K, Akahoshi M, Seto S, Yano K. Disappearance of the Brugada-type electrocardiogram after surgical castration: a role for testosterone and an explanation for the male preponderance. *Pacing Clin Electrophysiol PACE*. 2003;26:1551–1553.
277. Barajas-Martínez H, Hu D, Urrutia J, Wu Y, Panama BK, Goodrow RJ Jr, Sicouri S, Di Diego JM, Treat JA, Desai M, Doss MX, Antzelevitch C. Chronic Exposure to Testosterone Increases Expression of Transient Outward Current in Human Induced Pluripotent Stem Cell (hiPSC)-Derived Cardiomyocytes (CM). *Heart Rhythm Off J Heart Rhythm Soc*. 2013;10:1741.
278. Song M, Helguera G, Eghbali M, Zhu N, Zarei MM, Olcese R, Toro L, Stefani E. Remodeling of Kv4.3 potassium channel gene expression under the control of sex hormones. *J Biol Chem*. 2001;276:31883–31890.
279. Nagase S, Kusano KF, Morita H, Fujimoto Y, Kakishita M, Nakamura K, Emori T, Matsubara H, Ohe T. Epicardial electrogram of the right ventricular outflow tract in patients with the Brugada syndrome: using the epicardial lead. *J Am Coll Cardiol*. 2002;39:1992–1995.
280. Postema PG, van Dessel PFHM, Kors JA, Linnenbank AC, van Herpen G, Ritsema van Eck HJ, van Geloven N, de Bakker JMT, Wilde AAM, Tan HL. Local depolarization abnormalities are the dominant pathophysiologic mechanism for type 1 electrocardiogram in brugada syndrome a study of electrocardiograms, vectorcardiograms, and body surface potential maps during ajmaline provocation. *J Am Coll Cardiol*. 2010;55:789–797.
281. Takami M, Ikeda T, Enjoji Y, Sugi K. Relationship between ST-segment morphology

and conduction disturbances detected by signal-averaged electrocardiography in Brugada syndrome. *Ann Noninvasive Electrocardiol Off J Int Soc Holter Noninvasive Electrocardiol Inc*. 2003;8:30–36.
282. Tukkie R, Sogaard P, Vleugels J, de Groot IKLM, Wilde AAM, Tan HL. Delay in right ventricular activation contributes to Brugada syndrome. *Circulation*. 2004;109:1272–1277.
283. Nademanee K, Veerakul G, Chandanamattha P, Chaothawee L, Ariyachaipanich A, Jirasirirojanakorn K, Likittanasombat K, Bhuripanyo K, Ngarmukos T. Prevention of ventricular fibrillation episodes in Brugada syndrome by catheter ablation over the anterior right ventricular outflow tract epicardium. *Circulation*. 2011;123:1270–1279.
284. Coronel R, Casini S, Koopmann TT, Wilms-Schopman FJG, Verkerk AO, de Groot JR, Bhuiyan Z, Bezzina CR, Veldkamp MW, Linnenbank AC, van der Wal AC, Tan HL, Brugada P, Wilde AAM, de Bakker JMT. Right ventricular fibrosis and conduction delay in a patient with clinical signs of Brugada syndrome: a combined electrophysiological, genetic, histopathologic, and computational study. *Circulation*. 2005;112:2769–2777.
285. Corrado D, Nava A, Buja G, Martini B, Fasoli G, Oselladore L, Turrini P, Thiene G. Familial cardiomyopathy underlies syndrome of right bundle branch block, ST segment elevation and sudden death. *J Am Coll Cardiol*. 1996;27:443–448.
286. Frustaci A, Priori SG, Pieroni M, Chimenti C, Napolitano C, Rivolta I, Sanna T, Bellocci F, Russo MA. Cardiac histological substrate in patients with clinical phenotype of Brugada syndrome. *Circulation*. 2005;112:3680–3687.
287. Priori SG, Wilde AA, Horie M, Cho Y, Behr ER, Berul C, Blom N, Brugada J, Chiang C-E, Huikuri H, Kannankeril P, Krahn A, Leenhardt A, Moss A, Schwartz PJ, Shimizu W, Tomaselli G, Tracy C. HRS/EHRA/APHRS Expert Consensus Statement on the Diagnosis and Management of Patients with Inherited Primary Arrhythmia SyndromesExpert Consensus Statement on Inherited Primary Arrhythmia Syndromes: Document endorsed by HRS, EHRA, and APHRS in May 2013 and by ACCF, AHA, PACES, and AEPC in June 2013. *Heart Rhythm Off J Heart Rhythm Soc*. 2013;:e75–e106.
288. Maury P, Hocini M, Haïssaguerre M. Electrical storms in Brugada syndrome: review of pharmacologic and ablative therapeutic options. *Indian Pacing Electrophysiol J*. 2005;5:25–34.
289. Schweizer PA, Becker R, Katus HA, Thomas D. Successful acute and long-term management of electrical storm in Brugada syndrome using orciprenaline and quinine/quinidine. *Clin Res Cardiol Off J Ger Card Soc*. 2010;99:467–470.
290. Belhassen B, Viskin S, Fish R, Glick A, Setbon I, Eldar M. Effects of electrophysiologic-guided therapy with Class IA antiarrhythmic drugs on the long-term outcome of patients with idiopathic ventricular fibrillation with or without the Brugada syndrome. *J Cardiovasc Electrophysiol*. 1999;10:1301–1312.
291. Belhassen B, Glick A, Viskin S. Efficacy of quinidine in high-risk patients with Brugada syndrome. *Circulation*. 2004;110:1731–1737.
292. Hermida J-S, Denjoy I, Clerc J, Extramiana F, Jarry G, Milliez P, Guicheney P, Di Fusco S, Rey J-L, Cauchemez B, Leenhardt A. Hydroquinidine therapy in Brugada syndrome. *J Am Coll Cardiol*. 2004;43:1853–1860.
293. Belhassen B, Glick A, Viskin S. Excellent long-term reproducibility of the electrophysiologic efficacy of quinidine in patients with idiopathic ventricular fibrillation and Brugada syndrome. *Pacing Clin Electrophysiol PACE*. 2009;32:294–301.
294. Márquez MF, Bonny A, Hernández-Castillo E, De Sisti A, Gómez-Flores J, Nava S,

Hidden-Lucet F, Iturralde P, Cárdenas M, Tonet J. Long-term efficacy of low doses of quinidine on malignant arrhythmias in Brugada syndrome with an implantable cardioverter-defibrillator: a case series and literature review. *Heart Rhythm Off J Heart Rhythm Soc*. 2012;9:1995–2000.

295. Zipes DP, Camm AJ, Borggrefe M, Buxton AE, Chaitman B, Fromer M, Gregoratos G, Klein G, Moss AJ, Myerburg RJ, Priori SG, Quinones MA, Roden DM, Silka MJ, Tracy C, Smith SC Jr, Jacobs AK, Adams CD, Antman EM, Anderson JL, Hunt SA, Halperin JL, Nishimura R, Ornato JP, Page RL, Riegel B, Blanc J-J, Budaj A, Dean V, Deckers JW, Despres C, Dickstein K, Lekakis J, McGregor K, Metra M, Morais J, Osterspey A, Tamargo JL, Zamorano JL, American College of Cardiology/American Heart Association Task Force, European Society of Cardiology Committee for Practice Guidelines, European Heart Rhythm Association, Heart Rhythm Society. ACC/AHA/ESC 2006 Guidelines for Management of Patients With Ventricular Arrhythmias and the Prevention of Sudden Cardiac Death: a report of the American College of Cardiology/American Heart Association Task Force and the European Society of Cardiology Committee for Practice Guidelines (writing committee to develop Guidelines for Management of Patients With Ventricular Arrhythmias and the Prevention of Sudden Cardiac Death): developed in collaboration with the European Heart Rhythm Association and the Heart Rhythm Society. *Circulation*. 2006;114:e385–484.
296. Bohora S. Drug Therapy For Preventing Ventricular Arrhythmia In Brugada syndrome: Do We Have The Answers Yet? *Indian Pacing Electrophysiol J*. 2013;13:166–169.
297. Haïssaguerre M, Extramiana F, Hocini M, Cauchemez B, Jaïs P, Cabrera JA, Farré J, Farre G, Leenhardt A, Sanders P, Scavée C, Hsu L-F, Weerasooriya R, Shah DC, Frank R, Maury P, Delay M, Garrigue S, Clémenty J. Mapping and ablation of ventricular fibrillation associated with long-QT and Brugada syndromes. *Circulation*. 2003;108:925–928.
298. Darmon J-P, Bettouche S, Deswardt P, Tiger F, Ricard P, Bernasconi F, Saoudi N. Radiofrequency ablation of ventricular fibrillation and multiple right and left atrial tachycardia in a patient with Brugada syndrome. *J Interv Card Electrophysiol Int J Arrhythm Pacing*. 2004;11:205–209.
299. Nakagawa E, Takagi M, Tatsumi H, Yoshiyama M. Successful radiofrequency catheter ablation for electrical storm of ventricular fibrillation in a patient with Brugada syndrome. *Circ J Off J Jpn Circ Soc*. 2008;72:1025–1029.
300. Shah AJ, Hocini M, Lamaison D, Sacher F, Derval N, Haissaguerre M. Regional substrate ablation abolishes Brugada syndrome. *J Cardiovasc Electrophysiol*. 2011;22:1290–1291.
301. Nademanee K, Veerakul G, Chandanamattha P, Chaothawee L, Ariyachaipanich A, Jirasirirojanakorn K, Likittanasombat K, Bhuripanyo K, Ngarmukos T. Prevention of ventricular fibrillation episodes in Brugada syndrome by catheter ablation over the anterior right ventricular outflow tract epicardium. *Circulation*. 2011;123:1270–1279.
302. Postema PG, Wolpert C, Amin AS, Probst V, Borggrefe M, Roden DM, Priori SG, Tan HL, Hiraoka M, Brugada J, Wilde AAM. Drugs and Brugada syndrome patients: review of the literature, recommendations, and an up-to-date website (www.brugadadrugs.org). *Heart Rhythm Off J Heart Rhythm Soc*. 2009;6:1335–1341.
303. Nielsen MW, Holst AG, Olesen S-P, Olesen MS. The genetic component of Brugada syndrome. *Front Physiol*. 2013;4:179.
304. Hennessey JA, Marcou CA, Wang C, Wei EQ, Wang C, Tester DJ, Torchio M, Dagradi F, Crotti L, Schwartz PJ, Ackerman MJ, Pitt GS. FGF12 is a candidate

Brugada syndrome locus. *Heart Rhythm Off J Heart Rhythm Soc*. 2013;10:1886–1894.
305. Cerrone M, Lin X, Zhang M, Agullo-Pascual E, Pfenniger A, Chkourko-Gusky H, Novelli V, Kim C, Tirasawadichai T, Judge DP, Rothenberg E, Chen H-SV, Napolitano C, Priori S, Delmar M. Missense Mutations in Plakophilin-2 Cause Sodium Current Deficit and Associate with a Brugada Syndrome Phenotype. *Circulation*. 2013; Dec 18. [Epub ahead of print]
306. Kapplinger JD, Tester DJ, Alders M, Benito B, Berthet M, Brugada J, Brugada P, Fressart V, Guerchicoff A, Harris-Kerr C, Kamakura S, Kyndt F, Koopmann TT, Miyamoto Y, Pfeiffer R, Pollevick GD, Probst V, Zumhagen S, Vatta M, Towbin JA, Shimizu W, Schulze-Bahr E, Antzelevitch C, Salisbury BA, Guicheney P, Wilde AAM, Brugada R, Schott J-J, Ackerman MJ. An international compendium of mutations in the SCN5A-encoded cardiac sodium channel in patients referred for Brugada syndrome genetic testing. *Heart Rhythm Off J Heart Rhythm Soc*. 2010;7:33–46.
307. Schulze-Bahr E, Eckardt L, Breithardt G, Seidl K, Wichter T, Wolpert C, Borggrefe M, Haverkamp W. Sodium channel gene (SCN5A) mutations in 44 index patients with Brugada syndrome: different incidences in familial and sporadic disease. *Hum Mutat*. 2003;21:651–2.
308. Chen Q, Kirsch GE, Zhang D, Brugada R, Brugada J, Brugada P, Potenza D, Moya A, Borggrefe M, Breithardt G, Ortiz-Lopez R, Wang Z, Antzelevitch C, O'Brien RE, Schulze-Bahr E, Keating MT, Towbin JA, Wang Q. Genetic basis and molecular mechanism for idiopathic ventricular fibrillation. *Nature*. 1998;392:293–296.
309. Amin AS, Asghari-Roodsari A, Tan HL. Cardiac sodium channelopathies. *Pflüg Arch Eur J Physiol*. 2010;460:223–237.
310. Baroudi G, Pouliot V, Denjoy I, Guicheney P, Shrier A, Chahine M. Novel mechanism for Brugada syndrome: defective surface localization of an SCN5A mutant (R1432G). *Circ Res*. 2001;88:E78–83.
311. Valdivia CR, Tester DJ, Rok BA, Porter CJ, Munger TM, Jahangir A, Makielski JC, Ackerman MJ. A trafficking defective, Brugada syndrome-causing SCN5A mutation rescued by drugs. *Cardiovasc Res*. 2004;62:53–62.
312. Pfahnl AE, Viswanathan PC, Weiss R, Shang LL, Sanyal S, Shusterman V, Kornblit C, London B, Dudley SC Jr. A sodium channel pore mutation causing Brugada syndrome. *Heart Rhythm Off J Heart Rhythm Soc*. 2007;4:46–53.
313. Baroudi G, Acharfi S, Larouche C, Chahine M. Expression and intracellular localization of an SCN5A double mutant R1232W/T1620M implicated in Brugada syndrome. *Circ Res*. 2002;90:E11–16.
314. Clatot J, Ziyadeh-Isleem A, Maugenre S, Denjoy I, Liu H, Dilanian G, Hatem SN, Deschênes I, Coulombe A, Guicheney P, Neyroud N. Dominant-negative effect of SCN5A N-terminal mutations through the interaction of Nav1.5 α-subunits. *Cardiovasc Res*. 2012;96:53–63.
315. Mohler PJ, Rivolta I, Napolitano C, LeMaillet G, Lambert S, Priori SG, Bennett V. Nav1.5 E1053K mutation causing Brugada syndrome blocks binding to ankyrin-G and expression of Nav1.5 on the surface of cardiomyocytes. *Proc Natl Acad Sci U S A*. 2004;101:17533–17538.
316. Petitprez S, Zmoos AF, Ogrodnik J, Balse E, Raad N, El-Haou S, Albesa M, Bittihn P, Luther S, Lehnart SE, Hatem SN, Coulombe A, Abriel H. SAP97 and dystrophin macromolecular complexes determine two pools of cardiac sodium channels Nav1.5 in cardiomyocytes. *Circ Res*. 108:294–304.
317. Hennessey JA, Marcou CA, Wang C, Wei EQ, Wang C, Tester DJ, Torchio M, Dagradi F, Crotti L, Schwartz PJ, Ackerman MJ, Pitt GS. FGF12 is a candidate

Brugada syndrome locus. *Heart Rhythm Off J Heart Rhythm Soc*. 2013;10:1886–1894.
318. Vatta M, Dumaine R, Antzelevitch C, Brugada R, Li H, Bowles NE, Nademanee K, Brugada J, Brugada P, Towbin JA. Novel mutations in domain I of SCN5A cause Brugada syndrome. *Mol Genet Metab*. 2002;75:317–324.
319. Veldkamp MW, Viswanathan PC, Bezzina C, Baartscheer A, Wilde AAM, Balser JR. Two Distinct Congenital Arrhythmias Evoked by a Multidysfunctional Na+ Channel. *Circ Res*. 2000;86:e91–e97.
320. Keller DI, Rougier J-S, Kucera JP, Benammar N, Fressart V, Guicheney P, Madle A, Fromer M, Schläpfer J, Abriel H. Brugada syndrome and fever: genetic and molecular characterization of patients carrying SCN5A mutations. *Cardiovasc Res*. 2005;67:510–519.
321. Amin AS, Verkerk AO, Bhuiyan ZA, Wilde AAM, Tan HL. Novel Brugada syndrome-causing mutation in ion-conducting pore of cardiac Na+ channel does not affect ion selectivity properties. *Acta Physiol Scand*. 2005;185:291–301.
322. Hsueh C-H, Chen W-P, Lin J-L, Tsai C-T, Liu Y-B, Juang J-M, Tsao H-M, Su M-J, Lai L-P. Distinct functional defect of three novel Brugada syndrome related cardiac sodium channel mutations. *J Biomed Sci*. 2009;16:23.
323. Chiang K-C, Lai L-P, Shieh R-C. Characterization of a novel Nav1.5 channel mutation, A551T, associated with Brugada syndrome. *J Biomed Sci*. 2009;16:76.
324. Calloe K, Refaat MM, Grubb S, Wojciak J, Campagna J, Thomsen NM, Nussbaum RL, Scheinman MM, Schmitt N. Characterization and mechanisms of action of novel NaV1.5 channel mutations associated with Brugada syndrome. *Circ Arrhythm Electrophysiol*. 2013;6:177–184.
325. London B, Michalec M, Mehdi H, Zhu X, Kerchner L, Sanyal S, Viswanathan PC, Pfahnl AE, Shang LL, Madhusudanan M, Baty CJ, Lagana S, Aleong R, Gutmann R, Ackerman MJ, McNamara DM, Weiss R, Dudley SC Jr. Mutation in glycerol-3-phosphate dehydrogenase 1 like gene (GPD1-L) decreases cardiac Na+ current and causes inherited arrhythmias. *Circulation*. 2007;116:2260–2268.
326. Antzelevitch C, Pollevick GD, Cordeiro JM, Casis O, Sanguinetti MC, Aizawa Y, Guerchicoff A, Pfeiffer R, Oliva A, Wollnik B, Gelber P, Bonaros EP Jr, Burashnikov E, Wu Y, Sargent JD, Schickel S, Oberheiden R, Bhatia A, Hsu L-F, Haïssaguerre M, Schimpf R, Borggrefe M, Wolpert C. Loss-of-function mutations in the cardiac calcium channel underlie a new clinical entity characterized by ST-segment elevation, short QT intervals, and sudden cardiac death. *Circulation*. 2007;115:442–449.
327. Watanabe H, Koopmann TT, Le Scouarnec S, Yang T, Ingram CR, Schott J-J, Demolombe S, Probst V, Anselme F, Escande D, Wiesfeld ACP, Pfeufer A, Kääb S, Wichmann H-E, Hasdemir C, Aizawa Y, Wilde AAM, Roden DM, Bezzina CR. Sodium channel β1 subunit mutations associated with Brugada syndrome and cardiac conduction disease in humans. *J Clin Invest*. 2008;118:2260–2268.
328. Delpón E, Cordeiro JM, Núñez L, Thomsen PEB, Guerchicoff A, Pollevick GD, Wu Y, Kanters JK, Larsen CT, Hofman-Bang J, Burashnikov E, Christiansen M, Antzelevitch C. Functional effects of KCNE3 mutation and its role in the development of Brugada syndrome. *Circ Arrhythm Electrophysiol*. 2008;1:209–218.
329. Hu D, Barajas-Martinez H, Burashnikov E, Springer M, Wu Y, Varro A, Pfeiffer R, Koopmann TT, Cordeiro JM, Guerchicoff A, Pollevick GD, Antzelevitch C. A mutation in the beta 3 subunit of the cardiac sodium channel associated with Brugada ECG phenotype. *Circ Cardiovasc Genet*. 2009;2:270–278.
330. Ueda K, Hirano Y, Higashiuesato Y, Aizawa Y, Hayashi T, Inagaki N, Tana T, Ohya Y, Takishita S, Muratani H, Hiraoka M, Kimura A. Role of HCN4 channel in preventing ventricular arrhythmia. *J Hum Genet*. 2009;54:115–121.

331. Itoh H, Sakaguchi T, Ashihara T, Ding W-G, Nagaoka I, Oka Y, Nakazawa Y, Yao T, Jo H, Ito M, Nakamura K, Ohe T, Matsuura H, Horie M. A novel KCNH2 mutation as a modifier for short QT interval. *Int J Cardiol*. 2009;137:83–85.
332. Verkerk AO, Wilders R, Schulze-Bahr E, Beekman L, Bhuiyan ZA, Bertrand J, Eckardt L, Lin D, Borggrefe M, Breithardt G, Mannens MMAM, Tan HL, Wilde AAM, Bezzina CR. Role of sequence variations in the human ether-a-go-go-related gene (HERG, KCNH2) in the Brugada syndrome. *Cardiovasc Res*. 2005;68:441–453.
333. Burashnikov E, Pfeiffer R, Barajas-Martinez H, Delpón E, Hu D, Desai M, Borggrefe M, Häissaguerre M, Kanter R, Pollevick GD, Guerchicoff A, Laiño R, Marieb M, Nademanee K, Nam G-B, Robles R, Schimpf R, Stapleton DD, Viskin S, Winters S, Wolpert C, Zimmern S, Veltmann C, Antzelevitch C. Mutations in the cardiac L-type calcium channel associated with inherited J-wave syndromes and sudden cardiac death. *Heart Rhythm*. 2010;7:1872–1882.
334. Kattygnarath D, Maugenre S, Neyroud N, Balse E, Ichai C, Denjoy I, Dilanian G, Martins RP, Fressart V, Berthet M, Schott JJ, Leenhardt A, Probst V, Le Marec H, Hainque B, Coulombe A, Hatem SN, Guicheney P. MOG1: a new susceptibility gene for Brugada syndrome. *Circ Cardiovasc Genet*. 4:261–8.
335. Ohno S, Zankov DP, Ding W-G, Itoh H, Makiyama T, Doi T, Shizuta S, Hattori T, Miyamoto A, Naiki N, Hancox JC, Matsuura H, Horie M. KCNE5 (KCNE1L) variants are novel modulators of Brugada syndrome and idiopathic ventricular fibrillation. *Circ Arrhythm Electrophysiol*. 2011;4:352–361.
336. Giudicessi JR, Ye D, Tester DJ, Crotti L, Mugione A, Nesterenko VV, Albertson RM, Antzelevitch C, Schwartz PJ, Ackerman MJ. Transient outward current (I(to)) gain-of-function mutations in the KCND3-encoded Kv4.3 potassium channel and Brugada syndrome. *Heart Rhythm Off J Heart Rhythm Soc*. 2011;8:1024–1032.
337. Ishikawa T, Sato A, Marcou CA, Tester DJ, Ackerman MJ, Crotti L, Schwartz PJ, On YK, Park J-E, Nakamura K, Hiraoka M, Nakazawa K, Sakurada H, Arimura T, Makita N, Kimura A. A novel disease gene for Brugada syndrome: sarcolemmal membrane-associated protein gene mutations impair intracellular trafficking of hNav1.5. *Circ Arrhythm Electrophysiol*. 2012;5:1098–1107.
338. Liu H, Chatel S, Simard C, Syam N, Salle L, Probst V, Morel J, Millat G, Lopez M, Abriel H, Schott J-J, Guinamard R, Bouvagnet P. Molecular genetics and functional anomalies in a series of 248 Brugada cases with 11 mutations in the TRPM4 channel. *PloS One*. 2013;8:e54131.
339. Riuró H, Beltran-Alvarez P, Tarradas A, Selga E, Campuzano O, Vergés M, Pagans S, Iglesias A, Brugada J, Brugada P, Vázquez FM, Pérez GJ, Scornik FS, Brugada R. A missense mutation in the sodium channel β2 subunit reveals SCN2B as a new candidate gene for Brugada syndrome. *Hum Mutat*. 2013;34:961–966.
340. Wilde AAM, Antzelevitch C, Borggrefe M, Brugada J, Brugada R, Brugada P, Corrado D, Hauer RNW, Kass RS, Nademanee K, Priori SG, Towbin JA. Proposed Diagnostic Criteria for the Brugada Syndrome Consensus Report. *Circulation*. 2002;106:2514–2519.
341. Takagi M, Yokoyama Y, Aonuma K, Aihara N, Hiraoka M, Japan Idiopathic Ventricular Fibrillation Study (J-IVFS) Investigators. Clinical characteristics and risk stratification in symptomatic and asymptomatic patients with brugada syndrome: multicenter study in Japan. *J Cardiovasc Electrophysiol*. 2007;18:1244–1251.
342. Junttila MJ, Brugada P, Hong K, Lizotte E, DE Zutter M, Sarkozy A, Brugada J, Benito B, Perkiomaki JS, Mäkikallio TH, Huikuri HV, Brugada R. Differences in 12-lead electrocardiogram between symptomatic and asymptomatic Brugada syndrome patients. *J Cardiovasc Electrophysiol*. 2008;19:380–383.

343. Ohkubo K, Watanabe I, Okumura Y, Ashino S, Kofune M, Nagashima K, Kofune T, Nakai T, Kunimoto S, Kasamaki Y, Hirayama A. Prolonged QRS duration in lead V2 and risk of life-threatening ventricular Arrhythmia in patients with Brugada syndrome. *Int Heart J*. 2011;52:98–102.
344. Benito B, Sarkozy A, Mont L, Henkens S, Berruezo A, Tamborero D, Arzamendi D, Berne P, Brugada R, Brugada P, Brugada J. Gender Differences in Clinical Manifestations of Brugada Syndrome. *J Am Coll Cardiol*. 2008;52:1567–1573.
345. Schott JJ, Alshinawi C, Kyndt F, Probst V, Hoorntje TM, Hulsbeek M, Wilde AA, Escande D, Mannens MM, Le Marec H. Cardiac conduction defects associate with mutations in SCN5A. *Nat Genet*. 1999;23:20–21.
346. Probst V, Kyndt F, Potet F, Trochu J-N, Mialet G, Demolombe S, Schott J-J, Baró I, Escande D, Le Marec H. Haploinsufficiency in combination with aging causes SCN5A-linked hereditary Lenègre disease. *J Am Coll Cardiol*. 2003;41:643–652.
347. Balser JR. The cardiac sodium channel: gating function and molecular pharmacology. *J Mol Cell Cardiol*. 2001;33:599–613.
348. Wilde AAM, Brugada R. Phenotypical manifestations of mutations in the genes encoding subunits of the cardiac sodium channel. *Circ Res*. 2011;108:884–897.
349. Goldin AL. Mechanisms of sodium channel inactivation. *Curr Opin Neurobiol*. 2003;13:284–290.
350. Motoike HK, Liu H, Glaaser IW, Yang A-S, Tateyama M, Kass RS. The Na+ channel inactivation gate is a molecular complex: a novel role of the COOH-terminal domain. *J Gen Physiol*. 2004;123:155–165.
351. Scriven DR, Dan P, Moore ED. Distribution of proteins implicated in excitation-contraction coupling in rat ventricular myocytes. *Biophys J*. 2000;79:2682–2691.
352. Maier SKG, Westenbroek RE, McCormick KA, Curtis R, Scheuer T, Catterall WA. Distinct subcellular localization of different sodium channel alpha and beta subunits in single ventricular myocytes from mouse heart. *Circulation*. 2004;109:1421–1427.
353. Petitprez S, Zmoos A-F, Ogrodnik J, Balse E, Raad N, El-Haou S, Albesa M, Bittihn P, Luther S, Lehnart SE, Hatem SN, Coulombe A, Abriel H. SAP97 and dystrophin macromolecular complexes determine two pools of cardiac sodium channels Nav1.5 in cardiomyocytes. *Circ Res*. 2011;108:294–304.
354. Abriel H. Cardiac sodium channel Na(v)1.5 and interacting proteins: Physiology and pathophysiology. *J Mol Cell Cardiol*. 2010;48:2–11.
355. Shy D, Gillet L, Abriel H. Cardiac sodium channel Na(V)1.5 distribution in myocytes via interacting proteins: The multiple pool model. *Biochim Biophys Acta*. 2013;1833:886–894.
356. Lin X, Liu N, Lu J, Zhang J, Anumonwo JMB, Isom LL, Fishman GI, Delmar M. Subcellular heterogeneity of sodium current properties in adult cardiac ventricular myocytes. *Heart Rhythm Off J Heart Rhythm Soc*. 2011;8:1923–1930.
357. Remme CA, Verkerk AO, Hoogaars WMH, Aanhaanen WTJ, Scicluna BP, Annink C, van den Hoff MJB, Wilde AAM, van Veen TAB, Veldkamp MW, de Bakker JMT, Christoffels VM, Bezzina CR. The cardiac sodium channel displays differential distribution in the conduction system and transmural heterogeneity in the murine ventricular myocardium. *Basic Res Cardiol*. 2009;104:511–522.
358. Rook MB, Evers MM, Vos MA, Bierhuizen MFA. Biology of cardiac sodium channel Nav1.5 expression. *Cardiovasc Res*. 2012;93:12–23.
359. Meadows LS, Isom LL. Sodium channels as macromolecular complexes: implications for inherited arrhythmia syndromes. *Cardiovasc Res*. 2005;67:448–458.
360. Dhar Malhotra J, Chen C, Rivolta I, Abriel H, Malhotra R, Mattei LN, Brosius FC, Kass RS, Isom LL. Characterization of sodium channel alpha- and beta-subunits in rat

and mouse cardiac myocytes. *Circulation*. 2001;103:1303–1310.
361. Malhotra JD, Thyagarajan V, Chen C, Isom LL. Tyrosine-phosphorylated and nonphosphorylated sodium channel beta1 subunits are differentially localized in cardiac myocytes. *J Biol Chem*. 2004;279:40748–54.
362. Ishikawa T, Takahashi N, Ohno S, Sakurada H, Nakamura K, On YK, Park JE, Makiyama T, Horie M, Arimura T, Makita N, Kimura A. Novel SCN3B mutation associated with brugada syndrome affects intracellular trafficking and function of Nav1.5. *Circ J Off J Jpn Circ Soc*. 2013;77:959–967.
363. Valdivia CR, Medeiros-Domingo A, Ye B, Shen W-K, Algiers TJ, Ackerman MJ, Makielski JC. Loss-of-function mutation of the SCN3B-encoded sodium channel {beta}3 subunit associated with a case of idiopathic ventricular fibrillation. *Cardiovasc Res*. 2010;86:392–400.
364. Medeiros-Domingo A, Kaku T, Tester DJ, Iturralde-Torres P, Itty A, Ye B, Valdivia C, Ueda K, Canizales-Quinteros S, Tusié-Luna MT, Makielski JC, Ackerman MJ. SCN4B-encoded sodium channel beta4 subunit in congenital long-QT syndrome. *Circulation*. 2007;116:134–142.
365. Qin N, D'Andrea MR, Lubin M-L, Shafaee N, Codd EE, Correa AM. Molecular cloning and functional expression of the human sodium channel beta1B subunit, a novel splicing variant of the beta1 subunit. *Eur J Biochem FEBS*. 2003;270:4762–4770.
366. Brackenbury WJ, Isom LL. Na Channel β Subunits: Overachievers of the Ion Channel Family. *Front Pharmacol*. 2011;2:53.
367. Patino GA, Brackenbury WJ, Bao Y, Lopez-Santiago LF, O'Malley HA, Chen C, Calhoun JD, Lafrenière RG, Cossette P, Rouleau GA, Isom LL. Voltage-gated Na+ channel β1B: a secreted cell adhesion molecule involved in human epilepsy. *J Neurosci Off J Soc Neurosci*. 2011;31:14577–14591.
368. Zimmer T, Biskup C, Bollensdorff C, Benndorf K. The beta1 subunit but not the beta2 subunit colocalizes with the human heart Na+ channel (hH1) already within the endoplasmic reticulum. *J Membr Biol*. 2002;186:13–21.
369. Makita N, Bennett PB, George AL Jr. Molecular determinants of beta 1 subunit-induced gating modulation in voltage-dependent Na+ channels. *J Neurosci Off J Soc Neurosci*. 1996;16:7117–7127.
370. McCormick KA, Srinivasan J, White K, Scheuer T, Catterall WA. The extracellular domain of the beta1 subunit is both necessary and sufficient for beta1-like modulation of sodium channel gating. *J Biol Chem*. 1999;274:32638–32646.
371. Makita N, Bennett PB Jr, George AL Jr. Multiple domains contribute to the distinct inactivation properties of human heart and skeletal muscle Na+ channels. *Circ Res*. 1996;78:244–252.
372. Meadows L, Malhotra JD, Stetzer A, Isom LL, Ragsdale DS. The intracellular segment of the sodium channel beta 1 subunit is required for its efficient association with the channel alpha subunit. *J Neurochem*. 2001;76:1871–1878.
373. Qu Y, Isom LL, Westenbroek RE, Rogers JC, Tanada TN, McCormick KA, Scheuer T, Catterall WA. Modulation of cardiac Na+ channel expression in Xenopus oocytes by beta 1 subunits. *J Biol Chem*. 1995;270:25696–25701.
374. Fahmi AI, Patel M, Stevens EB, Fowden AL, John JE 3rd, Lee K, Pinnock R, Morgan K, Jackson AP, Vandenberg JI. The sodium channel beta-subunit SCN3b modulates the kinetics of SCN5a and is expressed heterogeneously in sheep heart. *J Physiol*. 2001;537:693–700.
375. Bezzina CR, Rook MB, Groenewegen WA, Herfst LJ, van der Wal AC, Lam J, Jongsma HJ, Wilde AAM, Mannens MMAM. Compound heterozygosity for

mutations (W156X and R225W) in SCN5A associated with severe cardiac conduction disturbances and degenerative changes in the conduction system. *Circ Res*. 2003;92:159–168.
376. Herfst LJ, Potet F, Bezzina CR, Groenewegen WA, Le Marec H, Hoorntje TM, Demolombe S, Baró I, Escande D, Jongsma HJ, Wilde AAM, Rook MB. Na+ channel mutation leading to loss of function and non-progressive cardiac conduction defects. *J Mol Cell Cardiol*. 2003;35:549–557.
377. Valdivia CR, Nagatomo T, Makielski JC. Late Na currents affected by alpha subunit isoform and beta1 subunit co-expression in HEK293 cells. *J Mol Cell Cardiol*. 2002;34:1029–1039.
378. Ko S-H, Lenkowski PW, Lee HC, Mounsey JP, Patel MK. Modulation of Na(v)1.5 by beta1-- and beta3-subunit co-expression in mammalian cells. *Pflüg Arch Eur J Physiol*. 2005;449:403–412.
379. Lopez-Santiago LF, Meadows LS, Ernst SJ, Chen C, Malhotra JD, McEwen DP, Speelman A, Noebels JL, Maier SKG, Lopatin AN, Isom LL. Sodium channel Scn1b null mice exhibit prolonged QT and RR intervals. *J Mol Cell Cardiol*. 2007;43:636–647.
380. Chen C, Westenbroek RE, Xu X, Edwards CA, Sorenson DR, Chen Y, McEwen DP, O'Malley HA, Bharucha V, Meadows LS, Knudsen GA, Vilaythong A, Noebels JL, Saunders TL, Scheuer T, Shrager P, Catterall WA, Isom LL. Mice lacking sodium channel beta1 subunits display defects in neuronal excitability, sodium channel expression, and nodal architecture. *J Neurosci Off J Soc Neurosci*. 2004;24:4030–4042.
381. Zimmer T, Benndorf K. The human heart and rat brain IIA Na+ channels interact with different molecular regions of the beta1 subunit. *J Gen Physiol*. 2002;120:887–895.
382. Johnson D, Bennett ES. Isoform-specific effects of the beta2 subunit on voltage-gated sodium channel gating. *J Biol Chem*. 2006;281:25875–25881.
383. Hakim P, Gurung IS, Pedersen TH, Thresher R, Brice N, Lawrence J, Grace AA, Huang CL-H. Scn3b knockout mice exhibit abnormal ventricular electrophysiological properties. *Prog Biophys Mol Biol*. 2008;98:251–266.
384. Tan B-H, Pundi KN, Van Norstrand DW, Valdivia CR, Tester DJ, Medeiros-Domingo A, Makielski JC, Ackerman MJ. Sudden infant death syndrome-associated mutations in the sodium channel beta subunits. *Heart Rhythm Off J Heart Rhythm Soc*. 2010;7:771–778.
385. Gee SH, Madhavan R, Levinson SR, Caldwell JH, Sealock R, Froehner SC. Interaction of muscle and brain sodium channels with multiple members of the syntrophin family of dystrophin-associated proteins. *J Neurosci Off J Soc Neurosci*. 1998;18:128–137.
386. Gavillet B, Rougier J-S, Domenighetti AA, Behar R, Boixel C, Ruchat P, Lehr H-A, Pedrazzini T, Abriel H. Cardiac sodium channel Nav1.5 is regulated by a multiprotein complex composed of syntrophins and dystrophin. *Circ Res*. 2006;99:407–414.
387. Albesa M, Ogrodnik J, Rougier J-S, Abriel H. Regulation of the cardiac sodium channel Nav1.5 by utrophin in dystrophin-deficient mice. *Cardiovasc Res*. 2011;89:320–328.
388. Rougier J-S, Gavillet B, Abriel H. Proteasome inhibitor (MG132) rescues Nav1.5 protein content and the cardiac sodium current in dystrophin-deficient mdx (5cv) mice. *Front Physiol*. 2013;4:51.
389. Wu G, Ai T, Kim JJ, Mohapatra B, Xi Y, Li Z, Abbasi S, Purevjav E, Samani K, Ackerman MJ, Qi M, Moss AJ, Shimizu W, Towbin JA, Cheng J, Vatta M. alpha-1-syntrophin mutation and the long-QT syndrome: a disease of sodium channel

disruption. *Circ Arrhythm Electrophysiol*. 2008;1:193–201.
390. Ueda K, Valdivia C, Medeiros-Domingo A, Tester DJ, Vatta M, Farrugia G, Ackerman MJ, Makielski JC. Syntrophin mutation associated with long QT syndrome through activation of the nNOS-SCN5A macromolecular complex. *Proc Natl Acad Sci U S A*. 2008;105:9355–9360.
391. Funke L, Dakoji S, Bredt DS. Membrane-associated guanylate kinases regulate adhesion and plasticity at cell junctions. *Annu Rev Biochem*. 2005;74:219–245.
392. Elias GM, Nicoll RA. Synaptic trafficking of glutamate receptors by MAGUK scaffolding proteins. *Trends Cell Biol*. 2007;17:343–352.
393. El-Haou S, Balse E, Neyroud N, Dilanian G, Gavillet B, Abriel H, Coulombe A, Jeromin A, Hatem SN. Kv4 potassium channels form a tripartite complex with the anchoring protein SAP97 and CaMKII in cardiac myocytes. *Circ Res*. 2009;104:758–769.
394. Godreau D, Vranckx R, Maguy A, Rücker-Martin C, Goyenvalle C, Abdelshafy S, Tessier S, Couétil JP, Hatem SN. Expression, regulation and role of the MAGUK protein SAP-97 in human atrial myocardium. *Cardiovasc Res*. 2002;56:433–442.
395. Godreau D, Vranckx R, Maguy A, Goyenvalle C, Hatem SN. Different isoforms of synapse-associated protein, SAP97, are expressed in the heart and have distinct effects on the voltage-gated K+ channel Kv1.5. *J Biol Chem*. 2003;278:47046–47052.
396. Leonoudakis D, Conti LR, Anderson S, Radeke CM, McGuire LMM, Adams ME, Froehner SC, Yates JR 3rd, Vandenberg CA. Protein trafficking and anchoring complexes revealed by proteomic analysis of inward rectifier potassium channel (Kir2.x)-associated proteins. *J Biol Chem*. 2004;279:22331–22346.
397. Cunha SR, Mohler PJ. Cardiac ankyrins: Essential components for development and maintenance of excitable membrane domains in heart. *Cardiovasc Res*. 2006;71:22–29.
398. Lemaillet G, Walker B, Lambert S. Identification of a conserved ankyrin-binding motif in the family of sodium channel alpha subunits. *J Biol Chem*. 2003;278:27333–27339.
399. Lowe JS, Palygin O, Bhasin N, Hund TJ, Boyden PA, Shibata E, Anderson ME, Mohler PJ. Voltage-gated Nav channel targeting in the heart requires an ankyrin-G dependent cellular pathway. *J Cell Biol*. 2008;180:173–186.
400. Marfatia KA, Harreman MT, Fanara P, Vertino PM, Corbett AH. Identification and characterization of the human MOG1 gene. *Gene*. 2001;266:45–56.
401. Wu L, Yong SL, Fan C, Ni Y, Yoo S, Zhang T, Zhang X, Obejero-Paz CA, Rho H-J, Ke T, Szafranski P, Jones SW, Chen Q, Wang QK. Identification of a new co-factor, MOG1, required for the full function of cardiac sodium channel Nav 1.5. *J Biol Chem*. 2008;283:6968–6978.
402. Kattygnarath D, Maugenre S, Neyroud N, Balse E, Ichai C, Denjoy I, Dilanian G, Martins RP, Fressart V, Berthet M, Schott JJ, Leenhardt A, Probst V, Le Marec H, Hainque B, Coulombe A, Hatem SN, Guicheney P. MOG1: a new susceptibility gene for Brugada syndrome. *Circ Cardiovasc Genet*. 2011;4:261–268.
403. Ziane R, Huang H, Moghadaszadeh B, Beggs AH, Levesque G, Chahine M. Cell membrane expression of cardiac sodium channel Na(v)1.5 is modulated by alpha-actinin-2 interaction. *Biochemistry (Mosc)*. 2010;49:166–178.
404. Staub O, Rotin D. Role of Ubiquitylation in Cellular Membrane Transport. *Physiol Rev*. 2006;86:669–707.
405. Jespersen T, Membrez M, Nicolas CS, Pitard B, Staub O, Olesen S-P, Baró I, Abriel H. The KCNQ1 potassium channel is down-regulated by ubiquitylating enzymes of the Nedd4/Nedd4-like family. *Cardiovasc Res*. 2007;74:64–74.

406. Abriel H, Kamynina E, Horisberger JD, Staub O. Regulation of the cardiac voltage-gated Na+ channel (H1) by the ubiquitin-protein ligase Nedd4. *FEBS Lett*. 2000;466:377–380.
407. Bemmelen MX van, Rougier J-S, Gavillet B, Apothéloz F, Daidié D, Tateyama M, Rivolta I, Thomas MA, Kass RS, Staub O, Abriel H. Cardiac Voltage-Gated Sodium Channel Nav1.5 Is Regulated by Nedd4-2 Mediated Ubiquitination. *Circ Res*. 2004;95:284–291.
408. Rougier J-S, van Bemmelen MX, Bruce MC, Jespersen T, Gavillet B, Apothéloz F, Cordonier S, Staub O, Rotin D, Abriel H. Molecular determinants of voltage-gated sodium channel regulation by the Nedd4/Nedd4-like proteins. *Am J Physiol Cell Physiol*. 2005;288:C692–701.
409. Abriel H, Staub O. Ubiquitylation of Ion Channels. *Physiology*. 2005;20:398–407.
410. Couchonnal LF, Anderson ME. The Role of Calmodulin Kinase II in Myocardial Physiology and Disease. *Physiology*. 2008;23:151–159.
411. Wagner S, Dybkova N, Rasenack ECL, Jacobshagen C, Fabritz L, Kirchhof P, Maier SKG, Zhang T, Hasenfuss G, Brown JH, Bers DM, Maier LS. Ca2+/calmodulin-dependent protein kinase II regulates cardiac Na+ channels. *J Clin Invest*. 2006;116:3127–3138.
412. Yoon J-Y, Ho W-K, Kim S-T, Cho H. Constitutive CaMKII activity regulates Na+ channel in rat ventricular myocytes. *J Mol Cell Cardiol*. 2009;47:475–484.
413. Ashpole NM, Herren AW, Ginsburg KS, Brogan JD, Johnson DE, Cummins TR, Bers DM, Hudmon A. Ca2+/calmodulin-dependent protein kinase II (CaMKII) regulates cardiac sodium channel NaV1.5 gating by multiple phosphorylation sites. *J Biol Chem*. 2012;287:19856–19869.
414. Ahern CA, Zhang J-F, Wookalis MJ, Horn R. Modulation of the cardiac sodium channel NaV1.5 by Fyn, a Src family tyrosine kinase. *Circ Res*. 2005;96:991–998.
415. Jespersen T, Gavillet B, van Bemmelen MX, Cordonier S, Thomas MA, Staub O, Abriel H. Cardiac sodium channel Na(v)1.5 interacts with and is regulated by the protein tyrosine phosphatase PTPH1. *Biochem Biophys Res Commun*. 2006;348:1455–1462.
416. Tan HL, Kupershmidt S, Zhang R, Stepanovic S, Roden DM, Wilde AAM, Anderson ME, Balser JR. A calcium sensor in the sodium channel modulates cardiac excitability. *Nature*. 2002;415:442–447.
417. Deschênes I, Neyroud N, DiSilvestre D, Marbán E, Yue DT, Tomaselli GF. Isoform-specific modulation of voltage-gated Na(+) channels by calmodulin. *Circ Res*. 2002;90:E49–57.
418. Kim J, Ghosh S, Liu H, Tateyama M, Kass RS, Pitt GS. Calmodulin mediates Ca2+ sensitivity of sodium channels. *J Biol Chem*. 2004;279:45004–45012.
419. Sarhan MF, Petegem FV, Ahern CA. A Double Tyrosine Motif in the Cardiac Sodium Channel Domain III-IV Linker Couples Calcium-dependent Calmodulin Binding to Inactivation Gating. *J Biol Chem*. 2009;284:33265–33274.
420. Potet F, Chagot B, Anghelescu M, Viswanathan PC, Stepanovic SZ, Kupershmidt S, Chazin WJ, Balser JR. Functional Interactions between Distinct Sodium Channel Cytoplasmic Domains through the Action of Calmodulin. *J Biol Chem*. 2009;284:8846–8854.
421. Aiba T, Hesketh GG, Liu T, Carlisle R, Villa-Abrille MC, O'Rourke B, Akar FG, Tomaselli GF. Na+ channel regulation by Ca2+/calmodulin and Ca2+/calmodulin-dependent protein kinase II in guinea-pig ventricular myocytes. *Cardiovasc Res*. 2010;85:454–463.
422. Young KA, Caldwell JH. Modulation of skeletal and cardiac voltage-gated sodium

channels by calmodulin. *J Physiol*. 2005;565:349–370.
423. Shah VN, Wingo TL, Weiss KL, Williams CK, Balser JR, Chazin WJ. Calcium-dependent regulation of the voltage-gated sodium channel hH1: intrinsic and extrinsic sensors use a common molecular switch. *Proc Natl Acad Sci U S A*. 2006;103:3592–3597.
424. Mazzone A, Strege PR, Tester DJ, Bernard CE, Faulkner G, De Giorgio R, Makielski JC, Stanghellini V, Gibbons SJ, Ackerman MJ, Farrugia G. A mutation in telethonin alters Nav1.5 function. *J Biol Chem*. 2008;283:16537–16544.
425. Valle G, Faulkner G, De Antoni A, Pacchioni B, Pallavicini A, Pandolfo D, Tiso N, Toppo S, Trevisan S, Lanfranchi G. Telethonin, a novel sarcomeric protein of heart and skeletal muscle. *FEBS Lett*. 1997;415:163–168.
426. Nigro V, Aurino S, Piluso G. Limb girdle muscular dystrophies: update on genetic diagnosis and therapeutic approaches. *Curr Opin Neurol*. 2011;24:429–436.
427. Hayashi T, Arimura T, Itoh-Satoh M, Ueda K, Hohda S, Inagaki N, Takahashi M, Hori H, Yasunami M, Nishi H, Koga Y, Nakamura H, Matsuzaki M, Choi BY, Bae SW, You CW, Han KH, Park JE, Knöll R, Hoshijima M, Chien KR, Kimura A. Tcap gene mutations in hypertrophic cardiomyopathy and dilated cardiomyopathy. *J Am Coll Cardiol*. 2004;44:2192–2201.
428. Kraichely RE, Farrugia G. Mechanosensitive ion channels in interstitial cells of Cajal and smooth muscle of the gastrointestinal tract. *Neurogastroenterol Motil*. 2007;19:245–252.
429. Weiss R, Barmada MM, Nguyen T, Seibel JS, Cavlovich D, Kornblit CA, Angelilli A, Villanueva F, McNamara DM, London B. Clinical and molecular heterogeneity in the Brugada syndrome: a novel gene locus on chromosome 3. *Circulation*. 2002;105:707–713.
430. London B, Michalec M, Mehdi H, Zhu X, Kerchner L, Sanyal S, Viswanathan PC, Pfahnl AE, Shang LL, Madhusudanan M, Baty CJ, Lagana S, Aleong R, Gutmann R, Ackerman MJ, McNamara DM, Weiss R, Dudley SC Jr. Mutation in glycerol-3-phosphate dehydrogenase 1 like gene (GPD1-L) decreases cardiac Na+ current and causes inherited arrhythmias. *Circulation*. 2007;116:2260–2268.
431. Van Norstrand DW, Valdivia CR, Tester DJ, Ueda K, London B, Makielski JC, Ackerman MJ. Molecular and functional characterization of novel glycerol-3-phosphate dehydrogenase 1 like gene (GPD1-L) mutations in sudden infant death syndrome. *Circulation*. 2007;116:2253–2259.
432. Valdivia CR, Ueda K, Ackerman MJ, Makielski JC. GPD1L links redox state to cardiac excitability by PKC-dependent phosphorylation of the sodium channel SCN5A. *Am J Physiol Heart Circ Physiol*. 2009;297:H1446–1452.
433. Liu M, Sanyal S, Gao G, Gurung IS, Zhu X, Gaconnet G, Kerchner LJ, Shang LL, Huang CL-H, Grace A, London B, Dudley SC Jr. Cardiac Na+ current regulation by pyridine nucleotides. *Circ Res*. 2009;105:737–745.
434. Murray KT, Hu NN, Daw JR, Shin HG, Watson MT, Mashburn AB, George AL Jr. Functional effects of protein kinase C activation on the human cardiac Na+ channel. *Circ Res*. 1997;80:370–376.
435. Morrison DK. The 14-3-3 proteins: integrators of diverse signaling cues that impact cell fate and cancer development. *Trends Cell Biol*. 2009;19:16–23.
436. Allouis M, Le Bouffant F, Wilders R, Péroz D, Schott J-J, Noireaud J, Le Marec H, Mérot J, Escande D, Baró I. 14-3-3 is a regulator of the cardiac voltage-gated sodium channel Nav1.5. *Circ Res*. 2006;98:1538–1546.
437. Sato PY, Musa H, Coombs W, Guerrero-Serna G, Patiño GA, Taffet SM, Isom LL, Delmar M. Loss of plakophilin-2 expression leads to decreased sodium current and

slower conduction velocity in cultured cardiac myocytes. *Circ Res*. 2009;105:523–526.
438. Cerrone M, Noorman M, Lin X, Chkourko H, Liang F-X, van der Nagel R, Hund T, Birchmeier W, Mohler P, van Veen TA, van Rijen HV, Delmar M. Sodium current deficit and arrhythmogenesis in a murine model of plakophilin-2 haploinsufficiency. *Cardiovasc Res*. 2012;95:460–468.
439. Delmar M, McKenna WJ. The Cardiac Desmosome and Arrhythmogenic Cardiomyopathies From Gene to Disease. *Circ Res*. 2010;107:700–714.
440. Rizzo S, Lodder EM, Verkerk AO, Wolswinkel R, Beekman L, Pilichou K, Basso C, Remme CA, Thiene G, Bezzina CR. Intercalated disc abnormalities, reduced Na(+) current density, and conduction slowing in desmoglein-2 mutant mice prior to cardiomyopathic changes. *Cardiovasc Res*. 2012;95:409–418.
441. Murphy BJ, Rogers J, Perdichizzi AP, Colvin AA, Catterall WA. cAMP-dependent phosphorylation of two sites in the alpha subunit of the cardiac sodium channel. *J Biol Chem*. 1996;271:28837–28843.
442. Frohnwieser B, Chen LQ, Schreibmayer W, Kallen RG. Modulation of the human cardiac sodium channel alpha-subunit by cAMP-dependent protein kinase and the responsible sequence domain. *J Physiol*. 1997;498 (Pt 2):309–318.
443. Zhou J, Yi J, Hu N, George AL Jr, Murray KT. Activation of protein kinase A modulates trafficking of the human cardiac sodium channel in Xenopus oocytes. *Circ Res*. 2000;87:33–38.
444. Zhou J, Shin H-G, Yi J, Shen W, Williams CP, Murray KT. Phosphorylation and Putative ER Retention Signals Are Required for Protein Kinase A-Mediated Potentiation of Cardiac Sodium Current. *Circ Res*. 2002;91:540–546.
445. Lu T, Lee HC, Kabat JA, Shibata EF. Modulation of rat cardiac sodium channel by the stimulatory G protein alpha subunit. *J Physiol*. 1999;518 (Pt 2):371–384.
446. Yarbrough TL, Lu T, Lee H-C, Shibata EF. Localization of Cardiac Sodium Channels in Caveolin-Rich Membrane Domains Regulation of Sodium Current Amplitude. *Circ Res*. 2002;90:443–449.
447. Williams TM, Lisanti MP. The Caveolin genes: from cell biology to medicine. *Ann Med*. 2004;36:584–595.
448. Vatta M, Ackerman MJ, Ye B, Makielski JC, Ughanze EE, Taylor EW, Tester DJ, Balijepalli RC, Foell JD, Li Z, Kamp TJ, Towbin JA. Mutant Caveolin-3 Induces Persistent Late Sodium Current and Is Associated With Long-QT Syndrome. *Circulation*. 2006;114:2104–2112.
449. Cronk LB, Ye B, Kaku T, Tester DJ, Vatta M, Makielski JC, Ackerman MJ. Novel mechanism for sudden infant death syndrome: persistent late sodium current secondary to mutations in caveolin-3. *Heart Rhythm Off J Heart Rhythm Soc*. 2007;4:161–166.
450. Goldfarb M. Fibroblast growth factor homologous factors: evolution, structure, and function. *Cytokine Growth Factor Rev*. 2005;16:215–220.
451. Munoz-Sanjuan I, Smallwood PM, Nathans J. Isoform diversity among fibroblast growth factor homologous factors is generated by alternative promoter usage and differential splicing. *J Biol Chem*. 2000;275:2589–2597.
452. Smallwood PM, Munoz-Sanjuan I, Tong P, Macke JP, Hendry SH, Gilbert DJ, Copeland NG, Jenkins NA, Nathans J. Fibroblast growth factor (FGF) homologous factors: new members of the FGF family implicated in nervous system development. *Proc Natl Acad Sci U S A*. 1996;93:9850–9857.
453. Liu Cj, Dib-Hajj SD, Waxman SG. Fibroblast growth factor homologous factor 1B binds to the C terminus of the tetrodotoxin-resistant sodium channel rNav1.9a (NaN).

J Biol Chem. 2001;276:18925–18933.
454. Liu C, Dib-Hajj SD, Renganathan M, Cummins TR, Waxman SG. Modulation of the cardiac sodium channel Nav1.5 by fibroblast growth factor homologous factor 1B. *J Biol Chem*. 2003;278:1029–1036.
455. Goetz R, Dover K, Laezza F, Shtraizent N, Huang X, Tchetchik D, Eliseenkova AV, Xu C-F, Neubert TA, Ornitz DM, Goldfarb M, Mohammadi M. Crystal Structure of a Fibroblast Growth Factor Homologous Factor (FHF) Defines a Conserved Surface on FHFs for Binding and Modulation of Voltage-gated Sodium Channels. *J Biol Chem*. 2009;284:17883–17896.
456. Wang C, Wang C, Hoch EG, Pitt GS. Identification of novel interaction sites that determine specificity between fibroblast growth factor homologous factors and voltage-gated sodium channels. *J Biol Chem*. 2011;286:24253–24263.
457. Wittmack EK, Rush AM, Craner MJ, Goldfarb M, Waxman SG, Dib-Hajj SD. Fibroblast Growth Factor Homologous Factor 2B: Association with Nav1.6 and Selective Colocalization at Nodes of Ranvier of Dorsal Root Axons. *J Neurosci*. 2004;24:6765–6775.
458. Wang C, Hennessey JA, Kirkton RD, Wang C, Graham V, Puranam RS, Rosenberg PB, Bursac N, Pitt GS. Fibroblast growth factor homologous factor 13 regulates Na+ channels and conduction velocity in murine hearts. *Circ Res*. 2011;109:775–782.
459. Hennessey JA, Wei EQ, Pitt GS. Fibroblast Growth Factor Homologous Factors Modulate Cardiac Calcium Channels. *Circ Res*. 2013;113:381–388.
460. Garbino A, Wehrens XHT. Emerging role of junctophilin-2 as a regulator of calcium handling in the heart. *Acta Pharmacol Sin*. 2010;31:1019–1021.
461. Van Swieten JC, Brusse E, de Graaf BM, Krieger E, van de Graaf R, de Koning I, Maat-Kievit A, Leegwater P, Dooijes D, Oostra BA, Heutink P. A mutation in the fibroblast growth factor 14 gene is associated with autosomal dominant cerebellar ataxia [corrected]. *Am J Hum Genet*. 2003;72:191–199.
462. Dalski A, Atici J, Kreuz FR, Hellenbroich Y, Schwinger E, Zühlke C. Mutation analysis in the fibroblast growth factor 14 gene: frameshift mutation and polymorphisms in patients with inherited ataxias. *Eur J Hum Genet EJHG*. 2005;13:118–120.
463. Brusse E, de Koning I, Maat-Kievit A, Oostra BA, Heutink P, van Swieten JC. Spinocerebellar ataxia associated with a mutation in the fibroblast growth factor 14 gene (SCA27): A new phenotype. *Mov Disord Off J Mov Disord Soc*. 2006;21:396–401.
464. Laezza F, Gerber BR, Lou J-Y, Kozel MA, Hartman H, Craig AM, Ornitz DM, Nerbonne JM. The FGF14(F145S) mutation disrupts the interaction of FGF14 with voltage-gated Na+ channels and impairs neuronal excitability. *J Neurosci Off J Soc Neurosci*. 2007;27:12033–12044.
465. Wang Q, Bardgett ME, Wong M, Wozniak DF, Lou J, McNeil BD, Chen C, Nardi A, Reid DC, Yamada K, Ornitz DM. Ataxia and paroxysmal dyskinesia in mice lacking axonally transported FGF14. *Neuron*. 2002;35:25–38.
466. Goldfarb M, Schoorlemmer J, Williams A, Diwakar S, Wang Q, Huang X, Giza J, Tchetchik D, Kelley K, Vega A, Matthews G, Rossi P, Ornitz DM, D'Angelo E. Fibroblast growth factor homologous factors control neuronal excitability through modulation of voltage-gated sodium channels. *Neuron*. 2007;55:449–463.
467. Chouabe C, Neyroud N, Guicheney P, Lazdunski M, Romey G, Barhanin J. Properties of KvLQT1 K+ channel mutations in Romano-Ward and Jervell and Lange-Nielsen inherited cardiac arrhythmias. *EMBO J*. 1997;16:5472–5479.
468. Keller DI, Rougier J-S, Kucera JP, Benammar N, Fressart V, Guicheney P, Madle A,

Fromer M, Schläpfer J, Abriel H. Brugada syndrome and fever: genetic and molecular characterization of patients carrying SCN5A mutations. *Cardiovasc Res*. 2005;67:510–519.
469. Shy D, Gillet L, Abriel H. Cardiac sodium channel NaV1.5 distribution in myocytes via interacting proteins: the multiple pool model. *Biochim Biophys Acta*. 2013;1833:886–894.
470. Burashnikov A, Di Diego JM, Zygmunt AC, Belardinelli L, Antzelevitch C. Atrium-selective sodium channel block as a strategy for suppression of atrial fibrillation: differences in sodium channel inactivation between atria and ventricles and the role of ranolazine. *Circulation*. 2007;116:1449–1457.
471. Golod DA, Kumar R, Joyner RW. Determinants of action potential initiation in isolated rabbit atrial and ventricular myocytes. *Am J Physiol*. 1998;274:H1902–13.
472. Body SC, Collard CD, Shernan SK, Fox AA, Liu K-Y, Ritchie MD, Perry TE, Muehlschlegel JD, Aranki S, Donahue BS, Pretorius M, Estrada J-C, Ellinor PT, Newton-Cheh C, Seidman CE, Seidman JG, Herman DS, Lichtner P, Meitinger T, Pfeufer A, Kääb S, Brown NJ, Roden DM, Darbar D. Variation in the 4q25 chromosomal locus predicts atrial fibrillation after coronary artery bypass graft surgery. *Circ Cardiovasc Genet*. 2009;2:499–506.
473. Husser D, Adams V, Piorkowski C, Hindricks G, Bollmann A. Chromosome 4q25 variants and atrial fibrillation recurrence after catheter ablation. *J Am Coll Cardiol*. 2010;55:747–753.
474. Parvez B, Shoemaker MB, Muhammad R, Richardson R, Jiang L, Blair MA, Roden DM, Darbar D. Common genetic polymorphism at 4q25 locus predicts atrial fibrillation recurrence after successful cardioversion. *Heart Rhythm Off J Heart Rhythm Soc*. 2013;10:849–855.
475. Chinchilla A, Daimi H, Lozano-Velasco E, Dominguez JN, Caballero R, Delpón E, Tamargo J, Cinca J, Hove-Madsen L, Aranega AE, Franco D. PITX2 Insufficiency Leads to Atrial Electrical and Structural Remodeling Linked to Arrhythmogenesis. *Circ Cardiovasc Genet*. 2011;4:269–279.
476. Bezzina CR, Barc J, Mizusawa Y, Remme CA, Gourraud J-B, Simonet F, Verkerk AO, Schwartz PJ, Crotti L, Dagradi F, Guicheney P, Fressart V, Leenhardt A, Antzelevitch C, Bartkowiak S, Schulze-Bahr E, Zumhagen S, Behr ER, Bastiaenen R, Tfelt-Hansen J, Olesen MS, Kääb S, Beckmann BM, Weeke P, Watanabe H, Endo N, Minamino T, Horie M, Ohno S, Hasegawa K, Makita N, Nogami A, Shimizu W, Aiba T, Froguel P, Balkau B, Lantieri O, Torchio M, Wiese C, Weber D, Wolswinkel R, Coronel R, Boukens BJ, Bézieau S, Charpentier E, Chatel S, Despres A, Gros F, Kyndt F, Lecointe S, Lindenbaum P, Portero V, Violleau J, Gessler M, Tan HL, Roden DM, Christoffels VM, Le Marec H, Wilde AA, Probst V, Schott J-J, Dina C, Redon R. Common variants at SCN5A-SCN10A and HEY2 are associated with Brugada syndrome, a rare disease with high risk of sudden cardiac death. *Nat Genet*. 2013;45:1044–1049.
477. Remme CA. Cardiac sodium channelopathy associated with SCN5A mutations: electrophysiological, molecular and genetic aspects. *J Physiol*. 2013; 591: 4099–4116.
478. Manganas LN, Trimmer JS. Subunit Composition Determines Kv1 Potassium Channel Surface Expression. *J Biol Chem*. 2000;275:29685–29693.
479. Thomas D, Kiehn J, Katus HA, Karle CA. Defective protein trafficking in hERG-associated hereditary long QT syndrome (LQT2): molecular mechanisms and restoration of intracellular protein processing. *Cardiovasc Res*. 2003;60:235–241.
480. Mercier A, Clément R, Harnois T, Bourmeyster N, Faivre J-F, Findlay I, Chahine M, Bois P, Chatelier A. The β1-Subunit of Nav1.5 Cardiac Sodium Channel Is Required

for a Dominant Negative Effect through α-α Interaction. *PLoS ONE*. 2012;7:e48690.
481. Owsianik G, Cao L, Nilius B. Rescue of functional DeltaF508-CFTR channels by co-expression with truncated CFTR constructs in COS-1 cells. *FEBS Lett*. 2003;554:173–178.
482. Cormet-Boyaka E, Jablonsky M, Naren AP, Jackson PL, Muccio DD, Kirk KL. Rescuing cystic fibrosis transmembrane conductance regulator (CFTR)-processing mutants by transcomplementation. *Proc Natl Acad Sci U S A*. 2004;101:8221–8226.
483. Poelzing S, Forleo C, Samodell M, Dudash L, Sorrentino S, Anaclerio M, Troccoli R, Iacoviello M, Romito R, Guida P, Chahine M, Pitzalis M, Deschênes I. SCN5A Polymorphism Restores Trafficking of a Brugada Syndrome Mutation on a Separate Gene. *Circulation*. 2006;114:368–376.
484. Shinlapawittayatorn K, Du XX, Liu H, Ficker E, Kaufman ES, Deschênes I. A common SCN5A polymorphism modulates the biophysical defects of SCN5A mutations. *Heart Rhythm*. 2011;8:455–462.
485. Undrovinas AI, Fleidervish IA, Makielski JC. Inward sodium current at resting potentials in single cardiac myocytes induced by the ischemic metabolite lysophosphatidylcholine. *Circ Res*. 1992;71:1231–1241.
486. Núñez L, Barana A, Amorós I, de la Fuente MG, Dolz-Gaitón P, Gómez R, Rodríguez-García I, Mosquera I, Monserrat L, Delpón E, Caballero R, Castro-Beiras A, Tamargo J. p.D1690N Nav1.5 rescues p.G1748D mutation gating defects in a compound heterozygous Brugada syndrome patient. *Heart Rhythm*. 2013;10:264–272.
487. Moran O, Nizzari M, Conti F. Endogenous expression of the beta1A sodium channel subunit in HEK-293 cells. *FEBS Lett*. 2000;473:132–134.
488. Brodsky JL, Scott CM. Tipping the delicate balance: defining how proteasome maturation affects the degradation of a substrate for autophagy and endoplasmic reticulum associated degradation (ERAD). *Autophagy*. 2007;3:623–625.
489. Sharkey LM, Cheng X-Y, Drews V, Buchner DA, Jones JM, Justice MJ, Waxman SG, Dib-Hajj SD, Meisler MH. The ataxia3 mutation in the N-terminal cytoplasmic domain of sodium channel Nav1.6 disrupts intracellular trafficking. *J Neurosci Off J Soc Neurosci*. 2009;29:2733–2741.
490. Gütter C, Benndorf K, Zimmer T. Characterization of N-terminally mutated cardiac Na(+) channels associated with long QT syndrome 3 and Brugada syndrome. *Front Physiol*. 2013;4:153.
491. Cormier JW, Rivolta I, Tateyama M, Yang A-S, Kass RS. Secondary Structure of the Human Cardiac Na+ Channel C Terminus EVIDENCE FOR A ROLE OF HELICAL STRUCTURES IN MODULATION OF CHANNEL INACTIVATION. *J Biol Chem*. 2002;277:9233–9241.
492. Dolz-Gaitón P, Núñez M, Núñez L, Barana A, Amorós I, Matamoros M, Pérez-Hernández M, González de la Fuente M, Alvarez-López M, Macías-Ruiz R, Tercedor-Sánchez L, Jiménez-Jáimez J, Delpón E, Caballero R, Tamargo J. Functional characterization of a novel frameshift mutation in the C-terminus of the Nav1.5 channel underlying a Brugada syndrome with variable expression in a Spanish family. *PloS One*. 2013;8:e81493.
493. DiFrancesco D, Noble D. A model of cardiac electrical activity incorporating ionic pumps and concentration changes. *Philos Trans R Soc Lond B Biol Sci*. 1985;307:353–398.
494. Maier LS. New treatment options for late Na current, arrhythmias, and diastolic dysfunction. *Curr Heart Fail Rep*. 2012;9:183–191.
495. Haïssaguerre M, Jaïs P, Shah DC, Takahashi A, Hocini M, Quiniou G, Garrigue S, Le Mouroux A, Le Métayer P, Clémenty J. Spontaneous initiation of atrial fibrillation by

ectopic beats originating in the pulmonary veins. *N Engl J Med*. 1998;339:659–666.
496. Wang J, Klysik E, Sood S, Johnson RL, Wehrens XHT, Martin JF. Pitx2 prevents susceptibility to atrial arrhythmias by inhibiting left-sided pacemaker specification. *Proc Natl Acad Sci*. 2010;107:9753–9758.
497. Kirchhof P, Kahr PC, Kaese S, Piccini I, Vokshi I, Scheld H-H, Rotering H, Fortmueller L, Laakmann S, Verheule S, Schotten U, Fabritz L, Brown NA. PITX2c is expressed in the adult left atrium, and reducing Pitx2c expression promotes atrial fibrillation inducibility and complex changes in gene expression. *Circ Cardiovasc Genet*. 2011;4:123–133.
498. Ritchie MD, Rowan S, Kucera G, Stubblefield T, Blair M, Carter S, Roden DM, Darbar D. Chromosome 4q25 variants are genetic modifiers of rare ion channel mutations associated with familial atrial fibrillation. *J Am Coll Cardiol*. 2012;60:1173–1181.
499. Ammirabile G, Tessari A, Pignataro V, Szumska D, Sutera Sardo F, Benes J Jr, Balistreri M, Bhattacharya S, Sedmera D, Campione M. Pitx2 confers left morphological, molecular, and functional identity to the sinus venosus myocardium. *Cardiovasc Res*. 2012;93:291–301.
500. Remme CA, Scicluna BP, Verkerk AO, Amin AS, van Brunschot S, Beekman L, Deneer VHM, Chevalier C, Oyama F, Miyazaki H, Nukina N, Wilders R, Escande D, Houlgatte R, Wilde AAM, Tan HL, Veldkamp MW, de Bakker JMT, Bezzina CR. Genetically determined differences in sodium current characteristics modulate conduction disease severity in mice with cardiac sodium channelopathy. *Circ Res*. 2009;104:1283–1292.
501. Arking DE, Pfeufer A, Post W, Kao WHL, Newton-Cheh C, Ikeda M, West K, Kashuk C, Akyol M, Perz S, Jalilzadeh S, Illig T, Gieger C, Guo C-Y, Larson MG, Wichmann HE, Marbán E, O'Donnell CJ, Hirschhorn JN, Kääb S, Spooner PM, Meitinger T, Chakravarti A. A common genetic variant in the NOS1 regulator NOS1AP modulates cardiac repolarization. *Nat Genet*. 2006;38:644–651.
502. Newton-Cheh C, Eijgelsheim M, Rice KM, de Bakker PIW, Yin X, Estrada K, Bis JC, Marciante K, Rivadeneira F, Noseworthy PA, Sotoodehnia N, Smith NL, Rotter JI, Kors JA, Witteman JCM, Hofman A, Heckbert SR, O'Donnell CJ, Uitterlinden AG, Psaty BM, Lumley T, Larson MG, Stricker BHC. Common variants at ten loci influence QT interval duration in the QTGEN Study. *Nat Genet*. 2009;41:399–406.
503. Pfeufer A, Sanna S, Arking DE, Müller M, Gateva V, Fuchsberger C, Ehret GB, Orrú M, Pattaro C, Köttgen A, Perz S, Usala G, Barbalic M, Li M, Pütz B, Scuteri A, Prineas RJ, Sinner MF, Gieger C, Najjar SS, Kao WHL, Mühleisen TW, Dei M, Happle C, Möhlenkamp S, Crisponi L, Erbel R, Jöckel K-H, Naitza S, Steinbeck G, Marroni F, Hicks AA, Lakatta E, Müller-Myhsok B, Pramstaller PP, Wichmann H-E, Schlessinger D, Boerwinkle E, Meitinger T, Uda M, Coresh J, Kääb S, Abecasis GR, Chakravarti A. Common variants at ten loci modulate the QT interval duration in the QTSCD Study. *Nat Genet*. 2009;41:407–414.
504. Sotoodehnia N, Isaacs A, de Bakker PIW, Dörr M, Newton-Cheh C, Nolte IM, van der Harst P, Müller M, Eijgelsheim M, Alonso A, Hicks AA, Padmanabhan S, Hayward C, Smith AV, Polasek O, Giovannone S, Fu J, Magnani JW, Marciante KD, Pfeufer A, Gharib SA, Teumer A, Li M, Bis JC, Rivadeneira F, Aspelund T, Köttgen A, Johnson T, Rice K, Sie MPS, Wang YA, Klopp N, Fuchsberger C, Wild SH, Mateo Leach I, Estrada K, Völker U, Wright AF, Asselbergs FW, Qu J, Chakravarti A, Sinner MF, Kors JA, Petersmann A, Harris TB, Soliman EZ, Munroe PB, Psaty BM, Oostra BA, Cupples LA, Perz S, de Boer RA, Uitterlinden AG, Völzke H, Spector TD, Liu F-Y, Boerwinkle E, Dominiczak AF, Rotter JI, van Herpen G, Levy D, Wichmann H-E, van

Gilst WH, Witteman JCM, Kroemer HK, Kao WHL, Heckbert SR, Meitinger T, Hofman A, Campbell H, Folsom AR, van Veldhuisen DJ, Schwienbacher C, O'Donnell CJ, Volpato CB, Caulfield MJ, Connell JM, Launer L, Lu X, Franke L, Fehrmann RSN, te Meerman G, Groen HJM, Weersma RK, van den Berg LH, Wijmenga C, Ophoff RA, Navis G, Rudan I, Snieder H, Wilson JF, Pramstaller PP, Siscovick DS, Wang TJ, Gudnason V, van Duijn CM, Felix SB, Fishman GI, et al. Common variants in 22 loci are associated with QRS duration and cardiac ventricular conduction. *Nat Genet*. 2010;42:1068–1076.

505. Cho YS, Go MJ, Kim YJ, Heo JY, Oh JH, Ban H-J, Yoon D, Lee MH, Kim D-J, Park M, Cha S-H, Kim J-W, Han B-G, Min H, Ahn Y, Park MS, Han HR, Jang H-Y, Cho EY, Lee J-E, Cho NH, Shin C, Park T, Park JW, Lee J-K, Cardon L, Clarke G, McCarthy MI, Lee J-Y, Lee J-K, Oh B, Kim H-L. A large-scale genome-wide association study of Asian populations uncovers genetic factors influencing eight quantitative traits. *Nat Genet*. 2009;41:527–534.
506. Eijgelsheim M, Newton-Cheh C, Sotoodehnia N, de Bakker PIW, Müller M, Morrison AC, Smith AV, Isaacs A, Sanna S, Dörr M, Navarro P, Fuchsberger C, Nolte IM, de Geus EJC, Estrada K, Hwang S-J, Bis JC, Rückert I-M, Alonso A, Launer LJ, Hottenga JJ, Rivadeneira F, Noseworthy PA, Rice KM, Perz S, Arking DE, Spector TD, Kors JA, Aulchenko YS, Tarasov KV, Homuth G, Wild SH, Marroni F, Gieger C, Licht CM, Prineas RJ, Hofman A, Rotter JI, Hicks AA, Ernst F, Najjar SS, Wright AF, Peters A, Fox ER, Oostra BA, Kroemer HK, Couper D, Völzke H, Campbell H, Meitinger T, Uda M, Witteman JCM, Psaty BM, Wichmann H-E, Harris TB, Kääb S, Siscovick DS, Jamshidi Y, Uitterlinden AG, Folsom AR, Larson MG, Wilson JF, Penninx BW, Snieder H, Pramstaller PP, van Duijn CM, Lakatta EG, Felix SB, Gudnason V, Pfeufer A, Heckbert SR, Stricker BHC, Boerwinkle E, O'Donnell CJ. Genome-wide association analysis identifies multiple loci related to resting heart rate. *Hum Mol Genet*. 2010;19:3885–3894.
507. Crotti L, Monti MC, Insolia R, Peljto A, Goosen A, Brink PA, Greenberg DA, Schwartz PJ, George AL Jr. NOS1AP is a genetic modifier of the long-QT syndrome. *Circulation*. 2009;120:1657–1663.
508. Tomás M, Napolitano C, De Giuli L, Bloise R, Subirana I, Malovini A, Bellazzi R, Arking DE, Marban E, Chakravarti A, Spooner PM, Priori SG. Polymorphisms in the NOS1AP gene modulate QT interval duration and risk of arrhythmias in the long QT syndrome. *J Am Coll Cardiol*. 2010;55:2745–2752.

Résumé en francais

Titre : Nouveaux mécanismes contribuant à la variabilité phénotypiques de mutations N- et C-terminales du canal sodique cardiaque

Les mutations du gène *SCN5A*, codant la sous-unité α du canal Na^+ cardiaque $Na_v1.5$, sont responsables d'arythmies cardiaques héréditaires. La pénétrance incomplète observée dans ces maladies suggère l'existence d'autres facteurs modulant le phénotype associé à ces mutations. Dans ce travail de thèse, nous avons caractérisé deux mutations identifiées dans *SCN5A*. Le mutant R104W, identifié chez un patient atteint du syndrome de Brugada, est retenu dans le réticulum endoplasmique (RE), dégradé par le protéasome et abolit le courant Na^+. Co-exprimé avec le canal sauvage, R104W conduit à la rétention de celui-ci dans le RE, résultant en un effet dominant négatif sur les canaux sauvages. Nous avons démontré que ce nouveau mécanisme mettait en jeu une interaction entre les sous-unités α de $Na_v1.5$. La mutation R1860Gfs*12 a été identifiée dans une famille présentant des arythmies auriculaires. Dans un système d'expression hétérologue, ce mutant induit à la fois une perte et un gain de fonction de $Na_v1.5$. La modélisation informatique nous a permis de montrer que la perte de fonction était plus prononcée dans les cellules auriculaires que ventriculaires. De plus, nous avons montré que la présence de polymorphismes en amont du gène *PITX2* dans cette famille pouvait expliquer la variabilité des phénotypes observés. En conclusion, l'interaction entre les sous-unités α de $Na_v1.5$, les propriétés électriques différentes entre oreillette et ventricule et la présence de polymorphismes chez les patients porteurs de mutations *SCN5A* sont des facteurs importants dans l'interprétation des effets fonctionnels de ces mutations, contribuant à la variabilité phénotypique des canalopathies Na^+.

Mots Clés : Arythmie, Syndrome de Brugada, Fibrillation auriculaire, $Na_v1.5$, *SCN5A*, *PITX2*, Polymorphisme